Springer Theses
Recognizing Outstanding Ph.D. Research

Simone Zoia

Modern Analytic Methods for Computing Scattering Amplitudes

With Application to Two-Loop Five-Particle Processes

Springer

Springer Theses

Recognizing Outstanding Ph.D. Research

Aims and Scope

The series "Springer Theses" brings together a selection of the very best Ph.D. theses from around the world and across the physical sciences. Nominated and endorsed by two recognized specialists, each published volume has been selected for its scientific excellence and the high impact of its contents for the pertinent field of research. For greater accessibility to non-specialists, the published versions include an extended introduction, as well as a foreword by the student's supervisor explaining the special relevance of the work for the field. As a whole, the series will provide a valuable resource both for newcomers to the research fields described, and for other scientists seeking detailed background information on special questions. Finally, it provides an accredited documentation of the valuable contributions made by today's younger generation of scientists.

Theses may be nominated for publication in this series by heads of department at internationally leading universities or institutes and should fulfill all of the following criteria

- They must be written in good English.
- The topic should fall within the confines of Chemistry, Physics, Earth Sciences, Engineering and related interdisciplinary fields such as Materials, Nanoscience, Chemical Engineering, Complex Systems and Biophysics.
- The work reported in the thesis must represent a significant scientific advance.
- If the thesis includes previously published material, permission to reproduce this must be gained from the respective copyright holder (a maximum 30% of the thesis should be a verbatim reproduction from the author's previous publications).
- They must have been examined and passed during the 12 months prior to nomination.
- Each thesis should include a foreword by the supervisor outlining the significance of its content.
- The theses should have a clearly defined structure including an introduction accessible to new PhD students and scientists not expert in the relevant field.

Indexed by zbMATH.

More information about this series at https://link.springer.com/bookseries/8790

Simone Zoia

Modern Analytic Methods for Computing Scattering Amplitudes

With Application to Two-Loop Five-Particle Processes

Doctoral Thesis accepted by
Ludwig-Maximilians-Universität München, Germany

Springer

Author
Dr. Simone Zoia
Department of Physics
University of Turin
Turin, Italy

Supervisor
Prof. Johannes M. Henn
Werner-Heisenberg-Institut
Max-Planck-Institut für Physik
München, Germany

ISSN 2190-5053 ISSN 2190-5061 (electronic)
Springer Theses
ISBN 978-3-031-01944-9 ISBN 978-3-031-01945-6 (eBook)
https://doi.org/10.1007/978-3-031-01945-6

This Springer imprint is published by the registered company Springer Nature Switzerland AG
The registered company address is: Gewerbestrasse 11, 6330 Cham, Switzerland

Supervisor's Foreword

Our ability to understand the fundamental laws of the universe rests on the comparison between theory and experiments. Scattering amplitudes are what makes this possible for the quantum field theories describing elementary particles and their interactions. Their computation to ever increasing accuracy is of the utmost importance. Simone Zoia's thesis offers insight into the dramatic progress the field of scattering amplitudes has undergone in the last years. We now understand much better the special functions appearing in the scattering amplitudes, in particular thanks to a deeper understanding of the differential equations satisfied by the loop Feynman integrals. This development was recently complemented by the application of finite field arithmetics, which allows us to handle efficiently the complicated multivariate rational functions appearing along with the special functions in the scattering amplitudes. This is especially relevant for processes involving many kinematical scales, which are of particular interest for phenomenological applications. These two tools constitute the backbone of the modern workflow for computing scattering amplitudes presented in this thesis.

This thesis is useful for master and Ph.D. students, as well as researchers who would like to get acquainted with the latest methods and results. Starting from a basic knowledge of quantum field theory, Dr. Zoia gives a pedagogical review of the basic notions of scattering amplitudes, and smoothly moves on to presenting some of the most advanced techniques for their computation. The discussion is thorough yet concise, enriched with interesting explicit examples, and culminates with the application to a problem of great relevance for the physics program of CERN's Large Hadron Collider: the computation of five-particle scattering amplitudes at two-loop order. The work presented in this thesis constitutes an important step forward in the field, and contributes significantly to making five-particle processes at two-loop order the new state of the art for scattering amplitudes in the Standard Model of Particle Physics. The techniques and the results discussed here open the door to precision phenomenology for several processes of great interest for the LHC programme,

such as three-photon production, three-jet production, and di-photon production in association with a jet.

München, Germany
April 2022

Prof. Johannes M. Henn

Abstract

The scientific approach to understanding the laws of nature is based on the comparison between theory and experiment. In laypersons' terms, a theory is a set of rules which describe mathematically how we think things work. We use these rules to predict the outcome of a certain experiment, and the comparison against the actual results of the experiment may disprove or uphold the theory.

Particle physics is concerned with the tiniest building blocks of the universe—the fundamental particles—and the way they interact. Our best description of fundamental particles is given by the Standard Model of particle physics (SM), which treats particles as oscillations of "quantum fields" permeating the space-time. The spectacular success of the SM at describing the microscopic world is one of humanity's greatest intellectual feats. Yet, this theory fails to address a variety of theoretical concerns and observed phenomena—gravity, to say the most obvious. Understanding the limitations of the SM and constraining its extensions is of primary importance.

Scattering amplitudes are the bridge between theory and experiments in Quantum Field Theories (QFTs). Roughly speaking, the amplitude of a scattering process encodes its probability distribution: for a given initial state—say two colliding protons—the scattering amplitude tells us how likely the production of certain other particles is according to the theory. The rules of QFT are however complicated, and scattering amplitudes can only be computed approximately as series in the coupling constants which weigh the interactions. We know—at least in principle—how to compute each term of the series, and including more terms makes the prediction more accurate. The computation however becomes more and more difficult as the order in the couplings—also called the "loop order"—or the number of particles increase. In practice, we need as many terms as is necessary to make the theoretical uncertainty comparable with the experimental one so that the comparison is statistically significant.

Exploiting fully the physics potential of CERN's Large Hadron Collider requires predictions at the Next-to-Next-to-Leading Order (NNLO) in the coupling of the strong interactions. This goal has already been reached for many $2 \to 1$ and $2 \to 2$ processes. Processes with three particles in the final state are however of great interest, as they would allow for precise measurements of the strong coupling constant and of

its scaling, in-depth studies of the Higgs couplings, better background estimates for yet unknown phenomena, and more. The main bottleneck towards NNLO predictions for $2 \to 3$ processes is the analytic computation of two-loop five-particle scattering amplitudes.

The most difficult part of computing a scattering amplitude is the computation of the Feynman integrals appearing in it. My collaborators and I computed the missing and most complicated set of massless two-loop five-particle Feynman integrals. This opened the doors to the computation of the amplitude for *any* process involving five massless particles at two-loop order. Such processes feature prominently in the LHC physics program. Cases in point are three-jet, three-photon, and di-photon + jet production. In order to compute these integrals we made use of cutting-edge mathematical techniques, and proposed a new strategy which has already been applied to other difficult problems.

Armed with analytic expressions for the Feynman integrals, we tackled the amplitudes. The challenge is one of enormous algebraic complexity. We developed a workflow based on the recent idea of evaluating the rational functions in the intermediate expressions numerically over finite fields. The analytic expression of the final result is then reconstructed by "bootstrapping" an Ansatz or through reconstruction algorithms. Before considering the SM, we tested our approach on the amplitudes in two supersymmetric theories: $\mathcal{N} = 4$ super Yang-Mills theory and $\mathcal{N} = 8$ supergravity. These were the very first complete five-particle scattering amplitudes to be computed analytically at two loops. Although these models do not seek to describe physical particles and forces, they are of great interest. They give precious insights into hidden structures of QFT in general and—thanks to their simplicity and elegance—they are a perfect testing ground for new techniques and ideas which can be later applied to the SM.

The successful computation of the supersymmetric amplitudes showed that our technology was mature enough to face the SM. We therefore computed the two-loop amplitude describing the scattering of five positive-helicity gluons in Quantum Chromodynamics (QCD), the part of the SM which describes the strong interactions. Despite the leap in complexity with respect to the supersymmetric theories, we managed to find an extremely compact and elegant analytic expression. Having compact results for the amplitudes is not only a theorist's delight but also is crucial for their use in phenomenology. The simplicity of the expression allowed us to notice that certain parts of the amplitude enjoy an unexpected property: they are invariant under conformal symmetry. We identified the origin of this property in the conformal invariance of the gluonic amplitudes in QCD at one loop, which we proved for any number of gluons.

After the publication of the results presented in this thesis, there has been a dramatic progress. Several other two-loop five-particle amplitudes have become available analytically, and this has already led to the first theoretical prediction at NNLO in QCD, for three-photon production. Partly using methods similar to those presented in this thesis, many more results are sure to follow in the near future.

Publications Related to This Thesis

This thesis is based on the author's work conducted at the Johannes Gutenberg University in Mainz from October 2017 to September 2018, and at the Max Planck Institute for Physics in Munich from October 2018 to September 2020. Parts of this work have already been presented in the following publications.

Refereed Research Papers

- D. Chicherin, T. Gehrmann, J. M. Henn, P. Wasser, Y. Zhang and **S. Zoia**, "*Analytic result for a two-loop five-particle amplitude*," Phys. Rev. Lett. 122 (2019) no.12, 121602;
- D. Chicherin, T. Gehrmann, J. M. Henn, P. Wasser, Y. Zhang and **S. Zoia**, "*All master integrals for three-jet production at NNLO*," Phys. Rev. Lett. 123 (2019) no.4, 041603;
- D. Chicherin, T. Gehrmann, J. M. Henn, P. Wasser, Y. Zhang and **S. Zoia**, "*The two-loop five-particle amplitude in $\mathcal{N} = 8$ supergravity*," JHEP 1903 (2019) 115;
- S. Badger, D. Chicherin, T. Gehrmann, G. Heinrich, J. M. Henn, T. Peraro, P. Wasser, Y. Zhang and **S. Zoia**, "*Analytic form of the full two-loop five-gluon all-plus helicity amplitude*," Phys. Rev. Lett. 123 (2019) no.7, 071601;
- J. M. Henn, B. Power and **S. Zoia**, "*Conformal Invariance of the One-Loop All-Plus Helicity Scattering Amplitudes*," JHEP 02 (2020) 019;
- S. Caron-Huot, D. Chicherin, J. M. Henn, Y. Zhang and **S. Zoia**, "*Multi-Regge Limit of the Two-Loop Five-Point Amplitudes in $\mathcal{N} = 4$ Super Yang-Mills and $\mathcal{N} = 8$* Supergravity," JHEP 10 (2020) 188.

Conference Proceedings

- S. Zoia, "*Conformal Symmetry and Feynman Integrals*," PoS LL2018 (2018) 037, based on a talk given at Loops and Legs in Quantum Field Theory, St. Goar, Germany (2018).

Acknowledgments

Throughout my doctoral studies, I had the luck of meeting many wonderful people. Their support was crucial to the completion of this dissertation.

First of all, I need to express my deepest gratitude to Johannes Henn, who managed to be at the same time an amazing supervisor and a friend. Needless to say, without his support this experience would not have been possible. His insightful guidance pushed me to sharpen my thinking way beyond the scope of theoretical physics. I wish all Ph.D. students could have a supervision as excellent as I did.

I am deeply indebted also to Dmitry Chicherin, for always finding the time to answer my countless questions. I already miss walking into his office and discussing thoroughly my doubts. I look up to him as an incredible model of efficiency, which will be very difficult to match.

I am thankful to Tiziano Peraro, for the great time I had sharing the office with him in Mainz and for teaching me everything I know about the "fake" finite fields he pioneered. Without his prompt assistance with his package FiniteFlow my work would be incredibly harder.

My gratitude goes to Emery Sokatchev, for the many inspiring discussions about conformal symmetry and for his relentless but constructive criticism. It was an honour to visit him at LAPTh in Annecy at the very beginning of my Ph.D. Though brief, that visit had a great impact on my research ever since.

My thanks go also to Yang Zhang, not only of the many inspiring discussions about algebraic geometry but also for his service as photographer, as well as guide and driver in California.

I am truly thankful to Robin Brüser, Christoph Dlapa, Daniele Lombardi, Leila Maestri, and Pascal Wasser. Doing a Ph.D. is a challenging endeavor, but sharing it with them made it a pleasant and often even fun experience. I learnt so much from them, and I consider meeting them as one of the best aspects of my time as a Ph.D. student.

I would like to thank also many other brilliant researchers I had the luck to discuss with during my doctoral studies: Taushif Ahmed, Long Chen, Verónica Errasti Díez, Amando Hala, Gudrun Heinrich, Stephan Jahn, Vladimir Mitev, Bláithín Power, Vasily Sotnikov, Maximilian Stahlhofen, Alexander Tumanov, Edward Wang,

Marius Wiesemann, Ekta Chaubey, Kai Yan, and Giulia Zanderighi. I am particularly thankful to Taushif Ahmed and Ekta Chaubey for cheering me up and enduring my grumbling while completing this thesis.

I am truly grateful to the University of Mainz and to the Max Planck Institute for Physics for providing excellent and pleasant working environments. In particular, my deepest gratitude goes to Silke Köster, Vera Kudrin, and Annette Sturm, for making all the paperwork so easy and hassle-free. I truly miss the help of such efficient and kind persons. The same goes for the IT support: I am indebted to Thomas Hahn and Cesare delle Fratte for their continuous and excellent assistance with the computing resources of the Max Planck Institute for Physics and of the Max Planck Computing and Data Facility. I am also thankful to Sorana Scholtes, for helping me in the difficult and fundamental task of explaining my job to people who have not studied theoretical physics, and to Frank Steffen, for his dedication in coordinating the International Max Planck Research School on Elementary Particle Physics (IMPRS).

It is a pleasure to thank also my collaborators Simon Badger, Simon Caron-Huot, and Thomas Gehrmann. Discussing with them has been extremely inspiring and instructive. I very much look forward to working with them again. I am also grateful to Martin Beneke for serving as external supervisor in the IMPRS advisory committee.

I am grateful to Taushif Ahmed, Ekta Chaubey, Antonela Matijasic, Fabian Wagner, and Christoph Dlapa for their constructive criticism on parts of this thesis. To Christoph Dlapa I am even more indebted for helping me out with the German language countless times, in particular with the summary of this thesis.

I will never be grateful enough to my family for their unconditional love, support, and sacrifices, without which I would have never been able to embark on such a challenging adventure. Finally, I must thank my girlfriend Lisa, for enduring the distance, for her love, and—especially—for the discovery of the Königlicher Hirschgarten.

This work received funding from the European Union's Horizon 2020 research and innovation programme *Novel structures in scattering amplitudes* (grant agreement No 725110).

Contents

Chapter 1
Introduction

Do I dare
Disturb the Universe?

What are the fundamental laws of the universe? Is it even possible for us to know them? After all, what we have is just our *experience* of things, the way they appear to us as observers. To put it in philosophical terms—the *phenomenon* [1]. We have no direct access to things in themselves, the *noumenon*. So how dare we "disturb the Universe"?[1]

After thousands of years of philosophical and scientific inquiry, the noumenon remains impenetrable. Still, I think we can safely claim that our understanding of the universe is better than it used to be, say, when Thales of Miletus—one of the first western philosophers—argued with confidence that everything is made of water. What has enabled this progress is the scientific method, a powerful practical approach which by-passes the inaccessibility of the noumenon. Based on our imagination and our experience, we make guesses for the form of the noumenon, which we call *models*. Necessary condition for a model to be acceptable is that it must allow us to make quantitative predictions which can be tested. We can then rule out the wrong models by comparing predictions based on them against the phenomenon. Theories can thus be falsified, never verified.[2] In the truest sense, we learn from our mistakes. While this approach might be unsatisfactory to some from the philosophical point of view, it has taken us very far. Our entire civilisation is built upon the technological progress stemmed from it.

[1] From "The Love Song of J. Alfred Prufrock," by T. S. Eliot.

[2] See Ref. [2] for the first systematic treatment of this methodology based on falsifiability, and Bertrand Russell's "inductivist turkey" for the dangers that reside in the idea of verifying models with repeated observations [3].

S. Zoia, *Modern Analytic Methods for Computing Scattering Amplitudes*, Springer Theses,
https://doi.org/10.1007/978-3-031-01945-6_1

Particle physics is concerned with the tiniest building blocks of the Universe—the fundamental particles—and their interactions. Our best description (so far) is given by the Standard Model of particle physics, a Quantum Field Theory (QFT) where fundamental particles are viewed as excitations of quantum fields which permeate a four-dimensional Minkowski space-time. The current formulation of the Standard Model dates back to the mid-Seventies. Ever since, it has been throughly scrutinised. Although a few tensions between theoretical predictions and experimental data do exist (e.g. see Ref. [4, 5]), none has reached sufficient statistical significance to claim a discovery. For example, the value of the electron magnetic moment predicted by the Standard Model agrees with the experimental measure to an astonishing part in a trillion [6, 7]! The fact that it is even possible to describe the Universe down to its (supposedly) fundamental constituents and to such a high accuracy continues to amaze me. In case you are not amazed yet—although you should—I will give you another—perhaps the most well-known—example of the success of the Standard Model: the Higgs boson. This particle and its properties were speculated in the Sixties to introduce masses in the model without spoiling its symmetry, and was first detected at CERN's Large Hadron Collider (LHC) in 2012. It took almost fifty years to develop the technology and the expertise to observe experimentally a particle whose existence had been suggested by the mathematical elegance and self-consistency of the Standard Model. To me, this is one of the supreme examples of "the unreasonable effectiveness of mathematics in the natural sciences" [8].

Ironically, the triumph of the Standard Model is reason not only for delight, but also for growing frustration. While none of its predictions has been clearly falsified yet, there are things it does not account for at all. Some of them are of a theoretical nature. For example, one concerns the sector of the Standard Model which describes the strong interaction: Quantum Chromodynamics (QCD). The symmetries of QCD would in principle allow a kind of interaction which breaks CP symmetry (the combination of charge and parity symmetry). There is no theoretical reason to rule it out, and yet this phenomenon has never been observed experimentally, thus requiring a fine tuning of a parameter of the model which many consider as "unnatural." This issue, referred to as strong CP problem, is not a problem per se, but the necessity for fine tuning often signals a lack of understanding. There are other theoretical issues of similar kind, such as the hierarchy problem and the Landau pole, but the most apparent shortcoming of the Standard Model is of a much more concrete nature: it does not explain gravity. Our best description of gravity so far is given by General Relativity, which has proven as successful at explaining the Universe on macroscopic scales as the Standard Model is with the microscopic world. Fitting the two descriptions in a unique framework is definitely one of the most important open problems in fundamental physics. The effects of gravity at the scales relevant for particle physics are however negligible, so that the Standard Model's accuracy in describing particle interactions in the experiments we can carry out is not affected. Another prominent and concrete issue not addressed by the Standard Model is the existence and nature of dark matter and dark energy. The Standard Model in fact accounts only for ordinary matter, which we know from cosmological observations to constitute just about five percent of the total energy of the Universe. And even within this five percent that is

described by the Standard Model there are issues. For instance, what we observe of the Universe is disproportionately made of matter, while, comparatively, there is not much anti-matter to be seen. This observed asymmetry cannot be explained by the Standard Model alone. Moreover, the Standard Model neutrinos are massless particles, whereas the observation of neutrino oscillations indicates that neutrinos do have small but non-vanishing masses. In short, we have an amazing model, mathematically elegant and astonishingly accurate, which however fails to address a variety of theoretical concerns and observed phenomena. Can we do better?

In order to go "beyond" the Standard Model, it is of primary importance to determine its range of validity, and to constrain its possible extensions. Our best probe into the microscopic world of fundamental particles is CERN's LHC,, where two beams of protons are accelerated to nearly the speed of light and smashed against each other to observe the products of their interaction. Originally intended as a "discovery" machine, after the discovery of the Higgs boson the LHC has revealed a great potential for "precision" measurements as well. So far, the observations at the LHC, as well as in the other particle colliders, have revealed only small tensions with the Standard Model, not considered to be statistically significant. However, not all hope is lost: we have only seen about one tenth of the total data that the full LHC programme is expected to deliver! [9] This stunning wealth of present and future precise measurements becomes however useless if it is not matched by a comparable accuracy in the theoretical predictions. It is in fact not possible to achieve an exact theoretical description of particle collisions. The current model consists of several very distinct parts, each associated with difficult challenges and sources of uncertainty. I will give a brief review of this "picture" in Sect. 2.1, but I must anticipate that in this thesis I focus on the high-energy (or equivalently short-distance) effects, captured by the *scattering amplitudes*. These objects, which I define in Sect. 2.1, are computed in perturbation theory, namely as power series in the coupling constants. Each coefficient of the series can in principle be determined systematically, e.g. using Feynman diagrams. The complexity of the computation however escalates very rapidly with the order in the couplings, so that scattering amplitudes in the Standard Model and candidate extensions can only be computed up to some finite order. The theoretical uncertainty reflects this truncation of the infinite perturbative series (see e.g. [10, 11] for some recent work on this topic). Clearly, the smaller are the values of the coupling constants, the better is the convergence of the perturbative series.

Among the coupling constants of the Standard Model, the one that takes the largest value at the energy scales relevant for the LHC—while still being in a perturbative regime—is that of the strong interactions, α_{QCD}. The higher orders in α_{QCD} are thus generally expected to give the most important corrections in a generic process at the LHC. Indeed, theoretical predictions truncated at the Leading Order (LO) in QCD typically provide only estimates of the order of magnitude, and are thus insufficient for precision studies. In order to exploit fully the enormous scientific potential of the LHC it is necessary to push the theoretical predictions for a number of phenomenologically relevant processes to the Next-to-Next-to-Leading Order (NNLO) in QCD. NNLO predictions for $2 \to 2$ processes have by

now become the state of the art (see e.g. Refs. [12, 13] for comprehensive reviews of the current status of precision collider physics). There is however great interest in higher-multiplicity processes as well. In this regard, the NNLO description of $2 \to 3$ processes represents the current challenge. Only very recently this was achieved for the first process, three-photon production [14–16], in the leading colour approximation (see Sect. 4.3.1 for the definition of this approximation).[3] Many other $2 \to 3$ processes feature in the so-called "precision wish-list," updated every two years in the workshop series "Physics at TeV Colliders" held in Les Houches [12]: $pp \to 3j$, $pp \to 2\gamma + j$, $pp \to V + 2j$, $pp \to H + 2j$, where p, j, γ, V and H stand for proton, jet, photon, vector bosons ($W^{\pm}$ and Z) and Higgs boson, respectively, just to name a few. One of the main bottlenecks is the computation and evaluation of the required two-loop five-particle scattering amplitudes. The last few years have seen tremendous progress in this direction by several groups and approaches. I have had the pleasure and the luck to take part in this endeavour, and in this thesis I present my contribution.

This thesis is addressed to readers with a basic knowledge of QFT, and who have already some familiarity with scattering amplitudes and their computation using Feynman diagrams. Chapter 2 is an attempt to provide a smooth and concise transition from a standard QFT course to the modern techniques presented in Chaps. 3 and 4. I discuss what, at first, I found most bewildering about scattering amplitudes beyond the tree level, namely that they diverge. I show where the divergences come from, where they go, and why they are there in the first place. Once we have made peace with the divergences, we focus on the analytic structure of scattering amplitudes viewed as functions of the momenta of the external particles, whose understanding plays a crucial role in the modern techniques presented in the following chapters. In particular, I discuss the most distinctive analytic features of scattering amplitudes, namely their singularities and their discontinuities, and relate them to the fundamental principles of locality and unitarity.

The main bottleneck in computing scattering amplitudes beyond the tree level is the loop integration. While Feynman diagrams allow us to write down the amplitude of any process and at any loop order in a completely algorithmic way,[4] the computation of the relevant loop integrals beyond one loop is still far from being systematic. In Chap. 3 I present one of the most powerful techniques for computing loop integrals analytically: the method of the differential equations in the canonical form [18–21]. I give a (hopefully) pedagogical and self-contained discussion, with a particular emphasis on the special functions which appear in the solution of the differential equations.

Finally, in Chap. 4 I put the techniques and ideas introduced in the previous chapter at the service of the two-loop five-particle cause, and present my and my collabora-

[3] The neglected contributions are estimated to be phenomenologically irrelevant for this process.

[4] Of course there are practical limitations, as the number of diagrams grows very rapidly with the number of external legs and of loops. For instance, the number of Feynman diagrams contributing to the tree-level amplitude for the process $gg \to ng$ grows factorially with n [17]. For this reason alternative approaches have been and are being developed. See e.g. Sect. 2.4.2 for a few words about unitarity-based methods.

tors' contributions. In Sect. 4.2 I discuss the analytic computation of the last missing "family" of massless two-loop five-particle Feynman integrals. In order to achieve it, we also developed a novel method to put the differential equations satisfied by the integrals in the so-called "canonical form," which we expect will be useful also in future applications. Together with the results already available in the literature, this work opened the door to the analytic computation of any massless five-particle amplitude at two loops, in any theory. Indeed, this allowed us to provide the very first analytic results for complete two-loop five-particle amplitudes. In Sect. 4.3 I present the computation of the (super) amplitudes in $\mathcal{N} = 4$ super Yang-Mills theory and $\mathcal{N} = 8$ supergravity. Moreover, I show how the method of the differential equations can be used very effectively to expand Feynman integrals and scattering amplitudes asymptotically in any kinematic limit. In particular, I discuss in detail how we computed the asymptotic expansion of the two supersymmetric amplitudes in the multi-Regge kinematics. After warming up with the super-symmetric amplitudes, we tackle Yang-Mills theory in Sect. 4.5, and compute analytically the complete two-loop five-gluon amplitude in the all-plus helicity configuration. Remarkable cancellations lead to an extremely compact expression, which exhibits intriguing signs of conformal symmetry. We expect that the integrals we computed and the workflow we developed will enable the computation of all the two-loop five-particle amplitudes required in the theoretical predictions for processes of great phenomenological interest, such as three-jet production and di-photon + jet production, at NNLO in QCD. I draw my conclusions and discuss the outlook of the work presented here in Chap. 5.

Bibliography

1. Kant I (1781) Kritik der reinen Vernunft. Johann Friedrich Hartknoch
2. Popper K (1934) Logik der Forschung. Julius Springer, Hutchinson & Co
3. Russell B (1912) The problems of philosophy
4. Muon g-2 collaboration (2006) Final report of the muon E821 anomalous magnetic moment measurement at BNL. Phys Rev D. https://doi.org/10.1103/PhysRevD.73.072003. arXiv:hep-ex/0602035
5. Aoyama T et al, The anomalous magnetic moment of the muon in the Standard Model. arXiv:2006.04822
6. Gabrielse G, Hanneke D, Kinoshita T, Nio M, Odom BC (2006) New determination of the fine structure constant from the electron g value and QED. Phys Rev Lett. https://doi.org/10.1103/PhysRevLett.97.030802
7. Hanneke D, Hoogerheide S, Gabrielse G (2011) Cavity control of a single-electron quantum cyclotron: measuring the electron magnetic moment. Phys Rev A. https://doi.org/10.1103/PhysRevA.83.052122. arXiv:1009.4831
8. Wigner E (1960) The unreasonable effectiveness of mathematics in the natural sciences. Commun Pure Appl Math 13:1. https://doi.org/10.1002/cpa.3160130102
9. Azzi P et al (2019) Report from working group 1: standard model physics at the HL-LHC and HE-LHC. CERN Yellow Rep: Monogr 7:1. https://doi.org/10.23731/CYRM-2019-007.1. arXiv:1902.04070
10. Cacciari M, Houdeau N (2011) Meaningful characterisation of perturbative theoretical uncertainties. https://doi.org/10.1007/JHEP09(2011)039. arXiv:1105.5152

11. Bonvini M, Probabilistic definition of the perturbative theoretical uncertainty from missing higher orders. arXiv:2006.16293
12. Amoroso S et al (2020) Les Houches 2019: physics at TeV colliders: standard model working group report. In: 11th Les Houches workshop on physics at TeV colliders: PhysTeV Les Houches, vol 3. arXiv:2003.01700
13. Heinrich G, Collider physics at the precision frontier. arXiv:2009.00516
14. Chawdhry HA, Czakon ML, Mitov A, Poncelet R, NNLO QCD corrections to three-photon production at the LHC. https://doi.org/10.1007/JHEP02(2020)057. arXiv:1911.00479
15. Kallweit S, Sotnikov V, Wiesemann M, Triphoton production at hadron colliders in NNLO QCD. arXiv:2010.04681
16. Abreu S, Page B, Pascual E, Sotnikov V, Leading-color two-loop QCD corrections for three-photon production at hadron colliders. arXiv:2010.15834
17. Mangano ML, Parke SJ (1991) Multiparton amplitudes in gauge theories. Phys Rep 200:301. https://doi.org/10.1016/0370-1573(91)90091-Y. arXiv:hep-th/0509223
18. Kotikov A (1991) Differential equations method: new technique for massive Feynman diagrams calculation. Phys Lett B 254:158. https://doi.org/10.1016/0370-2693(91)90413-K
19. Remiddi E (1997) Differential equations for Feynman graph amplitudes. Nuovo Cim A 110:1435. arXiv:hep-th/9711188
20. Gehrmann T, Remiddi E (2000) Differential equations for two loop four point functions. Nucl Phys B 580:485. https://doi.org/10.1016/S0550-3213(00)00223-6. arXiv:hep-ph/9912329
21. Henn JM (2013) Multiloop integrals in dimensional regularization made simple. https://doi.org/10.1103/PhysRevLett.110.251601. arXiv:1304.1806

Chapter 2
Scattering Amplitudes

In an attempt of making things more original, I will begin by telling you what this chapter is *not* about. I do not wish to introduce the complete theoretical framework of QFT. That has already been done elsewhere, and in a much better way than I could possibly do (see the many great textbooks, e.g. [1–3]). This thesis is aimed at people who have already some familiarity with QFT, and who can (at least in principle) write down the expression of a scattering amplitude using Feynman rules or whatever technique they are most comfortable with. I will also not introduce any specific theory. The techniques presented in Chaps. 3 and 4 are in fact very general and can be applied to the computation of scattering amplitudes in any QFT. In this chapter I content myself with discussing a few aspects of scattering amplitudes in general, with the goal of providing a smooth transition from a basic knowledge of QFT to the recent developments in the computation of scattering amplitudes presented in the next chapters. In this regard, I wish to point out the very useful textbooks [4, 5], which give a pedagogical and modern discussion of scattering amplitudes.

Since scattering amplitudes are the main character of this play, I feel like I should at least define them properly. This I do in Sect. 2.1, where I also discuss how these seemingly abstract mathematical constructs are related to actual scattering experiments. The interest in scattering amplitudes is however not solely due to their role in phenomenology. In Sect. 2.2 I motivate a more "pure" and formal study of scattering amplitudes in themselves, even in theories which have no pretence of describing the universe we live in. In doing so, I touch upon some of the inspiring ideas stemmed from the study of scattering amplitudes in the last few years, with the main intent of intriguing the reader and giving references. Then I move on to what is perhaps the most prominent and (at first) disconcerting feature of scattering amplitudes beyond the tree level, namely that they diverge. In Sect. 2.3 I discuss the origin of these divergences along with their underlying physical principles, how they are dealt with, and how they actually make sense and do not affect the theoretical predictions for physical observables. Once we have made peace with their divergent nature, I discuss the analytic structure of generic scattering amplitudes viewed as functions of the external

S. Zoia, *Modern Analytic Methods for Computing Scattering Amplitudes*, Springer Theses,
https://doi.org/10.1007/978-3-031-01945-6_2

momenta. Section 2.4 is devoted to their most important analytic features, namely where they blow up (the poles) and where they are discontinuous (the branch cuts). As we will see, these properties are deeply connected to fundamental postulates of quantum mechanics: locality and unitarity.

2.1 Scattering Amplitudes and the *Phenomenon*

In this section I define what scattering amplitudes are, and discuss briefly where they stand in the scientific process of understanding the laws of Nature. The rest of this thesis will be much more "theory oriented". Chapter 3 is about the mathematics of loop integrals, and most of the applications discussed in Chap. 4 deal with supersymmetric theories. It is however good to remember one's ties to reality from time to time. That is the purpose of this section.

Our goal is to understand the laws of nature. Having no direct access to things in themselves, the *noumenon*, we can only pursue this objective by looking at the *phenomenon*, namely how things appear to us as observers [6]. The keystone in the scientific approach to this problem is the possibility of falsifying a theoretical model of the noumenon by comparing quantitative predictions based on it against the data measured in an experiment. In order to proceed with this programme, we first need to understand what can actually be measured experimentally.

The typical particle-physics experiment is particle collision. Consider a bunch of N_a particles of type a colliding against a bunch of N_b particles of type b. If no black hole is created and swallows up the Earth [7], we expect the number of observed scattering events of a desired kind, say the detection of a certain final state c, to be proportional to the numbers of incoming particles N_a and N_b, and to the transverse area A common to the two bunches. The coefficient of proportionality defines the *total cross section* σ for the production of c from the collision of a and b,

$$\sigma = \frac{\text{Number of events}}{N_a N_b A} \,. \tag{2.1}$$

This simple formula (refined to take into account all the subtleties of a real-life experiment) has taken us very far. In fact, we can do much more than just counting the total number of events. We can count how many times an outgoing particle falls in a certain bin of energy, scattering angle, transverse momentum... leading to the definition of a differential cross section $d\sigma$. This is what our experimentalist friends give us. How do we, theorists, make contact with that? This is where scattering amplitudes enter the game.

In order to define what a scattering amplitude is, we need to refresh our quantum mechanics. I adopt the *interaction picture*. We split the Hamiltonian of the theory H into a free-field part H_0, and an interaction part V,

$$H = H_0 + V \,. \tag{2.2}$$

The operators behave as free-field operators, while the states evolve with the time-evolution operator associated with the interacting part of the Hamiltonian,

$$U(t, t_0) = \mathbb{T} \exp\left(-i \int_{t_0}^{t} dt' V_I(t')\right) , \tag{2.3}$$

where $\mathbb{T}$ is Dyson's time-ordering operator, and

$$V_I(t) = e^{i H_0 (t - t_0)} V(t_0) e^{-i H_0 (t - t_0)} \tag{2.4}$$

is the interacting part of the Hamiltonian, evolving freely—as prescribed by the interaction picture—from an arbitrary reference time t_0. From the theoretical point of view, the scattering process is idealised as follows. The initial state $|p_a, p_b; T_i\rangle$[1] is made of two freely-evolving wave-packets constructed at the asymptotically past time $T_i \to -\infty$, concentrated about the definite momenta p_a and p_b, respectively. The interaction is assumed to take place during a finite time interval, so that in the asymptotically far future, $T_f \to \infty$, the final state $\langle p_1, \ldots, p_n; T_f|$ again consists of n non-interacting wave-packets, each concentrated about a momentum p_i. The initial state evolves from T_i to T_f with the time-evolution operator U given by Eq. (2.3). The overlap between the two states defines the *S matrix* elements,

$$\langle p_1, \ldots, p_n | S | p_a, p_b \rangle := \lim_{T_i \to -\infty} \lim_{T_f \to \infty} \langle p_1, \ldots, p_n; T_f | U(T_f, T_i) | p_a, p_b; T_i \rangle \,. \tag{2.5}$$

The S matrix therefore is a unitary operator which encodes the probability amplitude that a given asymptotic state will evolve into some other state in the distant future. Even if the theory is interacting, there is always some probability that the colliding particles miss one another and do not interact at all. This implies that the S matrix has a term which is simply the identity. This is not particularly interesting, and we isolate the part which is due to interactions as

$$S = \mathbb{1} + i T \,. \tag{2.6}$$

Finally, we can define the *scattering amplitude* $\mathcal{A}$ for this process,

$$\langle p_1, \ldots, p_n | i T | p_a, p_b \rangle = (2\pi)^4 \delta^{(4)} \left(p_a + p_b - \sum_{i=1}^{n} p_i \right) i\mathcal{A}\,(p_a, p_b \to p_1, \ldots, p_n) \,, \tag{2.7}$$

[1] Of course the particle states can be labelled by other quantum numbers in general. I will keep the notation minimal, as the generalisation is straightforward.

where we factored out the overall momentum-conservation δ function. The scattering amplitude for any given process can be computed in perturbation theory using Feynman diagrams and Feynman rules. I assume the readers have some familiarity with this.

The absolute square of a scattering amplitude gives the probability that the initial state will evolve to the desired final state. It must be proportional to the cross section. The precise relation is given by

$$d\sigma = \frac{d\Phi_n}{\phi} |\mathcal{A}|^2 (2\pi)^4 \delta^{(4)} \left(p_a + p_b - \sum_{i=1}^{n} p_i \right) , \tag{2.8}$$

where $d\Phi_n$ is the volume element of the n-body phase space,

$$d\Phi_n = \prod_{i=1}^{n} \frac{d^3 p_i}{(2\pi)^3} \frac{1}{2E_i} , \tag{2.9}$$

and ϕ is a flux factor,

$$\phi = 2E_a 2E_b |v_a - v_b| , \tag{2.10}$$

with $|v_a - v_b|$ being the relative velocity of the beams as seen from the laboratory frame. Scattering amplitudes therefore offer a very concrete point of contact between theory and experiments.

Things get slightly more complicated when the scattering particles are bound states, rather than elementary fields. This is the case of QCD. The elementary fields are quarks and gluons but, because of colour confinement, we can only observe hadrons, i.e. colour-neutral composite states of quarks and gluons. In order to describe quantitatively the scattering of composite objects, therefore, one needs to supply some information about their structure in terms of elementary particles. Unfortunately, from the point of view of the elementary particles, this structure is a long distance effect. QCD is an asymptotically free theory, meaning that the coupling constant becomes weaker and weaker at high energy or, equivalently, at small distances. At large distances or low energies (roughly below the scale $\Lambda_{\text{QCD}} \sim 1$ GeV), the coupling becomes too large for a perturbative approach to be legitimate. The hadron states therefore cannot be described perturbatively.

As you might guess, it is not yet game over. Long and short distance effects do not talk to each other (up to power-suppressed terms), roughly speaking because they take place at such different scales. They can thus be disentangled, and the parton model [8] tells us how. Consider the scattering of two hadrons h_a and h_b, with momenta p_a and p_b, and center-of-mass energy $s = (p_a + p_b)^2$. We want to detect a certain final state X. The differential cross section of this process is given by the following convolution:

$$d\sigma_{h_a h_b \to X} = \sum_{i,j} \int_0^1 dx_1 dx_2 f_i^{(h_a)}(x_1, \mu_F^2) f_j^{(h_b)}(x_2, \mu_F^2) d\hat{\sigma}_{ij\to X} + \mathcal{O}\left(\frac{\Lambda_{\text{QCD}}}{s}\right). \tag{2.11}$$

The non-perturbative information about the structure of the hadron h is encoded in the Parton Distribution Function (PDF) $f_i^{(h)}(x, \mu_F^2)$. Roughly speaking, it gives the probability of finding a parton i (either a quark or a gluon) in h carrying a fraction x of the momentum of h. The PDFs are non-perturbative and, as such, they need to be extrapolated from experimental data. On the other hand, since the structure of the hadrons does not depend on the specific process under consideration, the PDFs are universal. In other words, we can determine them by measuring a set of particularly suitable processes, and then use them to make predictions about any other process. The PDFs are "renormalised" in order to absorb the divergent contributions from the emission of soft and collinear partons in the initial state (more about this in Sect. 2.3.3). This introduces the factorisation scale μ_F. The evolution of the PDFs with μ_F is governed by the DGLAP equations [9–11]. The perturbative information about the high-energy (often referred to as "hard") part interaction is instead encoded in the *partonic cross-section* $\hat{\sigma}_{ij\to X}$, i.e. the cross-section for the production of the desired final state X from the interaction of two partons i and j, carrying momenta $x_i p_a$ and $x_j p_b$, respectively. I stress that the interference between long and short-distance effects is power-suppressed by the energy scale Λ_{QCD} below which the QCD coupling becomes non-perturbative, but it is not zero. Eventually, as the experimental accuracy keeps increasing, it will become relevant.

The complications are not yet over. The final state of the hard interaction is in fact a collection of elementary particles. Quarks or gluons cannot be detected individually. Further non-perturbative information has thus to be supplied, describing the evolution of the final state of the hard interaction into physical states that can be detected in an actual collider experiment. The final state evolution is a combination of several ingredients: how the final-state partons radiate further partons (parton showers), how they combine into hadrons (hadronisation), and how the hadrons collimate into jets (jet algorithms). Similarly to the PDFs, these final-state ingredients are universal, and can usually be implemented in a process-independent way.

Each and every ingredient of this complicated recipe is crucial in order to produce a meaningful theoretical prediction that can be compared against the experimental data. In this picture, the scattering amplitude of the hard process is the main process-dependent and perturbative part. Increasing the accuracy of a theoretical prediction requires a joint effort to improve the entire theoretical description of the scattering process. From the point of view of scattering amplitudes, this means increasing the perturbative order. One should however keep in mind all the other steps that take from the elegant analytic expression of a scattering amplitude to the plots with error bands being compared against the experimental data. The impact of adding one more loop order to a partonic scattering amplitude might in fact be negligible if, say, the final-state evolution is described at a lower accuracy. A close cooperation

between physicists working on the different aspects of theoretical predictions, and experimentalists, is fundamental.

There is one last comment I would like to make about the role of scattering amplitudes in the theoretical description of the universe. Our current understanding of fundamental physics is broken into two theories: quantum mechanics and general relativity. Scattering amplitudes were "born" in the former context and that is where they have been conventionally used, but recently they have started playing an increasingly important role in the latter as well. In 2016 the LIGO and Virgo collaboration detected the first gravitational wave signal, coming from a binary black hole merger [12]. This spectacular achievement heralded the dawn of a new exciting era for astronomy and physics in general. Several other gravitational-wave signals have been observed ever since, and the detectors will become increasingly sensitive in the future. There is therefore urgency to produce accurate theoretical predictions to interpret the data. In a somewhat surprising twist of events, it is possible to compute perturbative contributions of classical General Relativity using the loop expansion of QFT. The amplitude techniques developed over the last decades for particle physics can now be put at the service of gravitational-wave physics as well. I refer the interested reader e.g. to Ref. [13] for an outline of this exciting program, and Ref. [14] for a recent review. This very exciting avenue calls for an even more invigorated effort to improve the technology to compute scattering amplitudes.

2.2 Scattering Amplitudes and the *Noumenon*

After such a "pheno-oriented" section, I feel like I should stress that computing theoretical predictions for collider or gravitational-wave physics is not at all the only reason of interest for scattering amplitudes. Their privileged position as bridge between theory and experiments makes them invaluable for phenomenology, but this direct computational access to the underlying theory is extremely precious in itself, even when the considered theory has no pretence of describing Nature. In a sense, scattering amplitudes give us an insight in the noumenon—the thing in itself—of quantum field theory, even without any reference to the phenomenon. In other words, the analytic computation of scattering amplitudes may allow us to discover properties of the underlying quantum field theory that are not visible in the traditional Lagrangian formulation. In this view, since computing multi-loop and multi-particle scattering amplitudes remains a formidable problem, it is useful to look at theories which are simpler than the Standard Model.

The best playground for "amplitudeologists" is $\mathcal{N} = 4$ super Yang-Mills theory.[2] Its elegance and simplicity makes it easier to spot patterns. It is the perfect testing ground for new techniques and ideas. Indeed, the study of scattering amplitudes in this theory has brought about many conceptual and technical advances, which have

[2] I refer the readers to the textbooks [4, 5] for an introduction to $\mathcal{N} = 4$ super Yang-Mills theory in the context of scattering amplitudes.

boosted the computation of quantities of phenomenological interest as well (see Ref. [15] for a recent review). My thesis fits in perfectly in this story. We begin by computing analytically the $\mathcal{N} = 4$ super Yang-Mills amplitude, and then gradually increase the complexity, passing through $\mathcal{N} = 8$ supergravity and finally arriving at Yang-Mills theory (with no supersymmetry), the core of the Standard Model. In doing so, we make use of several ideas and techniques that stemmed from $\mathcal{N} = 4$ super Yang-Mills theory.

The analytic computation of scattering amplitudes has revealed many remarkable properties of quantum field theory. We will encounter some of them later on in this thesis, but I will make a few examples here, in the hope of convincing those readers who are more interested in the fundamental aspects of quantum field theory rather than in phenomenology to continue further.

Dual (super)conformal symmetry is a hidden symmetry of planar $\mathcal{N} = 4$ super Yang-Mills theory. By "hidden" I mean that it is nowhere to be seen in the Lagrangian. Nonetheless, it emerges spectacularly at the level of the scattering amplitudes, imposing very tight constraints on their analytic structure [16–20]. Dual conformal symmetry was instrumental for many developments in planar $\mathcal{N} = 4$ super Yang-Mills theory, but its importance goes beyond that theory and the planar limit. For instance, certain non-planar Feynman integrals,[3] in generic quantum field theories, were only recently discovered to be invariant under a subset of dual conformal transformations [21–23].

Another fundamental property of quantum field theory which cannot be appreciated in the Lagrangian is the factorisation of the infrared singularities [24–29]. Scattering amplitudes in quantum field theories involving massless particles are affected by singularities which arise from the infrared regions of loop integration. Remarkably, these singularities factorise and the operator which captures them satisfies renormalisation group evolution equations, whose solution can be written down in closed form. The treatment of infrared singularities is of crucial importance in the computation of scattering amplitudes, and is therefore treated in some detail in this thesis, starting from Sect. 2.3.3.

A fascinating relation between gauge and gravity theories stems from the so-called colour/kinematics duality of scattering amplitudes [30, 31] (see Ref. [32] for a recent review). To understand this, consider a scattering amplitude in a gauge theory written as a sum of Feynman diagrams. The analytic expression of each diagram can be factored in a kinematic factor and a colour one. The colour factors obey algebraic relations such as Jacobi and commutation identities. Remarkably, it is possible to rearrange the scattering amplitudes so that the kinematic factors obey the same algebraic relations as the corresponding colour factors. Once the amplitudes are in this form—dubbed the Bern, Carrasco and Johansson (BCJ) form—replacing the colour factors with kinematic ones produces scattering amplitudes in a gravity theory. Which gravity theory depends on which gauge theories we take the kinematic factors from. In this sense, we may say that gravity is a double-copy of gauge theories. In Sect. 4.3, for instance, we will see how the two-loop five-particle amplitude in

[3] The difference between Feynman integrals and Feynman diagrams is clarified in Sect. 3.1.1.

$\mathcal{N} = 8$ supergravity is obtained through a double-copy of its $\mathcal{N} = 4$ super Yang-Mills counterpart. Although formal proofs of this construction are so far limited to tree level, there is solid evidence that it holds for a variety of theories also at loop level.

The rising role of mathematical structures in our understanding of quantum field theories is also driven by the study of scattering amplitudes. Some of them will play a lead role in this thesis: the notions of leading singularities, d log forms, and transcendental weight—to mention the most relevant here, but this is just the tip of an ever growing iceberg. A rich variety of unexpected geometric constructions have been discovered in scattering amplitudes. The best known instance is perhaps the "amplituhedron" [33], a Grassmannian generalisation of polygons and polytopes whose geometry captures the scattering amplitudes in planar $\mathcal{N} = 4$ super Yang-Mills. In this formulation there is no reference to space-time or Hilbert space, and the fundamental properties of locality and unitarity emerge as consequences of the geometry. The amplituhedron is just the first of several fascinating constructions which reformulate scattering amplitudes in terms of geometry (see e.g. [34] for a recent review).

Another mathematical concept for which there is growing interesting in the context of scattering amplitudes is that of cluster algebras [35–38]. For example, it is well known that the branch-cut structure of scattering amplitudes is constrained by physical constraints called Steinmann relations [39, 40]. In planar $\mathcal{N} = 4$ super Yang-Mills theory, the Steinmann relations have been found to be a special case of a cluster algebra property called cluster adjacency [41–43], which puts even tighter constraints on scattering amplitudes. This enabled to bootstrap—i.e. to fix from first principles—certain amplitudes to astonishing loop orders [44, 45] (see Ref. [46] for a review). On the whole, there is mounting evidence that cluster algebras play an important role for scattering amplitudes both at the level of the loop "integrand" [47]—i.e. prior to carrying out the loop integration—and for the special function which arise upon loop integration [48].

Determining which special functions are allowed to appear in scattering amplitudes in general is still an open problem, and a very inspiring one. It has led to a fruitful interplay between physicists and mathematicians from which both the disciplines are profiting enormously. As we will see in Sect. 2.4.2, unitarity implies that scattering amplitudes must have discontinuities. They must thus contain special functions with a non-trivial branch-cut structure, such as the logarithm. In Sect. 3.3 I will talk profusely about the multiple polylogarithms, a class of functions that covers most of the scattering amplitudes computed so far, but there is much more. Elliptic multiple polylogarithms [49–55], and iterated integrals of 1-forms defined on even more complicated geometries—e.g. hyperelliptic curves [56, 57] and Calabi-Yau geometries [58–62]—become relevant as we look to higher numbers of loops and variables.

The special functions appearing in scattering amplitudes have extremely rich algebraic structures. The multiple polylogarithms, in particular, are endowed with a Hopf algebra coaction [63–66], of which we will encounter the maximal iteration, called the symbol [67] (see Sect. 3.3.6). Some of these structures emerge also at the

level of the loop integrals. We now know that one-loop Feynman integrals can also be endowed with a coaction [68, 69], which encodes their analytic properties [70, 71]. While a higher-loop generalisation is under study [72], the idea of a "coaction principle" [73–75] has already been used to bootstrap certain amplitudes [76, 77]. Another branch of mathematics that has recently started playing a role is that of intersection theory [78–80], where Feynman integrals are thought of as elements of a vector space over which it is possible to define a notion of "scalar product."

This list could be made almost arbitrarily long and I am probably doing wrong to many by cutting it here. I make amends by inviting the interested reader to have a look at the talks of the last "Amplitudes" conference [81] to get a sense of how many exciting research directions are being explored in this field.

2.3 Loop Scattering Amplitudes

In Sects. 2.1 and 2.2 I have stressed the importance of scattering amplitudes from both a phenomenological and a theoretical point of view. Whether we aim at computing theoretical predictions or at unveiling a new geometrical principle underlying quantum field theory, restricting ourselves to tree-level amplitudes only is unacceptable. The main difference of loop amplitudes with respect to their tree-level counterparts is the appearance of Feynman integrals. The entire Chap. 3 is devoted to the computation of the latter. In preparation for that, I now want to talk about what is perhaps their most uncomfortable feature for a beginner in this field: the Feynman integrals, as they come out of the Feynman rules, may not converge. Scattering amplitudes are therefore typically divergent at loop level, a rather awkward feature for an object which encodes the probability distribution of a physical particle scattering experiment. In this section I discuss how these divergences can be regularised by analytically continuing the space-time to a generic number of dimensions. I distinguish two regions—ultraviolet and infrared—where the loop integration may not converge, and touch upon the deeper physical reason behind the appearance of such divergences. Finally, I outline briefly how the physically-relevant cross-sections manage to be finite, and preserve the physical interpretation I presented in Sect. 2.1.

2.3.1 Dimensional Regularisation

Quantum field theories are defined in some integer number of space-time dimensions d_0. For the Standard Model $d_0 = 4$, but it is sometimes interesting to study theories in other dimensions. We regularise the loop integrations by analytically continuing the number of space-time dimensions from d_0 to $d = d_0 - 2\epsilon$, and use the parameter ϵ as a regulator [82]. The loop integration measure is modified as

$$\int \prod_{i=1}^{\ell} \frac{d^{d_0}k_i}{(2\pi)^{d_0}} \longrightarrow (\mu^2)^{\ell\epsilon} \int \prod_{i=1}^{\ell} \frac{d^{d}k_i}{(2\pi)^{d}} \,, \tag{2.12}$$

where μ is an arbitrary mass scale which we need to introduce in order to preserve the dimensionality of the coupling constants. Scattering amplitudes and Feynman integrals are then computed as Laurent series around $\epsilon = 0$, and the loop-integration divergences show up as poles in ϵ. The Laurent series is typically truncated to the finite term, of order ϵ^0, or to some low power of ϵ. In Sect. 4.3.4 we will see explicitly one reason why the first few orders in ϵ may sometimes be needed.

Dimensional regularisation is particularly convenient because it preserves gauge and Lorentz invariance, and allows us to regularise at the same time both ultraviolet and infrared divergences. As we will see in the next sections, the ultraviolet divergences are regularised by assuming that $\epsilon > 0$, whereas $\epsilon < 0$ regularises the infrared ones. In practice, we can keep ϵ generic and regularise both simultaneously.

Dimensional regularisation however has drawbacks as well. For instance, it fails to regularise chiral theories consistently [83–88]. The source of contradictions is the Dirac matrix γ_5. The latter is defined in $d = 4$ dimensions as

$$\gamma_5 = \frac{i}{4!}\epsilon_{\mu_1\mu_2\mu_3\mu_4}\gamma^{\mu_1}\gamma^{\mu_2}\gamma^{\mu_3}\gamma^{\mu_4} \,. \tag{2.13}$$

Its continuation to generic d dimensions is however not uniquely defined. One could assume that Eq. (2.13) holds as-is also in d dimensions, but this would result in a breakdown of all Ward identities relying on $\{\gamma_5, \gamma^\mu\} = 0$. Dimensional regularisation can still be used in such cases, but some manual intervention may be required. The theories considered in this thesis are not affected by this problem.

Similarly, it is not uniquely defined how to continue the Dirac algebra to d dimensions. Several variants have been proposed, which share the continuation of the loop momenta to d dimensions, but differ in how the external states and the spin degrees of freedom are handled. I list here the most popular. In the original dimensional regularisation scheme, known as the "'t Hooft-Veltman" (HV) scheme [82], the external states are treated as d_0-dimensional, while the internal states are in d dimensions. In the "conventional dimensional regularisation" (CDR) scheme [89], all states are treated in d dimensions. In the "four-dimensional helicity" (FDH) scheme [90, 91], instead, only the internal momenta are d-dimensional, whereas the external states and the internal polarisation vectors are to be treated in d_0 dimensions. This is particularly convenient for the unitarity-based approaches, where the loop amplitudes are constructed by "gluing" together tree-level ones (more about unitarity in Sect. 2.4.2). It is therefore useful that both the internal and the external states have the same spin degrees of freedom. Furthermore, the FDH scheme preserves supersymmetry. I will therefore adopt the FDH scheme in the supersymmetric applications discussed in Sect. 4.3. In the Yang-Mills computation presented in Sect. 4.5, instead, I will not commit to any specific scheme, and keep the spin-dimension of the internal gluon generic.

In the next two sections I will show how divergences in the loop integration may arise from two distinct regions, the ultraviolet and the infrared, and how both are regularised by dimensional regularisation.

2.3.2 Ultraviolet Divergences and Renormalisation

Ultraviolet (UV) divergences arise when the integration does not converge in the large loop momentum region. Consider a generic one-loop integral with p propagators (which we assume to be quadratic) and a generic numerator N. At large loop-momentum k, it behaves as

$$\int d^d k \frac{N(k)}{(k^2)^p} \sim \int d|k| \, |k|^{d+r-1-2p} \,, \tag{2.14}$$

where r, also known as rank, counts the powers of loop momentum k in the numerator N. If $d + r - 2p \geq 0$, the integration does not converge and the integral exhibits a UV divergence. This combination of numerator rank and number of propagators takes the name of (superficial) degree of divergence,

$$\omega = d + r - 2p \,. \tag{2.15}$$

If $\omega = 0, 1, 2, \ldots$ the integral is logarithmically, linearly, quadratically... divergent in the UV region. If it is negative, the integral is UV finite. The multi-loop generalisation is almost straightforward. In order to ensure a complete absence of UV divergences, one must check the convergence in all the possible regions where the loop momenta become large. In other words, we need to check the power-counting for every subgraph. Note that this counting does not take into account potential cancellations of terms. These may reduce—never increase—the degree of divergence. That is the reason for the attribute "superficial" to this degree of divergence.

Dimensional regularisation is sensitive only to logarithmic divergences, which manifest themselves as poles in the regulator ϵ. Power-like divergences instead vanish (I will discuss this in Sect. 3.1.1). Clearly, an integral with degree of divergence $\omega = 0$ in d_0 dimensions has $\omega = -2\epsilon$ in $d = d_0 - 2\epsilon$ dimensions. UV divergences are therefore regulated by assuming that $\epsilon > 0$, so that the degree of divergence is negative.

The Standard Model and the theories considered in this thesis are renormalisable. This means that the UV divergences can be absorbed in a re-definition of the Lagrangian parameters: fields, coupling constants and masses. I expect that, if you are reading this thesis, you have already encountered this procedure called *renormalisation*. Still, I find a quick refresher always useful. Consider the coupling constant. There is a distinction between the "bare" coupling constant that appears in the Lagrangian, and the "physical" coupling constant. Of course we need to define what we mean by "physical" coupling constant, e.g. by relating it to some measured

quantity, which is definitely not divergent. We can compute this quantity in terms of the bare parameters up to a certain order in perturbation theory, this way relating the physical to the bare coupling constant. The relation may contain UV divergences, but the physical coupling constant is by definition finite. We can then use this relation to substitute the bare with the physical, renormalised coupling constant in any other computation. In this way we absorb the UV divergences in the definition of an unobservable quantity—the bare coupling—in terms of a finite and observable one—the renormalised coupling. Doing this for all the parameters of the Lagrangian removes the UV divergences altogether (provided that the theory can be renormalised). The renormalised quantities are defined at a specific value μ_R of the mass scale μ introduced by dimensional regularisation. This renormalisation scale is unphysical, and physical quantities do not depend on it. This translates into renormalisation group equations, which govern the evolution of the renormalised parameters with respect to the renormalisation scale. In Sect. 4.5 I will discuss in some detail the renormalisation of Yang-Mills theory. I refer to the standard QFT textbooks (e.g. [1, 89]) for a thorough discussion.

In summary, the UV divergences are just an artefact of computing the S-matrix elements using unphysical fields and in terms of unphysical (bare) parameters. Computing the S-matrix elements with physical—i.e. renormalised—fields in terms of physical parameters removes the UV divergences.

2.3.3 Infrared Divergences

Whenever the scattering process involves massless particles, the loop integral may develop IR divergences, stemming from regions of the loop integration where sufficiently many propagators go on shell simultaneously. This may occur when the loop momentum becomes soft, or when it becomes collinear to the momentum of an external massless particle. In the next subsections I discuss these two mechanisms separately, and then show how IR divergences cancel out in any "legitimate" physical observable.

Soft divergences

The loop momentum k is said to become *soft* when all its components become small, $k^\mu \to 0$. A toy example to understand this is given by the scalar loop diagram shown in Fig. 2.1. The particles are massless and the external momenta p_1 and p_2 are on shell, $p_i^2 = 0$. The integrand has the form

$$\int \frac{d^d k}{(2\pi)^d} \frac{F(k)}{(k-p_1)^2 k^2 (k+p_2)^2} \,, \tag{2.16}$$

where I have made explicit only the part that is relevant in the soft region, and F denotes the rest of the diagram. We rescale the loop momentum as

$$k^\mu = \lambda \hat{k}^\mu \,. \tag{2.17}$$

The soft region then corresponds to the small-λ region, while $\hat{k}^\mu$ is kept fixed. The propagators scale as

$$k^2 \sim \lambda^2 \,, \qquad (k - p_1)^2 \sim \lambda \,, \qquad (k + p_2)^2 \sim \lambda \,, \tag{2.18}$$

so that the relevant part of the integrand scales as

$$\frac{d^d k}{(k - p_1)^2 k^2 (k + p_2)^2} \sim \frac{d\lambda}{\lambda} \lambda^{d-4} \,. \tag{2.19}$$

Assuming that the rest of the diagram stays finite in the soft region, the integral has a clear logarithmic divergence if $d = 4$. In dimensional regularisation around four dimensions, $d = 4 - 2\epsilon$, the integration converges for $\epsilon < 0$, and produces a pole $1/\epsilon$. The integration instead converges in six dimensions. As we will see, the same is true also in the collinear region. It is therefore sometimes interesting to look at Feynman integrals in six dimensions, as they are free of IR divergences.

Collinear divergences

Collinear divergences may instead occur when the loop momentum becomes collinear to the on-shell momentum of an external massless particle. Let us consider once again the diagram shown in Fig. 2.1, and let us study the region of the loop integration where the loop momentum k becomes collinear to the external momentum p_1. It is convenient to parameterise the loop momentum as

$$k^\mu = \alpha_1 p_1^\mu + \alpha_2 p_2^\mu + k_\perp^\mu \,, \tag{2.20}$$

such that

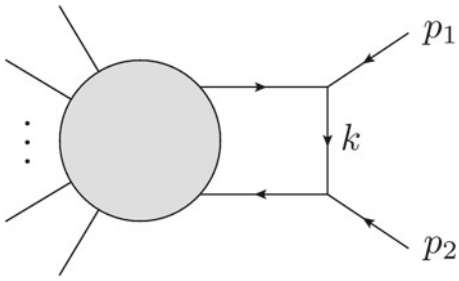

Fig. 2.1 Example of loop Feynman diagram to illustrate the origin of IR divergences. The arrows denote momentum flow

$$k_\perp \cdot p_1 = 0 = k_\perp \cdot p_2 \,. \tag{2.21}$$

We control the collinear limit with a parameter, ρ, such that the collinear region $k \parallel p_1$ corresponds to $\rho = 0$. The new integration variables $\left(\alpha_1, \alpha_2, k_\perp^\mu\right)$ scale as

$$\alpha_1 \sim \mathcal{O}(1)\,, \qquad \alpha_2 \sim \mathcal{O}(\rho^2)\,, \qquad k_\perp^\mu \sim \mathcal{O}(\rho)\,. \tag{2.22}$$

In the small ρ region the relevant part of the integrand behaves as

$$\frac{d^d k}{(k-p_1)^2 k^2 (k+p_2)^2} \sim \frac{d\rho}{\rho}\rho^{d-4}\,. \tag{2.23}$$

The same considerations we have made for the soft limit hold here as well. The integral diverges logarithmically in $d = 4$, and is regulated by analytically continuing to $d = 4 - 2\epsilon$ dimensions with $\epsilon < 0$. In $d = 6$, instead, the integral converges in the collinear region. It is important to stress that, in order to assess the presence of collinear singularities in a loop integral, one should check systematically *all* the regions where one or more loop momenta become collinear to some of the external momenta.

Factorisation of the infrared divergences

In the previous sections we have seen that the IR divergences in loop scattering amplitudes arise from the soft and collinear regions of the loop integration. In general, soft and collinear divergences may occur simultaneously. In this thesis we will be concerned with massless gauge and gravity theories in $d = 4 - 2\epsilon$. The leading IR pole in a ℓ-loop amplitude or integral in $d = 4 - 2\epsilon$ is typically of order $1/\epsilon^{2\ell}$. Remarkably, the IR divergences of a renormalised scattering amplitude $\mathcal{A}$ factorise, schematically as

$$\mathcal{A}\left(\frac{p_i \cdot p_j}{\mu_R^2}, g(\mu_R^2), \epsilon\right) = \mathcal{Z}\left(\frac{p_i \cdot p_j}{\mu_F^2}, g(\mu_F^2), \epsilon\right) \mathcal{A}_f\left(\frac{p_i \cdot p_j}{\mu_R^2}, \frac{\mu_F^2}{\mu_R^2}, g(\mu_R^2), \epsilon\right), \tag{2.24}$$

where $\{p_i\}_{i=1}^n$ are the external momenta, g is the renormalised coupling, μ_R is the renormalisation scale and μ_F is a factorisation scale. Most importantly, $\mathcal{Z}$ is an operator which captures all the IR divergences, i.e. all the $1/\epsilon$ poles, so that $\mathcal{A}_f$ is finite at $\epsilon = 0$. We can thus define a four-dimensional object called hard or remainder function by letting $\epsilon = 0$ in the finite amplitude,

$$\mathcal{H} = \lim_{\epsilon \to 0} \mathcal{A}_f\,. \tag{2.25}$$

The precise form of the IR pole operator $\mathcal{Z}$ depends on the specific theory. In Sects. 4.3.4 and 4.5.2 I discuss in some detail how IR divergences factorise in massless gauge theories and in gravity theories.

Cancellation of the infrared divergences

Just like UV divergences, also the appearance of IR divergences in massless theories is not a "bug," but the manifestation of a deep physical principle. We have seen in Sect. 2.1 that, in order to define a scattering amplitude, one must have a well-defined notion of asymptotic states, which correspond to the scattering particles in the idealised collision. States with a fixed number of massless particles are however not well defined: it is in fact impossible to distinguish between a single particle with a definite light-like momentum p ($p^2 = 0$) from a bunch of particles with collinear momenta which sum up to p, or from the same particle surrounded by a cloud of soft particles. These states are degenerate, and this ambiguity is the source of the IR divergences in the loop integration, as well as of the singularities exhibited by the amplitudes as the external momenta become soft or collinear (see Sect. 2.4.1).

The most common way of dealing with IR divergences is referred to as the *cross-section method* [92, 93]. The basic idea is that the S-matrix elements are not observable quantities, and we can therefore live with the fact that they have IR divergences. What is important is that observable quantities are instead finite. This seemingly innocent statement puts strong constraints on what we can call "observables": they must be *infrared safe*, i.e. they must be insensitive to the addition of soft particles, and to the exchange of a massless particle with momentum p with a bunch of collinear particles whose momenta sum up to p. An example of infrared-safe observable is the cross section for jet production defined by Sterman and Weinberg [94]. This makes very much sense from the experimental point of view: the detectors have a finite energy resolution, and cannot detect a particle with arbitrarily small momentum or distinguish two particles moving in the same direction. What guarantees that this actually works out also from the theoretical point of view is the fundamental theorem by Kinoshita, Lee and Nauenberg (KLN) [95, 96]. In its original formulation, the KLN theorem states that, for any given process, the IR divergences cancel out in the cross section order by order in perturbation theory when summing over all the degenerate initial and final states. The theorem was later gradually revisited and made stronger, so as to prove that a more general class of infrared-safe observables are finite (see e.g. Weinberg's classic textbook [2], and Ref. [97] for recent developments). In practice, the cancellation of IR divergences in physical observables takes place because of a conspiracy between the "virtual" divergences, i.e. those coming from the loop integrations, and the "real-emission" divergences, which instead arise from the phase space integration of squared amplitudes with fewer loops but extra radiation in the final state. This distinction makes it very challenging to rearrange the terms so that they can be integrated numerically.

When considering the scattering of composite objects there is one further subtlety. Consider the (QCD-improved) parton model, which I briefly presented in Sect. 2.1. The initial state of the hard scattering is precisely defined: there is exactly one parton coming from each of the incoming hadrons, and it is not possible to accommodate other degenerate states. This results in un-cancelled collinear divergences, which arise from the radiation of massless partons from the incoming partons taking part in the hard scattering process. The careful readers might recall that I have already

hinted at the solution to this problem in Sect. 2.1 (below Eq. (2.11)). Similarly to renormalisation, the initial state singularities can be absorbed into the "bare" PDFs to obtain the physical ones. The latter depend on an unphysical factorisation scale μ_F, of which the physical observables must be independent. This dictates the evolution of the PDFs according to the DGLAP equations [9–11].

The appearance of IR divergences in the scattering amplitudes therefore does not pose an obstacle for computing physical observables (although it is certainly a complication). From the formal point of view it is however disturbing that the S-matrix is not well defined in presence of massless particles, and the search for more satisfactory formulations is an active area of research. See e.g. Refs. [98, 99] for recent work on this topic.

2.4 Analytic Structure of Scattering Amplitudes

In this section I discuss some of the most salient analytic features of scattering amplitudes viewed as functions of the external momenta, and show how they are related to fundamental physical principles. Once again I want to keep the discussion as general as possible, without specialising to a specific theory. We start in Sect. 2.4.1 with the singularity structure of scattering amplitudes, tightly connected to the postulate of locality. Then, in Sect. 2.4.2 I discuss how the non-trivial branch-cut structure of scattering amplitudes follows from the unitarity of the S matrix. Indeed, it is the dream of many to construct explicit expressions for scattering amplitudes based solely on physical principles and a precise knowledge of their analytic structure. This is a long-standing goal of the so-called "S-matrix program," initiated in the early Sixties [100–102] and recently revived. The interplay between the "old" ideas of the S-matrix program with perturbation theory, especially in $\mathcal{N} = 4$ super Yang-Mills theory, has led to major advances in our understanding of quantum field theory and scattering amplitudes: generalised unitarity [103, 104], the Britto-Cachazo-Feng-Witten recursion relations [105–107], and on-shell diagrams [47], just to name a few. My goal in this thesis is more modest, but a thorough understanding of the analytic structure of scattering amplitudes is at the basis of the techniques presented in Chaps. 3 and 4.

2.4.1 Poles and Locality

The structure of the poles in scattering amplitudes as functions of the external momenta is tightly connected to the fundamental principle of *locality*. Loosely speaking, locality means that an object can be influenced only by its immediate surroundings. More rigorously, locality implies that the Lagrangian density, defined in position space, can only be a function of fields and of their derivatives at a single point in spacetime. In momentum space, this means that the interaction vertices are

either constant or polynomial in the momenta. Only the propagators contribute in the denominator.

At tree level, locality implies that the only poles with non-vanishing residues arise from the propagators of physical particles going on shell, i.e. from the exchanges of physical particles. Tree-level amplitudes therefore may have poles only where the sum of a subset of the momenta of the external particles goes on shell. More explicitly, a n-particle tree-level amplitude with external momenta $p_1, \ldots, p_n$, such that $\sum_{i=1}^{n} p_i = 0$, may only have poles of the form

$$\frac{1}{\left(\sum_{i\in\mathcal{I}} p_i\right)^2 - m^2}\,, \tag{2.26}$$

where $\mathcal{I} \subset \{1, \ldots, n\}$, and m is the mass of any one-particle state of the theory (including the case $m = 0$) which can couple to the external particles with momenta in the subset $\mathcal{I}$. Poles of the form given by Eq. (2.26) are called *multi-particle poles* in the literature. Certain representations of a scattering amplitude or separate parts of an amplitude (e.g. individual Feynman diagrams with obscure field redefinitions or gauge choices) may contain poles of a different form, but they are *spurious*, and the corresponding residues in the complete amplitude must vanish. The residues of the poles associated with the exchange of physical particles instead factorise into lower-point amplitudes, as shown in Fig. 2.2. This can be understood easily from Feynman diagrams: the propagator going on shell splits the Feynman diagrams into two parts, each containing all the Feynman diagrams required to compute a scattering amplitude. The fact that the residues of a tree amplitude at all its poles are products of lower-point amplitudes allows one to set up recursive relations to compute higher-point amplitudes without using Feynman diagrams. The Britto-Cachazo-Feng-Witten (BCFW) on-shell recursion relations [106, 107] are the most notable example of such a technique. I refer the interested readers e.g. to the textbooks [4, 5].

In massive quantum field theories the factorisation on the multi-particle poles represented in Fig. 2.2 can be shown to hold beyond the tree level, non-perturbatively [2]. This is a generalisation of the well known Lehmann-Symanzik-Zimmermann (LSZ) reduction formula [108] for the correlation functions, which corresponds to the special case where only one of the external momenta is put on shell (see e.g. the

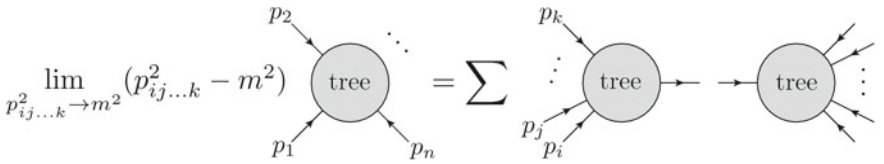

Fig. 2.2 Factorisation of a n-particle tree-level amplitude. The arrows denote momentum flow, $p_{ij\ldots k} = p_i + p_j + \ldots + p_k$, and m is the mass of any one-particle state of the theory (including $m = 0$) that can couple to the states with momenta $p_i, p_j, \ldots, p_k$. The sum runs over all the possible intermediate states

standard textbook [1] for a pedagogical discussion). The mass appearing in this non-perturbative factorisation must be a physical, renormalised mass, not the bare one appearing in the Lagrangian.

As for quantum field theories with massless particles, the standard theory of scattering needs to be modified because the states with a fixed number of massless particles are not well defined. As we have seen in Sect. 2.3.3, this implies the existence of infrared divergences in the S-matrix elements, but does not prevent us from computing physical observables. Generalisations of the LSZ formula to accommodate massless particles as well are being explored (see e.g. Refs. [109, 110] for recent work on this topic). The presence of IR divergences make the factorisation of scattering amplitudes with massless particles substantially more complicated than in the massive case. Even in the case of IR-finite loop amplitudes, the factorisation is made more complicated by the presence of special functions, necessary because of unitarity (see Sect. 2.4.2). Nonetheless, on-shell recursion methods similar to those used at tree-level can be used to compute finite loop amplitudes (see e.g. Refs. [111–113]). The special case where the sum of the momenta of exactly two particles goes on shell is of particular interest. In the massless case, the two external momenta become collinear in the limit, and the universal factorisation of the residue is well understood also at loop level. In Sects. 4.3.5 and 4.5.6 I discuss in some detail the factorisation in the collinear limit of the amplitudes in gauge and gravity theories at two-loop order. Another limit where the amplitudes exhibit a universal factorisation that is understood beyond the tree level is the soft limit, in which one of the momenta of the external particles vanishes. I discuss the factorisation of gravity amplitudes in the soft limit at two-loop order in Sect. 4.3.5.

The complications for loop amplitudes are of course due to the loop integration, which is responsible for the appearance of both special functions and divergences. The problem of integrating—to which Chap. 3 is devoted—is however separate from that of constructing an un-integrated expression for a loop amplitude. We can strip off the integral sign from an ℓ-loop amplitude $\mathcal{A}^{(\ell)}$,

$$\mathcal{A}^{(\ell)}\left(p_1, \ldots, p_n\right) = \int \left(\prod_{i=1}^{\ell} d^d k_i\right) \mathcal{I}^{(\ell)}\left(k_1, \ldots, k_\ell, p_1, \ldots, p_n\right) , \tag{2.27}$$

this way defining a *loop integrand* $\mathcal{I}^{(\ell)}$. Setting aside the issue that such an object is not uniquely defined, the loop integrand is just a rational function. Indeed, its properties are very similar to those of tree-level amplitudes, the only difference being that the topology of the associated Feynman graphs is more general, including also loops. On-shell methods based on the factorisation in terms of lower-point objects can therefore be used to compute the loops integrands, by-passing the Feynman diagrams. Perhaps the most notable result of this approach is the explicit recursive formula for the (four-dimensional) integrands of scattering amplitudes in planar $\mathcal{N} = 4$ super Yang-Mills theory at any loop order [114] (see also Ref. [115]).

As for the integrated amplitudes, it is known that for individual Feynman integrals (whose integrands have only local propagators in the denominator) the loci

where they may potentially be singular are determined by the solution of the *Landau equations* [102, 116, 117] (see also Refs. [118, 119] for some recent work). The latter however offer a necessary condition, not a sufficient one. Moreover, the singularities of the individual Feynman diagrams may cancel out in the complete amplitude, which ultimately is the physical object of interest. In Sect. 4.2.4 I give an interesting example of a non-trivial hypersurface in kinematic space where some of the Feynman integrals are singular, whereas the amplitudes they contribute to are finite. Understanding the singularity structure of the integrated amplitudes remains an important and ambitious goal.

2.4.2 Discontinuities and Unitarity

Another important feature of the analytic structure of scattering amplitudes is the presence of branch cuts. Their appearance follows from a fundamental postulate of quantum mechanics: the *unitarity* of the S matrix,

$$SS^\dagger = \mathbb{1}\,, \tag{2.28}$$

or

$$TT^\dagger = i\left(T^\dagger - T\right)\,, \tag{2.29}$$

in terms of the interacting part of the S matrix. In other words, the probability is conserved in the scattering process. This observation seems innocent, but has far-reaching implications for scattering amplitudes. In order to spell them out, we take the matrix element of both sides of Eq. (2.29) between two generic states $|i\rangle$ and $|f\rangle$, with total momenta p_i and p_f, respectively. Next, we insert in the left-hand side the resolution of the identity in Fock space,

$$\mathbb{1} = \sum_{n\geq 0}\int d\Phi_n |\{n\}\rangle\langle\{n\}|\,, \tag{2.30}$$

where $|\{n\}\rangle$ denotes loosely a n-particle state, with total momentum $p_{\{n\}}$, and $d\Phi_n$ is the n-body phase space defined by Eq. (2.9). Strictly speaking, the sum in Eq. (2.30) runs over the particle species and polarisations as well, but the generalisation is straightforward and I prefer to keep the notation simple. Then, recalling the definition of a scattering amplitude (2.7) and appealing to invariance under time reversal gives

$$2\mathrm{Im}\mathcal{A}_{i\to f} = \sum_{n\geq 0}\int\left(\prod_{i=1}^{n} d\Phi_i\right)(2\pi)^4\delta^{(4)}\left(p_f - p_{\{n\}}\right)\mathcal{A}_{\{n\}\to f}\mathcal{A}^*_{\{n\}\to i}\,, \tag{2.31}$$

where the overall conservation of momentum, $p_i = p_f$, is understood. This result, known as the *optical theorem*, has profound consequences. Let us consider the amplitude $\mathcal{A}_{i\to f}$ as a function of some kinematic variable s, e.g. $s = p_i^2$. For real momenta s is real, but allowing it to take complex values, although unphysical, leads to important insights. Schwarz's reflection principle,

$$\mathcal{A}^*_{i\to f}(s) = \mathcal{A}_{i\to f}(s^*)\,, \tag{2.32}$$

relates the imaginary part of the amplitude to its discontinuity as s crosses the real axis,

$$\underset{s}{\text{Disc}}\mathcal{A}_{i\to f}(s) := \lim_{\delta\to 0^+}\left[\mathcal{A}_{i\to f}(s+i\delta) - \mathcal{A}_{i\to f}(s-i\delta)\right] = 2i\,\text{Im}\mathcal{A}_{i\to f}(s)\,. \tag{2.33}$$

For instance, the discontinuity of a logarithm is given by

$$\underset{s}{\text{Disc}}\log(s) = 2\pi i\,\Theta(-s)\,, \tag{2.34}$$

where Θ is the Heaviside step function. The optical theorem then implies that scattering amplitude have branch points in the thresholds, i.e. where intermediate physical states become kinematically accessible. By convention we take the branch cuts to lie along the real axes.

These discontinuities may be traced back to the regions of the loop integration where some virtual particles go on shell. The only source of non-vanishing imaginary parts in a Feynman integral (for real kinematics) is the Feynman "$+i0^+$" prescription in the propagators,

$$\frac{1}{k^2 - m^2 + i0^+}\,, \tag{2.35}$$

where 0^+ is an infinitesimal positive real number.[4] This prescription becomes relevant only where the momentum flowing in the internal propagator goes on shell, $k^2 = m^2$, and the propagator becomes purely imaginary. This also suggests a way of computing the discontinuities across the branch cuts of a scattering amplitude through an operation called *unitarity cut* [120]. The Sokhotski-Plemelj theorem implies that

$$\lim_{\alpha\to 0^+}\text{Im}\left(\frac{1}{k^2 - m^2 + i\alpha}\right) = -\pi\delta\left(k^2 - m^2\right)\,, \tag{2.36}$$

to be understood in a distributional sense. A more careful derivation shows that causality requires the virtual particles put on shell to have positive energies, so that the δ function on the right-hand side of Eq. (2.36) has to be traded for

[4] The infinitesimal positive real number 0^+ in the Feynman prescription for the propagators is often denoted by ϵ in the literature. I use 0^+ to avoid confusion with the dimensional regulator ϵ.

$$\delta^{(+)}\left(k^2 - m^2\right) = \delta\left(k^2 - m^2\right)\Theta\left(k^0\right) , \tag{2.37}$$

where k^0 is the energy component of k^μ. The discontinuity of an amplitude across a branch cut can then be computed by "cutting," in all the relevant Feynman diagrams, the propagators in a given channel, i.e. by replacing them with δ functions which put the corresponding momenta on shell [120].

The fact that the relation given by Eq. (2.31) is non-linear in the scattering amplitudes grants unitarity an extraordinary predictive power. In order to simplify the notation, let us focus for a moment on a generic theory with trivalent vertices of order g. The n-particle scattering amplitude $\mathcal{A}_n$ can be series-expanded in the coupling constant g as

$$\mathcal{A}_n = g^{n-2} \sum_{\ell \geq 0} g^{2\ell} \mathcal{A}_n^{(\ell)} . \tag{2.38}$$

Substituting this expansion into the optical theorem given by Eq. (2.31), it becomes clear that the discontinuity of the ℓ-loop amplitude is entirely determined by lower-loop information. In particular, tree-level amplitudes have no discontinuity, as expected, whereas the discontinuities of one-loop amplitudes, or equivalently their unitarity cuts, are given by a product of tree-level amplitudes integrated over the remaining internal degrees of freedom. This is graphically represented in Fig. 2.3. The same result can be shown to hold for a generic theory. If the ℓ-loop amplitudes are known, then unitarity gives a strong handle over the $(\ell + 1)$-loop ones. The branch cuts of the integrated amplitude are in fact constrained by unitarity in terms of lower loop information. The unitarity cuts on the other hand relate the branch cut structure of the integrated amplitude to the pole structure of its un-integrated expression, its integrand. We can therefore make a generic ansatz for the integrand of an amplitude, which is just a rational function, and fix the coefficients by analysing different sets of unitarity cuts. This unitarity-based method to construct the amplitude integrands has proven extremely useful, but can be made even more powerful by generalising the concept of unitarity cut. Cutkosky's rules to compute the discontinuity of a one-loop amplitude in a given channel prescribe to cut the two propagators in that channel [120]. Nothing prevents us from cutting more than two propagators.

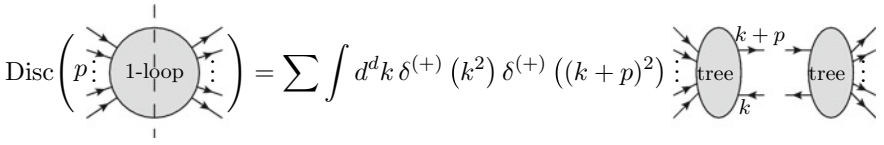

Fig. 2.3 Pictorial representation of the optical theorem for a generic one-loop amplitude in a massless theory. The dashed line denotes that we are computing the discontinuity in the p^2-channel, i.e. across the branch cut along the real p^2 axis. The arrows indicate the momentum flow. The sum runs over all the possible physical on-shell two-particle intermediate states. The constant overall prefactors are omitted

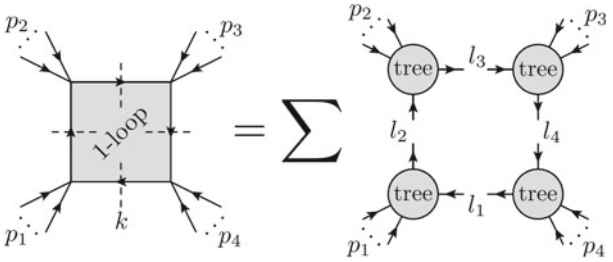

Fig. 2.4 Factorisation of a massless one-loop amplitude on the quadruple cut $l_i^2\big|_{k=k^*} = 0\,, \forall i = 1, \ldots, 4$, with $l_1 = k, l_2 = k + p_1, l_3 = k + p_1 + p_2, l_4 = k - p_4$. The arrows denote momentum flow, and the dashed lines denote the cut propagators. The sum runs over all the possible intermediate states, which carry momenta $\{l_i\}_{i=1}^4$ evaluated in one of the two solutions k^* of the quadruple cut

For instance, at one-loop and treating the loop momentum as four dimensional, we can cut up to four propagators. This quadruple cut localises entirely the internal degrees of freedom, and the result factorises in terms of tree amplitudes, as shown in Fig. 2.4. Strictly speaking, the factorisation of the generalised unitarity cuts in terms of lower-loop amplitudes does not follow directly from unitarity, but can be shown to hold e.g. by analysing the contributing Feynman diagrams [102]. For this reason we talk of *generalised unitarity* [103–105] (see e.g. Refs. [121, 122] for a review). One subtlety of generalised unitarity cuts is that the solution of the cuts is in general complex. If any number of propagators is substituted by δ functions and the loop integration is carried out in Minkowski space $\mathbb{R}^{1,3}$, the result may vanish, because the support of the δ function may be complex. Generalised unitarity cuts should therefore be viewed as the deformation of the integration contour around the poles of the cut propagators, rather than the substitution of the latter with δ functions. In order to understand this point, consider the following toy example:

$$f(z) = \int_{-\infty}^{\infty} dz' f\left(z'\right) \delta\left(z - z'\right)\,, \tag{2.39}$$

$$f(z) = \frac{1}{2\pi i} \oint_{\partial D} dz' \frac{f\left(z'\right)}{z' - z}\,, \tag{2.40}$$

where D is a closed disk around $z \in \mathbb{C}$, and f is holomorphic in D. While Eq. (2.39) works only if $z \in \mathbb{R}$, Cauchy's integral formula (2.40) makes sense for $z \in \mathbb{C}$. Computing generalised unitarity cuts therefore amounts to computing (possibly multivariate) residues. From this point of view, a Feynman integral and its cuts differ only in the integration contour, and it is thus reasonable to expect that they share common properties. Since computing the cuts is easier than computing the original integral, generalised unitarity cuts can be useful to anticipate certain properties of the integrated expressions. In fact, we will see in Sect. 3.6.1 that a further generalisation of the concept of unitarity cut—the leading singularity—plays a central role in the method to compute Feynman integrals presented in the next chapter.

Bibliography

1. Peskin ME, Schroeder DV (1995) An introduction to quantum field theory. Addison-Wesley, Reading, USA
2. Weinberg S (2005) The quantum theory of fields. Vol. 1: foundations, vol 6. Cambridge University Press
3. Srednicki M (2007) Quantum field theory, vol 1. Cambridge University Press
4. Henn JM, Plefka JC (2014) Scattering amplitudes in gauge theories, vol 883. Springer, Berlin. https://doi.org/10.1007/978-3-642-54022-6
5. Elvang H, Huang Y-t (2015) Scattering amplitudes in gauge theory and gravity, vol 4. Cambridge University Press
6. Kant I (1781) Kritik der reinen Vernunft. Johann Friedrich Hartknoch
7. Will CERN generate a black hole? https://home.cern/resources/faqs/will-cern-generate-black-hole
8. Feynman RP (1969) Very high-energy collisions of hadrons. Phys Rev Lett 23: 1415. https://doi.org/10.1103/PhysRevLett.23.1415
9. Dokshitzer YL (1977) Calculation of the structure functions for deep inelastic scattering and e+ e- annihilation by perturbation theory in quantum chromodynamics. Sov Phys JETP 46:641
10. Gribov V, Lipatov L (1972) Deep inelastic ep-scattering in perturbation theory. Sov J Nucl Phys 15:438
11. Altarelli G, Parisi G (1977) Asymptotic freedom in parton language. Nucl Phys B 126:298. https://doi.org/10.1016/0550-3213(77)90384-4
12. LIGO Scientific, Virgo Collaboration (2016) Observation of gravitational waves from a binary black hole merger. Phys Rev Lett 116:061102. https://doi.org/10.1103/PhysRevLett.116.061102. arXiv:1602.03837
13. Bjerrum-Bohr NEJ, Damgaard PH, Festuccia G, Planté L, Vanhove P (2018) General relativity from scattering amplitudes. Phys Rev Lett 121:171601. https://doi.org/10.1103/PhysRevLett.121.171601
14. Levi M. Field theory for gravity at all scales. arXiv:1901.01282
15. Henn JM. What can we learn about QCD and collider physics from $N = 4$ super Yang-Mills? arXiv:2006.00361
16. Drummond JM, Henn J, Smirnov VA, Sokatchev E (2007) Magic identities for conformal four-point integrals. JHEP 01:064. https://doi.org/10.1088/1126-6708/2007/01/064. arXiv:hep-th/0607160
17. Alday LF, Maldacena JM (2007) Gluon scattering amplitudes at strong coupling. JHEP 06:064. https://doi.org/10.1088/1126-6708/2007/06/064. arXiv:0705.0303
18. Drummond J, Henn J, Korchemsky G, Sokatchev E (2010) Dual superconformal symmetry of scattering amplitudes in $N = 4$ super-Yang-Mills theory. Nucl Phys B 828:317. https://doi.org/10.1016/j.nuclphysb.2009.11.022. arXiv:0807.1095
19. Berkovits N, Maldacena J (2008) Fermionic T-duality, dual superconformal symmetry, and the amplitude/Wilson loop connection. JHEP 09:062. https://doi.org/10.1088/1126-6708/2008/09/062. arXiv:0807.3196
20. Drummond JM, Henn JM, Plefka J (2009) Yangian symmetry of scattering amplitudes in $N = 4$ super Yang-Mills theory. JHEP 05:046. https://doi.org/10.1088/1126-6708/2009/05/046. arXiv:0902.2987
21. Bern Z, Enciso M, Ita H, Zeng M (2017) Dual conformal symmetry, integration-by-parts reduction, differential equations and the nonplanar sector. Phys Rev D96:096017. https://doi.org/10.1103/PhysRevD.96.096017. arXiv:1709.06055
22. Bern Z, Enciso M, Shen C-H, Zeng M. Dual conformal structure beyond the planar limit. arXiv:1806.06509
23. Chicherin D, Henn J, Sokatchev E (2018) Implications of nonplanar dual conformal symmetry. JHEP 09:012. https://doi.org/10.1007/JHEP09(2018)012. arXiv:1807.06321
24. van Neerven WL (1986) Infrared behavior of on-shell form-factors in a $N = 4$ supersymmetric Yang-Mills field theory. Z Phys C30:595. https://doi.org/10.1007/BF01571808

25. Korchemsky GP (1994) On near forward high-energy scattering in QCD. Phys Lett B 325:459. https://doi.org/10.1016/0370-2693(94)90040-X. arXiv:hep-ph/9311294
26. Korchemskaya IA, Korchemsky GP (1995) High-energy scattering in QCD and cross singularities of Wilson loops. Nucl Phys B 437:127. https://doi.org/10.1016/0550-3213(94)00553-Q. arXiv:hep-ph/9409446
27. Korchemskaya IA, Korchemsky GP (1996) Evolution equation for gluon Regge trajectory. Phys Lett B 387:346. https://doi.org/10.1016/0370-2693(96)01016-7. arXiv:hep-ph/9607229
28. Bern Z, Dixon LJ, Smirnov VA (2005) Iteration of planar amplitudes in maximally supersymmetric Yang-Mills theory at three loops and beyond. Phys Rev D72:085001. https://doi.org/10.1103/PhysRevD.72.085001. arXiv:hep-th/0505205
29. Almelid O, Duhr C, Gardi E (2016) Three-loop corrections to the soft anomalous dimension in multileg scattering. Phys Rev Lett 117:172002. https://doi.org/10.1103/PhysRevLett.117.172002. arXiv:1507.00047
30. Bern Z, Carrasco J, Johansson H (2008) New relations for gauge-theory amplitudes. Phys Rev D 78:085011. https://doi.org/10.1103/PhysRevD.78.085011. arXiv:0805.3993
31. Bern Z, Carrasco JJM, Johansson H (2010) Perturbative quantum gravity as a double copy of gauge theory. Phys Rev Lett 105:061602. https://doi.org/10.1103/PhysRevLett.105.061602. arXiv:1004.0476
32. Bern Z, Carrasco JJ, Chiodaroli M, Johansson H, Roiban R. The duality between color and kinematics and its applications. arXiv:1909.01358
33. Arkani-Hamed N, Trnka J (2014) The Amplituhedron. JHEP 10:030. https://doi.org/10.1007/JHEP10(2014)030. arXiv:1312.2007
34. Ferro L, Lukowski T. Amplituhedra, and beyond. arXiv:2007.04342
35. Fomin S, Zelevinsky A (2002) Cluster algebras I: foundations. J Am Math Soc 15:497. https://doi.org/10.1090/S0894-0347-01-00385-X. arXiv:math/0104151
36. Fomin S, Zelevinsky A (2003) Cluster algebras II: finite type classification. Invent Math 154:63. https://doi.org/10.1007/s00222-003-0302-y. arXiv:math/0208229
37. Gekhtman M, Shapiro M, Vainshtein A (2003) Cluster algebras and poisson geometry. Mosc Math J 3:899. arXiv:math/0208033
38. Fock VV, Goncharov AB (2009) Cluster ensembles, quantization and the dilogarithm. Ann Sci Éc Norm Supér (4) 42:865. arXiv:math/0311245
39. Steinmann O (1960) Über den Zusammenhang zwischen den Wightmanfunktionen und der-retardierten Kommutatoren. Helv Physica Acta 33:257
40. Steinmann O (1960) Wightman-Funktionen und retardierten Kommutatoren. II Helv Physica Acta 33:347
41. Drummond J, Foster J, Gürdoğan Ö (2018) Cluster adjacency properties of scattering amplitudes in $N = 4$ supersymmetric Yang-Mills theory. Phys Rev Lett 120:161601. https://doi.org/10.1103/PhysRevLett.120.161601. arXiv:1710.10953
42. Drummond J, Foster J, Gürdoğan Ö (2019) Cluster adjacency beyond MHV. JHEP 03:086. https://doi.org/10.1007/JHEP03(2019)086. arXiv:1810.08149
43. Caron-Huot S, Dixon LJ, von Hippel M, McLeod AJ, Papathanasiou G (2018) The double pentaladder integral to all orders. JHEP 07:170. https://doi.org/10.1007/JHEP07(2018)170. arXiv:1806.01361
44. Caron-Huot S, Dixon LJ, McLeod A, von Hippel M (2016) Bootstrapping a five-loop amplitude using Steinmann relations. Phys Rev Lett 117:241601. https://doi.org/10.1103/PhysRevLett.117.241601. arXiv:1609.00669
45. Dixon LJ, Drummond J, Harrington T, McLeod AJ, Papathanasiou G, Spradlin M (2017) Heptagons from the Steinmann cluster bootstrap. JHEP 02:137. https://doi.org/10.1007/JHEP02(2017)137. arXiv:1612.08976
46. Caron-Huot S, Dixon LJ, Drummond JM, Dulat F, Foster J, Gürdoğan O, et al (2020) The Steinmann cluster bootstrap for $N = 4$ super Yang-Mills amplitudes. PoS CORFU2019:003. https://doi.org/10.22323/1.376.0003. arXiv:2005.06735
47. Arkani-Hamed N, Bourjaily JL, Cachazo F, Goncharov AB, Postnikov A, Trnka J (2016) Grassmannian geometry of scattering amplitudes, vol 4. Cambridge University Press. https://doi.org/10.1017/CBO9781316091548. arXiv:1212.5605

48. Golden J, Goncharov AB, Spradlin M, Vergu C, Volovich A (2014) Motivic amplitudes and cluster coordinates. JHEP 01:091. https://doi.org/10.1007/JHEP01(2014)091. arXiv:1305.1617
49. Brown FCS, Levin A (2011) Multiple elliptic polylogarithms
50. Adams L, Bogner C, Weinzierl S (2014) The two-loop sunrise graph in two space-time dimensions with arbitrary masses in terms of elliptic dilogarithms. J Math Phys 55:102301. https://doi.org/10.1063/1.4896563. arXiv:1405.5640
51. Broedel J, Mafra CR, Matthes N, Schlotterer O (2015) Elliptic multiple zeta values and one-loop superstring amplitudes. JHEP 07:112. https://doi.org/10.1007/JHEP07(2015)112. arXiv:1412.5535
52. Broedel J, Duhr C, Dulat F, Tancredi L (2018) Elliptic polylogarithms and iterated integrals on elliptic curves. Part I: general formalism. JHEP 05:093. https://doi.org/10.1007/JHEP05(2018)093. arXiv:1712.07089
53. Broedel J, Duhr C, Dulat F, Tancredi L (2018) Elliptic polylogarithms and iterated integrals on elliptic curves II: an application to the sunrise integral. Phys Rev D 97:116009. https://doi.org/10.1103/PhysRevD.97.116009. arXiv:1712.07095
54. Adams L, Weinzierl S (2018) The ε-form of the differential equations for Feynman integrals in the elliptic case. Phys Lett B 781:270. https://doi.org/10.1016/j.physletb.2018.04.002. arXiv:1802.05020
55. Bogner C, Müller-Stach S, Weinzierl S (2020) The unequal mass sunrise integral expressed through iterated integrals on $\overline{\mathcal{M}}_{1,3}$. Nucl Phys B 954:114991. https://doi.org/10.1016/j.nuclphysb.2020.114991. arXiv:1907.01251
56. Huang R, Zhang Y (2013) On genera of curves from high-loop generalized unitarity cuts. JHEP 04:080. https://doi.org/10.1007/JHEP04(2013)080. arXiv:1302.1023
57. Hauenstein JD, Huang R, Mehta D, Zhang Y (2015) Global structure of curves from generalized unitarity cut of three-loop diagrams. JHEP 02:136. https://doi.org/10.1007/JHEP02(2015)136. arXiv:1408.3355
58. Vanhove P (2019) Feynman integrals, toric geometry and mirror symmetry. In: KMPB conference: elliptic integrals, elliptic functions and modular forms in quantum field theory, pp 415–458. https://doi.org/10.1007/978-3-030-04480-0_17. arXiv:1807.11466
59. Klemm A, Nega C, Safari R (2020) The l-loop banana amplitude from GKZ systems and relative Calabi-Yau periods. JHEP 04:088. https://doi.org/10.1007/JHEP04(2020)088. arXiv:1912.06201
60. Bourjaily JL, He Y-H, Mcleod AJ, Von Hippel M, Wilhelm M (2018) Traintracks through Calabi-Yau manifolds: scattering amplitudes beyond elliptic polylogarithms. Phys Rev Lett 121:071603. https://doi.org/10.1103/PhysRevLett.121.071603. arXiv:1805.09326
61. Bourjaily JL, McLeod AJ, von Hippel M, Wilhelm M (2019) Bounded collection of Feynman integral Calabi-Yau geometries. Phys Rev Lett 122:031601. https://doi.org/10.1103/PhysRevLett.122.031601. arXiv:1810.07689
62. Bourjaily JL, McLeod AJ, Vergu C, Volk M, Von Hippel M, Wilhelm M (2020) Embedding Feynman integral (Calabi-Yau) geometries in weighted projective space. JHEP 01:078. https://doi.org/10.1007/JHEP01(2020)078. arXiv:1910.01534
63. Goncharov AB. Multiple polylogarithms and mixed tate motives. arXiv:math/0103059
64. Brown FCS (2006) Multiple zeta values and periods of moduli spaces $\mathfrak{M}_{0,n}$
65. Duhr C, Gangl H, Rhodes JR (2012) From polygons and symbols to polylogarithmic functions. JHEP 10:075. https://doi.org/10.1007/JHEP10(2012)075. arXiv:1110.0458
66. Duhr C (2012) Hopf algebras, coproducts and symbols: an application to Higgs boson amplitudes. JHEP 08:043. https://doi.org/10.1007/JHEP08(2012)043. arXiv:1203.0454
67. Goncharov AB, Spradlin M, Vergu C, Volovich A (2010) Classical polylogarithms for amplitudes and Wilson loops. Phys Rev Lett 105:151605. https://doi.org/10.1103/PhysRevLett.105.151605. arXiv:1006.5703
68. Goncharov AB (2002) Galois symmetries of fundamental groupoids and noncommutative geometry. arXiv Mathematics e-prints (2002). arXiv:math/0208144
69. Brown F (2015) Notes on motivic periods

70. Abreu S, Britto R, Duhr C, Gardi E (2017) Algebraic structure of cut Feynman integrals and the diagrammatic coaction. Phys Rev Lett 119:051601. https://doi.org/10.1103/PhysRevLett.119.051601. arXiv:1703.05064
71. Abreu S, Britto R, Duhr C, Gardi E (2017) Diagrammatic hopf algebra of cut Feynman integrals: the one-loop case. J High Energy Phys 2017. https://doi.org/10.1007/jhep12(2017)090
72. Abreu S, Britto R, Duhr C, Gardi E, Matthew J (2019) Diagrammatic coaction of two-loop Feynman integrals. In: 14th international symposium on radiative corrections: application of quantum field theory to phenomenology, vol 12. https://doi.org/10.22323/1.375.0065. arXiv:1912.06561
73. Brown F (2015) Feynman amplitudes and cosmic Galois group
74. Schnetz O (2014) Graphical functions and single-valued multiple polylogarithms. Commun Num Theor Phys 08:589. https://doi.org/10.4310/CNTP.2014.v8.n4.a1. arXiv:1302.6445
75. Panzer E, Schnetz O (2017) The Galois coaction on ϕ^4 periods. Commun Num Theor Phys 11:657. https://doi.org/10.4310/CNTP.2017.v11.n3.a3. arXiv:1603.04289
76. Caron-Huot S, Dixon LJ, Dulat F, Von Hippel M, McLeod AJ, Papathanasiou G (2019) The cosmic Galois group and extended Steinmann relations for planar $\mathcal{N} = 4$ SYM amplitudes. JHEP 09:061. https://doi.org/10.1007/JHEP09(2019)061. arXiv:1906.07116
77. Caron-Huot S, Dixon LJ, Dulat F, von Hippel M, McLeod AJ, Papathanasiou G (2019) Six-Gluon amplitudes in planar $\mathcal{N} = 4$ super-Yang-Mills theory at six and seven loops. JHEP 08:016. https://doi.org/10.1007/JHEP08(2019)016. arXiv:1903.10890
78. Mizera S (2018) Scattering amplitudes from intersection theory. Phys Rev Lett 120:141602. https://doi.org/10.1103/PhysRevLett.120.141602. arXiv:1711.00469
79. Mastrolia P, Mizera S (2019) Feynman integrals and intersection theory. JHEP 02:139. https://doi.org/10.1007/JHEP02(2019)139. arXiv:1810.03818
80. Mizera S. Status of intersection theory and Feynman integrals. arXiv:2002.10476
81. Amplitudes 2020. https://indico.cern.ch/event/908370/
82. 't Hooft G, Veltman MJG (1972) Regularization and renormalization of Gauge fields. Nucl Phys B44:189. https://doi.org/10.1016/0550-3213(72)90279-9
83. Bonneau G (1980) Consistency in dimensional regularization with γ_5. Phys Lett B 96:147. https://doi.org/10.1016/0370-2693(80)90232-4
84. Kreimer D (1990) The γ_5-problem and anomalies – a Clifford algebra approach. Phys Lett B 237:59. https://doi.org/10.1016/0370-2693(90)90461-E
85. Baikov P, Ilyin V (1991) Status of gamma(5) in dimensional regularization. Theor Math Phys 88:789. https://doi.org/10.1007/BF01019107
86. Larin S (1993) The renormalization of the axial anomaly in dimensional regularization. Phys Lett B 303:113. https://doi.org/10.1016/0370-2693(93)90053-K. arXiv:hep-ph/9302240
87. Jegerlehner F (2001) Facts of life with gamma(5). Eur Phys J C 18:673. https://doi.org/10.1007/s100520100573. arXiv:hep-th/0005255
88. Bruque A, Cherchiglia A, Pérez-Victoria M (2018) Dimensional regularization vs methods in fixed dimension with and without γ_5. JHEP 08:109. https://doi.org/10.1007/JHEP08(2018)109. arXiv:1803.09764
89. Collins JC (1986) Renormalization: an introduction to renormalization, the renormalization group, and the operator product expansion. Cambridge monographs on mathematical physics, vol 26. Cambridge University Press, Cambridge. https://doi.org/10.1017/CBO9780511622656
90. Bern Z, Kosower DA (1992) The computation of loop amplitudes in gauge theories. Nucl Phys B379:451. https://doi.org/10.1016/0550-3213(92)90134-W
91. Bern Z, De Freitas A, Dixon LJ, Wong HL (2002) Supersymmetric regularization, two loop QCD amplitudes and coupling shifts. Phys Rev D66:085002. https://doi.org/10.1103/PhysRevD.66.085002. arXiv:hep-ph/0202271
92. Nelson C (1981) Origin of cancellation of infrared divergences in coherent state approach: forward process $qq \to qq$ + *Gluon*. Nucl Phys B 181:141. https://doi.org/10.1016/0550-3213(81)90511-3

93. Contopanagos HF, Einhorn MB (1992) Interpretation of the asymptotic s matrix for massless particles. Phys Rev D 45:1291. https://doi.org/10.1103/PhysRevD.45.1291
94. Sterman GF, Weinberg S (1977) Jets from quantum chromodynamics. Phys Rev Lett 39:1436. https://doi.org/10.1103/PhysRevLett.39.1436
95. Kinoshita T (1962) Mass singularities of Feynman amplitudes. J Math Phys 3:650. https://doi.org/10.1063/1.1724268
96. Lee T, Nauenberg M (1964) Degenerate systems and mass singularities. Phys Rev 133:B1549. https://doi.org/10.1103/PhysRev.133.B1549
97. Frye C, Hannesdottir H, Paul N, Schwartz MD, Yan K (2019) Infrared finiteness and forward scattering. Phys Rev D 99:056015. https://doi.org/10.1103/PhysRevD.99.056015. arXiv:1810.10022
98. Kapec D, Perry M, Raclariu A-M, Strominger A (2017) Infrared divergences in QED, revisited. Phys Rev D 96:085002. https://doi.org/10.1103/PhysRevD.96.085002. arXiv:1705.04311
99. Hannesdottir H, Schwartz MD (2020) S-matrix for massless particles. Phys Rev D 101:105001. https://doi.org/10.1103/PhysRevD.101.105001. arXiv:1911.06821
100. Olive DI (1964) Exploration of s-matrix theory. Phys Rev 135:B745. https://doi.org/10.1103/PhysRev.135.B745
101. Chew GF (1966) The analytic S-matrix: a basis for nuclear democracy. W. A. Benjamin, New York
102. Eden RJ, Landshoff PV, Olive DI, Polkinghorne JC (1966) The analytic S-matrix. Cambridge University Press, Cambridge
103. Bern Z, Dixon LJ, Dunbar DC, Kosower DA (1995) Fusing gauge theory tree amplitudes into loop amplitudes. Nucl Phys B 435:59. https://doi.org/10.1016/0550-3213(94)00488-Z. arXiv:hep-ph/9409265
104. Bern Z, Dixon LJ, Dunbar DC, Kosower DA (1994) One loop n point gauge theory amplitudes, unitarity and collinear limits. Nucl Phys B 425:217. https://doi.org/10.1016/0550-3213(94)90179-1. arXiv:hep-ph/9403226
105. Britto R, Cachazo F, Feng B (2005) Generalized unitarity and one-loop amplitudes in $N = 4$ super-Yang-Mills. Nucl Phys B 725:275. https://doi.org/10.1016/j.nuclphysb.2005.07.014. arXiv:hep-th/0412103
106. Britto R, Cachazo F, Feng B (2005) New recursion relations for tree amplitudes of gluons. Nucl Phys B 715:499. https://doi.org/10.1016/j.nuclphysb.2005.02.030. arXiv:hep-th/0412308
107. Britto R, Cachazo F, Feng B, Witten E (2005) Direct proof of tree-level recursion relation in Yang-Mills theory. Phys Rev Lett 94:181602. https://doi.org/10.1103/PhysRevLett.94.181602. arXiv:hep-th/0501052
108. Lehmann H, Symanzik K, Zimmermann W (1955) On the formulation of quantized field theories. Nuovo Cim 1:205. https://doi.org/10.1007/BF02731765
109. Collins J. A new approach to the LSZ reduction formula. arXiv:1904.10923
110. Gillioz M, Meineri M, Penedones J. A scattering amplitude in conformal field theory. arXiv:2003.07361
111. Bern Z, Dixon LJ, Kosower DA (2005) On-shell recurrence relations for one-loop QCD amplitudes. Phys Rev D 71:105013. https://doi.org/10.1103/PhysRevD.71.105013. arXiv:hep-th/0501240
112. Berger CF, Bern Z, Dixon LJ, Forde D, Kosower DA (2006) Bootstrapping one-loop QCD amplitudes with general helicities. Phys Rev D 74:036009. https://doi.org/10.1103/PhysRevD.74.036009. arXiv:hep-ph/0604195
113. Henn J, Power B, Zoia S (2020) Conformal invariance of the one-loop all-plus helicity scattering amplitudes. JHEP 02:019. https://doi.org/10.1007/JHEP02(2020)019. arXiv:1911.12142
114. Arkani-Hamed N, Bourjaily JL, Cachazo F, Caron-Huot S, Trnka J (2011) The all-loop integrand for scattering amplitudes in planar $N = 4$ SYM. JHEP 01:041. https://doi.org/10.1007/JHEP01(2011)041. arXiv:1008.2958
115. Boels RH (2010) On BCFW shifts of integrands and integrals. JHEP 11:113. https://doi.org/10.1007/JHEP11(2010)113. arXiv:1008.3101

116. Landau L (1960) On analytic properties of vertex parts in quantum field theory. Nucl Phys 13:181. https://doi.org/10.1016/B978-0-08-010586-4.50103-6
117. Coleman S, Norton R (1965) Singularities in the physical region. Nuovo Cim 38:438. https://doi.org/10.1007/BF02750472
118. Prlina I, Spradlin M, Stanojevic S (2018) All-loop singularities of scattering amplitudes in massless planar theories. Phys Rev Lett 121:081601. https://doi.org/10.1103/PhysRevLett.121.081601. arXiv:1805.11617
119. Collins J. A new and complete proof of the Landau condition for pinch singularities of Feynman graphs and other integrals. arXiv:2007.04085
120. Cutkosky R (1960) Singularities and discontinuities of Feynman amplitudes. J Math Phys 1:429. https://doi.org/10.1063/1.1703676
121. Britto R (2011) Loop amplitudes in gauge theories: modern analytic approaches. J Phys A 44:454006. https://doi.org/10.1088/1751-8113/44/45/454006. arXiv:1012.4493
122. Carrasco JJM, Johansson H (2011) Generic multiloop methods and application to $N = 4$ super-Yang-Mills. J Phys A 44:454004. https://doi.org/10.1088/1751-8113/44/45/454004. arXiv:1103.3298

Chapter 3
The Art of Integrating by Differentiating

The good, old Feynman rules offer a completely algorithmic way of writing down the expression of any scattering amplitude. The number of Feynman diagrams grows badly with the number of loops and of external particles, and the search of alternative methods is an exciting area of research. However, it is fair to say that, given a Lagrangian and an arbitrary amount of computing power, it is no mystery how to write down *some* expression of the scattering amplitude for a certain process at a certain loop order. Yet, even once such an expression is available and properly massaged, one has to face the hard truth that she is still quite far from the finishing line. The main obstacle standing in the way are the Feynman integrals. Despite tremendous progress in the last decades, the computation of Feynman integrals beyond one loop is far from being an algorithmic process. In this chapter I will discuss the analytic strategy which I am convinced is the most systematic at our disposal: the method of the differential equations [1–5].

Before doing so, I feel that I owe the reader some words of persuasion on the necessity of computing Feynman integrals *analytically*. I invite those who need no persuasion to skip the following paragraphs.

First of all, there is a practical reason. Scattering amplitudes are the ultimate gauge-invariant building blocks of cross sections. In order to compute a cross section, however, the scattering amplitudes have to be integrated over the phase space. This means evaluating them hundreds of thousands of times. Speed and numerical stability are crucial. Despite the enormous progress in numerical integration, which has given us extremely powerful tools such as FIESTA [6] and pySecDec [7], this approach is still no match for a fully analytic result in the case of multi-loop integrals, in particular if evaluated in the region of the kinematic space which is of interest for phenomenology.

Yet, even if it were possible to evaluate numerically any Feynman integral in such a way that our phenomenologist friends would be entirely satisfied, I argue that it would still be worth pursuing a fully analytic computation. Scattering amplitudes and Feynman integrals are more than numbers. Their analytic structure contains

S. Zoia, *Modern Analytic Methods for Computing Scattering Amplitudes*, Springer Theses,
https://doi.org/10.1007/978-3-031-01945-6_3

much more information than it is possible to read off from plots, and gives extremely precious insights in the underlying theory. I have given a few examples in Sect. 2.2.

Finally, it is worth mentioning that hybrid analytic/numeric approaches are also being explored [8], and have already lead to several promising applications [9–13].

Hopefully galvanised by this motivation, we can now move on to discussing the method of the differential equation for the analytic computation of Feynman integrals. I wish to make the presentation rather pedagogical and self-contained.[1] For this reason I complement the presentation of each technique and idea with its application to an explicit case, the so-called "three-mass triangle" integral family, which we will compute together step by step throughout this chapter. I begin in Sect. 3.1.1 by defining the fundamental notion of integral family, roughly speaking the set of all integrals with the same propagator structure and any numerator. I show that an integral family admits a basis, and that the latter satisfies a system of first-order linear differential equations. The choice of basis is arbitrary and the differential equations can in general be very complicated. In Sect. 3.2 I argue that a natural choice of basis exists, for which the differential equations simplify dramatically and take the so-called "canonical form." In order to write down the solution of the differential equations, in Sect. 3.3 I define and discuss the analytic properties of the multiple polylogarithms, and introduce some technology to work with them. In Sect. 3.4 I show three different approaches to write down the solution of the canonical differential equations, and discuss the benefits and the limitations of each of them. The differential equations are also an extremely convenient tool to compute the asymptotic expansion of the Feynman integrals in any kinematic limit. I show how to do this systematically in Sect. 3.5. Finally, in Sect. 3.6 I show how certain properties of the loop integrands, prior to integration, can be used to construct canonical bases systematically.

3.1 Feynman Integrals and Differential Equations

In this section I introduce the important concept of "family" of Feynman integrals associated with a given loop Feynman diagram. Although an integral family contains infinite Feynman integrals, only a finite number of them are actually independent, which naturally implies the notion of an integral basis. I discuss how the Integration-by-Parts (IBP) relations can be used to rewrite any integral of the family in terms of elements of the basis. The computation of the entire integral family therefore reduces to that of the basis integrals, often called master integrals in the literature. I then show that the basis integrals satisfy a system of first-order linear differential equations.

[1] For an even more thorough discussion of this method I recommend the notes [14].

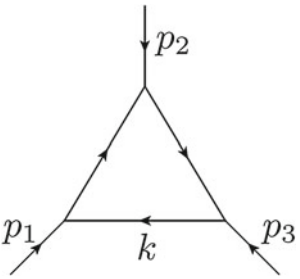

Fig. 3.1 Graph representing the propagator-structure of the three-mass triangle integral family defined by Eq. (3.1). The arrows denote momentum flow

3.1.1 Integral Families and Integration-by-Parts Identities

Depending on the theory and on the process under consideration, a loop Feynman diagram may have a non-trivial spinor structure. While the denominator is always given by a product of scalar propagators of the form $k_i^2 - m_i^2$ because of locality (see Sect. 2.4.1),[2] the numerator can carry several Lorentz or Weyl indices in the loop momenta k_i^μ. With some manipulations—called tensor reduction—it is possible to rewrite any tensor quantity as a combination of tensor monomials in the external momenta p_i^μ with scalar coefficients. As a result, we can restrict our analysis to scalar Feynman integrals. Through the tensor reduction, however, a given Feynman diagram can generate various scalar Feynman integrals with the same propagator structure, but with different powers of propagators. For example, certain powers may be negative, originating from a polynomial in the numerator of the original expression. This suggests to generalise the idea of Feynman integral by allowing arbitrary integer powers of the propagators. The resulting object is called integral family.

In general the propagators of the representative Feynman diagram may not be sufficient in order to express any possible numerator. In other words, it may not be possible to rewrite certain scalar products of the momenta in terms of propagators. We talk in this case of Irreducible Scalar Products (ISPs). The standard procedure to handle them is to add a minimal set of ISPs as auxiliary propagators. We will see an example of this in the next chapter, when discussing the two-loop five-particle integral families.

In order to be more explicit and to define the notation, let me give an explicit example. Let us consider the integral family corresponding to the one-loop three-particle graph with massless propagators shown in Fig. 3.1 [15],

$$I_{a_1,a_2,a_3} = e^{\epsilon\gamma_\mathrm{E}} \int \frac{d^D k}{i\pi^{\frac{D}{2}}} \frac{1}{\left(k^2 + i0^+\right)^{a_1} \left((k+p_1)^2 + i0^+\right)^{a_2} \left((k+p_1+p_2)^2 + i0^+\right)^{a_3}} \,. \tag{3.1}$$

[2] The propagators can also be linear in the loop momenta, e.g. in the context of Wilson lines. In this thesis I focus on quadratic propagators. The treatment of the linear ones follows analogously.

The overall prefactor of $e^{\epsilon\gamma_E}$ is conventional, and serves the purpose of removing Euler's constant $\gamma_E = -\Gamma'(1)$ from the results. We take the external momenta p_i, with $i = 1, 2, 3$, to be all incoming. They satisfy the on-shell conditions and momentum conservation,

$$p_i^2 = m_i^2\,, \quad \forall i = 1, 2, 3\,, \tag{3.2}$$

$$p_1 + p_2 + p_3 = 0\,. \tag{3.3}$$

The loop momentum k lives in $D = 4 - 2\epsilon$ dimensions in order to regulate the divergences, while the external momenta can be chosen to lie either in a four- or in a D-dimensional space. The choice has no effect in this case, but it is in general important (see Sect. 2.3.1). The Feynman prescription $+i0^+$ in the propagators specifies how to perform the Wick rotation from Minkowski space with metric $+ - \cdots -$ to Euclidean space. In most of the following we will omit it in order to simplify the notation. Poincaré invariance and momentum conservation imply that the integrals of this family depend only on three kinematic variables, which we choose as the external masses m_i^2, $\forall i = 1, 2, 3$, and on the dimensional regulator ϵ. In order to simplify the notation, I denote the kinematic variables cumulatively by m,

$$m := \left(m_1^2, m_2^2, m_3^2\right)\,. \tag{3.4}$$

It is important to stress that it is not necessary to specify the underlying theory and Feynman rules. The propagators are in fact always the same, and the integral family is defined by allowing arbitrary powers of the propagators so as to accommodate any numerator. The graph in Fig. 3.1, therefore, is not to be mistaken for a Feynman diagram. It is a pictorial representation of the propagator structure of the integral family we are considering. Once the integral family has been computed, the results can be used for the calculation of scattering amplitudes or correlation functions in any theory.

We started off with the goal of computing a Feynman integral and we ended up with a family of infinite integrals. At first glance it might seem like we did not make a particularly good deal. However, the integrals in a given family are in general not independent. They satisfy linear relations called Integration-by-Parts relations (IBPs) [16]. They originate from the fact that total derivatives vanish in dimensional regularisation. Given the important role played by this theorem in the method of the differential equations, it is worth trying to understand why it holds—at least qualitatively. Let $f(k)$ be the integrand of a Feynman integral $\int d^D k f(k)$. The Poincaré invariance of the integrand allows us to translate the loop momentum k by some external momentum p,

$$\int d^D k f(k) = \int d^D k f(k + p)\,. \tag{3.5}$$

Assuming that p is infinitesimally small, the following series expansion holds,

$$\begin{aligned}\int d^D k f(k) &= \int d^D k f(k) + p^\mu \int d^D k \frac{\partial}{\partial p^\mu} f(k+p)\Big|_{p=0} + \mathcal{O}\left(p^2\right) \\ &= \int d^D k f(k) + p^\mu \int d^D k \frac{\partial}{\partial k^\mu} f(k) + \mathcal{O}\left(p^2\right) ,\end{aligned} \tag{3.6}$$

which implies that total derivatives vanish in dimensional regularisation,

$$\int d^D k \frac{\partial}{\partial k^\mu} f(k) = 0 . \tag{3.7}$$

In order to perform all these manipulations the integral must be well defined. This is why dimensional regularisation is crucial. Similarly, one can also prove that scaleless integrals vanish in dimensional regularisation,

$$\int d^D k \left(k^2\right)^a = 0 . \tag{3.8}$$

This is often referred to as Veltman's formula in the literature [17, 18].

Going back to the three-mass triangle integral family (3.1), we have that

$$e^{\epsilon\gamma_{\mathrm{E}}} \int \frac{d^D k}{i\pi^{\frac{D}{2}}} \frac{\partial}{\partial k^\mu} \left(\frac{q^\mu}{\left(k^2\right)^{a_1} \left((k+p_1)^2\right)^{a_2} \left((k+p_1+p_2)^2\right)^{a_3}} \right) = 0 , \tag{3.9}$$

for any momentum q. In this case there are three independent choices, $q \in \{p_1, p_2, k\}$. It is sufficient to perform a bit of algebra to show that the action of the differential operator on the rest of the integrand in Eq. (3.9) can be rewritten in terms of members of the integral family with different powers of the propagators $\{a_1, a_2, a_3\}$. For instance, choosing $q = k$ gives the IBP relation

$$\begin{aligned}&(D - 2a_1 - a_2 - a_3) I_{a_1,a_2,a_3} - a_3 I_{a_1-1,a_2,a_3+1} - a_2 I_{a_1-1,a_2+1,a_3} + \\ &+ m_3^2 a_3 I_{a_1,a_2,a_3+1} + m_1^2 a_2 I_{a_1,a_2+1,a_3} = 0 .\end{aligned} \tag{3.10}$$

The IBPs therefore relate integrals with different powers of the propagators a_i. As already anticipated, only a finite number of them are independent [19]. The members of an integral family therefore form a finite-dimensional vector space. As we will see in the next section, the choice of the basis of such a vector space is crucial. In the three-mass triangle case, the basis or master integrals can be chosen for instance as

$$\vec{f} = \{I_{1,1,0}, I_{1,0,1}, I_{0,1,1}, I_{1,1,1}\} , \tag{3.11}$$

corresponding pictorially to bubble-graphs in the three different channels, and a triangle, as shown in Fig. 3.2.

It is then possible to make use of the IBPs iteratively to expand any integral of the family in the chosen basis, with rational prefactors in the kinematic variables and

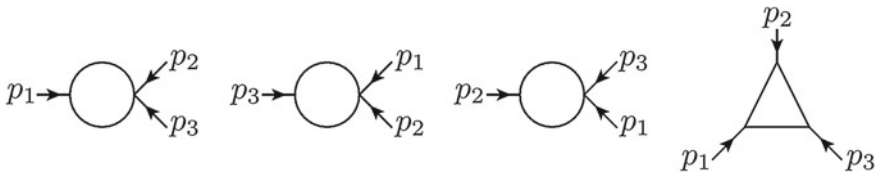

Fig. 3.2 Integral basis of the three-mass triangle family given by Eq. (3.11)

the spacetime dimension D. For example,

$$I_{2,1,1} = \frac{D-3}{m_1^2 m_3^2}\left(I_{0,1,1} - I_{1,0,1} - I_{1,1,0}\right) - (D-4)\frac{m_1^2 - m_2^2 + m_3^2}{2m_1^2 m_3^2} I_{1,1,1}\,. \tag{3.12}$$

This procedure is called IBP reduction. Although in principle straightforward, this task is rather tedious to do by hand, and can become very heavy from the computational point of view. Several algorithms have been devised to perform it in an automatic and efficient way, notably Laporta's algorithm [20, 21]. Various implementations are publicly available [22–26].

3.1.2 Differential Equations

Thanks to the IBPs the computation of all the integrals of a given family reduces to that of the basis integrals. We will now see how we can compute these integrals—quite ironically—by differentiating them.

We want to compute the basis integrals as functions of the kinematic invariants, but their defining expression (3.1) is written in terms of momenta. The first step is thus to construct differential operators $\partial/\partial m_i^2$ that can act on the integral representation (3.1). This can be easily done by writing down ansätze for them, e.g. for $\partial/\partial m_1^2$

$$\frac{\partial}{\partial m_1^2} = \left(a_1(m)\,p_1^\mu + a_2(m)\,p_2^\mu\right)\frac{\partial}{\partial p_1^\mu} + \left(b_1(m)\,p_1^\mu + b_2(m)\,p_2^\mu\right)\frac{\partial}{\partial p_2^\mu}\,. \tag{3.13}$$

Imposing that the operator behaves as expected, namely that

$$\frac{\partial}{\partial m_1^2} p_1^2 = 1\,, \qquad \frac{\partial}{\partial m_1^2} p_2^2 = 0\,, \qquad \frac{\partial}{\partial m_1^2}(p_1+p_2)^2 = 0\,, \tag{3.14}$$

fixes three of the free coefficients,

$$\begin{cases} a_2 = \frac{-1+2a_1 m_1^2}{m_1^2+m_2^2-m_3^2}\,, \\ b_1 = \frac{2m_2^2}{m_1^2+m_2^2-m_3^2}\left(\frac{m_1^2-m_2^2-m_3^2}{\lambda(m_1^2,m_2^2,m_3^2)} - a_1\right)\,, \\ b_2 = \frac{m_1^2-m_2^2-m_3^2}{\lambda(m_1^2,m_2^2,m_3^2)} - a_1\,, \end{cases} \tag{3.15}$$

where λ denotes the Källen function,

$$\lambda\,(x,\,y,\,z) = x^2 + y^2 + z^2 - 2xy - 2xz - 2yz\,. \tag{3.16}$$

The remaining freedom can be used to simplify the expression. For instance, by choosing $a_1 = (m_1^2 - m_2^2 - m_3^2)/\lambda(m_1^2, m_2^2, m_3^2)$, we obtain

$$\frac{\partial}{\partial m_1^2} = \frac{\left(m_1^2 - m_2^2 - m_3^2\right) p_1^\mu + \left(m_1^2 - m_2^2 + m_3^2\right) p_2^\mu}{\lambda\left(m_1^2, m_2^2, m_3^2\right)} \frac{\partial}{\partial p_1^\mu}\,. \tag{3.17}$$

The other operators can be constructed the same way, using the remaining freedom to ensure that they all commute,

$$\left[\frac{\partial}{\partial m_i^2}, \frac{\partial}{\partial m_j^2}\right] = 0\,,\ \forall i,\, j = 1, 2, 3\,. \tag{3.18}$$

Now that we have differential operators at our disposal, we can differentiate the basis integrals $\vec{f}$ (3.11). It takes just a little amount of algebra to show that one obtains integrals within the same family. We can thus re-express the result of the differentiation as a linear combination of basis integrals using IBPs. To put it differently, the fact that a family of Feynman integrals admits an integral basis implies that the latter satisfy a system of first-order linear homogeneous differential equations,

$$\begin{cases} \dfrac{\partial \vec{f}}{\partial m_1^2} = B_1(m, \epsilon) \cdot \vec{f} \\ \dfrac{\partial \vec{f}}{\partial m_2^2} = B_2(m, \epsilon) \cdot \vec{f} \\ \dfrac{\partial \vec{f}}{\partial m_3^2} = B_3(m, \epsilon) \cdot \vec{f} \end{cases}, \tag{3.19}$$

where we stress that B_i is a 4×4 matrix function of both the kinematics and ϵ. For example, the derivative with respect to m_1^2 gives

$$B_1 = \begin{pmatrix} -\frac{\epsilon}{m_1^2} & 0 & 0 & 0 \\ 0 & 0 & 0 & 0 \\ 0 & 0 & 0 & 0 \\ \frac{4\epsilon-2}{\lambda} & (1-2\epsilon)\frac{m_1^2-m_2^2+m_3^2}{m_1^2\lambda} & (1-2\epsilon)\frac{m_1^2+m_2^2-m_3^2}{m_1^2\lambda} & \frac{m_1^2\left(m_2^2+m_3^2-m_1^2\right)+\epsilon\left(m_1^4-(m_2^2-m_3^2)^2\right)}{m_1^2\lambda} \end{pmatrix}, \tag{3.20}$$

where we denote $\lambda \equiv \lambda(m_1^2, m_2^2, m_3^2)$ for simplicity.

A few comments on the matrices of the differential equations B_i are in order. First of all, Euler's theorem on homogeneous functions implies that

$$\sum_{i=1}^{3} m_i^2 B_i = \text{diag}\left(-\epsilon, -\epsilon, -\epsilon, -1-\epsilon\right) , \tag{3.21}$$

where on the diagonal are the scaling dimensions of the integrals. We can set them to zero by normalising the integrals with appropriate dimensional factors, so that they only depend on two non-trivial dimensionless variables.

Secondly, the matrices B_i must satisfy certain integrability conditions,

$$\frac{\partial B_i}{\partial m_j^2} - \frac{\partial B_j}{\partial m_i^2} = \left[B_j, B_i\right] , \qquad \forall i, j = 1, 2, 3 . \tag{3.22}$$

They follow through the differential equations (3.19) from the requirement that partial derivatives of the basis integrals commute,

$$\left[\frac{\partial}{\partial m_i^2}, \frac{\partial}{\partial m_j^2}\right] \vec{f} = 0 . \tag{3.23}$$

In practice, the scaling dimensions (3.21) and the integrability conditions (3.22) offer a very precious opportunity to check one's implementation of the differential equations. Such an opportunity should never be missed.

The differential equations for the bubble integrals are trivial, as can be seen e.g. for f_1 from Eq. (3.20). Since they depend only on one scale, m_1^2 for f_1, their functional dependence is entirely fixed by dimensional analysis. We can thus read off from Eq. (3.21) that $f_i \propto (m_i^2)^{-\epsilon}$ for $i = 1, 2, 3$. The overall kinematic-independent normalisation cannot be determined from the differential equations. Its full expression is rather easy to compute in closed-form, e.g. by straightforward integration of the Feynman parametrisation,

$$f_i = e^{\epsilon\gamma_{\text{E}}} \frac{\Gamma^2(1-\epsilon)\Gamma(\epsilon)}{\Gamma(2-2\epsilon)} \left(-m_i^2\right)^{-\epsilon} = \frac{1}{\epsilon} + 2 - \log\left(-m_i^2\right) + \mathcal{O}(\epsilon) , \qquad \forall i = 1, 2, 3 . \tag{3.24}$$

The expression for the bubble integrals given by Eq. (3.24) is well defined in the so-called Euclidean region, where $m_i^2 < 0 \, \forall i = 1, 2, 3$. I postpone the discussion of the kinematic regions and of how to analytically continue away from the Euclidean region to Sect. 3.4.1.

Finally, the differential equations exhibit manifestly the loci of the potential singularities of the integrals. By looking at Eq. (3.20) and at the corresponding expressions for B_2 and B_3, it is clear that the basis integrals can diverge when one of the external masses vanishes, $m_i^2 = 0$, or on the hypersurface $\lambda(m_1^2, m_2^2, m_3^2) = 0$. The latter singularity may sound surprising. It has no physical meaning and therefore must not appear in the Feynman integrals. The presence of such spurious singularities in the differential equations is actually valuable: imposing their absence provides us with constraints to fix the boundary constants, as discussed in Sect. 3.4.2.

To summarise, we have seen that any integral family admits an integral basis, and that the latter satisfies a linear system of first-order differential equations (3.19), whose expression can be computed in a completely algorithmic way. Their solution is however not systematic, in general. Moreover, the choice of basis is arbitrary. We are always free to switch to a different basis $\vec{g}$,

$$\vec{g} = T \cdot \vec{f}, \tag{3.25}$$

for some invertible matrix T. The new basis integrals $\vec{g}$ satisfy a system of differential equations equivalent to Eqs. (3.19),

$$\frac{\partial \vec{g}}{\partial m_i^2} = A_i \, (m, \epsilon) \cdot \vec{g} \, , \qquad \forall i = 1, 2, 3 \, , \tag{3.26}$$

where

$$A_i = T \cdot B_i \cdot T^{-1} + \frac{\partial T}{\partial m_i^2} \cdot T^{-1} \, . \tag{3.27}$$

In the next section we will see that there is a natural choice of basis for which the differential equations simplify dramatically.

3.2 Differential Equations in the Canonical Form

In Sect. 3.1.2 we have seen that the basis of an integral family satisfies a linear system of first-order differential equations. The latter can be rather complicated for a generic choice of basis, so that its solution remains a difficult problem. In [5] it was conjectured that there exist special choices of basis for which the differential equations take a certain "canonical" form. The canonical form of the differential equations is dramatically simpler, so that the solution can be simply read off in terms

of special functions. In this section I discuss the main features of the canonical form by working out explicitly the case of the three-mass triangle family (3.1).

Let us make the following educated choice of integral basis,

$$\begin{aligned} g_1 &= \epsilon m_1^2 I_{2,1,0}\,, \\ g_2 &= \epsilon m_2^2 I_{0,2,1}\,, \\ g_3 &= \epsilon m_3^2 I_{1,0,2}\,, \\ g_4 &= \epsilon^2 \sqrt{\lambda} I_{1,1,1}\,. \end{aligned} \tag{3.28}$$

The corresponding transformation matrix in Eq. (3.25) simply amounts to changing the normalisation of the integrals,

$$T = \text{diag}\left(\epsilon(2\epsilon-1), \epsilon(2\epsilon-1), \epsilon(2\epsilon-1), \epsilon^2\sqrt{\lambda}\right)\,. \tag{3.29}$$

For the bubble integrals this can be seen e.g. by setting $a_1 = a_2 = 1$ and $a_3 = 0$ in Eq. (3.10), which yields the relation

$$I_{2,1,0} = \frac{2\epsilon - 1}{m_1^2}\, I_{1,1,0}\,. \tag{3.30}$$

Analogous relations for the other bubbles, $I_{0,1,1}$ and $I_{1,0,1}$, can be deduced from Eq. (3.30) by symmetry or determined using other IBP relations.

The basis defined by Eq. (3.28) might look more complicated than the one given by Eq. (3.11), since we have introduced a square root. This is a fair price to pay for the drastic simplification we achieve. The new integral basis $\{g_i\}_{i=1}^4$ satisfies the system of differential equations (3.26). The matrices of the differential equations A_i can either be obtained from those of the previous basis through Eq. (3.27) or computed following the procedure outlined in Sect. 3.1.2. Let us take a look for instance at A_1,

$$A_1 = \epsilon \begin{pmatrix} -\frac{1}{m_1^2} & 0 & 0 & 0 \\ 0 & 0 & 0 & 0 \\ 0 & 0 & 0 & 0 \\ \frac{2}{\sqrt{\lambda}} & \frac{m_3^2-m_1^2-m_2^2}{m_1^2\sqrt{\lambda}} & \frac{m_2^2-m_1^2-m_3^2}{m_1^2\sqrt{\lambda}} & \frac{(m_1^2+m_2^2-m_3^2)(m_1^2-m_2^2+m_3^2)}{\lambda} \end{pmatrix}\,. \tag{3.31}$$

The first striking simplification is that the dependence on ϵ is factorised. The system of differential equations can therefore be rewritten as

$$\frac{\partial \vec{g}}{\partial m_i^2} = \epsilon\, \tilde{A}_i\,(m) \cdot \vec{g}\,, \qquad \forall i = 1,2,3\,, \tag{3.32}$$

where we stress that the matrices $\tilde{A}_i = A_i/\epsilon$ depend only on the kinematic variables. As a result, the two sides of the integrability conditions, given by Eq. (3.22) with B_i

traded for A_i, have a different order in ϵ. Since they must hold for any value of ϵ, they split into

$$\begin{aligned} &\frac{\partial \tilde{A}_i}{\partial m_j^2} - \frac{\partial \tilde{A}_j}{\partial m_i^2} = 0\,, \\ &\left[\tilde{A}_i, \tilde{A}_j\right] = 0\,, \end{aligned} \qquad \forall i, j = 1, 2, 3\,. \tag{3.33}$$

Moreover, the integrals of the new basis $\{g_i\}_{i=1}^4$ all have the same scaling dimensions,

$$\sum_{i=1}^{3} m_i^2 \tilde{A}_i = \text{diag}\,(-1, -1, -1, -1)\ . \tag{3.34}$$

One could therefore extract a factor of, say, $\left(m_1^2\right)^{-\epsilon}$ from the integrals g_i, leaving a non-trivial dependence on two dimensionless variables only.

The kinematic dependence simplifies enormously as well. In order to appreciate this in full glory, it is convenient to combine the differential equations (3.26) and write the full system in differential form,

$$d\vec{g} = \epsilon\, d\tilde{A}(m) \cdot \vec{g}\,, \tag{3.35}$$

where

$$\frac{\partial \tilde{A}}{\partial m_i^2} = \tilde{A}_i\,, \quad \forall i = 1, 2, 3\,. \tag{3.36}$$

The matrix $\tilde{A}$ can be obtained from the $\tilde{A}_i$ by solving algorithmically the Eqs. (3.36)—see for instance [9]—or bootstrapped as I discuss below. It takes the form

$$\widetilde{A} = \begin{pmatrix} -\log\alpha_1 & 0 & 0 & 0 \\ 0 & -\log\alpha_2 & 0 & 0 \\ 0 & 0 & -\log\alpha_3 & 0 \\ -\log\alpha_4 & -\log\alpha_5 & \log\alpha_4 + \log\alpha_5 & -\log\alpha_1 - \log\alpha_2 - \log\alpha_3 + 2\log\alpha_6 \end{pmatrix}, \tag{3.37}$$

where $\{\alpha_i\}_{i=1}^6$ are algebraic functions of the kinematics,

$$\{\alpha_i\}_{i=1}^6 = \left\{ m_1^2, m_2^2, m_3^2, \frac{m_1^2 - m_2^2 - m_3^2 - \sqrt{\lambda}}{m_1^2 - m_2^2 - m_3^2 + \sqrt{\lambda}}, \frac{m_2^2 - m_3^2 - m_1^2 - \sqrt{\lambda}}{m_2^2 - m_3^2 - m_1^2 + \sqrt{\lambda}}, \sqrt{\lambda} \right\}. \tag{3.38}$$

The differential equations (3.35) with $\tilde{A}$ given by Eq. (3.37) make beautifully manifest not only the loci of the (physical and spurious) singularities, but also their regular nature. It is worth spending a few words to clarify this concept. It is possible

to prove, e.g. by analysing the Feynman parameterisation, that a Feynman integral is always bounded in a limit by a power with a certain exponent (see e.g. [14]). This means that Feynman integrals can only have regular singularities in the kinematic variables. In other words, it is not possible for a Feynman integral to develop an essential singularity, such as $e^{1/x}$ at $x = 0$. This observation has strong implications for the differential equations. In order to appreciate this, let $h(x)$ be a Feynman integral depending on a kinematic variable x. Let $x_s \neq \infty$ be a singular point of $h(x)$.[3] There exists a constant a such that $h(x) \sim (x - x_s)^a$ in the limit $x \to x_s$. This means that $h(x)$ satisfies a first-order differential equation which exhibits a simple pole at $x = x_s$,

$$\frac{\partial h(x)}{\partial x} \underset{x \to x_s}{\sim} \frac{a}{x - x_s} h(x) \,. \tag{3.39}$$

A differential equation which exhibits this behaviour around all its singular points is called fuchsian. Higher poles would lead to essential singularities, absent in Feynman integrals. In the case of an integral basis, the matrix nature of the differential equations they satisfy may obscure the fuchsian property with spurious higher poles. However, the fact that Feynman integrals can have only regular singularities implies the existence of a basis whose differential equations are in fuchsian form. The matrix $\tilde{A}$ in Eq. (3.37) makes the system of differential equations (3.35) manifestly fuchsian.

Equation (3.35) with a manifestly fuchsian matrix $\tilde{A}$ is called the *canonical form* of the differential equations [5]. The integral basis for which the differential equations takes this form is dubbed *canonical basis*.

Once the differential equations are cast into the canonical form, the problem of solving them for the basis integrals as Laurent expansions around $\epsilon = 0$ is essentially solved. Formally, the solution can be written down straightforwardly as

$$\vec{g}\,(m, \epsilon) = \mathbb{P} \exp\left(\epsilon \int_\gamma d\tilde{A}\right) \cdot \vec{b}(\epsilon) \,, \tag{3.40}$$

where $\mathbb{P}$ denotes the path ordering, γ is a path in the kinematic space going from some boundary point $m^{(0)}$ to m, and $\vec{b}(\epsilon) = \vec{g}_0(\epsilon)$ are the values of the basis integrals at $m^{(0)}$. Equation (3.40) is to be understood in a Laurent expansion around $\epsilon = 0$,

$$\vec{g}(m, \epsilon) = \sum_{k=0}^{\infty} \epsilon^k \vec{g}^{(k)}(m) \,, \tag{3.41}$$

and similarly for the boundary values $\vec{b}(\epsilon)$. Note that it is always possible to rescale the basis integrals such that they are finite as $\epsilon \to 0$, since the differential equation is not affected by any overall kinematic-independent normalisation of the integrals. This motivates the overall factor of ϵ in the definition of the canonical basis given by

[3] Singularities at infinity, $x_s \to \infty$, can be analysed in the same way by first doing a variable transformation $x \to z = 1/x$ and then studying the singular point $z_s = 0$.

Eq. (3.28). The kth term in the expansion is then given by a k-fold iterated integral along the contour γ of the matrix differential form $d\widetilde{A}$,

$$\vec{g}^{(k)}(m) = \sum_{j=0}^{k} \int_{\gamma} \underbrace{d\widetilde{A} \cdot \cdots \cdot d\widetilde{A}}_{j} \cdot \vec{b}^{(k-j)} \,, \tag{3.42}$$

with the empty iterated integral defined to be 1. I postpone to Sect. 3.3.1 the precise definition of iterated integral. For now it suffices to understand that, once the differential equations are cast into the canonical form, the problem of solving them can be considered as solved, at least formally. The 1-forms appearing in the matrix $d\widetilde{A}$ constitute the integration kernels in the iterated-integral solution, and therefore encode which class of special functions is required to write down the solution.

In the three-mass triangle case, we see from Eq. (3.37) that all the integration kernels are logarithmic,

$$d\widetilde{A} = \sum_{i=1}^{6} a_i d\log\alpha_i \,, \tag{3.43}$$

where a_i are constant rational matrices and α_i are algebraic functions given by Eq. (3.38). This is the most well understood case and it covers a great number of applications. The 1-forms $\{d\log\alpha_i\}_{i=1}^{6}$ are called *letters*, and the set of linearly independent letters is dubbed *alphabet*. If the alphabet can be rationalised with an appropriate change of kinematic variables, then it is possible to express the result algorithmically in terms of Multiple Polylogarithms (MPLs) [27–31]. I discuss how to do that in Sect. 3.4.3. This is often possible even in the presence of non-rational letters (see e.g. [32]), although it is not true in general. Reference [33], for instance, provides an explicit example of an iterated integral with logarithmic kernels which cannot be written as a linear combination of MPLs. In such a case, and whenever the integration kernels in Eq. (3.42) are not logarithmic, more complicated functions may be required. One practical way of assessing this is the analysis of the maximal cuts, i.e. the generalised unitarity cuts where all propagators are cut. If all maximal cuts of a Feynman integral and of its sub-topologies are algebraic, for instance, it is typically possible to express it in terms of MPLs. Maximal cuts that evaluate to elliptic integrals, on the other hand, are the smoking gun of Elliptic Multiple Polylogarithms [34–40]. Iterated integrals of 1-forms defined on even more complicated geometries—e.g. hyperelliptic curves [41, 42] and Calabi–Yau geometries [43–47]—become relevant as we keep increasing the number of loops and of variables.

For the work presented in this thesis it suffices to consider logarithmic 1-forms only. From now on I will thus specialise in this case and, for simplicity, I will refer to the arguments of the logarithms $\{\alpha_i\}_{i=1}^{6}$ as letters, rather than to the full 1-forms $\{d\log\alpha_i\}_{i=1}^{6}$. I will therefore assume that the matrix $\tilde{A}$ in the canonical differential equations (3.35) has the form given by Eq. (3.43). Since the alphabet $\{\alpha_i\}_{i=1}^{6}$ can

be determined by looking at the $\tilde{A}_i$ matrices, $\tilde{A}$ can be computed by writing down an ansatz of the form (3.43), and fixing the constant matrices a_i by imposing that it satisfies the differential equations (3.36). This can be done numerically, which often makes it advantageous with respect to integrating the Eqs. (3.36) analytically.

3.2.1 A Note on the Choice of the Letters

Of course there is freedom in the specific expression of the letters, and finding the simplest alphabet is an art. For instance, one might as well choose the letters α_4 and α_5 in Eq. (3.38) to have only the numerator or the denominator, since

$$\begin{aligned} \text{num}\,[\alpha_4]\,\text{den}\,[\alpha_4] &= 4\alpha_2\alpha_3\,, \\ \text{num}\,[\alpha_5]\,\text{den}\,[\alpha_5] &= 4\alpha_1\alpha_3\,, \end{aligned} \tag{3.44}$$

where $\text{den}\,[x]$ and $\text{num}\,[x]$ denote the denominator and the numerator of x, respectively. I prefer the choice made in Eq. (3.38) because, in the kinematic region where $\lambda(m_1^2, m_2^2, m_3^2) < 0$, all the letters have a well-defined transformation under complex conjugation. They are either even,

$$d\log\alpha_i^* = d\log\alpha_i\,, \qquad i = 1, 2, 3, 6\,, \tag{3.45}$$

or odd,

$$d\log\alpha_i^* = -d\log\alpha_i\,, \qquad i = 4, 5\,. \tag{3.46}$$

This property gives a useful criterion of classification of the functions appearing in the solution.

In general, thus, whenever the alphabet contains a square root $\sqrt{\lambda}$, it is convenient that the letters depending on it have the form

$$\frac{P - \sqrt{\lambda}}{P + \sqrt{\lambda}}\,, \tag{3.47}$$

where P is a polynomial in the kinematic variables. While it is typically easy to identify a square root in the alphabet by looking at the differential equations even in a form that is not canonical (see e.g. Eq. (3.31)), finding the corresponding polynomials P to construct letters of the form (3.47) may be non-trivial, especially in the presence of multiple square roots. This can be done algorithmically as follows. If a letter of the form (3.47) belongs to the alphabet, it must be possible to factorise both numerator and denominator separately in the alphabet. This implies that their product is given by a product of letters which are even under the exchange $\sqrt{\lambda} \leftrightarrow -\sqrt{\lambda}$,

$$P^2 - \lambda = c \prod_{\alpha_i \text{ even}} \alpha_i^{e_i}\,, \tag{3.48}$$

where $c, e_i \in \mathbb{Q}$. Since the left-hand side of Eq. (3.48) is polynomial, the right-hand side must be polynomial as well. There is therefore only a finite number of combinations of exponents $\{e_i\}$ such that the right-hand side of the equation is a polynomial with the right dimensions. We can therefore make an ansatz for P and look for a solution for its free coefficients and for the constant c in Eq. (3.48) by scanning systematically over all the allowed products of even letters. In the three-mass triangle case, for instance, with λ given by Eq. (3.16), one solution is given by $P = m_1^2 - m_2^2 - m_3^2$, for which Eq. (3.48) becomes

$$P^2 - \lambda = 4\alpha_2\alpha_3 \,. \tag{3.49}$$

In this section I have introduced the canonical form of the differential equations for an integral basis, and praised its many virtues. It encodes in a minimal way all the information about the basis integrals: the alphabet defines which class of special functions is needed to write down the answer, and the coefficient matrices a_i in Eq. (3.43) specify which linear combinations of those functions are required. It is now high time we take a look at what these special functions look like. I collect their definitions and main properties in Sect. 3.3. After this mathematical interlude, I will discuss a few approaches to write down the explicit solution in practice in Sect. 3.4, and in Sect. 3.5 I will show how even the asymptotic expansion in a limit can be computed systematically using the differential equations. The problem of computing a family of Feynman integrals therefore reduces to the task of finding a canonical basis. I will tackle this issue in Sect. 3.6.

3.3 Special Functions

The canonical form of the differential equations (3.158) makes it manifest that the solution can be written down perturbatively in terms of iterated integrals with logarithmic integration kernels. In Sect. 3.3.1 I give a precise mathematical definition of what we call iterated integrals, and discuss some of their salient properties. For a thorough discussion I refer to the notes by F. Brown [48]. While iterated integrals can be very convenient to work with, it is often desirable to have expressions in terms of more specific special functions, which for instance allow for a more efficient numerical evaluation. We know that the unitarity of the S-matrix demands the presence of special functions with branch cuts in its matrix elements. The simplest example is of course the logarithm, but much wilder functions show up in scattering amplitudes. In Sects. 3.3.2 and 3.3.3 I present the classical polylogarithms and the multiple polylogarithms. These generalisations of the logarithm play a prominent role in the computation of scattering amplitudes. Their importance stems from the fact that, whenever the letters of an alphabet are d logs with rational arguments, the iterated integrals can be expressed in terms of multiple polylogarithms. This is often true even in the presence of square roots, as we will see. Having defined these special functions is however not particularly useful unless we can work with them comfort-

ably. To this end, I first define some vocabulary in Sect. 3.3.4, where I introduce the notions of transcendental weight and of pure functions. Next, I argue that any pure function generates a system of differential equations in the canonical form, and that the latter can be used very conveniently to manipulate the multiple polylogarithms. Finally, in Sect. 3.3.6 I introduce our most powerful weapon to simply expressions containing multiple polylogarithms—the symbol—and show how it encodes in a minimal and elegant way the analytic information.

3.3.1 Chen's Iterated Integrals

Let $\omega_1, \ldots, \omega_n$ be smooth 1-forms on a smooth manifold M, and let $\gamma : [0, 1] \to M$ be a piecewise smooth path on M. In the context of Feynman integrals, M is the kinematic space and $\{\omega_i\}_{i=1}^n$ is the alphabet. The (Chen) iterated integral of $\omega_1, \ldots, \omega_n$ along γ is defined by [49]

$$\int_\gamma \omega_1 \ldots \omega_n = \int_{0 \le t_1 \le \cdots \le t_n \le 1} f_1(t_1) dt_1 \ldots f_n(t_n) dt_n \,, \qquad \forall n > 0 \,, \tag{3.50}$$

where the functions f_i are defined by pulling back the 1-forms ω_i to the interval $[0, 1]$,

$$f_i(t) dt = \gamma^* \omega_i \,. \tag{3.51}$$

For an exact 1-form $d\Omega(z)$ the pull-back with the contour γ is given by

$$\left(\gamma^* d\Omega\right)(t) = \frac{\partial \Omega\big|_{z=\gamma(t)}}{\partial t} dt \,. \tag{3.52}$$

The empty iterated integral, namely the case $n = 0$, is defined to be the constant 1. In general, we will consider $\mathbb{Q}$-linear combinations of iterated integrals of the form (3.50). In this thesis we will be interested in logarithmic 1-forms only, $\omega_i = d \log \alpha_i$.

Let us look at a few basic properties. The iterated integrals are independent on the parameterisation of the path γ. Given two paths $\alpha, \beta : [0, 1] \to M$ such that $\alpha(1) = \beta(0)$, let $\alpha\beta$ denote the composed path obtained by integrating first along α and next along β. Then,

$$\int_{\alpha\beta} \omega_1 \ldots \omega_n = \sum_{i=0}^{n} \int_\alpha \omega_1 \ldots \omega_i \int_\beta \omega_{i+1} \ldots \omega_n \,. \tag{3.53}$$

The iterated integrals satisfy the shuffle relations

$$\int_\gamma \omega_{a_1} \ldots \omega_{a_s} \int_\gamma \omega_{b_1} \ldots \omega_{b_t} = \sum_{\vec{c} \in \vec{a} \sqcup\!\sqcup \vec{b}} \int_\gamma \omega_{c_1} \ldots \omega_{c_{s+t}} \,, \tag{3.54}$$

where $\vec{a} = (a_1, \ldots, a_s)$, and similarly for $\vec{b}$ and $\vec{c}$. The sum runs over the shuffle product of the lists $\vec{a}$ and $\vec{b}$, namely the set of the lists which contain all the elements of $\vec{a}$ and $\vec{b}$, for which the ordering of the elements of $\vec{a}$ and $\vec{b}$ is preserved.

Integrability Conditions

Let us now consider a contour γ from a fixed base point $z_0 = \gamma(0) \in M$ to a generic point $z = \gamma(1) \in M$. We would like the iterated integral $\int_\gamma \omega_1 \ldots \omega_n$ to be a (multi-valued) function of z. In general, this is not the case, because the iterated integrals depend on the choice of γ. Since there is an infinite continuum of contours from z_0 to z, the iterated integral does not evaluate to a (multi-valued) function. In order for this to be the case, the iterated integral must be a homotopy functional. In other words, given two contours with the same endpoints that can be deformed continuously into each other, the value of the integral along the two must be the same. As a result, if the manifold M is contractible, the iterated integral depends only on the end-point z (we consider the base point z_0 as fixed) and is thus a single-valued function. If the manifold M has punctures, the iterated integral is a multi-valued function of z, since it also depends on the homotopy class of the contour γ, namely on how it wiggles around the punctures to reach to end-point. This defines the choice of the branch of the multi-valued function. This requirement imposes constraints on the set of 1-forms $\{\omega_i\}_{i=1}^n$.

Let us consider the 1-fold iterated integral $I_1 = \int_\gamma \omega$. It is a homotopy functional if and only if ω is closed, namely if $d\omega = 0$. This is a consequence of Stokes' theorem,

$$\oint_\gamma \omega = \int_D d\omega \,, \tag{3.55}$$

where γ is a closed loop encircling the disk $D \subset M$. If we assume that I_1 is a homotopy functional, then the integral on the left-hand side of Eq. (3.55) vanishes for any closed loop. The integral on the right-hand side thus vanishes for every small disk D centered in any point of M. This implies that $d\omega = 0$ everywhere in M. On the other hand, any closed form is locally exact by Poincaré's lemma, namely there exists a potential function α such that $\omega = d\alpha$ locally. Therefore, $d\omega = 0$ implies that the integral around any small loop vanishes. As a result, the first constraint is that the 1-forms are closed,

$$d\omega_i = 0 \,, \qquad \forall i = 1, \ldots, n \,. \tag{3.56}$$

Let us now consider the 2-fold iterated integral $\int_\gamma \omega_1 \omega_2$. The constraint (3.56) implies that there exists a function $F_2(z) = \int_\gamma \omega_2$. The 2-fold iterated integral can thus be expressed as a 1-fold one,

$$\int_\gamma \omega_1 \omega_2 = \int_\gamma F_2 \omega_1 \,, \tag{3.57}$$

and we know that this is a homotopy functional if and only if $d(F_2\omega_1) = 0$. Since $d\omega_1 = 0$ and $dF_2 = \omega_2$, $\int_\gamma \omega_1\omega_2$ is a homotopy functional if and only if $\omega_1 \wedge \omega_2 = 0$. We see therefore that, for generic 1-forms ω_1 and ω_2, the iterated integral $\int_\gamma \omega_1\omega_2$ is not a homotopy functional, but the symmetric combination

$$\int_\gamma (\omega_1\omega_2 + \omega_2\omega_1) \tag{3.58}$$

is. In general we are therefore interested in $\mathbb{Q}$-linear combinations of integrals of the form (3.50).

By iterating this procedure one can work out the constraints for a generic $\mathbb{Q}$-linear combination of n-fold iterated integrals. Given a set of closed 1-forms $\{\omega_1, \ldots, \omega_n\}$, the iterated integral

$$\int_\gamma \sum_{I=(i_1,\ldots,i_n)} c_I\, \omega_{i_1} \ldots \omega_{i_n} \qquad (c_I \in \mathbb{Q}) \tag{3.59}$$

is a homotopy functional if and only if [49, 50]

$$\sum_{I=(i_1,\ldots,i_n)} c_I\, \omega_{i_1} \otimes \cdots \otimes \omega_{i_k} \wedge \omega_{i_{k+1}} \otimes \cdots \otimes \omega_{i_n} = 0\,, \qquad \forall k = 1, \ldots, n-1\,. \tag{3.60}$$

These constraints are referred to as *integrability conditions*.

In this thesis we will be concerned with iterated integrals of logarithmic forms, or d log forms, $\omega_i = d\log\alpha_i$ on the kinematic space. In this case it is customary to label the d log form $d\log\alpha_i$ by its argument α_i only. Denoting by $\{x_a\}_{a=1}^m$ the set of independent kinematic variables, the integrability conditions (3.60) become

$$\sum_{I=(i_1,\ldots,i_n)} c_I \left(\frac{\partial \log\alpha_{i_k}}{\partial x_a} \frac{\partial \log\alpha_{i_{k+1}}}{\partial x_b} - (a \leftrightarrow b) \right) \alpha_{i_1} \otimes \cdots \otimes \hat{\alpha}_{i_k} \wedge \hat{\alpha}_{i_{k+1}} \otimes \cdots \otimes \alpha_{i_n} = 0\,, \tag{3.61}$$

for all $k = 1, \ldots, n-1$, and for all pairs of kinematic variables (x_a, x_b). The hat denotes omission as usual. Clearly, if the kinematic space is described by only one variable the integrability conditions are automatically satisfied.

Therefore, an integrable iterated integral with fixed base point $\gamma(0) = z_0$ and variable end-point $\gamma(1) = z$ defines a multivalued function of z. This motivates the following notation

$$[\alpha_1, \ldots, \alpha_n]_{z_0}(z) = \int_\gamma d\log\alpha_1 \ldots d\log\alpha_n\,, \qquad \forall n > 1\,, \tag{3.62}$$

and $[]_{z_0}(z) = 1$. Note that such a function vanishes by definition at the base point, $[\alpha_1, \ldots, \alpha_n]_{z_0}(z_0) = 0$. The differential is given by

$$d\,[\alpha_1, \ldots, \alpha_n]_{z_0}(z) = d\log\alpha_n(z)\,\big[\alpha_1, \ldots, \alpha_{n-1}\big]_{z_0}(z)\,. \tag{3.63}$$

The definition (3.62) and the differential rule (3.63) generalise to $\mathbb{Q}$-linear combinations of iterated integrals in the obvious way. A function which can be expressed as a linear combination of integrable iterated integrals of $d\log$ forms is assigned a *transcendental weight*, which is loosely defined as the number of iterated integrations. For now it will play the role of a useful label for the functions and constants presented in Sects. 3.3.2 and 3.3.3. The precise definition and its importance will be discussed in full glory in Sect. 3.3.4.

Linear Independence of the Iterated Integrals

If we consider a set of linearly independent $d\log$ forms $\{d\log\alpha_i\}_{i=1}^n$, namely if

$$\sum_{i=1}^{n} c_i\, d\log\alpha_i = 0 \quad\Longleftrightarrow\quad c_i = 0\;\forall i = 1\ldots, n\,, \tag{3.64}$$

then (integrable) iterated integrals $[\alpha_1, \ldots, \alpha_n]_{z_0}(z)$ with the same argument z but different entries drawn from $\{\alpha_i\}_{i=1}^n$ give rise to linearly independent functions. This means that all the complicated functional relations satisfied by transcendental functions—we will see many examples in the next sections—are automatically implemented when they are expressed in terms of iterated integrals. In the context of scattering amplitudes, this means that we can check all sorts of cancellations, e.g. when subtracting UV/IR poles, at the level of the iterated integrals. This is a great advantage, since solving the differential equations for the basis integrals in terms of iterated integrals is completely straightforward, as we will see in Sect. 3.4.4. In general, the non-trivial aspect remains how to express a given function in terms of iterated integrals with letters drawn from a given alphabet. In Sects. 3.3.5 and 3.3.6 I discuss how to do this using the canonical differential equations and the symbol associated with an iterated integral.

Tangential Base Points

It is sometimes convenient to integrate starting from a pole of the integrand or, in other words, from a point which does not belong to the space M where the differential form is defined. We talk in this case of a *tangential base point*. For instance, consider the 1-form $d\log z$. It is defined on $M = \mathbb{C}\backslash\{0\}$, but it is possible to define the iterated integral $[d\log z]_0$ with base point at $z = 0$ in a regulated sense. Let $\gamma : [0, 1] \to M$ be a smooth path from 0 to some point $z \in M$. Let us make an educated choice,

$$\gamma(t) = t + t^2(z-1)\,. \tag{3.65}$$

We can regulate the divergence by integrating on the interval $[\delta, 1]$, with δ small and positive ($0 < \delta \ll 1$),

$$\int_\delta^1 (\gamma^* d\log z) = \log z - \log(1 + \delta(z-1)) - \log\delta\,. \tag{3.66}$$

In general, one has the expansion

$$\int_\delta^1 (\gamma^* d\log z)(\gamma^*\omega_2)\ldots(\gamma^*\omega_n) = a_0(z,\delta) + a_1(z,\delta)\log\delta + \cdots + a_n(z,\delta)\log^n\delta\,, \tag{3.67}$$

where the functions $a_i(z,\delta)$ are analytic at $\delta = 0$. The regularised value is defined by formally setting $\log\delta$ to 0, and letting $\delta = 0$ in the remaining, e.g.

$$\mathrm{Reg}\left[d\log z, \omega_2, \ldots, \omega_n\right]_0(z) = a(z,0)\,. \tag{3.68}$$

From Eq. (3.66) we therefore see that

$$\mathrm{Reg}[d\log z]_0(z) = \log z\,. \tag{3.69}$$

This definition is of course not unique. If we integrate along a straight line from 0 to z, $\rho(t) = tz$, then

$$\int_{\delta'}^1 (\rho^* d\log z) = -\log\delta'\,. \tag{3.70}$$

which in turn results in an awkward

$$\mathrm{Reg}[d\log z]_0(z) = 0\,. \tag{3.71}$$

This is where the *tangential* nature of the base point becomes relevant. Consider a generic change of the regularisation parameter $\delta' = c_1\delta + c_2\delta^2 + \cdots$, where $c_1 \neq 0$. Then,

$$\log\delta' = \log\delta + \log c_1 + \mathcal{O}(\delta)\,. \tag{3.72}$$

This means that the result of the regularisation depends on $c_1 = \partial\delta'/\partial\delta$ only. The difference between Eqs. (3.69) and (3.71) is therefore due to a different regulator, with $c_1 = 1/z$. This is related to the derivative of the path at the base point, hence the adjective "tangential." We see in fact that $\gamma'(0) = 1$, whereas $\rho'(0) = z$. Therefore, an iterated integral with a tangential base point depends not only on the end-points of the integration path γ, but also on the tangent $\gamma'(0)$. One can define a corresponding notion of homotopy for paths γ with the same values of $\gamma(0)$, $\gamma(1)$ and $\gamma'(0)$.

3.3.2 Classical Polylogarithms

The classical polylogarithm Li_n is defined by the power series

$$\mathrm{Li}_n(z) = \sum_{k=1}^{\infty} \frac{z^k}{k^n}, \qquad \forall n \in \mathbb{N}, \tag{3.73}$$

which converges to a holomorphic function in the unit circle $|z| \leq 1$. The first polylogarithm is simply the ordinary logarithm, $\mathrm{Li}_1(z) = -\ln(1-z)$. The second, called dilogarithm, was defined and studied by Landen and Euler more than two centuries ago. The higher polylogarithms were defined in [51]. The definition (3.73) can be analytically continued to a multivalued holomorphic function on $\mathbb{C}/\{0,1\}$ through the differential relation

$$\frac{d}{dz}\mathrm{Li}_n(z) = \frac{1}{z}\mathrm{Li}_{n-1}(z), \qquad \forall n > 1, \tag{3.74}$$

or equivalently through the iterated integration

$$\mathrm{Li}_n(z) = \int_0^z \frac{dt}{t}\mathrm{Li}_{n-1}(t), \qquad \forall n > 1, \tag{3.75}$$

with the recursion starting from the logarithm. Equation (3.73) defines the principal branch for $|z| \leq 1$. It is straightforward to verify that the classical polylogarithm Li_n can be expressed as a Chen iterated integral of $d\log$ forms,

$$\mathrm{Li}_n(z) = -\big[1-z, \underbrace{z, \ldots, z}_{n-1}\big]_0(z). \tag{3.76}$$

The points 0 and 1 are special. The monodromies around them are given respectively by [48]

$$\mathcal{M}_0\mathrm{Li}_n(z) = \mathrm{Li}_n(z), \tag{3.77}$$

$$\mathcal{M}_1\mathrm{Li}_n(z) = \mathrm{Li}_n(z) + \frac{2i\pi}{(n-1)!}\log^{n-1}(z). \tag{3.78}$$

This result has important consequences. First of all, we see that it still makes sense to talk about the value of the classical polylogarithm at 0 and 1,

$$\mathrm{Li}_n(0) = 0, \qquad \mathrm{Li}_n(1) = \zeta(n)\ (\mathrm{Re}(n) > 1). \tag{3.79}$$

Secondly, $z = 1$ is a branch point. We take the branch cut to lie along the interval $[1, \infty)$. Finally, although the principal branch of $\mathrm{Li}_n(z)$ defined by Eq. (3.73) is holomorphic at the origin $z = 0$, its Riemann surface is ramified there. Analytically continuing around $z = 1$ in fact brings in a term $\log^{n-1}(z)$, which is singular at the origin.

The knowledge of the monodromies of the classical polylogarithm can be used to construct a single-valued version of it, by combining classical polylogarithms in z and its complex conjugate $\bar{z}$ in such a way that all the discontinuities cancel. One way to do so is [52]

$$D_n(z) = \mathfrak{R}_n\left[\sum_{k=0}^{n-1} \frac{2^k B_k}{k!} \log^k |z| \mathrm{Li}_{n-k}(z)\right], \tag{3.80}$$

where $\mathfrak{R}_n$ denotes

$$\mathfrak{R}_n(f) = \begin{cases} 2\mathrm{Re}(f), & \text{if } n \text{ odd}, \\ 2i\mathrm{Im}(f), & \text{if } n \text{ even}, \end{cases} \tag{3.81}$$

and B_k are the Bernoulli numbers

$$B_0 = 1, \qquad B_1 = -\frac{1}{2}, \qquad B_2 = \frac{1}{6}, \qquad \ldots \tag{3.82}$$

The single-valued classical polylogarithms $D_n(z)$ are real-analytic functions on the punctured complex plane $\mathbb{C}\backslash\{0, 1\}$, namely they are infinitely smooth and their Taylor series around any point has a finite radius of convergence. In 0 and 1 they are continuous but not differentiable, due to singularities of the type $x \log x$ there. For $n = 2$, Eq. (3.80) reproduces the well-known Bloch–Wigner dilogarithm [53],

$$D_2(z) = \mathrm{Li}_2(z) - \mathrm{Li}_2(\bar{z}) + \frac{1}{2}(\log(1-z) - \log(1-\bar{z}))\log(z\bar{z}), \tag{3.83}$$

where $\bar{z}$ is the complex conjugate of z.

The classical polylogarithms satisfy a plethora of functional identities. The classic example are the two reflection rules of the dilogarithm,

$$\mathrm{Li}_2\left(\frac{1}{z}\right) = -\mathrm{Li}_2(z) - \frac{1}{2}\log^2(-z) - \frac{\pi^2}{6}, \qquad \forall z \in D_1, \tag{3.84}$$

$$\mathrm{Li}_2(1-z) = -\mathrm{Li}_2(z) - \log(z)\log(1-z) + \frac{\pi^2}{6}, \qquad \forall z \in D_2, \tag{3.85}$$

valid in the domains $D_1 = \mathbb{C}\backslash[0, \infty)$ and $D_2 = \mathbb{C}\backslash\{(-\infty, 0] \cup [1, \infty)\}$, respectively. Much more complicated relations exist, even for the dilogarithm. For instance, the exotic two-variable five-term relation,

$$\begin{aligned} &\mathrm{Li}_2(x) + \mathrm{Li}_2(y) + \mathrm{Li}_2\left(\frac{1-x}{1-xy}\right) + \mathrm{Li}_2(1-xy) + \mathrm{Li}_2\left(\frac{1-y}{1-xy}\right) \\ &= \frac{\pi^2}{2} - \log(x)\log(1-x) - \log(y)\log(1-y) + \log\left(\frac{1-x}{1-xy}\right)\log\left(\frac{1-y}{1-xy}\right), \end{aligned} \tag{3.86}$$

for $x, y \in \mathbb{C}\backslash\{(-\infty, 0] \cup [1, \infty)\}$, which provides an intriguing link to cluster algebras discussed in Sect. 3.3.6. While the reflection rules are rather easy to prove by differentiating, the five-term relation is already more cumbersome. The complexity escalates quickly as we go to higher n. This can be a serious concern if we want to use the classical polylogarithms to express scattering amplitudes and Feynman integrals. Indeed, finding compact expressions is not only a matter of aesthetic elegance, which of course is indispensable. From the theoretical point of view, elegant formulae allow us to highlight properties and spot patterns otherwise obscured. From the phenomenological point of view, we want to be able to evaluate the scattering amplitudes numerically in a fast and reliable way. Expressions containing very complicated zeros due to unresolved functional identities are no good. In Sect. 3.3.6 I will discuss a method to derive and implement these relations in a simple and systematic way.

3.3.3 Goncharov Polylogarithms

The Goncharov Polylogarithms (GPLs) (or multiple polylogarithms) constitute a particularly important representative of Chen iterated integrals of logarithmic 1-forms $d \log \alpha_i$. We refer to any function which can be expressed in terms of GPLs as "polylogarithmic." The reason of this importance is that, if the arguments α_i are rational functions and the base point is algebraic, it is always possible to express an integrable iterated integral in terms of GPLs evaluated at algebraic arguments. What is more, this can be done algorithmically. If the α_i are not rational, however, this is no longer possible in general. No algorithm exists and we know at least one explicit example of iterated integral of d log forms with arguments that cannot be rationalised which evaluates to non-polylogarithmic functions [33]. Nevertheless, we also know of many examples of iterated integrals of non-rational d log forms which can be evaluated in terms of GPLs (see e.g. [32]).

The GPLs can be defined recursively through the iterated integral [31, 54]

$$G(a_1, a_2, \ldots, a_n; x) := \int_0^x \frac{dt}{t - a_1} G(a_2, \ldots, a_n; t)\,, \qquad \forall n \in \mathbb{N}\,, a_n \neq 0\,, \tag{3.87}$$

with the recursion starting from

$$G(; x) := \begin{cases} 0\,, & \text{if } x = 0\,, \\ 1\,, & \text{otherwise}\,. \end{cases} \tag{3.88}$$

It is customary to refer to $\vec{a} = (a_1, \ldots, a_n)$ and to x as the indices and the argument of $G(a_1, \ldots, a_n; x)$, respectively, although we will consider it to be a function of the indices as well. The number of iterated integrations, or equivalently the number of indices, is called the transcendental weight of a GPL.

Trailing zeros, namely zeros on the right-most side of the index vector (e.g. $a_n = a_{n-1} = \cdots = a_p = 0$ for some p, $1 \leq p \leq n$), are special, because the integral in Eq. (3.87) diverges. One can however define the GPLs with trailing zeros in a regularised sense as Chen iterated integrals with a tangential base point with unit tangent. In fact, this is exactly what we have done in Eq. (3.69) for the weight-1 case. In practice, GPLs with trailing zeros are allowed through the definition

$$G(\vec{0}_n; x) := \frac{1}{n!} \log^n x \,, \tag{3.89}$$

where we have introduced the short-hand notation $\vec{a}_n = (a, \ldots, a)$, with a repeated n times.

The GPLs have an extremely rich structure, and enjoy a variety of interesting mathematical properties. I will content myself with mentioning those which are useful in the applications presented in this thesis. A useful reference for a more complete discussion is [55], where the authors also present the useful MATHEMATICA package POLYLOGTOOLS to work with the GPLs. The more demanding reader is invited to take on the original papers [31, 54].

First of all, GPLs satisfy a *shuffle algebra* [56]: any product of two GPLs of weights w_1 and w_2 can be expressed as a linear combination with integer coefficients of GPLs of weight $w_1 + w_2$ through the shuffle product relation

$$G(\vec{a}; x)G(\vec{b}; x) = \sum_{\vec{c} \in \vec{a} \sqcup\!\sqcup \vec{b}} G(\vec{c}; x) \,, \tag{3.90}$$

where $\vec{a} \sqcup\!\sqcup \vec{b}$ denotes the shuffle product of the lists $\vec{a}$ and $\vec{b}$.

If there are no trailing zeros, the Goncharov polylogarithms are invariant under the rescaling of all their arguments,

$$G(ka_1, \ldots, ka_n; kx) = G(a_1, \ldots, a_n; x) \,, \quad \forall k \in \mathbb{C}\backslash\{0\} \quad (a_n \neq 0) \,, \tag{3.91}$$

In the presence of trailing zeros, it is possible to shuffle them away through Eq. (3.90) and rescale the arguments in the separate terms (see [28, 30] for an explicit algorithm). Only if all the indices a_i are zero this is not possible, but then Eq. (3.89) holds. In practice, one can study $G(a_1, \ldots, a_n; 1)$ without loss of generality.

The GPLs can have a very rich branch cut structure. Let us focus on GPLs of the form $G(a_1, \ldots, a_n; 1)$ to simplify the discussion. As can be seen from the definition (3.87), $G(a_1, \ldots, a_n; 1)$ is in general not well defined whenever one of the indices a_i lies along the integration contour, namely whenever $a_i \in [0, 1]$ for some $i = 1, \ldots, n$. In fact, there is a discontinuity whenever some index a_i crosses the real axis between 0 and 1. These segments define all the branch cuts of the GPLs. Therefore, if one of the indices $a_i \in [0, 1]$, it is necessary to choose which branch of the function we are interested in. In practice, this is done by perturbing slightly the indices lying on the integration path with the addition of a small positive or negative imaginary part.

The GPLs of the form $G(a_1, \ldots, a_n; 1)$ have an end-point singularity if the left-most indices are 1 ($a_1 = a_2 = \cdots = a_p = 1$ for some p, $0 \leq p \leq n$). We can regularise them by introducing a small positive cutoff $0 < \delta \ll 1$ as $G(a_1, \ldots, a_n; 1 - \delta)$. This defines a *tangential end-point* (see the discussion of the tangential base points in Sect. 3.3.1), which depends on the tangent at the end-point $\gamma'(1)$. The logarithmic divergences $\log \delta$ can then be extracted easily using the shuffle algebra (3.90). E.g., for $a \neq 1$,

$$\begin{aligned} G(1, a; 1 - \delta) &= G(a, 1; 1 - \delta) - G(a; 1 - \delta) G(1; 1 - \delta) = \\ &= G(a, 1; 1) - G(a; 1) \log \delta + \mathcal{O}(\delta) \,. \end{aligned} \tag{3.92}$$

If more than one of the left-most indices is equal to 1, the GPL can be expanded as

$$G(\vec{1}_p, a_{p+1}, \ldots, a_n; 1 - \delta) = \sum_{k=0}^{p} c^{(n-k)}(\delta) \log^k \delta \,, \qquad a_{p+1} \neq 1, \tag{3.93}$$

where the coefficients $c^{(w)}$ are given by weight-w GPLs with indices drawn from the set $\{1, a_{p+1}, \ldots, a_n\}$ and are finite in the limit $\delta \to 0$. They can be determined by applying the shuffle algebra iteratively, in the very same way one can shuffle the trailing zeros away. The regularised value is then defined by formally setting $\log \delta$ to 0, but it is often useful to keep track of the logarithmic divergences as well. It is worth stressing one more time that the result of the end-point regularisation depends on the tangent at the end-point, $\gamma'(1)$.

The GPLs, seen as functions of all the arguments, satisfy the first-order differential equation [54]

$$\begin{aligned} dG(a_{n-1}, \ldots, a_1; a_n) = \sum_{i=1}^{n-1} & G(a_{n-1}, \ldots, \hat{a}_i, \ldots, a_1; a_n) \\ & \times (d \log (a_i - a_{i+1}) - d \log (a_i - a_{i-1})) \,, \end{aligned} \tag{3.94}$$

where the hatted indices are removed. This formula is valid in the generic case where all the arguments are mutually different and do not take particular values.

An important subset of the Goncharov polylogarithms are the Harmonic Polylogarithms (HPLs) $H(a_1, \ldots, a_n; x)$ [28], corresponding to the case where all the indices a_i are 0 or ± 1. The harmonic polylogarithms are equal to the Goncharov polylogarithms up to the sign,

$$H(a_1, \ldots, a_n; x) = (-1)^p G(a_1, \ldots, a_n; x) \,, \qquad a_i \in \{0, \pm 1\} \; \forall i = 1, \ldots, n \,, \tag{3.95}$$

where p is the number of indices a_i equal to $+1$. A vast collection of useful routines to work with the HPLs is implemented in the MATHEMATICA package HPL [57].

It is also worth mentioning that the GPLs are equivalent to another class of functions often used in the physics literature, the MPLs [31]. The latter are defined by

generalising the sum which defines the classical polylogarithms (3.73) to the multivariate case,[4]

$$\mathrm{Li}_{m_1,\ldots,m_n}(x_1,\ldots,x_n) := \sum_{0<k_1<\cdots<k_n}^{\infty} \frac{x_1^{k_1}}{k_1^{m_1}} \cdots \frac{x_n^{k_n}}{k_n^{m_n}}\,, \tag{3.96}$$

for $|x_i| < 1\ \forall i = 1,\ldots,n$. The two classes of functions are related by

$$\mathrm{Li}_{m_1,\ldots,m_k}(x_1,\ldots,x_k) = (-1)^k G\left(\vec{0}_{m_k-1}, \frac{1}{x_k}, \ldots, \vec{0}_{m_1-1}, \frac{1}{x_1\ldots x_k}; 1\right)\,. \tag{3.97}$$

This formula provides the analytic continuation of the nested-sum definition of the MPLs by Eq. (3.96).

While the iterated integral definition (3.87) induces on the GPLs the shuffle algebra structure thanks to the shuffle product (3.90), the nested sum definition (3.96) leads to another algebra structure, called the *stuffle algebra*. Since this will not play a role in the applications presented in this thesis, I will content myself with an example,

$$\mathrm{Li}_{k_1,k_2}(x,y) + \mathrm{Li}_{k_2,k_1}(y,x) = \mathrm{Li}_{k_1}(x)\mathrm{Li}_{k_2}(y) - \mathrm{Li}_{k_1+k_2}(xy)\,. \tag{3.98}$$

The connection between classical polylogarithms and the values of the Riemann zeta function $\zeta(n)$ at positive integers n given by Eq. (3.79) generalises to the MPLs. Just like the values at 1 of the classical polylogarithms define the ordinary zeta values $\zeta(n)$, the values at 1 of the MPLs define the Multiple Zeta Values (MZVs),

$$\zeta(m_1,\ldots,m_k) = \mathrm{Li}_{m_k,\ldots,m_1}(1,\ldots,1)\,, \qquad m_1,\ldots m_k \in \mathbb{N}\,. \tag{3.99}$$

It is conjectured that all the relations among the MZVs follow from the shuffle and stuffle algebras. This implies that no relation among MZVs of different weight exists. Moreover, writing down and solving all the shuffle and stuffle relations systematically allows us to construct an explicit basis of the MZVs at each weight [58–60]. Remarkably, the first MZV that cannot be written as a polynomial in ordinary zeta values appears only at weight eight. In this thesis we will content ourselves with using functions with transcendental weight up to four. The corresponding MZVs can all be written in terms of $\zeta(2) = \pi^2/6$ and $\zeta(3)$ only.

In a few special cases, the GPLs can be rewritten for arbitrary weight in terms of classical polylogarithms. We have already seen one such case in Eq. (3.89). Other examples are

$$G(\vec{a}_n; x) = \frac{1}{n!}\log^n\left(1-\frac{x}{a}\right)\,, \qquad G(\vec{0}_{n-1}, a; x) = -\mathrm{Li}_n\left(\frac{x}{a}\right)\,. \tag{3.100}$$

[4] Note that the reverse summation convention is sometimes used.

Moreover, all GPLs up to weight 3 can be rewritten in terms of classical polylogarithms [54, 61, 62]. For instance,

$$G(a,b;x) = \mathrm{Li}_2\left(\frac{b-x}{b-a}\right) - \mathrm{Li}_2\left(\frac{b}{b-a}\right) + \log\left(1-\frac{x}{b}\right)\log\left(\frac{x-a}{b-a}\right), \tag{3.101}$$

valid for $|\mathrm{Im}(a/x)| > |\mathrm{Im}(b/x)|$ [63]. Only starting from weight 4 we can see a genuine MPL, $\mathrm{Li}_{2,2}$, that cannot be expressed in terms of classical polylogarithms. Reference [63] provides the relations to rewrite any GPL up to weight 4 in terms of classical polylogarithms and $\mathrm{Li}_{2,2}$.

Let me finish this excursus with a practical note. Routines for the numerical evaluations of the GPLs without any restrictions on the weight and the number of variables are implemented with arbitrary precision arithmetic in C++ within the GiNaC framework [64]. Therefore, once a result is written in terms of GPLs, it can be evaluated easily and reliably. However, expressions in terms of GPLs are in general not the most compact, due to the abundance of functional equations between them. I discuss how find and implement the latter systematically in Sect. 3.3.6.

3.3.4 The Transcendental Weight

Given a polylogarithmic function f that can be expressed as a $\mathbb{Q}$-linear combination of integrable iterated integrals of $d\log$ forms with an algebraic base point z_0,

$$f(z) = \sum_{I=(i_1,\ldots,i_W)} c_I \left[\alpha_{i_1},\ldots,\alpha_{i_W}\right]_{z_0}(z), \qquad (c_I \in \mathbb{Q}), \tag{3.102}$$

its *transcendental weight* (or transcendentality) $\mathcal{T}$ is defined as the number of iterated integrations,

$$\mathcal{T}(f) = W. \tag{3.103}$$

Clearly, $\mathcal{T}(f_1 f_2) = \mathcal{T}(f_1) + \mathcal{T}(f_2)$. On the other hand, $\mathcal{T}(f_1 + f_2)$ is well defined only if $\mathcal{T}(f_1) = \mathcal{T}(f_2)$. The transcendental weights of the special functions introduced in the previous sections are

$$\mathcal{T}(\log z) = 1, \qquad \mathcal{T}(\mathrm{Li}_n(z)) = n, \qquad \mathcal{T}(G(a_1,\ldots,a_n;z)) = n. \tag{3.104}$$

This definition generalises straightforwardly to any constant that can be expressed as a $\mathbb{Q}$-linear combination of integrable iterated integrals of $d\log$ forms with algebraic end-points. For instance, $\mathcal{T}(\pi) = 1$, since $\log(-1) = \pm i\pi$, and i and -1 are algebraic. Similarly, one can show that

$$\mathcal{T}(\log c) = 1\,, \qquad \mathcal{T}\left(\zeta(n)\right) = n\,, \qquad \mathcal{T}\left(\zeta(m_1,\ldots,m_k)\right) = m_1 + \cdots + m_k\,, \tag{3.105}$$

for any algebraic constant $c \neq 0, 1$.

The rigorous mathematician might rightfully feel uneasy. Not much is known about the transcendentality of the polylogarithms and of the MZVs. For instance, we know that π, e, and $\log q$ for any algebraic $q \neq 0, 1$ are transcendental. It follows that the even zeta values $\zeta(2n)$ are also transcendental, since

$$\zeta(2n) = \frac{(-1)^{n+1} B_{2n} (2\pi)^{2n}}{2(2n)!}\,. \tag{3.106}$$

For the odd zeta values, we basically only know that $\zeta(3)$ is irrational [65]. Even less is known about the transcendentality of the classical polylogarithms at values other than 1, or of the more general GPLs. Nonetheless, it proves useful to adopt the widely-accepted conjecture that all polylogarithmic functions and MZVs are transcendental.

The careful reader might have noticed that all the relations I presented are uniform in the transcendental weight. Whether there exist relations among polylogarithms or zeta values of different weight is an extremely interesting and still open problem. As we conjecture that the polylogarithms are transcendental, it is also convenient to conjecture that relations which are not uniform in the transcendental weight are not possible. This has very strong implications. Let $\mathcal{P}_n$ be the vector space over $\mathbb{Q}$ spanned by all the weight-n GPLs and their values at algebraic arguments. We set $\mathcal{P}_0 = \mathbb{Q}$. The conjecture implies that the vector space of all GPLs, $\mathcal{P}$, is the direct sum of all the $\mathcal{P}_n$,

$$\mathcal{P} = \bigoplus_{n=0}^{\infty} \mathcal{P}_n\,. \tag{3.107}$$

The vector space $\mathcal{P}$ can be equipped with a product, e.g. the shuffle product (3.90), thus becoming a commutative algebra. Since the shuffle product preserves the weight, the GPLs form a graded algebra. One could go very far along this road. The algebra $\mathcal{P}$ can in fact be equipped also with a coproduct as well [66], leading to the conclusion that the GPLs form a Hopf algebra. Clearly there are a lot of interesting aspects to be discussed here, but this would take us too far. The purpose of this paragraph is to get the mathematically-inclined readers interested in the topic. In the hope I succeeded, I refer them to [67] for a thorough and pedagogical discussion.

The notion of transcendental weight is very tightly related to the differential equations in the canonical form. In order to see this, we need to introduce two more concepts. A function f which is given by a sum of terms with the same transcendental degree is said to have a *uniform transcendental degree*. An ever stronger property with respect to the transcendentality is that of purity. A function f is *pure* if its transcendental weight is lowered by differentiation, i.e. if $\mathcal{T}(df) = \mathcal{T}(f) - 1$. While the uniform transcendentality can accommodate algebraic factors, the latter spoil the

purity of a function, as they are "seen" by the differential operators (unless they are constant, of course). The canonical differential equations (3.35) imply that the canonical basis integrals $\vec{g}$ have uniform transcendental weight at each order in ϵ.[5] This becomes clear e.g. in Eq. (3.42): the kth term in the Laurent expansion around $\epsilon = 0$ is given by a $\mathbb{Q}$-linear combination of weight-k iterated integrals. There is more. It is conventional to assign transcendental weight -1 to the dimensional regulator $\epsilon = (4-d)/2$. One way to justify this is to think of the poles in ϵ as logarithms in some cut-off Λ, $1/\epsilon \sim \log \Lambda$. Then, it follows from the canonical differential equations that

$$\mathcal{T}(d\vec{g}) = \mathcal{T}(d\widetilde{A}) + \mathcal{T}(\vec{g}) - 1\,. \tag{3.108}$$

In the cases we are interested in, $d\widetilde{A}$ is a logarithmic 1-form, as in Eq. (3.43), and therefore it has transcendental weight 0. As a result, $\mathcal{T}(d\vec{g}) = \mathcal{T}(\vec{g}) - 1$, namely the canonical basis integrals are pure functions. This is not just a mathematical fun fact. The idea that the transcendental purity is marred by algebraic factors, for instance, gives us a precious hint on how to find a canonical basis of integrals, as I discuss in Sect. 3.6.

The transcendental weight is also related to a very fascinating conjecture about scattering amplitudes. Let us consider an ℓ-loop scattering amplitude $\mathcal{A}^{(\ell)}$ computed in dimensional regularisation in $D = D_0 - 2\epsilon$ dimensions for some even positive integer D_0,

$$\mathcal{A}^{(\ell)} = \sum_{k \geq k_0} \epsilon^k \mathcal{A}_k^{(\ell)}\,, \tag{3.109}$$

where $k_0 \in \mathbb{Z}$. If the coefficients of the series $\mathcal{A}_k^{(\ell)}$ can be written in terms of iterated integrals of logarithmic 1-forms, the empirical observation leads to the conjecture that

$$\mathcal{T}\left(\mathcal{A}_k^{(\ell)}\right) \leq \frac{D_0 \ell}{2} + k\,. \tag{3.110}$$

For instance, if we are interested in computing a two-loop amplitude for $D_0 = 4$ up to the finite part, we need functions with transcendental weight up to four. A lot of empirical evidence suggests that this bound is exactly saturated in $\mathcal{N} = 4$ super Yang–Mills theory. This conjecture, apart from being of great theoretical interest, has also very important practical consequences. It opens the door to bootstrap approaches for computing scattering amplitudes or Feynman integrals. For instance, the kth term in the ϵ-expansion of the ℓ-loop amplitude $\mathcal{A}^{(\ell)}$ has the generic form

$$\mathcal{A}_k^{(\ell)} = \sum_{w=0}^{\ell D_0/2+k} \sum_{i,j} c_{ij} R_i F_j^{(w)}\,, \tag{3.111}$$

[5] Of course I am assuming that the base point is algebraic. It would be unreasonable to do differently.

where $c_{ij} \in \mathbb{Q}$, R_i are algebraic functions, and $F_j^{(w)}$ are weight-w integrable iterated integrals (eventually allowing also for special values). Given an alphabet, the integrability conditions imply there is only a finite number of integrable iterated integrals at each transcendental weight. Constructing them explicitly can be reduced to a linear algebra problem, and can thus be done very efficiently (see e.g. [68, 69]). It is sometimes possible to make a guess for the algebraic functions R_i as well. For instance, the notion of leading singularity discussed in Sect. 3.6.1 gives a handle on them. Then, only the rational constants c_{ij} remain the be fixed. The problem of computing $\mathcal{A}_k^{(\ell)}$ therefore reduces to finding a sufficient number of constraints to determine the constant coefficients (e.g. collinear and soft limits, symmetries...). In [70], for instance, I bootstrap a two-loop five-particle integral using conformal symmetry.

3.3.5 *On the Naturalness of the Canonical Form*

We have seen that the differential equations in the canonical form imply that the canonical integral bases are given by transcendental pure functions. The reverse is true as well. Any pure function satisfies a differential equation in the canonical form.

Consider a weight-w (integrable) iterated integral $s^{(w)}$. Since it is a pure function, its differential is expressed in terms of weight-$(w-1)$ iterated integrals. Choose a set of linearly independent ones, $\vec{s}^{\,(w-1)}$, and differentiate them too. Their differential involves weight-$(w-2)$ iterated integrals, out of which we extract a basis $\vec{s}^{\,(w-2)}$. Continue differentiating until we reach the bottom, weight zero, where by definition we have the constant 1. Then, it is convenient to introduce a parameter, ϵ, to which we assign transcendental weight $\mathcal{T}(\epsilon) = -1$. This auxiliary parameter merely serves to package all the iterated integrals together in a vector with a uniform transcendental weight,

$$\vec{S} = \left(\epsilon^w s^{(w)}, \epsilon^{w-1}\vec{s}^{\,(w-1)}, \ldots, \epsilon\vec{s}^{\,(1)}, 1\right)^T . \tag{3.112}$$

In Feynman integral computations this role is played by the dimensional regulator. It is easy to see that the vector $\vec{S}$ satisfies a differential equation in the canonical form,

$$d\vec{S} = \epsilon\, d\tilde{B} \cdot \vec{S} . \tag{3.113}$$

In particular, since the differential lowers strictly by 1 the transcendental weight of a pure symbol, the matrix $\tilde{B}$ is strictly block upper triangular. It is thus nilpotent, $\tilde{B}^{w+1} = 0$. If it were not nilpotent, the solution of the differential equation would in general be non-zero at orders in ϵ higher than w. This is the norm in the case of a Feynman integral, but here it would be absurd, since we know exactly the dependence on ϵ of $\vec{S}$, given by Eq. (3.112).

For example, let us consider the weight-2 iterated integral

$$s^{(2)} = -\left[1-z, z\right]_0(z) . \tag{3.114}$$

Upon differentiation it generates the vector

$$\vec{S}(z,\epsilon) = \left(-\epsilon^2[1-z,z]_0(z), \epsilon[1-z]_0(z), 1\right)^T . \tag{3.115}$$

The corresponding differential equation is

$$d\vec{S} = \epsilon \begin{pmatrix} 0 & -d\log z & 0 \\ 0 & 0 & d\log(1-z) \\ 0 & 0 & 0 \end{pmatrix} \cdot \vec{S} . \tag{3.116}$$

Thanks to its (strictly) upper triangular form, this equation is very easy to solve by hand (and even easier using MATHEMATICA's DSOLVE). Since we know the expression of $\vec{S}$ in terms of iterated integrals, given by Eq. (3.115), we can just read off the boundary values at the base point $z = 0$,

$$\vec{S}(0,\epsilon) = (0,0,1)^T . \tag{3.117}$$

The solution for $z < 1$ is then given by

$$\vec{S} = \left(\epsilon^2 \mathrm{Li}_2(z) , \epsilon \log(1-z), 1\right)^T . \tag{3.118}$$

Once we are able to solve the differential equations in the canonical form, the procedure I just outlined can also be used to switch from one representation of a function to another. In this case we started off with an iterated integral and solved the associated differential equation in terms of classical polylogarithms. We could have solved it in terms of GPLs or HPLs as well. Similarly, we could have started from $\mathrm{Li}_2(z)$ and solved the differential equation in terms of iterated integrals. I will give a more interesting example in Sect. 3.4.4.

This simple argument shows that the canonical form (3.113) is the natural form of the differential equations for any family of Feynman integrals which can be expressed in terms of polylogarithmic functions. An arbitrary choice of integral basis may obscure the underlying elegance of the differential equations and it may be very difficult to unveil it, but we must have faith that it is there.

3.3.6 The Symbol

The story of the first application of the symbol in theoretical physics is a very inspiring one. A heroic computation—in its own inspiring!—led to a 17-page expression in terms of thousands of GPLs for a quantity called the six-point remainder function in $\mathcal{N} = 4$ super Yang–Mills theory [71, 72]. Strongly motivated by a firm belief in the beauty of that theory, the authors of [73] took a rather abstract mathematical construct, the symbol [66, 74], and used it to simplify the known expression for the

six-point remainder function. The result was astonishingly simple: just a few lines of classical polylogarithms. Since then, the symbol has been used in many successful applications, and has by now become a standard weapon in multi-loop computations.

The reason for its success is that the symbol is an extremely simple tool that manages to capture the main analytical and combinatorial properties of the polylogarithmic functions. In particular, all functional equations among MPLs are conjectured to be in the kernel of the symbol. In other words, a necessary condition for two expressions written in terms of MPLs to be equal is that they have the same symbol. As we will see, this is much simpler to check. Going back from symbol to function is a much harder problem, for which no algorithm that works in general is known. The methods presented in Sects. 3.3.6, 3.4.3 and 3.4.5 can be used for this purpose. I refer to [75] for a complete discussion.

The symbol map can be defined by its action on the Chen iterated integrals of logarithmic 1-forms. It maps linearly a k-fold iterated integral to the k-fold tensor product of its 1-forms,

$$\mathcal{S}\left(\int_\gamma d\log\alpha_1 \dots d\log\alpha_n\right) := d\log\alpha_1 \otimes \dots \otimes d\log\alpha_n \equiv \alpha_1 \otimes \dots \otimes \alpha_n \,. \tag{3.119}$$

This definition generalises to all functions of uniform transcendental weight by linearity. It is customary to omit the $d\log$ sign to simplify the notation, but really we should keep in mind that each entry α of a symbol actually stands for the 1-form $d\log\alpha$. The symbol in fact inherits from the $d\log$ differential a number of basic properties,

$$A \otimes (a \times b) \otimes B = A \otimes a \otimes B + A \otimes b \otimes B \,, \tag{3.120}$$

$$A \otimes \left(\frac{a}{b}\right) \otimes B = A \otimes a \otimes B - A \otimes b \otimes B \,, \tag{3.121}$$

where A and B denote elementary tensors of arbitrary length, and a and b are algebraic functions. Consequently,

$$A \otimes a^n \otimes B = n\,(A \otimes a \otimes B) \,, \tag{3.122}$$

where we stress that, on the right-hand side, n is a coefficient in front of the symbol in the parenthesis, rather than part of the first entry. Moreover, any symbol with a constant entry vanishes,

$$A \otimes c \otimes B = 0 \,, \qquad \text{if } c \text{ constant} \,. \tag{3.123}$$

This follows trivially from the fact that the differential of any constant is zero, in other words $d\log c = 0$ for any constant c. Of course part of the information is lost as a result of this. It is possible to extend the notion of symbol so as to accommodate rational numbers in the entries as well, this way recovering part of the informa-

tion [75]. This is not necessary for the work presented here, and I therefore adopt the original convention of [73] given by Eq. (3.123).

The symbol inherits straightforwardly many properties from the iterated integrals as well. The symbols satisfy the shuffle product relations (3.54),

$$(\alpha_{a_1} \otimes \cdots \otimes \alpha_{a_s}) \times (\alpha_{b_1} \otimes \cdots \otimes \alpha_{b_t}) = \sum_{\vec{c} \in \vec{a} \sqcup\!\sqcup \vec{b}} \alpha_{c_1} \otimes \cdots \otimes \alpha_{c_{s+t}} \,. \tag{3.124}$$

Furthermore, a $\mathbb{Q}$-linear combination of tensors,

$$S = \sum_{I=(i_1,\ldots,i_n)} c_I \, \alpha_{i_1} \otimes \cdots \otimes \alpha_{i_n} \qquad (c_I \in \mathbb{Q}) \,, \tag{3.125}$$

represents a function if and only if it satisfies the integrability conditions given by Eq. (3.61). As a result, given an alphabet, there is only a finite number of integrable symbols at each transcendental weight.

Despite its simplicity, the symbol retains most of the analytic information of the corresponding function. From the formula for the differential of the (integrable) iterated integrals (3.63) it follows that

$$d\,(\alpha_1 \otimes \cdots \otimes \alpha_n) = d \log \alpha_n \, (\alpha_1 \otimes \cdots \otimes \alpha_{n-1}) \,. \tag{3.126}$$

The last entry of an (integrable) symbol therefore encodes its differential information. The first entry, on the other hand, captures the branch cut structure in a beautifully manifest way. A function $f(z)$ whose symbol has the schematic form

$$\mathcal{S}\,[f(z)] = \alpha_1(z) \otimes \cdots \otimes \alpha_n(z) \,, \tag{3.127}$$

has branch cuts (in its canonical sheet) starting at the points z_i such that $\alpha_1(z_i) = 0$ or $\alpha_1(z_i) = \infty$. The symbol of the discontinuity across the branch cut is given by

$$\mathcal{S}\,[\mathrm{Disc}\, f(z)] = \mathrm{Disc}\,(\log \alpha_1(z)) \;\; \alpha_2(z) \otimes \cdots \otimes \alpha_n(z) \,. \tag{3.128}$$

If $f(z)$ is a Feynman integral or a scattering amplitude, its discontinuities are determined by the Cutkosky's rules. As a result, the first entries are subject to constraints. I address this and other important aspects of the symbol more in detail in the next few sections.

How to Compute the Symbol

The differential rule given by Eq. (3.126) can be seen as an iterative definition of the symbol. If the differential of a weight-w function $\mathcal{F}^{(w)}$ has the form

$$d\mathcal{F}^{(w)} = \sum_i c_i \, \mathcal{F}_i^{(w-1)} \, d \log \alpha_i \,, \tag{3.129}$$

where $c_i \in \mathbb{Q}$, $\mathcal{F}_i^{(w-1)}$ are weight-$(w-1)$ functions and α_i are algebraic functions, then

$$\mathcal{S}\left(\mathcal{F}^{(w)}\right) = \sum_i c_i \, \mathcal{S}\left(\mathcal{F}_i^{(w-1)}\right) \otimes \alpha_i \,. \tag{3.130}$$

The recursion starts with $\mathcal{S}(\log \alpha) = (\alpha)$, understood as a 1-fold tensor product. Computing the symbol of a function can therefore be done systematically by taking derivatives. For instance, let us consider the classical polylogarithm. From

$$d\mathrm{Li}_n(z) = \mathrm{Li}_{n-1}(z) d\log z \qquad \forall n \in \mathbb{N}\,, \tag{3.131}$$

together with the starting point of the recursion $\mathrm{Li}_1(z) = -\log(1-z)$, one can immediately read off the symbol,

$$\mathcal{S}\left(\mathrm{Li}_n(z)\right) = -(1-z) \otimes \underbrace{z \otimes \cdots \otimes z}_{n-1} \,. \tag{3.132}$$

This is in manifest agreement with the iterated integral representation given in Eq. (3.76). The symbol of the GPLs can be computed iteratively using the differentiation formula (3.94).

Beyond the Symbol

The iterative definition of the symbol makes it clear that the symbol captures the *leading functional transcendentality* part of a function. Any term given by a transcendental constant times a lower-weight function is annihilated by the symbol map. It can be useful to be pedantic once in a while, so consider for example the dummy expression

$$a = \mathrm{Li}_2(z) + i\pi \log z + \pi^2 \,. \tag{3.133}$$

Differentiating removes the constant piece,

$$da = -\log(1-z) d\log z + i\pi d\log z \,. \tag{3.134}$$

By applying the iterative definition the symbol we obtain

$$\mathcal{S}(a) = -\mathcal{S}\left(\log(1-z)\right) \otimes z + \mathcal{S}(i\pi) \otimes z \,. \tag{3.135}$$

Since symbols with constant entries vanish, we can conclude that

$$\mathcal{S}\left(\mathrm{Li}_2(z) + i\pi \log z + \pi^2\right) = \mathcal{S}\left(\mathrm{Li}_2(z)\right) \,, \tag{3.136}$$

namely only the leading functional transcendentality part of the function is captured by the symbol. The terms which are in the kernel of the symbol map are referred to as "beyond-the-symbol" terms.

This is not a tragic loss. The symbol in fact keeps track of the most complicated part of the function. What is lost has a lower transcendental weight, from the functional point of view, and it is therefore easier to recover a posteriori. From this very simple example we understand that what we lose when taking the symbol are the "$i\pi$"-terms, which encode the information on the branch of the function, and the constant terms, related to the boundary constants of the iterated integrals. In this sense, the symbol is equivalent to an iterated integral stripped of the information on the integration contour,

$$\alpha_1 \otimes \cdots \otimes \alpha_n \equiv [\alpha_1, \ldots, \alpha_n] \,, \tag{3.137}$$

where I intentionally omit the argument and the base point in the iterated integral on the right-hand side. In order to obtain a function corresponding to a given symbol, therefore, it is sufficient to upgrade the latter to iterated integral by making a physically motivated choice of the branch, and an arbitrary choice of the base point. This straightforwardly produces a legitimate function with the correct symbol. Nonetheless, one might not be satisfied with an iterated integral, and would like to have a more explicit expression in terms of standard functions.

One way to do so is offered by the differential equations in the canonical form. The symbol in fact retains all the differential information of the corresponding iterated integral. Given a symbol S, we may want to find a function f such that $\mathcal{S}(f) = S$. We can write down a canonical differential equation for a vector of functions which contains f together with a tower of lower-weight functions, the very same way we did in Sect. 3.3.5 for the iterated integrals. Starting from the symbol of the iterated integral in Eq. (3.115), for example, we can write down the same differential equation shown in Eq. (3.116). The only difference is that we can no longer fix the boundary values (except for the weight-0 function, which is always 1 by definition). This freedom reflects the freedom of the terms beyond the symbol. For example, the solution of Eq. (3.116) with no boundary values fixed for the symbols has the form

$$\vec{S} = \left(\epsilon^2 \left(\mathrm{Li}_2(z) - c_1 \log(z) + c_2\right) \,, \epsilon \left(\log(1-x) + c_1\right) \,, 1\right)^T \,, \tag{3.138}$$

where c_1 and c_2 are arbitrary weight-1 and 2 constants. The problem of associating a function to a symbol therefore is equivalent to that of solving the differential equations in the canonical form. Section 3.4 is devoted to discussing several approaches to do so.

The take-home message of this section is that the symbol encodes all the information on the branch cuts of the function and on how to differentiate it, and captures entirely its most complicated part. Considering what a simple object the symbol is, that is pretty good.

Proving Functional Relations with the Symbol

In the previous sections we have seen many functional identities relating polylogarithmic functions. All these complicated relations simply reduce to the algebraic rules given by Eqs. (3.120), (3.121) and (3.123) at the symbol level. Proving a relation among polylogarithmic functions using the symbol is therefore straightforward. First, one computes the symbol of both sides of the equation, either iteratively using Eq. (3.130) or by applying known rules such as the one for the classical polylogarithms given by Eq. (3.132). For example, for the dilogarithm relation (3.84) this gives

$$-\left(1-\frac{1}{z}\right)\otimes\frac{1}{z}=(1-z)\otimes z-z\otimes z\,. \tag{3.139}$$

Next, the separate symbols have to be expanded out by factorising their entries and then applying Eqs. (3.120), (3.121) and (3.123) until all the entries are simple factors. This makes the cancellations apparent. From Eq. (3.139) we get

$$(z-1)\otimes z-z\otimes z=(1-z)\otimes z-z\otimes z\,. \tag{3.140}$$

Note that Eqs. (3.120) and (3.123) imply that

$$A\otimes(-a)\otimes B=A\otimes a\otimes B\,, \tag{3.141}$$

for any elementary tensors A and B. The two sides of Eq. (3.140) are thus the same, which proves that the most complicated part of the relation is correct. Finally, one has to fix the terms beyond the symbol. This can be done using various arguments, such as analyticity at some point, differentiation and numerical evaluations. In this case, we can miss terms of the generic form "$\pi\times\log$" and "π^2", where log and π denote generically a weight-1 function and constant, respectively. One way to constrain the "$\pi\times\log$"-terms is by differentiating. This in fact produces a strictly-lower weight relation, which is simpler to prove than the original one. In the case at hand we immediately see that no "$\pi\times\log$" is needed. The constant can be determined with a single evaluation of both sides of the relation, this way completing the proof of Eq. (3.84). It is important to stress that any relation has a precise domain of validity, to which the point where we decide to evaluate must belong. The domain of validity of the relation also suggests a heuristic but faster way of ruling out the "$\pi\times\log$"-terms. Since the arguments of the functions in the relation (3.84) do not involve constants other than ±1, it is reasonable to assume that the only weight-1 constant that can potentially show up is $i\pi$, which typically comes from the analytic continuations. For $z<0$ the weight-2 functions captured by the symbol are manifestly real, so that no $i\pi$ is needed. If we traded $\log(-z)$ for $\log(z)$ on the right-hand side of Eq. (3.84), the symbol would still vanish, but there would be no domain where all the functions are well-defined. As a result, the analytic continuation would be required, together with factors of $i\pi$.

This first example was almost trivial. Let us look at the much more interesting five-term identity (3.86). A theorem states that all the relations among dilogarithms

follow from the five-term identity [76]. Moreover, it has a hidden $\mathbb{Z}_5$ symmetry, and a fascinating connection with cluster algebras. In order to unveil these two aspects, it is convenient to introduce the Rogers L-function,

$$L(x) = \mathrm{Li}_2(x) + \frac{1}{2}\log x \log(1-x)\,. \tag{3.142}$$

It captures the part of the dilogarithm whose symbol is anti-symmetric,

$$\mathcal{S}\left[L(x)\right] = -\frac{1}{2}(1-x)\wedge x\,, \tag{3.143}$$

where the factor of $1/2$ is a prefactor of the tensor, and $a\wedge b := a\otimes b - b\otimes a$. Note that the symmetric part of a weight-2 symbol can always be written in terms of products through the shuffle relations (3.124),

$$a\otimes b + b\otimes a = \mathcal{S}(\log a \log b)\,. \tag{3.144}$$

The logarithms on the right-hand side of Eq. (3.86) can then be absorbed in the definition of the Rogers L-function, so that the five-term identity takes a tidier form,

$$L(x) + L(y) + L\left(\frac{1-x}{1-xy}\right) + L(1-xy) + L\left(\frac{1-y}{1-xy}\right) = \frac{\pi^2}{2}\,. \tag{3.145}$$

Next, consider the recursive sequence

$$1 - a_i = a_{i-1}a_{i+1}\,. \tag{3.146}$$

It is easy to prove that it has periodicity 5, namely that $a_{i+5} = a_i$. This recursion is (a slightly modified version of) the cluster coordinate mutation of the cluster algebra A_2 [77]. The five-term identity can then be expressed as

$$\sum_{i=1}^{5} L(a_i) = \frac{\pi^2}{2}\,, \tag{3.147}$$

which makes manifest the $\mathbb{Z}_5$ symmetry. The choice $a_1 = x, a_2 = (1-x)/(1-xy)$ produces the identity as in Eq. (3.145). In order to prove Eq. (3.147), let us compute the symbol of the right-hand side,

$$\mathcal{S}\left[\sum_{i=1}^{5} L(a_i)\right] = -\frac{1}{2}\sum_{i=1}^{5}(1-a_i)\wedge a_i\,. \tag{3.148}$$

Using the definition of the sequence in Eq. (3.146) and the multi-linearity of the symbol (3.120) gives

$$\mathcal{S}\left[\sum_{i=1}^{5} L(a_i)\right] = -\frac{1}{2}\sum_{i=1}^{5} (a_{i-1} \wedge a_i + a_{i+1} \wedge a_i) \,. \tag{3.149}$$

Next, we use the periodicity of the sequence to shift the indices in the first term of the summand,

$$\mathcal{S}\left[\sum_{i=1}^{5} L(a_i)\right] = -\frac{1}{2}\sum_{i=1}^{5} (a_i \wedge a_{i+1} + a_{i+1} \wedge a_i) \,. \tag{3.150}$$

Finally, the anti-symmetry implies that the symbol vanishes,

$$\mathcal{S}\left[\sum_{i=1}^{5} L(a_i)\right] = 0 \,. \tag{3.151}$$

The beyond-the-symbol terms can only be of the generic form "$\pi \times \log$" and "π^2", where log and π denote generically a weight-1 function and constant, respectively. It is easy to see that the derivatives of $\sum_{i=1}^{5} L(a_i)$ vanish, so that there is no "$\pi \times \log$" term. Also in this case, these terms could be excluded heuristically by noting that all the functions are real in the region $0 < x, y < 1$. The remaining weight-2 constant can be determined with a single evaluation, e.g. at $x = 0$, $y = 0$. Using that $L(0) = 0$ and $L(1) = \pi^2/6$ gives the complete functional identity,

$$\sum_{i=1}^{5} L(a_i) = \frac{\pi^2}{2} \,. \tag{3.152}$$

Symbols and Branch Cuts

We have seen that the first entry of a symbol encodes its branch cut structure. In particular, a function has branch cuts starting where the first entry of its symbol vanishes or diverges. This means that the first entries of the symbol of a Feynman integral or a scattering amplitude are constrained by physics through the Cutkosky's rules. For Feynman integrals with massless propagators, this implies that the first entry in the symbol can only be a Mandelstam invariant, i.e. of the form $(p_i + \cdots + p_k)^2$ [78].

One might naïvely expect that only the functions which satisfy the first-entry condition appear in the result for a scattering amplitude or a Feynman integral. For instance, consider the scattering of four massless particles. The kinematics is described by two independent Mandelstam invariants, say s and t, and a third one is related to them by momentum conservation, $u = -s - t$. Only the functions $\log s$, $\log t$ and $\log u$ are allowed by the first-entry condition at weight 1. The hasty physicist might conclude that no other logarithm can appear. Let us make an explicit example to see why this expectation is wrong.

The function

$$\mathrm{Li}_2\left(1-\frac{t}{s}\right) \tag{3.153}$$

is well-defined in the region $t/s \in \mathbb{C}\backslash(-\infty, 0]$, and it satisfies the first-entry condition, since

$$\mathcal{S}\left[\mathrm{Li}_2\left(1-\frac{t}{s}\right)\right] = -t \otimes \left(1-\frac{t}{s}\right) + s \otimes \left(1-\frac{t}{s}\right). \tag{3.154}$$

Our goal is to analytically continue it from the Euclidean region $\{s < 0, t < 0\}$ to the s-channel $\{s > 0, t < 0\}$.

One simple way to do it is through Euler's inversion formula (3.85),

$$\mathrm{Li}_2\left(1-\frac{t}{s}\right) = -\mathrm{Li}_2\left(\frac{t}{s}\right) - \log\left(\frac{t}{s}\right)\log\left(1-\frac{t}{s}\right) + \frac{\pi^2}{6}, \tag{3.155}$$

which is valid in the region $t/s \in \mathbb{C}\backslash\{(-\infty, 0] \cup [1, \infty)\}$. Of the functions on the right-hand side, only $\log(t/s)$ is problematic for $s > 0, t < 0$. Analytically continuing a logarithm is however very simple. The Feynman prescription for the propagators instructs us to add a small, positive imaginary part to each Mandelstam invariant, i.e. $s \to s + i0^+$ and similarly for t. As a result, the analytic continuation of the function in Eq. (3.153) to the s-channel is given by

$$-\mathrm{Li}_2\left(\frac{t}{s}\right) - \log\left(\frac{-t}{s}\right)\log\left(1-\frac{t}{s}\right) - i\pi\log\left(1-\frac{t}{s}\right) + \frac{\pi^2}{6}. \tag{3.156}$$

This expression has the same symbol as the original function (3.153), and therefore it satisfies the first entry condition. The "$i\pi$"-term at first sight does not. It has a branch cut along $t > s$. The latter, however, does not lie in the s-channel, where $s > 0$ and $t < 0$. In order to access it, e.g. to compute the discontinuity, one would therefore have to analytically continue to a region where t can be greater than s, e.g. the original Euclidean region. There, we know that the function is given by Eq. (3.153), which is clearly well-defined for $t > s$. In summary,

$$\underbrace{\mathrm{Li}_2\left(1-\frac{t}{s}\right)}_{s<0,\,t<0} \longleftrightarrow \underbrace{-\mathrm{Li}_2\left(\frac{t}{s}\right) - \log\left(\frac{-t}{s}\right)\log\left(1-\frac{t}{s}\right) - i\pi\log\left(1-\frac{t}{s}\right) + \frac{\pi^2}{6}}_{s>0,\,t<0}. \tag{3.157}$$

So we see that, in order to represent the result in a certain region, e.g. $\{s > 0, t < 0\}$, it may be necessary to use functions which do not satisfy the first entry condition on their own, such as $\log(1 - t/s)$ on the right-hand side of Eq. (3.157).

This is a practical complication, but it does not mean that the full result has unphysical discontinuities. In fact, it is very important to highlight that dropping the "$i\pi$"-term on the right-hand side of Eq. (3.157) would produce a function whose

symbol still satisfies the first entry condition, but which does have the unphysical discontinuity across the surface $s = t$.

The take-home message here is that the absence of certain discontinuities implies first entry conditions, but not vice versa. A function which satisfies a first entry condition at symbol level may still exhibit the forbidden branch cut.

Deeper entries in the symbol contain valuable information on the branch cut structure as well. The first entry conditions imply that certain discontinuities, e.g. those associated with letters that are not Mandelstam invariants, are not visible in the canonical Riemann sheet of the Feynman integrals (or scattering amplitudes). It does not mean that they are completely absent. They can in fact be exposed through analytic continuation. Actually, we have already seen this for the classical polylogarithm $\mathrm{Li}_n(z)$ in Sect. 3.3.2. It is holomorphic at the origin $z = 0$, but its Riemann surface is ramified there. We see from the monodromy around $z = 1$ (3.77) that the analytic continuation across the branch cut $[1, \infty)$ introduces a term with $\log^{n-1} z$, which has a branch cut along the negative real axis $(-\infty, 0]$. This information is contained in the second entry of the symbol, $\mathcal{S}[\mathrm{Li}_n(z)] = -(1-z) \otimes z \otimes \cdots \otimes z$. The formula for the discontinuity (3.128) can in fact be iterated: as the first entry encodes the discontinuity of the principal sheet of the function, the second entry does the same for the discontinuity of the discontinuity, and so on deeper into the symbol.

Physics can therefore impose constraints also on the second entries. An important example of this is given by the Steinmann relations [79–81], which state that a scattering amplitude cannot have double discontinuities in overlapping channels. This constrains strongly the space of functions, and was in fact instrumental in pushing the computations in planar $\mathcal{N} = 4$ super Yang–Mills to astonishing results: the 5-loop six-particle amplitude [82], and the 3-loop NMHV and 4-loop MHV seven-particle amplitudes [83]. As we will see in the next chapter, certain pairs of letters never show up in the first two entries of the massless two-loop five-particle integrals. This is an empirical observation, but it is not outrageous to believe in a physical explanation along the lines of the Steinmann relations. Moreover, other observations have lead to the conjecture that the Steinmann relations actually hold to all depths in the symbol in planar $\mathcal{N} = 4$ super Yang–Mills [84]. Remarkably, the ensuing restrictions on multiple discontinuities are equivalent to the conditions coming from the cluster algebra approach in the form of the cluster adjacency property [85, 86]. Clearly this is a very active area of research. The symbol has still a lot to offer.

3.4 Solving the Differential Equations

Our goal in this section is to solve the system of differential equations in the canonical form,

$$d\vec{g} = \epsilon\, d\widetilde{A} \cdot \vec{g}\,, \tag{3.158}$$

where

$$d\widetilde{A} = \sum_i a_i d\log\alpha_i(m)\,. \tag{3.159}$$

The α_i are algebraic functions of the kinematic variables m called letters, and the a_i are constant rational matrices. We continue with the example of the three-mass triangle integral family, for which the alphabet is shown in Eq. (3.38), and the vector $\vec{g}$ is the (canonical) integral basis given by Eq. (3.28). It is worth stressing that this system of differential equations has a much more general nature, tightly linked with the polylogarithmic nature of the functions. As I argued in Sect. 3.3.5, the differential equations take the canonical form (3.158) for any set of pure functions $\vec{g}$. The parameter ϵ plays the role of bookkeeper of the transcendental weight, and its factorisation is the hallmark of transcendental purity. Being able to solve such a system of differential equations therefore also allows one to manipulate in a very powerful way the polylogarithmic functions introduced in Sect. 3.3.

We have seen that the formal solution of the system (3.158) is given by the path-ordered exponential in Eq. (3.40), which produces $\mathbb{Q}$-linear combinations of iterated integrals of $d\log$ forms at each order in ϵ, as can be seen in Eq. (3.42). In practice, it is convenient to view the formal solution (3.40) as a neat iterative procedure to determine each order in the ϵ-expansion (3.41) in terms of the previous one,

$$\begin{aligned}\vec{g}^{(0)}(m) &= \vec{b}^{(0)}\,,\\ \vec{g}^{(k)}(m) &= \int_\gamma d\tilde{A}\cdot\vec{g}^{(k-1)} + \vec{b}^{(k)}\,, \qquad \forall k>0\,,\end{aligned} \tag{3.160}$$

where $\gamma : [0,1] \to M$ is an integration contour in the kinematic space M from some boundary point $\gamma(0) = m^{(0)}$ to a generic point $\gamma(1) = m$. The details of how this iterative integration is to be interpreted are given in Sect. 3.3.1. In Sect. 3.3 we armed ourselves with a mathematical toolkit to handle such functions. It is time we put it to good use.

Since the solution of the differential equations (3.158) is in general a vector of multi-valued functions, it is crucial to define the domain of the kinematic variables m where we want the result to be valid. I address this in Sect. 3.4.1. Next, in Sect. 3.4.2 I show how the boundary constants $\vec{b}^{(k)}$ can be determined straightforwardly from the differential equations themselves by imposing certain physical constraints. Then, we will finally be in a position to discuss how the solution of the differential equations can be written down. In Sects. 3.4.3, 3.4.4 and 3.4.5 I offer you three different approaches: we can express the solution in terms of GPLs, iterated integrals/symbols or a tailored basis of polylogarithmic functions, respectively. Each of these approaches has its pros and cons, but they should all be in our arsenal.

3.4.1 Kinematic Region and Analytic Continuation

The integrability conditions of the differential equations (3.33) guarantee that the iterated integrals appearing in the solution at each order in ϵ are homotopy functionals. In other words, the result of the integration depends only on the endpoints $m^{(0)}$ and m, and on the homotopy class of the contour γ. Since the $d\log$ forms in the iterated integrals have poles associated with the zeros of the letters, the kinematic space M is punctured, and the basis integrals $\vec{g}$ are thus multi-valued functions. The choice of the branch is dictated by the Feynman prescription in the propagators of Eq. (3.1).

This is a crucial point. It is thus worthwhile to be pedantic at least once. The readers who are even just slightly familiar with the concept of analytic continuation are advised to skip this paragraph, as we are going to make the simplest example possible. Consider the iterated integral

$$h(m_1^2) := \left[m_1^2\right]_{-1}(m_1^2) = \int_\gamma d\log m_1^2\,, \tag{3.161}$$

with the integration contour γ going from $m_1^2 = -1$ to a generic point m_1^2. Here one must not get confused between the m_1^2 in the square brackets, which defines the 1-form $d\log m_1^2$ on the kinematic space, and the one on the parentheses, end-point of the integration contour and argument of the function h. Integrating along a straight line,

$$\gamma(t) = -1 + t(m_1^2 + 1)\,, \qquad t \in [0,1]\,, \tag{3.162}$$

gives

$$h(m_1^2) = \int_0^1 dt \frac{1+m_1^2}{-1+t(1+m_1^2)}\,. \tag{3.163}$$

The integrand has a simple pole at $t = 1/(1+m_1^2)$. If $m_1^2 < 0$, the pole lies outside of the integration domain. The integral is thus well defined and evaluates to

$$h(m_1^2) = \log(-m_1^2)\,, \qquad (m_1^2 < 0)\,. \tag{3.164}$$

If instead $m_1^2 > 0$, the pole lies right on the integration path. In this case, one has to specify whether the contour γ goes around the pole from above or from below. The Feynman prescription tells us to add a small positive imaginary part "$+i0^+$" to each of the masses m_i^2, so that

$$h(m_1^2) = \int_\gamma d\log\left(m_1^2 + i0^+\right) = \int_0^1 \frac{(1+m_1^2)dt}{-1+(1+m_1^2)t+i0^+} = \log(m_1^2) - i\pi\,, \quad (m_1^2 > 0)\,. \tag{3.165}$$

This choice of branch of the logarithm differs from the canonical one, for which we would have that $\log(-1) = +i\pi$. Getting the analytic continuation wrong is therefore

as easy as dangerous. In Sect. 3.4.1 we will see this is in fact the analytic continuation of the logarithm from the so-called Euclidean region, in Eq. (3.164), to the physical scattering region, in Eq. (3.165).

In summary, Feynman integrals evaluate to multi-valued functions, and it is therefore crucial to specify the domain of the variables, which depends on the kinematics of the scattering process. The differential equations are then solved in a specific kinematic region. Results valid in other regions can be obtained through analytic continuation (see e.g. [87]).

The three-mass triangle integrals (3.1) are functions of the masses of the three external legs, $m = (m_1^2, m_2^2, m_3^2)$. The kinematic region of phenomenological interest is given by $m_i^2 > 0 \ \forall i = 1, 2, 3$, which describes the decay of the particle with greatest mass into two lighter particles. Moreover, the triangle integrals in this region contribute also to the scattering amplitude for the production of a pair of weak gauge bosons at higher orders in perturbation theory [15]. I will refer to this region as the *physical region*. The values of the kinematic invariants m in this region correspond to actual angles θ between the particle trajectories (i.e., such that $\sin\theta \in [-1, 1]$) and positive energies.

There is a more convenient region to solve the differential equations in than the physical one. In order to define it, let us take a look at the Feynman parameterisation of a generic element of the three-mass triangle family,

$$I_{a_1,a_2,a_3} = (-1)^a \Gamma\left(a - \frac{d}{2}\right) \int_0^\infty \left(\prod_{i=1}^3 d\alpha_i \frac{\alpha_i^{a_i-1}}{\Gamma(a_i)}\right) \delta\left(1 - \sum_{j\in B} \alpha_j\right) \times \\ (\alpha_1 + \alpha_2 + \alpha_3)^{a-D} \left(-m_1^2\alpha_2\alpha_3 - m_2^2\alpha_1\alpha_2 - m_3^2\alpha_1\alpha_3\right)^{D/2-a}, \tag{3.166}$$

where $a = a_1 + a_2 + a_3$ and B is any non-empty subset of $\{1, 2, 3\}$. Since all the integration variables α_i are non-negative, the entire integrand is manifestly non-negative for $m_i^2 < 0 \, \forall i = 1, 2, 3$. As a result, the integral in Eq. (3.166) is manifestly real, which constitutes a useful simplification in the computation of a Feynman integral. The kinematic region where all the integrals[6] in a family are real is called *Euclidean region*. While all planar integrals have such a region, this is not true in general for non-planar integrals.

In the three-mass triangle case there is an even simpler kinematic region. In order to define it, let us consider the change of variables

$$m_2^2 = m_1^2 z\bar{z}\,, \qquad m_3^2 = m_1^2(1-z)(1-\bar{z})\,. \tag{3.167}$$

[6] Strictly speaking, here I mean only the scalar integrals of the form I_{a_1,a_2,a_3}. One can always rescale any real integral by some square root such that it becomes imaginary. In fact, this is what happens with g_4 (3.28).

The inverse transformation is given by

$$z = \frac{m_1^2 + m_2^2 - m_3^2 + \sqrt{\lambda(m)}}{2m_1^2}, \qquad \bar{z} = \frac{m_1^2 + m_2^2 - m_3^2 - \sqrt{\lambda(m)}}{2m_1^2}. \tag{3.168}$$

The new variables $\{m_1^2, z, \bar{z}\}$ are extremely convenient. First of all, z and $\bar{z}$ are dimensionless. As a result, the dimensionality of the basis integrals g_i is entirely given by an overall factor of $(m_1^2)^{-\epsilon}$. What remains are dimensionless functions of the two variables only, z and $\bar{z}$. Moreover, the change of variables given by Eq. (3.167) rationalises the square root of the Källen function, since $\lambda(m) = m_1^4(z - \bar{z})^2$. The branch of the square root corresponding to Eq. (3.168) is

$$\sqrt{\lambda(m)} = m_1^2(z - \bar{z}). \tag{3.169}$$

In terms of the new variables $\{m_1^2, z, \bar{z}\}$, the Euclidean region is defined by

$$m_1^2 < 0, \qquad z\bar{z} > 0, \qquad (1 - z)(1 - \bar{z}) > 0. \tag{3.170}$$

The presence of the square root of the Källen function divides the Euclidean region into five sub-regions, shown in Fig. 3.3. If $\lambda(m) > 0$, Eq. (3.168) implies that $z, \bar{z} \in \mathbb{R}$. Equation (3.170) then implies three sub-regions: $z, \bar{z} < 0, 0 < z, \bar{z} < 1$, and $z, \bar{z} > 1$. If $\lambda(m) < 0$, instead, we see from Eq. (3.168) that z and $\bar{z}$ are complex conjugate to each other. Finally, the boundary surface $\lambda(m) = 0$ constitutes the fifth sub-region.

It is convenient to choose the region where $\lambda(m) < 0$. There, in fact, the three-mass triangle integrals are single valued [15]. The results can then be analytically continued

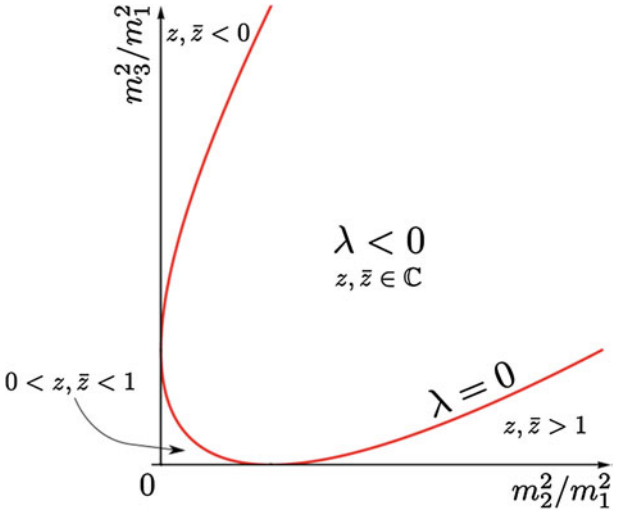

Fig. 3.3 Subdivision of the Euclidean kinematic region for the three-mass triangle integrals. All masses are negative, $m_i^2 < 0 \, \forall i = 1, 2, 3$. The red line denotes the surface $\lambda \equiv \lambda\left(m_1^2, m_2^2, m_3^2\right) = 0$

to any region. In particular, the analytic continuation to the physical scattering region where $m_i^2 > 0 \; \forall i = 1, 2, 3$ is performed by adding a small positive imaginary part to each invariant m_i^2. For the logarithm we have seen that this yields

$$\log(-m_i^2) \longrightarrow \log(-m_i^2 - i0) = \log(m_i^2) - i\pi \,. \tag{3.171}$$

This operation is equivalent to the substitution

$$-m_i^2 \longrightarrow e^{-i\pi} m_i^2 \,. \tag{3.172}$$

The analytic continuation of the three-mass triangle integrals is therefore straightforward. We single out an overall scale from the canonical basis integrals computed in the Euclidean region,

$$g_i(m) = \left(-m_1^2\right)^{-\epsilon} \tilde{g}_i \left(\frac{m_2^2}{m_1^2}, \frac{m_3^2}{m_1^2}\right) , \qquad \text{with } m_i^2 < 0 \; \forall i = 1, 2, 3 \,, \tag{3.173}$$

so that $\tilde{g}_i$ are dimensionless functions of two ratios. Then, the phase factor on the right-hand side of Eq. (3.172) cancels out in the arguments of $\tilde{g}_i$, and the analytic continuation simply amounts to an overall phase factor,

$$g_i(m) = e^{i\pi\epsilon} \left(m_1^2\right)^{-\epsilon} \tilde{g}_i \left(\frac{m_2^2}{m_1^2}, \frac{m_3^2}{m_1^2}\right) , \qquad \text{with } m_i^2 > 0 \; \forall i = 1, 2, 3 \,. \tag{3.174}$$

In general, the analytic continuation of high transcendental weight functions of many variables can be significantly involved. In such a situation, it may be more convenient to by-pass the problem by solving the differential equations separately in each of the kinematic regions we are interested in. In practice, we pick a different base point in each of the kinematic regions and fix the boundary constants there. Then we solve the differential equations in such a way that the integration contour γ never leaves the region the base point lies in. In this way the analytic continuation is avoided altogether, and we obtain separate and reliable expressions for the solution in each of the relevant kinematic regions. In give an example of this strategy in Sect. 4.2.3.

Now that we have decided which region of the kinematic space we want to solve the differential equations in, we need to choose a base point in it. It is convenient to choose a point with as few and as simple numbers as possible. The boundary constants are the values of the basis integrals at the base point. If the latter contains complicated numbers, the resulting expressions for the integrals are polluted by a proliferation of awful constants. See Eq. (3.186) for an example of this. A rather good choice in this case is

$$m^{(0)} := (-1, -1, -1) \,. \tag{3.175}$$

Since the problem involves a square root and we are interested in the kinematic region where its argument is negative, the kinematics is not entirely specified by the values of the three kinematic invariants m_i^2. One must also choose a branch of the square root. My choice is

$$\sqrt{\lambda(m^{(0)})} = +i\sqrt{3}\,, \tag{3.176}$$

which corresponds through Eq. (3.169) to

$$z^{(0)} = e^{-i\pi/3}\,, \qquad \bar{z}^{(0)} = e^{i\pi/3}\,. \tag{3.177}$$

Since no letter of the alphabet (3.38) vanishes at $m^{(0)}$ (3.175), the basis integrals are finite there. It may sometimes be convenient to choose a singular point as base point. We talk in this case of tangential base point (see Sect. 3.3.1). I show in Sect. 3.5 how to integrate the differential equations starting from a singular base point. Having one or more of the kinematic variables set to 0 can in fact simplify dramatically the constants appearing in the expressions of the integrals. I present an example of this in Sect. 4.4.2.

To summarise, we have chosen to solve the differential equations (3.158) in the kinematic region defined by

$$m_i^2 < 0 \;\forall i = 1, 2, 3\,, \qquad \lambda(m) < 0\,, \tag{3.178}$$

where the integrals are single valued. Results valid outside of this region can be obtained through analytic continuation. However, as long as the base point $m^{(0)}$ and the integration contour γ in Eqs. (3.40) or (3.160) stay within the region (3.178), we do not need to worry about the analytic continuation at all.

3.4.2 Boundary Constants

The goal of this section is to determine the boundary constants $\vec{b}(\epsilon)$, namely the values of the basis integrals $\vec{g}$ at the base point $m^{(0)}$ given by Eqs. (3.175) and (3.176). One approach consists in evaluating the integrals numerically, e.g. using pySecDec [7] or FIESTA [6]. At two or more loops, this is very challenging, and even in the best-case scenario gives only a limited accuracy. The approach we are going to follow is instead completely analytical. The basic idea is quite simple. The generic solution of the differential equations in the canonical form (3.158) has singularities on all the hypersurfaces where one of the letters vanishes. Some of these singularities are however unphysical, and must be absent in the solution of the differential equations which corresponds to Feynman integrals. This gives constraints on the boundary constants, which are "fine-tuned" in such a way that the unphysical divergences cancel out. Solving the physical constraints allows one to relate the boundary constants

to a small set of values of the simplest integrals in the family. Typically, only one trivial integral—e.g. a bubble or a product of bubbles in the multi-loop case—has to be computed in some other way to fix entirely the boundary constants. The differential equations are in fact homogeneous, and it is thus inevitable that the overall normalisation is given by some external input.

The three-mass triangle integral family at one loop is particularly simple, as the three single-scale integrals can be easily computed in closed-form,

$$g_i = -e^{\epsilon\gamma_{\mathrm{E}}} \frac{\Gamma^2(1-\epsilon)\Gamma(1+\epsilon)}{\Gamma(1-2\epsilon)} \left(-m_i^2\right)^{-\epsilon} , \qquad \forall i = 1, 2, 3 . \tag{3.179}$$

This result is obtained by rescaling the bubble integral (3.24) according to Eq. (3.25), with the transformation matrix given by Eq. (3.29). From Eq. (3.179) we can immediately read off the boundary values,

$$b_i = -1 + \frac{\pi^2}{6}\epsilon^2 + \mathcal{O}\left(\epsilon^3\right) , \qquad \forall i = 1, 2, 3 . \tag{3.180}$$

The boundary value of the genuine triangle integral g_4 is determined in terms of the previous ones from physical constraints. For arbitrary boundary constants $\vec{b}$ the solution of the differential equations (3.158) is singular on the hypersurface $\lambda(m) = 0$ because of the letter $\alpha_6 = \sqrt{\lambda(m)}$. This singularity is spurious and the solution of the differential equations which corresponds to Feynman integrals must be free of it. We can thus tune the boundary values in such a way that this singularity drops out from the solution.

In practice, we integrate the differential equation (3.158) from $m^{(0)}$ to some point on the hypersurface $\lambda(m) = 0$. The result diverges logarithmically for arbitrary values of the missing constants $b_4^{(k)}$. We fix the latter by requiring that the divergences cancel out. The integration can be performed easily in terms of GPLs or simpler subsets of them. One choice of integration contour is particularly convenient. We keep m_1^2 fixed to its value at the boundary point, and vary m_2^2 and m_3^2 together going to the point $m^* = (-1, -1/4, -1/4)$ such that $\lambda(m^*) = 0$. A convenient parameterisation which rationalises the square root of the Källen function is given by

$$\gamma(t) = \left(-1, \frac{(t-1)(t+1)}{4}, \frac{(t-1)(t+1)}{4}\right) , \tag{3.181}$$

where the parameter t is purely imaginary and ranges from $i\sqrt{3}$ to 0, so that $\gamma(i\sqrt{3}) = m^{(0)}$ and $\gamma(0) = m^*$. This is just a straight line in terms of z and $\bar{z}$ (3.167). The unusual range of the parameter t makes it possible to perform the integration straightforwardly in terms of HPLs, a special subset of the GPLs where the indices are drawn from $\{0, \pm 1\}$ (see Eq. (3.95)). Pulling the letters of the three-mass triangle alphabet (3.38) back with γ (3.181) in fact gives

$$(\gamma^* d\log\alpha_i)(t) = \operatorname*{span}_{\mathbb{Q}}\Big(d\log t, d\log(t-1), d\log(t+1)\Big), \qquad \forall i = 1,\ldots,6, \tag{3.182}$$

which is the alphabet of the HPLs. Moreover, the path (3.181) never leaves the kinematic region $\lambda(m) < 0$, since $\lambda(\gamma(t)) = t^2$ and t is purely imaginary. No analytic continuation is thus required, and the integration can be straightforwardly performed by simply implementing the rules defining the HPLs, given by Eqs. (3.87) and (3.89) with $a_i \in \{0, \pm 1\}$.

As expected, the result of the integration for g_4 diverges. We regulate the divergences by truncating the integration before it reaches the end-point, as discussed in Sect. 3.3.3. In practice, this simply amounts to giving them a name,

$$L := \lim_{t\to 0} H(0;t) = \lim_{t\to 0} \log t\,. \tag{3.183}$$

Up to order ϵ^2, for instance, we have

$$\begin{aligned} g_4\left(m^*\right) = & b_4^{(0)} + \epsilon\left(2b_4^{(0)}L + \cdots\right) + \\ & + \epsilon^2\left[2b_4^{(0)}L^2 + \left(2b_4^{(1)} - 4\log\left(\frac{i\sqrt{3}}{4}\right)b_4^{(0)}\right)L + \cdots\right] + \mathcal{O}\left(\epsilon^3\right), \end{aligned} \tag{3.184}$$

where the dots denote finite terms. Requiring that the integrals are finite at the point m^* thus fixes $b_4^{(0)} = 0 = b_4^{(1)}$.

From this very simple example we can already infer one important feature of this approach: we need to integrate the differential equations up to weight $w+1$ in order to fix the weight-w boundary constants. Up to which weight to integrate thus depends on which order in ϵ the boundary values are needed at. For instance, let us say we are interested in the expression for the triangle integral $I_{1,1,1}$ up to the finite part, namely up to order ϵ^0. We see from the transformation matrix in Eq. (3.29) that

$$I_{1,1,1} = \frac{g_4}{\epsilon^2\sqrt{\lambda}}, \tag{3.185}$$

so that we need the boundary value of g_4 up to order ϵ^2. By integrating the differential equations up to weight 3 and imposing finiteness we obtain

$$b_4(\epsilon) = \epsilon^2 4i\,\mathrm{Im}\left[\mathrm{Li}_2\left(e^{-i\pi/3}\right)\right] + \mathcal{O}\left(\epsilon^3\right). \tag{3.186}$$

The constant appearing at order ϵ^2 might appear surprising. First, it is imaginary although the boundary point is in the Euclidean region. All the scalar Feynman integrals I_{a_1,a_2,a_3} of the family are real in this region, but g_4 has an overall factor of $\sqrt{\lambda}$, which is purely imaginary in the region of interest. Secondly, its value might look rather unnatural. Why would a Feynman integral depend on $e^{-i\pi/3}$? Indeed this is just

an artefact of the representation we are using. Solving the differential equations forces us to choose a boundary point. This point feeds into the intermediate expressions. In fact, note that $e^{-i\pi/3}$ is just the value of z at the boundary point (3.177). Once the full integral g_4 is expressed in terms of functions, this constant drops out. We will see this explicitly in Eq. (3.240).

The appearance of such complicated constants, satisfying highly non-trivial relations, makes this approach unfeasible in the generic case, where the integration is carried out in terms of GPLs. A good strategy consists in evaluating numerically the functions appearing in the result of the integration. It is worth stressing that the integration is carried out analytically in terms of GPLs or other classes of functions, and that only the latter are evaluated numerically (e.g. using the C++ library GiNaC [64]), if necessary with an outrageous number of digits. In this way all the simplifications are immediate and the expressions are as compact as they could possibly be. Once the boundary constants are known numerically, their fully analytic expression can be recovered. In fact, while the constants appearing in the integration depend on the arbitrary choice of contour, the boundary values are strictly related to the alphabet and to the boundary point. It is therefore possible to guess which constants might appear. The numerical boundary constants can then be related to such analytic constants through the PSLQ algorithm [88] or MATHEMATICA's built-in function FINDINTEGERNULLVECTOR.

Finally, note that the approach here described for the three-mass triangle integrals may not give enough constraints to fix all the boundary constants in more complicated cases. For the applications presented in the next chapter, a more refined method was used, based on the same idea of removing unphysical singularities. Applying it to the three-mass triangle case would be an overkill, to put it mildly. Therefore, I refer to [89] for a thorough discussion.

3.4.3 *Solution in Terms of Goncharov Polylogarithms*

Whenever the alphabet is rational, the canonical differential equations can be integrated algorithmically in terms of GPLs (or subsets thereof). Let us consider a rational letter R, and let us assume that, on the integration contour γ, it is given by a degree-n polynomial,

$$R(t) := R\left(m = \gamma(t)\right) = \sum_{k=0}^{n} c_k t^k \,. \tag{3.187}$$

We do not lose generality, since any rational letter can be expressed in terms of polynomial letters through $d\log(N/D) = d\log N - d\log D$. The pull-back of R with the contour γ can then be partial fractioned over $\mathbb{C}$ as

$$(\gamma^* d\log R)(t) = \sum_{t_s : R(t_s)=0} \frac{dt}{t - t_s} \,. \tag{3.188}$$

As a result, the iterated integrations given by Eq. (3.160) can be performed straightforwardly in terms of GPLs by simply implementing their defining formulae (3.87) and (3.89). Loosely speaking, the roots t_s in Eq. (3.188) are added as new indices in the GPLs of the previous order in ϵ.

Clearly there is a practical limitation: if the degree of the polynomial is too high, it might not be possible to express its roots in a closed form. Physics has been gracious enough not to put me in such an uncomfortable situation so far. The letters of the alphabets discussed in this thesis, pulled back with the relevant contours, have at most degree 2. The choice of the contour is however crucial. We want it to rationalise the square roots in the alphabet (at least those which appear simultaneously in a given integration). If possible, we want it to lie within a chosen region of analyticity, to avoid the worry of analytic continuation. And now we see that we also want it to be simple enough that the numerators and denominators of the letters do not have prohibitive polynomial degrees. While the rationalisation of the square roots—if possible—is algorithmic to some extent (see e.g. [90–93]), finding a *good* contour which satisfies all the criteria is an art.

The three-mass triangle alphabet (3.38) becomes rational in the variables $(m_1^2, z, \bar{z})$ defined by Eq. (3.167). In terms of the latter, the letters simplify significantly,

$$\left\{m_1^2, z, \bar{z}, 1-z, 1-\bar{z}, z-\bar{z}\right\} . \tag{3.189}$$

As a result, we can straightforwardly integrate the differential equation along a straight line γ in these variables from the base point (3.175) to a generic point $(m_1^2, z, \bar{z})$,

$$\gamma(t) = \left(m_1^{2(0)}, z^{(0)}, \bar{z}^{(0)}\right) + t\left(m_1^2 - m_1^{2(0)}, z - z^{(0)}, \bar{z} - \bar{z}^{(0)}\right), \tag{3.190}$$

where $m_1^{2(0)} = -1$, and $z^{(0)}$ and $\bar{z}^{(0)}$ are given by Eq. (3.177). I do not spell them out to keep the expressions tidier. It is worth stressing that, as long as the entire contour γ lies in the same kinematic region, no analytic continuation is needed. Moreover, I recall that, thanks to the homotopy invariance, we can choose the path arbitrarily. Sometimes it is more convenient to vary one variable at a time, effectively integrating along a zig-zag path. Different paths can lead to substantially different, although equivalent, expressions.

Pulling back $d\widetilde{A}$ (3.37) with γ (3.190) gives

$$(\gamma^* d\widetilde{A})(t) = \sum_{i=1}^{6} Q_i \frac{dt}{t - q_i} , \tag{3.191}$$

where the Q_i are constant rational matrices and

$$\{q_i\}_{i=1}^6 = \left\{ \frac{m_1^{2(0)}}{m_1^{2(0)} - m_1^2}, \frac{1-z^{(0)}}{z-z^{(0)}}, \frac{z^{(0)}}{z-z^{(0)}}, \frac{1-\bar{z}^{(0)}}{\bar{z}-\bar{z}^{(0)}}, \frac{\bar{z}^{(0)}}{\bar{z}-\bar{z}^{(0)}}, 1 - \frac{z-\bar{z}}{z^{(0)}-\bar{z}^{(0)}} \right\} . \tag{3.192}$$

Substituting the pulled-back $d\tilde{A}$ into the iterative solution of the canonical differential equations (3.160) we immediately recognise the definition of the GPLs (3.87), with argument 1 and indices drawn from the set $\{q_i\}_{i=1}^6$. The constant matrices Q_i tell us which combinations of GPLs are required. A potentially complicated integration therefore reduces to a very basic task of pattern recognition, easy to implement in a computer algebra system.

The differential equations can now be algorithmically solved to any order in ϵ (provided that the boundary constants are available). The solution, however, looks awfully complicated. For example, let us take a look at g_2. It is a bubble, and its closed-form expression is given by Eq. (3.179). It is the archetypical simple integral. Yet, its expression in terms of GPLs coming from the differential equations obscures this simplicity,

$$g_2 = -1 + \epsilon \left[G\left(\frac{m_1^{2(0)}}{m_1^{2(0)} - m_1^2}; 1 \right) + G\left(\frac{z^{(0)}}{z^{(0)} - z}; 1 \right) + G\left(\frac{\bar{z}^{(0)}}{\bar{z}^{(0)} - \bar{z}}; 1 \right) \right] + \mathcal{O}\left(\epsilon^2\right) . \tag{3.193}$$

The first GPL at order ϵ is single valued for $m_1^2 < 0$, but the other two GPLs each have a branch cut for $\mathrm{Re}(z) < 0 \wedge \mathrm{Im}(z) = -\sqrt{3}\mathrm{Re}(z)$. This is spurious, of course, and the discontinuity cancels out between the two. Using Eq. (3.100) to rewrite the weight-1 GPLs in terms of logarithms, massaging the result, and going back to the original variables via Eq. (3.168) then gives

$$g_2 = -1 + \epsilon \log\left(-m_2^2\right) + \mathcal{O}\left(\epsilon^2\right) , \tag{3.194}$$

as expected. Clearly these manipulations become more and more complicated at higher orders in ϵ. For instance, the expression we obtain for g_4 using this approach reads

$$\begin{aligned} g_4 = \epsilon^2 \Big[& \Big(G(q_2, q_3; 1) - G(q_3, q_2; 1) + G(q_2, q_5; 1) - G(q_3, q_4; 1) + 2i\,\mathrm{Im}\left[\mathrm{Li}_2(z^{(0)}) \right] \Big) \\ & - (\text{complex conjugate}) \Big] + \mathcal{O}\left(\epsilon^3\right) . \end{aligned} \tag{3.195}$$

This expression is manifestly anti-symmetric under complex conjugation, i.e. under the exchange $z \leftrightarrow \bar{z}$ or equivalently $\sqrt{\lambda} \leftrightarrow -\sqrt{\lambda}$. This property was expected. The pure integral g_4 is in fact defined by normalising the scalar triangle integral by the square root of the Källen function (see Eq. (3.28)). Since the prefactor is odd and the scalar integral is even under this transformation, it follows that g_4 is odd. All the other features of g_4 are however obscured. This representation in fact exhibits several spurious branch cuts and a spurious dependence on the base point. We must be able to do better than this.

Whenever one is handed over a polylogarithmic function which looks more complicated than it needs to be, the first thing to do is to compute its symbol. Let us define

$$g_4 = \epsilon^2 \tilde{g}_4 + \mathcal{O}\left(\epsilon^3\right) , \tag{3.196}$$

and focus on the function $\tilde{g}_4$. Using the technique discussed in Sect. 3.3.6, it is rather easy to show that the symbol of $\tilde{g}_4$ is given by

$$\mathcal{S}\left(\tilde{g}_4\right) = ([z, 1-z] - [1-z, z] + [1-z, \bar{z}] - [z, 1-\bar{z}]) - (z \leftrightarrow \bar{z}) . \tag{3.197}$$

This formula unveils a lot properties. The dependence on the base point has disappeared, as it should, and the anti-symmetry under the exchange $z \leftrightarrow \bar{z}$ is even more manifest. A few easy algebraic manipulations allow one to rewrite it as

$$\mathcal{S}\left(\tilde{g}_4\right) = \left[z\bar{z}, \frac{1-z}{1-\bar{z}}\right] + \left[(1-z)(1-\bar{z}), \frac{\bar{z}}{z}\right] , \tag{3.198}$$

which manifestly satisfies the first-entry condition, since we recognise that only the Mandelstam invariants m_i^2 appear in the first entries (see Eq. (3.167)). There is even more. The symbol in Eq. (3.198) appears to have branch cuts in the complex plane starting at $z = 0$, $z = 1$ or $z = \infty$. The discontinuities across these branch cuts however cancel out. The discontinuity across the branch cut starting at $z = 0$, for instance, receives contributions from the part of the symbol which has first entry z and the one which has first entry $\bar{z}$,

$$\mathrm{Disc}_{z=0}\left[\mathcal{S}\left(\tilde{g}_4\right)\right] = \mathrm{Disc}_{z=0}\left[\log z\right]\left(\frac{1-z}{1-\bar{z}}\right) + \mathrm{Disc}_{z=0}\left[\log \bar{z}\right]\left(\frac{1-z}{1-\bar{z}}\right) , \tag{3.199}$$

where the parenthesis denote 1-fold symbols. The two terms cancel out, because—in the kinematic region we are considering—z and $\bar{z}$ are complex conjugate to each other,

$$\mathrm{Disc}_{z=0}\left[\mathcal{S}\left(\tilde{g}_4\right)\right] = 0 . \tag{3.200}$$

The same holds for the other branch cuts. The symbol-level analysis thus suggests that $\tilde{g}$ is single valued. I stress that this is just a hint, not a proof. As I argued in Sect. 3.3.6, the absence of a certain discontinuity in a function implies a first-entry condition in its symbol, but the reverse is more subtle due to the terms beyond the symbol. A more careful analysis based on the Hopf algebra of the MPLs can legitimately extend this conclusion to function level [15].

In conclusion, we have seen that it is very simple to solve the differential equations in the canonical form in terms of GPLs if the alphabet is rational. Although the resulting expressions may sometimes be rather complicated, they can be straightforwardly evaluated numerically with arbitrary accuracy (e.g. using GiNaC [64]). This is extremely valuable. In the context of the differential equations, the solution in terms of GPLs plays a particularly important role in determining the boundary

constants, as we have seen in Sect. 3.4.2. Extracting the logarithmic divergences from the GPLs is in fact made extremely simple by the shuffle algebra (3.90).

Before moving on to the other approaches, I want to stress that a surprisingly—for someone who has mainly used the differential equation method like I did—large number of Feynman integrals can actually be integrated directly in terms of GPLs starting from a suitable parametrisation (e.g. the Feynman parameterisation), thanks to powerful algorithms for the symbol integration of GPLs [94, 95]. The three-mass triangle integral g_4 considered here in fact provides a very simple example of this [15]. These algorithms are implemented in the MAPLE package HYPERINT [95].

3.4.4 Solution in Terms of Chen's Iterated Integrals

In the previous section we have seen that, if the alphabet can be rationalised, the solution of the canonical differential equations can be written down in terms of GPLs algorithmically. This approach has the advantage that the result can be straightforwardly evaluated numerically, but the need to rationalise the square roots in the alphabet is a serious limitation. Even when that is possible, the new variables might make the expressions of the integrals rather complicated. Moreover, the separate functions appearing in the results satisfy a multitude of complicated functional identities. Writing the solution of the differential equations in terms of Chen's iterated integrals, on the other hand, is straightforward regardless of how many square roots are present in the alphabet. Moreover, if the alphabet has been chosen so that the letters $\{\alpha_i\}$ are linearly independent—as it should always be—the separate "words" $[\alpha_1, \ldots, \alpha_n]$ are guaranteed to be independent as well. The functional identities are thus automatically implemented, and the expression in terms of iterated integrals is uniquely determined by the choice of letters and of the base point. As a result, even though they cannot be evaluated numerically directly, the iterated integrals are very useful to check cancellations and to study the analytic properties of the result.

In practice, solving the canonical differential equations in terms of iterated integrals is as easy as it could possibly be. Because of the differentiation formula given by Eq. (3.63), each integration in the iterative solution (3.160) just adds one of the letters at the right end of the iterated integrals in the previous order in ϵ,

$$\int_\gamma d\log\alpha_k \, \left[\alpha_{i_1}, \ldots, \alpha_{i_{k-1}}\right]_{m^{(0)}} = \left[\alpha_{i_1}, \ldots, \alpha_{i_{k-1}}, \alpha_{i_k}\right]_{m^{(0)}} . \tag{3.201}$$

If one is interested only in the symbol of the solution, it is sufficient to solve the differential equations with the weight-0 boundary constants $\vec{b}^{(0)}$, neglecting the higher-weight ones, namely $\vec{b}^{(k)}$ for $k \geq 1$. The latter produce terms beyond the symbol. The procedure is then identical to the one for the iterated integrals.

Let us make some explicit examples for the three-mass triangle integrals. The pure bubbles are given by

$$g_i = -1 + \epsilon\,[\alpha_i]_{m^{(0)}} + \epsilon^2 \left(\frac{\pi^2}{12} - [\alpha_i, \alpha_i]_{m^{(0)}} \right) + \mathcal{O}\left(\epsilon^3\right), \quad \forall i = 1, 2, 3\,. \tag{3.202}$$

Since they involve iterated integrals with only one entry, it is trivial to upgrade these expressions to explicit functions. At weight one we only have logarithms,

$$[\alpha_i]_{m^{(0)}}(m) = \log\left(-m_i^2\right), \qquad \forall i = 1, 2, 3\,. \tag{3.203}$$

Through the shuffle product (3.54) this implies that

$$\underbrace{\left[m_i^2, \ldots, m_i^2\right]}_{k \text{ times}}{}_{m^{(0)}}(m) = \frac{1}{k!} \log^k\left(-m_i^2\right). \tag{3.204}$$

Plugging this into Eq. (3.202), it is easy to check that it matches the closed-form formula given by Eq. (3.179).

More interesting is the expression of g_4 in terms of iterated integrals,

$$\begin{aligned} g_4 = \epsilon^2 \Big\{ & [\alpha_3, \alpha_4]_{m^{(0)}} + [\alpha_3, \alpha_5]_{m^{(0)}} - [\alpha_1, \alpha_4]_{m^{(0)}} - [\alpha_2, \alpha_5]_{m^{(0)}} \\ & + 4i\,\mathrm{Im}\left[\mathrm{Li}_2\left(e^{-i\pi/3}\right)\right] \Big\} + \mathcal{O}\left(\epsilon^3\right). \end{aligned} \tag{3.205}$$

This expression satisfies manifestly the first entry condition. Moreover, it is clear its symbol is odd, since the letters α_4 and α_5 are odd, while α_1, α_2 and α_3 are even (see Eqs. (3.45) and (3.46)). Applying the change of variables given by Eq. (3.167) to the letters in Eq. (3.205) and doing some easy algebraic manipulations, it is straightforward to check that the symbol of g_4 is in agreement with Eq. (3.197). Proving that Eq. (3.205) is equivalent to Eq. (3.195) also beyond the symbol is left as an exercise to the reader.

3.4.5 *Solution in Terms of a Basis of Functions*

The two approaches presented in Sects. 3.4.3 and 3.4.4 are extremely valuable, but have both some limitations. The iterated integrals offer an elegant and unique way of expressing the solution, well suited for analytic studies, whereas the GPLs may be messy—especially if the contour of integration is chosen poorly—but can be evaluated numerically with arbitrary accuracy. In this sense they complement each other. However, it is of course preferable to have a representation which enjoys the advantages of both iterated integrals and GPLs, but is exempt from their limitations. In this section I suggest an approach to achieve this. The main idea is to construct a basis of pure functions that have all the properties we would like to see manifestly in the integrals or the scattering amplitudes, e.g. absence spurious dependence on

Table 3.1 Basic functions needed to express any polylogarithmic function up to weight four

Transcendental weight	Pure function types
1	$\log x$
2	$\mathrm{Li}_2(x)$
3	$\mathrm{Li}_3(x)$
4	$\mathrm{Li}_4(x)$, $\mathrm{Li}_{2,2}(x, y)$

the base point of the integrals and absence of spurious singularities and branch cuts. The fact that it is a basis guarantees that no functional identities are left, so that the expression is unique. Moreover, the basis is made of explicit functions, which can be evaluated numerically directly. The price to pay for all this is that constructing such a basis is not algorithmic, and definitely requires more effort than the other approaches I presented. It is however an effort worth doing.

The goal therefore is to construct a basis that spans all the functions produced by a given alphabet up to a certain transcendental weight. The key observation is that only a small number of elementary functions is needed to express any polylogarithmic function. They are shown in Table 3.1 up to weight four. Up to weight three only classical polylogarithms are required, and the first genuine multiple polylogarithm appears at weight four. What remains to be understood is which arguments to use for these elementary functions so that their symbol belongs to the given alphabet and that they form a basis. On top of these necessary requirements, the more demanding physicists may also want the resulting functions to satisfy certain constraints, such as the first-entry condition, and to be "simple," e.g. to be well-defined in a certain kinematic region. This is in general a complicated problem, and there is no completely algorithmic approach. Nonetheless, a systematic strategy [75] combined with enough will power has proven successful even in highly non-trivial cases, such as the massless two-loop five-particle alphabet discussed in [96, 97].

In this section I show how to construct a basis of polylogarithmic functions for the one-loop three-mass triangle integrals. For simplicity let us work with the variables $(m_1^2, z, \bar{z})$ defined by Eq. (3.167), so that the square root rationalises. In particular, we are interested in the kinematic region where $m_1^2 < 0$, and z and $\bar{z}$ are complex conjugate. The alphabet can be chosen as

$$\{\beta_i\}_{i=1}^6 = \left\{m_1^2, z\bar{z}, (1-z)(1-\bar{z}), \frac{z}{\bar{z}}, \frac{1-z}{1-\bar{z}}, z-\bar{z}\right\}, \tag{3.206}$$

so that each letter has a well-defined transformation under complex conjugation: the letters β_i with $i = 1, 2, 3, 6$ are even, while β_4 and β_5 are odd. The Cutkosky rules imply that, for Feynman integrals with massless propagators, the first entry in the symbol can only be a Mandelstam invariant [78], in this case m_i^2 for $i = 1, 2, 3$. Through the change of variables (3.167), this means that only the letters β_i with $i = 1, 2, 3$ are allowed as first entries in the symbol.

Table 3.2 Number of integrable symbols in the three-mass triangle alphabet (3.206) with the first-entry condition, divided into even|odd under the exchange $z \leftrightarrow \bar{z}$. A symbol is said to be irreducible if it cannot be expressed as product of lower-weight symbols

Transcendental weight	1	2	3	4
Total	3|0	6|1	12|4	24|13
Irreducible	3|0	0|1	2|1	2|4

The integrability conditions for the iterated integrals or the symbols given by Eq. (3.61) inform us about how many linearly independent functions are produced by an alphabet at each transcendental weight. Solving them is a linear algebra problem and can thus be done very efficiently using e.g. the method described in [69], or the ad hoc MATHEMATICA package SYMBUILD [68]. The results up to weight 4 are presented in Table 3.2. It is possible to write down explicitly the integrable symbols, which is very valuable in view of a bootstrap approach, but for now we are only interested in their number.

At one loop we only need functions up to weight two, because of the conjecture on the transcendental weight shown in Eq. (3.110). I will therefore discuss explicitly the construction of the basis at weights one and two, and only make some comments about the higher weights.

Weight-1 Functions

At weight one the number of integrable symbols is clearly equal to the number of letters of the alphabet. Moreover, since the only possible elementary function is the logarithm, the basis is simply given by the logarithms of the letters. Only three satisfy the first-entry condition. We just need to make sure that they are well defined in the kinematic region of interest. The most obvious choice is given by

$$w_1^{(1)} = \log\left(-m_1^2\right) , \quad w_2^{(1)} = \log\left(z\bar{z}\right) , \quad w_3^{(1)} = \log\left((1-z)(1-\bar{z})\right) . \tag{3.207}$$

These functions are manifestly well defined in the region $m_1^2 < 0, z \in \mathbb{C}\backslash\{0, 1\}$, with $\bar{z}$ complex conjugate of z.

As I argued in Sect. 3.3.6, it is possible that weight-one functions which do not satisfy the first-entry condition on their own are needed to express the terms beyond the symbol at weight two. They can be chosen as

$$w_4^{(1)} = \log\left(\frac{z}{\bar{z}}\right) , \quad w_5^{(1)} = \log\left(\frac{1-z}{1-\bar{z}}\right) , \quad w_6^{(1)} = \log\left(z-\bar{z}\right) . \tag{3.208}$$

Some extra work is required to make these functions well defined. For $w_4^{(1)}$, we parametrise z using polar coordinates as $z = |z|e^{i\phi}$ with $\phi \in [0, \pi]$ for $\mathrm{Im}(z) > 0$, and as $z = |z|e^{-i\phi}$ with $\phi \in [0, \pi]$ for $\mathrm{Im}(z) < 0$. Then,

$$w_4^{(1)} = \begin{cases} 2i\phi\,, & \text{if } \mathrm{Im}(z) > 0\,, \\ -2i\phi\,, & \text{if } \mathrm{Im}(z) < 0\,. \end{cases} \tag{3.209}$$

The function $w_4^{(1)}$ is thus well defined in both the upper and the lower half of the complex plane, but has a branch cut along the negative real axis. Similarly for $w_5^{(1)}$ we parametrise z as $z = 1 + re^{i\phi}$ for $\mathrm{Im}(z) > 0$, and as $z = 1 + re^{-i\phi}$ for $\mathrm{Im}(z) < 0$. In both cases $\phi \in [0, \pi]$ and $r > 0$. Then,

$$w_5^{(1)} = \begin{cases} 2i\phi\,, & \text{if } \mathrm{Im}(z) > 0\,, \\ -2i\phi\,, & \text{if } \mathrm{Im}(z) < 0\,, \end{cases} \tag{3.210}$$

so that $w_5^{(1)}$ has a branch cut along the real axis for $\mathrm{Re}(z) < 1$. Finally, for $w_6^{(1)}$ we have that

$$w_6^{(1)} = \begin{cases} i\frac{\pi}{2} + \log\left(2|\mathrm{Im}(z)|\right)\,, & \text{if } \mathrm{Im}(z) > 0\,, \\ -i\frac{\pi}{2} + \log\left(2|\mathrm{Im}(z)|\right)\,, & \text{if } \mathrm{Im}(z) < 0\,, \end{cases} \tag{3.211}$$

and there is a branch cut along the entire real axis.

Weight-2 Functions

At weight two there are seven iterated integrals which satisfy the integrability and the first-entry conditions. Six of them are even under complex conjugation, one is odd. Clearly we can construct six even weight-2 functions by multiplying together the three even weight-1 functions shown in Eq. (3.207). In principle we could also multiply together two odd weight-1 functions, but there is none which satisfies the first-entry condition. The resulting functions are by construction linearly independent, and therefore span the entire even part of the weight-2 function space. We call the functions which can be expressed as products of lower-weight functions *reducible*. The shuffle product (3.54) implies that the reducible weight-2 iterated integrals or symbols are symmetric under the exchange of the entries,

$$a \times b = a \otimes b + b \otimes a\,. \tag{3.212}$$

Given a generic weight-2 iterated integral it therefore possible to separate the reducible and the irreducible parts by simply symmetrising and anti-symmetrising the entries. This allows one to identify the genuine weight-2 part of the expression by projecting away the products of logarithms. This operation can be generalised to higher weight through the operator [98–100]

$$\rho_w\left(a_1 \otimes \cdots \otimes a_w\right) = \rho_{w-1}\left(a_1 \otimes \cdots \otimes a_{w-1}\right) \otimes a_w - \rho_{w-1}\left(a_2 \otimes \cdots \otimes a_w\right) \otimes a_1\,, \tag{3.213}$$

for $w \geq 2$, with the recursion starting from $\rho_1 = \mathbb{1}$. This operator annihilates all shuffle products,

$$\rho_{w_1+w_2}\Big((a_1 \otimes \cdots \otimes a_{w_1}) \sqcup\!\sqcup (b_1 \otimes \cdots \otimes b_{w_2})\Big) = 0\,, \tag{3.214}$$

and can therefore be used to extract the irreducible part of a symbol. Other useful projectors in this context can be found in [75].

The weight-2 basis lacks only one irreducible function. Since it is a genuine weight-2 function, its expression must contain dilogarithms. We must then understand which arguments are allowed for a dilogarithm in the alphabet given by Eq. (3.206). We know that the symbol of a dilogarithm is

$$\mathcal{S}\left[\mathrm{Li}_2(R)\right] = -(1-R) \otimes R\,, \tag{3.215}$$

where R is a rational—in general algebraic—function of the kinematic variables. The argument R is allowed only if both R and $1-R$ factorise in terms of letters of the alphabet $\{\beta_i\}_{i=1}^6$, namely if there exist $c, c', e_i, e_i' \in \mathbb{Q}$ such that

$$R = c\prod_{i=1}^{6}\beta_i^{e_i}\,, \qquad 1-R = c'\prod_{i=1}^{6}\beta_i^{e_i'}\,. \tag{3.216}$$

Requiring that the argument R is dimensionless imposes a constraint on the exponents e_i and e_i', which depends on the dimensions of the letters. In our case only $\beta_1 = m_1^2$ is dimensionful, and we can thus immediately deduce that $e_1 = e_1' = 0$. More formally, following [75], we define the group of all the functions which factorise into letters of the alphabet as

$$\mathcal{R} = \left\{ c\prod_{i=1}^{6}\beta_i^{e_i} | e_i, c \in \mathbb{Q} \right\}\,. \tag{3.217}$$

The allowed arguments of the dilogarithm are then given by the subset

$$\mathcal{R}^{(1)} = \{R \in \mathcal{R} | 1-R \in \mathcal{R}\}\,. \tag{3.218}$$

The constraints in Eq. (3.216) cannot be solved in an algorithmic way, but it is straightforward to verify whether they are satisfied for a given R. A typical strategy consists in making a list of "reasonable" candidate arguments R of the form given by Eq. (3.216) and in selecting those for which also $1-R$ factorises in the alphabet. This constraint can be checked numerically in a very efficient way, as it is equivalent to asking whether the linear system of rational (or algebraic) equations

$$d\log(1-R) = \sum_{i=1}^{6} e_i' d\log\beta_i \tag{3.219}$$

admits a solution for the constant parameters e_i'. If enough arguments are found one can move on to the next step, otherwise she needs to enlarge to set of candidates for R and hope to be luckier. This procedure typically converges, because, for the applications we are interested in, we do not expect to see functions whose arguments are given by very high powers of the letters.

The alphabet of the three-mass triangle integrals is rather simple, and a quick search returns

$$\mathcal{R}^{(1)} = \left\{ z, 1-z, \frac{1}{z}, \frac{1}{1-z}, 1-\frac{1}{z}, \frac{z}{z-1}, \bar{z}, 1-\bar{z}, \frac{1}{\bar{z}}, \frac{1}{1-\bar{z}}, 1-\frac{1}{\bar{z}}, \frac{\bar{z}}{\bar{z}-1} \right\} . \tag{3.220}$$

It looks like we have found many arguments, but it is too early to celebrate. The reflection identities of the dilogarithm, given by Eqs. (3.84) and (3.85), imply that $\mathrm{Li}_2(R)$, $\mathrm{Li}_2(1-R)$ and $\mathrm{Li}_2(1/R)$ are equivalent up to powers of logarithms. The space of the allowed arguments R of the dilogarithm is therefore closed under the action of the operators

$$\sigma_2(R) = 1 - R\,, \qquad \sigma_3(R) = \frac{1}{R}\,. \tag{3.221}$$

This simple observation has important implications. The two operators in Eq. (3.221) in fact generate a group of transformations $\{\sigma_j\}_{j=1}^{6}$, with

$$\sigma_1(R) = R\,, \quad \sigma_4(R) = \frac{1}{1-R}\,, \quad \sigma_5(R) = 1 - \frac{1}{R}\,, \quad \sigma_6(R) = \frac{R}{R-1}\,, \tag{3.222}$$

which is isomorphic to the permutation group S_3. So what we should be looking for is not $\mathcal{R}^{(1)}$, but $\mathcal{R}^{(1)}/S_3$. Looking at Eq. (3.220) we can see that all the elements belong to two equivalence classes. The choice of the representatives can make a significant difference. Arguments in the same equivalence class may in fact produce branch cuts in different locations of the kinematic space. The choice must thus be pondered with special attention to the kinematic region under consideration. For the three-mass triangle case, we have chosen a region where the integrals are single-valued. Any branch cut will therefore cancel out, and we can choose the arguments which look simpler,

$$\mathcal{R}^{(1)}/S_3 = \{z, \bar{z}\}\,. \tag{3.223}$$

We now have at our disposal two dilogarithms: $\mathrm{Li}_2(z)$ and $\mathrm{Li}_2(\bar{z})$. We need only one function, which must be odd under complex conjugation and must obey the first-entry condition. The former constraint is simple. We just need to consider the odd combination $\mathrm{Li}_2(z) - \mathrm{Li}_2(\bar{z})$. In order to obtain a function which satisfies the first-entry condition, we need to use products of lower-weight functions to "correct" the branch-cut structure. We can do so by making an ansatz,

$$w^{(2)}_{\text{ansatz}} = \text{Li}_2(z) - \text{Li}_2(\bar{z}) + c_1 \log\left(\frac{z}{\bar{z}}\right)\log(z\bar{z}) + c_2 \log\left(\frac{z}{\bar{z}}\right)\log\left((1-z)(1-\bar{z})\right) + c_3 \log\left(\frac{1-z}{1-\bar{z}}\right)\log(z\bar{z}) + c_4 \log\left(\frac{1-z}{1-\bar{z}}\right)\log\left((1-z)(1-\bar{z})\right) , \tag{3.224}$$

where we included only the odd products of logarithms. One could also consider the logarithm of $z - \bar{z}$, but it is simple to argue that it cannot help this cause. In general one should also include products involving transcendental constants, but we have seen in Sect. 3.4.2 that the one-loop three-mass triangle integrals do not involve any weight-1 constant in this kinematic region. Finally, we compute the symbol of the ansatz and fix the free coefficients so that it satisfies the first-entry condition. There is only one solution,

$$w^{(2)}_1 = \text{Li}_2(z) - \text{Li}_2(\bar{z}) + \frac{1}{2}\log(z\bar{z})\log\left(\frac{1-z}{1-\bar{z}}\right) , \tag{3.225}$$

which—perhaps unsurprisingly—coincides with the Bloch–Wigner dilogarithm given by Eq. (3.83), $w^{(2)}_1 = D_2(z)$. This completes the basis of functions required to express the three-mass triangle integrals up to transcendental weight two.

It is worth stressing that in no point of this procedure the alphabet is required to be rational. The absence of square roots of course helps a lot, but it is not necessary. Armed with some more resolution, we can construct the genuine weight-2 function $w^{(2)}_1$ also in terms of the original variables m_i^2. The search for allowed arguments for the dilogarithm is made slower by the presence of the square root, but it nonetheless returns several possibilities. For instance, we can choose

$$\tau_2(m) = \frac{-2m_2^2}{m_1^2 - m_2^2 - m_3^2 - \sqrt{\lambda(m)}} , \qquad \tau_3(m) = \frac{-2m_3^2}{m_1^2 - m_2^2 - m_3^2 - \sqrt{\lambda(m)}} . \tag{3.226}$$

It is easy to check a posteriori that these functions belong to the set $\mathcal{R}^{(1)}$ for the alphabet (3.38). For τ_2, for instance, we have

$$d\log\tau_2 = \frac{1}{2} d\log\left(\frac{\alpha_2}{\alpha_3\alpha_4}\right) , \qquad d\log(1-\tau_2) = \frac{1}{2} d\log\left(\frac{\alpha_1\alpha_5}{\alpha_3}\right) . \tag{3.227}$$

Repeating the procedure described above we arrive at[7]

$$w^{(1)}_2 = -\text{Li}_2(\tau_2) - \text{Li}_2(\tau_3) - \frac{\pi^2}{6} - \frac{1}{2}\log\left(\frac{\tau_3}{\tau_2}\right)\log\left(\frac{1-\tau_3}{1-\tau_2}\right) - \frac{1}{2}\log(-\tau_2)\log(-\tau_3) . \tag{3.228}$$

[7] I thank Dmitry Chicherin for showing me this expression of the Bloch–Wigner dilogarithm.

The equivalence between Eqs. (3.225) and (3.228) can be proven using the symbol.

Higher-Weight Functions

The construction discussed in the previous section is conceptually straightforward to extend to higher weights. The functions in the set $\mathcal{R}^{(1)}$ defined by Eq. (3.218) are in fact allowed arguments of the classical polylogarithms at any transcendental weight, since the symbol of $\mathrm{Li}_n(R)$ involves only the entries R and $1-R$ for any n. The difference is that we can no longer mod out the action of the permutation group S_3. Polylogarithms with weight higher than two still satisfy identities which relate the different arguments in Eq. (3.220), but they become increasingly complicated. For instance, at weight three we have the identity

$$\mathrm{Li}_3(z)+\mathrm{Li}_3(1-z)+\mathrm{Li}_3\left(1-\frac{1}{z}\right)=\zeta(3)+\frac{1}{6}\log^3 z+\frac{\pi^2}{6}\log z-\frac{1}{2}\log^2 z\log(1-z)\,, \tag{3.229}$$

so that only two out of the arguments $\{z, 1-z, 1-1/z\}$ are inequivalent. In fact, one can choose $D_3(z)$ and $D_3(1-z)$, defined by Eq. (3.80), as the independent irreducible functions which, together with products of lower-weight functions, span the even part of three-mass triangle function space at weight three. The complete function basis up to weight four is discussed in [15].

Starting from weight four, genuine multiple polylogarithms become necessary. The search for allowed arguments for the multiple polylogarithms is the natural generalisation of what we have seen for the classical polylogarithms, and I will not go into any detail of it. I refer the interested reader to [75] for a thorough discussion.

I prefer to present here a different approach. The explicit polylogarithmic expressions at low transcendental weights offer important advantages, from both the analytical and the numerical point of view. In particular, fast and reliable implementations of the basic functions are immediately available. As we go to higher weights, however, the polylogarithmic expressions become increasingly bulkier and more difficult to construct. Moreover, although the separate terms can be evaluated numerically efficiently, their proliferation may lead to a significant slowdown and to a loss in accuracy. For these reasons, the following hybrid approach suggested in [101] is sometimes preferable.

Suppose we have an explicit representation in terms of polylogarithmic functions for any weight-n iterated integral in a given alphabet $\{\alpha_i\}$,

$$f_{\vec{\alpha}}(m)=\left[\vec{\alpha}\right]_{m^{(0)}}(m)\,, \tag{3.230}$$

where I introduced the short-hand notation $\vec{\alpha}=\alpha_{i_1},\ldots,\alpha_{i_n}$. Consider a generic weight-$(n+2)$ (integrable) iterated integral

$$\left[\vec{\alpha},\alpha_a,\alpha_b\right]_{m^{(0)}}(m)=\int_\gamma d\log\alpha_{i_1}\ldots d\log\alpha_{i_n}d\log\alpha_a d\log\alpha_b\,, \tag{3.231}$$

where γ is a piece-wise smooth path from a fixed base point $\gamma(0) = m^{(0)}$ to a generic end point $\gamma(1) = m$. Since we have an explicit polylogarithmic expression for the first n integrations, only two remain to be performed,

$$\left[\vec{\alpha}, \alpha_a, \alpha_b\right]_{m^{(0)}}(m) = \int_0^1 dt \frac{\partial \log W_b(\gamma(t))}{\partial t} \int_0^t dt' \frac{\partial \log W_a\left(\gamma(t')\right)}{\partial t'} f_{\vec{\alpha}}\left(\gamma(t')\right) . \tag{3.232}$$

If we exchange the order of integration over the variables t and t', the integration over t can be immediately done in terms of logarithms,

$$\begin{aligned}\left[\vec{\alpha}, \alpha_a, \alpha_b\right]_{m^{(0)}}(m) &= \int_0^1 dt' \int_{t'}^1 dt \frac{\partial \log \alpha_b(\gamma(t))}{\partial t} \frac{\partial \log \alpha_a\left(\gamma(t')\right)}{\partial t'} f_{\vec{\alpha}}\left(\gamma(t')\right) \\ &= \int_0^1 dt \left[\log \alpha_b(m) - \log \alpha_b(\gamma(t))\right] \frac{\partial \log \alpha_a(\gamma(t))}{\partial t} f_{\vec{\alpha}}(\gamma(t)) .\end{aligned} \tag{3.233}$$

Care must be taken that the logarithms in the integrand are evaluated on the right Riemann sheet and that the appropriate analytic continuation is performed if the contour γ leaves the region of analyticity where the base point $m^{(0)}$ lies. If we have control over the weight-n functions, this simple trick gives us a one-fold integral representation for the weight-$(n+2)$ iterated integrals. The latter might not look particularly elegant, but it is often rather convenient for numerical evaluations. From the computational point of view, the explicit polylogarithmic expressions at high transcendental weight are often outperformed by the one-fold integral representations [96, 97, 101]. Therefore, having an explicit basis of functions up to weight two allows us to evaluate numerically in an efficient way all the functions up to weight four, which is the highest transcendental weight required in two-loop computations in $D = 4 - 2\epsilon$ dimensions.

How to Express the Solution in the Function Basis

Once a basis of functions is available, one may wish to use it. In this section I discuss a way to express the solution of the differential equations in the canonical form in terms of a function basis.

The starting point is the observation that the solution in terms of Chen's iterated integrals can always be written down with no effort, even in the presence of multiple square roots. A practical strategy therefore consists in first solving the canonical differential equations in terms of iterated integrals, and then rewriting the latter in terms of the function basis. The only extra step we need to take is to rewrite the function basis in terms of iterated integrals. Once that is done, it becomes a mere linear algebra problem to translate an expression written in terms of iterated integrals to the function basis.

One way to rewrite a given function in terms of iterated integrals with letters drawn from a given alphabet makes use, one more time, of the differential equation

in the canonical form. In Sect. 3.3.5 we have seen that any polylogarithmic function satisfies, together with all its derivatives, a system of differential equations in the canonical form. So if we want to rewrite a function in terms of iterated integrals, we just need to write down the associated differential equation and solve the latter in terms of iterated integrals. Since we already know from the start the solution written in at least one form, we can also evaluate it in some point and immediately get the boundary values. Moreover, since the matrix in the differential equation depends on the kinematics only through d log forms, it is very easy to change variables or letters of the alphabet at the level of the differential equations.

Let me show the explicit example of the Bloch–Wigner dilogarithm $w_2^{(2)}$ given by Eq. (3.225). Differentiating it all the way down to weight zero produces a vector of linearly independent functions,

$$\vec{h} = \left(\epsilon^2 w_2^{(2)}, \epsilon w_2^{(1)}, \epsilon w_3^{(1)}, 1\right) , \tag{3.234}$$

which satisfies a differential equation in the canonical form,

$$d\vec{h} = \epsilon\, d\tilde{B} \cdot \vec{h} \, . \tag{3.235}$$

The function we started from, $w_2^{(2)}$, is given by Eq. (3.225) in terms of the z-variables. One may wish to write it in terms of iterated integrals in the alphabet of the physical variables m_i^2, given by Eq. (3.38). We can then change variables through Eq. (3.168) in the d log-forms contained in the matrix $d\tilde{B}$, obtaining

$$\tilde{B} = \begin{pmatrix} 0 & -\frac{1}{2}\log\alpha_5 & \frac{1}{2}\log\alpha_4 + \frac{1}{2}\log\alpha_5 & 0 \\ 0 & 0 & 0 & \log\alpha_2 - \log\alpha_1 \\ 0 & 0 & 0 & \log\alpha_3 - \log\alpha_1 \\ 0 & 0 & 0 & 0 \end{pmatrix} . \tag{3.236}$$

Next, we evaluate the functions $\vec{h}$ at the base point $m^{(0)}$, given in terms of the z-variables by Eq. (3.177),

$$\vec{h}(m^{(0)}, \epsilon) = \left(\epsilon^2 2i\,\mathrm{Im}\left[\mathrm{Li}_2\left(e^{-i\pi/3}\right)\right], 0, 0, 1\right)^T . \tag{3.237}$$

Finally, we solve the differential equation (3.235) in terms of iterated integrals as discussed in Sect. 3.4.4. This way we obtain the expression of $w_1^{(2)}$ in terms of iterated integrals in the alphabet (3.38),

$$w_1^{(2)} = \frac{1}{2}\left([\alpha_3, \alpha_4] + [\alpha_3, \alpha_5] - [\alpha_1, \alpha_4] - [\alpha_2, \alpha_5] + 4i\,\mathrm{Im}\left[\mathrm{Li}_2\left(e^{-i\pi/3}\right)\right]\right) , \tag{3.238}$$

where the subscript $m^{(0)}$ in the iterated integrals is omitted to simplify the expression. As a bonus, we also obtain the expressions for the weight-1 functions that appear in

the differential of $w_1^{(2)}$,

$$w_2^{(1)} = [\alpha_2]_{m^{(0)}} - [\alpha_1]_{m^{(0)}} \,, \qquad w_3^{(1)} = [\alpha_3]_{m^{(0)}} - [\alpha_1]_{m^{(0)}} \,, \tag{3.239}$$

which are however trivial and can be written down without too much thinking.

By comparing Eq. (3.238) to Eq. (3.205), we can immediately rewrite the triangle pure integral g_4 as

$$g_4 = 2\epsilon^2 w_1^{(2)} + \mathcal{O}\left(\epsilon^3\right) \,. \tag{3.240}$$

The simplification in the expression of g_4 from the GPLs of Eqs. (3.195)–(3.240) is dramatic. The latter is much more compact, and it is manifestly single valued in the punctured complex plane $\mathbb{C}\backslash\{0, 1\}$ and anti-symmetric under the exchange $z \leftrightarrow \bar{z}$. Moreover, the awful spurious dependence on the base point we see in Eq. (3.195) is completely absent in Eq. (3.240).

3.5 Asymptotic Solution of the Differential Equations

The differential equations in the canonical form (3.158) allow us to determine the asymptotic behaviour of the solution close to any regular singular point. I first present the general procedure, and then apply it to a soft limit of the one-loop three-mass triangle integrals. A complete discussion of this technique can be found e.g. in [102].

3.5.1 General Procedure

Let us consider a generic singular point $x = 0$, for some kinematic variable x. In order to simplify the notation, I denote cumulatively by y the set of variables which are fixed in the limit. The multi-variable generalisation can be recovered straightforwardly. By definition, the canonical basis integrals $\vec{g}$ satisfy a system of differential equations of the form

$$\begin{cases} \dfrac{\partial}{\partial x}\vec{g}(x, y, \epsilon) = \epsilon A_x(x, y)\vec{g}(x, y, \epsilon) \,, \\ \dfrac{\partial}{\partial y}\vec{g}(x, y, \epsilon) = \epsilon A_y(x, y)\vec{g}(x, y, \epsilon) \,. \end{cases} \tag{3.241}$$

As discussed in Sect. 3.2, this system is fuchsian. This implies that $x = 0$ is a regular singular point for the matrix A_x, namely that

$$A_x(x, y) = \frac{A_0}{x} + \sum_{k\geq 0} x^k A_{k+1}(y) \,, \tag{3.242}$$

where A_0 is a matrix of rational numbers. The matrix A_y, on the other hand, is regular at $x = 0$.

The first step consists in performing a "gauge transformation" with a holomorphic matrix $T(x, y, \epsilon)$,

$$\vec{g}(x, y, \epsilon) = T(x, y, \epsilon)\vec{h}(x, y, \epsilon)\,, \tag{3.243}$$

so that the new basis $\vec{h}$ obeys a simplified differential equation with respect to x,

$$\frac{\partial}{\partial x}\vec{h}(x, y, \epsilon) = \epsilon\frac{A_0}{x}\vec{h}(x, y, \epsilon)\,. \tag{3.244}$$

For this to hold, $T(x, y, \epsilon)$ must satisfy the differential equation

$$T^{-1}\left(\epsilon A_x T - \frac{\partial T}{\partial x}\right) = \epsilon\frac{A_0}{x}\,. \tag{3.245}$$

We can solve the latter for $T(x, y, \epsilon)$ as a series expansion around $x = 0$,

$$T(x, y, \epsilon) = \sum_{k\geq 0} x^k T_k(y, \epsilon)\,. \tag{3.246}$$

Substituting this formula into Eq. (3.245) and expanding both sides around $x = 0$ produces an equation at each order in x. The first, at order $1/x$, implies that

$$[A_0, T_0] = 0\,. \tag{3.247}$$

The simplest choice is given by

$$T_0(y, \epsilon) = \mathbb{1}\,. \tag{3.248}$$

This means that the transformation matrix becomes the identity at $x = 0$. The higher orders in x give a system of contiguous relations,

$$\epsilon A_k(y) + \epsilon A_0 T_k(y, \epsilon) - \epsilon T_k(y, \epsilon)A_0 - kT_k(y, \epsilon) + \epsilon\sum_{j=1}^{k-1} A_{k-j}(y)T_j(y, \epsilon) = 0\,, \quad \forall k \geq 1\,. \tag{3.249}$$

These equations imply in particular that $T_k(y, \epsilon) = \mathcal{O}(\epsilon)$. Since we are interested in the asymptotic solution as a Laurent expansion around $\epsilon = 0$, it is convenient to further series expand $T_k(y, \epsilon)$ in ϵ,

$$T_k(y, \epsilon) = \sum_{m\geq 1} \epsilon^m\, T_{k,m}(y)\,. \tag{3.250}$$

The contiguous relations (3.249) then take the form

$$\begin{aligned} T_{k,1}(y) &= \frac{1}{k} A_k(y)\,, \\ T_{k,m}(y) &= \frac{1}{k}\left[A_0 T_{k,m-1}(y) - T_{k,m-1}(y) A_0 + \sum_{j=1}^{k-1} A_{k-j}(y) T_{j,m-1}(y) \right], \quad \forall m > 1\,, \end{aligned} \tag{3.251}$$

which can be solved order by order in x and ϵ, giving an explicit expression for T as a double series,

$$T(x, y, \epsilon) = \mathbb{1} + \sum_{k\geq 1} \sum_{m\geq 1} x^k \epsilon^m T_{k,m}(y)\,. \tag{3.252}$$

After the gauge transformation, the system of differential equations for $\vec{h}$ takes the form

$$\begin{cases} \dfrac{\partial}{\partial x}\vec{h}(x, y, \epsilon) = \epsilon \dfrac{A_0}{x}\vec{h}(x, y, \epsilon) \\ \dfrac{\partial}{\partial y}\vec{h}(x, y, \epsilon) = B(x, y, \epsilon)\vec{h}(x, y, \epsilon) \end{cases}, \tag{3.253}$$

where

$$B(x, y, \epsilon) = T^{-1}\left(\epsilon A_y T - \frac{\partial T}{\partial y}\right). \tag{3.254}$$

Our goal is to solve this system of differential equations using a boundary point in the limit, namely at $x = 0$. We can achieve this by integrating the system along the piecewise path

$$(x = 0, y = y_0) \longrightarrow (x = 0, y) \longrightarrow (x, y)\,, \tag{3.255}$$

for some values y_0 of the other kinematic variables. In other words, we restore the dependence first on y and then on x. Since

$$B(x = 0, y, \epsilon) = \epsilon A_y(0, y)\,, \tag{3.256}$$

the solution is

$$\vec{h}(x, y, \epsilon) = x^{\epsilon A_0}\, \mathbb{P} \exp\left[\epsilon \int_{y_0}^{y} A_y(0, y')dy'\right] \vec{h}_0(\epsilon)\,. \tag{3.257}$$

Finally, the solution of the initial system of differential equations (3.241) is given by

$$\vec{g}(x, y, \epsilon) = T(x, y, \epsilon)\, x^{\epsilon A_0}\, \mathbb{P} \exp\left[\epsilon \int_{\gamma} d\tilde{A}(x = 0, y)\right] \vec{h}_0(\epsilon)\,, \tag{3.258}$$

where I have also made the straightforward generalisation to the multi-variable case. Note that $d\tilde{A}$ has to be evaluated at $x = 0$ *after* the differentiation, as can be understood from Eq. (3.256). This subtle point is very important, because differentiation and limit do not commute in general. In Eq. (3.258), γ is a path starting from a base-point in the limit, $(x = 0, y = y_0)$, and ending in the generic point (x, y), while $\vec{h}_0(\epsilon)$ are the boundary constants $\vec{h}_0(\epsilon) = \vec{h}(y = y_0, \epsilon)$ for the equation

$$\frac{\partial}{\partial y}\vec{h}(y, \epsilon) = \epsilon A_y(0, y)\vec{h}(y, \epsilon)\,. \tag{3.259}$$

The boundary constants $\vec{h}_0(\epsilon)$ can be computed by integrating the canonical differential equations (3.158) from a base point in the bulk of the kinematic space, where the values of the integrals are known, to the point in the limit $(x = 0, y = y_0)$. This can be done efficiently in terms of GPLs (if the alphabet is rationalised along the integration contour). Of course the integrals develop logarithmic singularities at the end-point, which is defined in a tangential sense (see Sect. 3.3.1). In particular, these logarithmic divergences as $x \to 0$ conspire together to produce the matrix exponential $x^{\epsilon A_0}$ in Eq. (3.258). It is therefore important that the regularisation procedure at the tangential end-point is compatible with the asymptotic solution given by Eq. (3.258). In other words, we need to make sure that, when integrating from the bulk to the end-point in the limit $x \to 0$, we discard the same logarithmic divergences which are produced by the matrix exponential $x^{\epsilon A_0}$ in Eq. (3.258). I will stress this again in the explicit example below.

This procedure allows us to solve the differential equations in canonical form (3.158) asymptotically starting from any regular singular point, say $x = 0$. The result contains divergent logarithms stemming from the matrix exponential $x^{\epsilon A_0}$. The path-ordered exponential in Eq. (3.258), on the other hand, produces iterated integrals which depend on the other kinematic variables. The gauge transformation matrix $T(x, y, \epsilon)$ is instead responsible for the power corrections in x.

3.5.2 *Soft Limit of the One-Loop Three-Mass Triangle Integrals*

Let us now make an explicit example: the soft limit $p_2^\mu \to 0$ of the one-loop three-mass triangle integrals. At the level of the kinematic variables m this implies that both m_2^2 and m_3^2 go to zero, because of momentum conservation. The first step is to determine the boundary constants $\vec{h}_0(\epsilon)$ in Eq. (3.258). As base point in the limit we choose

$$m_{\text{soft}} := \left(m_1^2 = -1\,, m_2^2 = 0\,, m_3^2 = -1\right)\,. \tag{3.260}$$

In order to reach it from the base point in the bulk $m^{(0)}$ (3.175) we only need to vary m_2^2. A convenient path is given by

$$m = \gamma(t) = \left(-1\,, \frac{(1-t)^2}{t}\,, -1\right)\,, \tag{3.261}$$

with t varying along the complex ray from $t = e^{i\pi/3}$ to $t = 0$. This path in fact rationalises the square root,

$$\sqrt{\lambda(\gamma(t))} = \frac{(-1+t)(1+t)}{t}\,. \tag{3.262}$$

The real parts of m_2^2 and of $\lambda(m)$ are always negative along the path, so that no analytic continuation is needed. Moreover, the alphabet pulled back with this path becomes that of the HPLs. The result of the integration contains logarithmic divergences, which we denote as $L := \lim_{t\to 1} H(1;t)$. For instance,

$$g_2(m_{\text{soft}}, \epsilon) = -1 + \epsilon\,(-2L + i\pi) + \mathcal{O}\left(\epsilon^2\right)\,. \tag{3.263}$$

Here comes a subtle point. We know that the result of the regularisation depends on an arbitrary choice. Naïvely, one would regularise Eq. (3.263) by formally setting $L = 0$. Another possibility consists in formally setting $\log(-m_2^2)$ to 0 in the limit. Since

$$\lim_{t\to 1} \log\left(-m_2^2 - i0\right)\big|_{m=\gamma(t)} = -2L + i\pi\,, \tag{3.264}$$

this choice amounts to setting $L = i\pi/2$. Although perhaps counterintuitive, the second choice is preferable. In the first regularisation scheme we are in fact setting to zero a logarithmic divergence which depends strongly on the specific path given by Eq. (3.261). In the second, instead, we are setting to zero a quantity which does not depend on the specific path, namely $\log(-m_2^2)$. This is the physical quantity that is vanishing in the soft limit $p_2^\mu \to 0$, and I therefore refer to this kind of regularisation as "physical." The values of the integrals at m_{soft} in the physical regularisation scheme,

$$\begin{aligned}
&\text{Reg}\left[g_i(m_{\text{soft}}, \epsilon)\right] = -1 + \epsilon^2\frac{\pi^2}{12} + \epsilon^3\frac{7}{3}\zeta(3) + \mathcal{O}\left(\epsilon^4\right)\,, \quad \forall i = 1,2,3\,,\\
&\text{Reg}\left[g_i(m_{\text{soft}}, \epsilon)\right] = \mathcal{O}\left(\epsilon^4\right)\,,
\end{aligned} \tag{3.265}$$

can be used as the boundary constants to write down the asymptotic solution in the soft limit.

In order to parameterise the soft limit, let us make the change of variables

$$m_2^2 = m_1^2 x^2\,, \qquad m_3^2 = m_1^2\,(1-xy)\left(1 - \frac{x}{y}\right)\,. \tag{3.266}$$

The new variables x and y are related to z and $\bar{z}$ defined by Eq. (3.167) through $z = xy$ and $\bar{z} = x/y$, and they also rationalise the square root,

$$\sqrt{\lambda(m)} = m_1^2 x \frac{y^2 - 1}{y} . \tag{3.267}$$

The soft limit is then represented by the regular singular point $x = 0$. The logarithmic divergences are produced by the matrix exponential

$$x^{\epsilon A_0} = \text{diag}\left(1, x^{-2\epsilon}, 1, 1\right) . \tag{3.268}$$

It is crucial to check that they are compatible with the regularisation used in the computation of the boundary constants at m_{soft}. There, we have regularised by setting $\log(-m_2^2)$ to 0. The latter is related to $\log x$ by

$$\log\left(-m_2^2\right) = 2\log(x) + \log\left(-m_1^2\right) . \tag{3.269}$$

Since at m_{soft} we have $m_1^2 = -1$, setting $\log(-m_2^2) = 0$ there is equivalent to setting $\log(x) = 0$ in the new variables. No correction in the regularisation scheme is thus needed. It would have been necessary if instead we had chosen the "unphysical" regularisation discussed above. The gauge transformation matrix T can be computed at any order in x and ϵ through the recursive relations given by Eqs. (3.251). Up to the first order in ϵ and in x, for instance, it is given by

$$T = \begin{pmatrix} 1 & 0 & 0 & 0 \\ 0 & 1 & 0 & 0 \\ 0 & 0 & 1 + \epsilon x \frac{y^2+1}{y} & 0 \\ \epsilon x \frac{y^2-1}{y} & -\epsilon x \frac{y^2-1}{y} & 0 & 1 + \epsilon x \frac{y^2+1}{y} \end{pmatrix} + o(\epsilon x) . \tag{3.270}$$

The last piece of the asymptotic solution is the path ordered exponential,

$$\vec{g}^{\,\prime} = \mathbb{P} \exp\left(\epsilon \int_\gamma d\tilde{A}(x=0)\right) \text{Reg}\left[\vec{g}(m_{\text{soft}}, \epsilon)\right] , \tag{3.271}$$

with the boundary constants given by Eqs. (3.265). I stress one more time that $d\tilde{A}$ has to be evaluated at $x = 0$ after the differentiation. The function space is particularly simple. Up to order ϵ^3—the order at which we have determined the boundary constants—we only need iterated integrals of the form

$$\underbrace{\left[m_1^2, \ldots, m_1^2\right]}_{k \text{ times}}_{m_{\text{soft}}}(m) = \frac{1}{k!} \log^k\left(-m_1^2\right) . \tag{3.272}$$

The result is given by

$$\vec{g}^{\,\prime} = \begin{cases} -1 + \epsilon \log\left(-m_1^2\right) + \epsilon^2 \left(\frac{\pi^2}{12} - \frac{1}{2}\log^2\left(-m_1^2\right)\right) + \mathcal{O}\left(\epsilon^3\right), & i = 1,2,3, \\ 0, & i = 4. \end{cases} \tag{3.273}$$

Substituting Eqs. (3.268), (3.270) and (3.273) into Eq. (3.258) finally gives the asymptotic expansion of the canonical basis integrals in the soft limit. The first integral, g_1, is a bubble in the m_1^2 channel, and is thus unaffected by the limit $p_2^\mu \to 0$. The second integral, a bubble in the m_2^2 channel, is given in the limit by

$$g_2 = -1 + \epsilon\left(\log\left(-m_1^2\right) + 2\log x\right) - \epsilon^2\left[\frac{1}{2}\left(\log\left(-m_1^2\right) + 2\log x\right)^2 - \frac{\pi^2}{12}\right] + \mathcal{O}\left(\epsilon^3\right). \tag{3.274}$$

No rational function appears. It is easy to check that this expression matches the closed-form expression in Eq. (3.179) after the change of variables given by Eq. (3.266). The bubble in m_3^2, g_3, is more interesting, as it features also rational functions

$$\begin{aligned} g_3 = & -1 + \epsilon\left(\log\left(-m_1^2\right) - x\frac{y^2+1}{y} + \mathcal{O}\left(x^2\right)\right) \\ & - \epsilon^2\left(\frac{1}{2}\log^2\left(-m_1^2\right) - x\frac{y^2+1}{y}\log\left(-m_1^2\right) - \frac{\pi^2}{12} + \mathcal{O}\left(x^2\right)\right) + \mathcal{O}\left(\epsilon^3\right). \end{aligned} \tag{3.275}$$

Also this expansion is easy to check against the closed-form expression (3.179). In the limit $x \to 0$ it matches the bubble in m_1^2, as expected since $m_3^2 \to m_1^2$. Finally, the triangle integral g_4 vanishes in the limit,

$$g_4 = \epsilon^2\left[-2x\frac{y^2-1}{y}\left(-1 + \log x\right) + \mathcal{O}\left(x^2\right)\right] + \mathcal{O}\left(\epsilon^3\right). \tag{3.276}$$

It is a nice exercise to check that this expansion is equal to that of the known solution written in terms of the Bloch–Wigner function, given by Eq. (3.240). Since the square root $\sqrt{\lambda}$ vanishes too $\sim x$ in the soft limit, the infinitesimal power corrections in g_4 become relevant for the triangle integral $I_{1,1,1}$, related to g_4 through Eq. (3.185). We find that it is divergent in the soft limit,

$$I_{1,1,1} = \left[-\frac{2}{m_1^2}\left(-1 + \log x\right) + \mathcal{O}\left(x\right)\right] + \mathcal{O}\left(\epsilon\right). \tag{3.277}$$

This divergence corresponds to an infrared pole $1/\epsilon$ that would show up in the two-mass triangle integral if we used dimensional regularisation to regularise the infrared divergences as well.

In conclusion, it is worth stressing that this procedure can be applied to any basis of functions which satisfies a system of differential equations in the canonical form.

They do not need to be Feynman integrals. This technique therefore offers a useful approach to the series expansion of polylogarithmic functions in general.

3.6 How to Find a Canonical Basis

Throughout this chapter we have seen that, whenever the differential equations for a basis of Feynman integrals are cast into the canonical form, the problem of solving them can essentially be considered as solved. Finding a canonical basis is therefore crucial. Several different approaches has been proposed. One may for instance simplify systematically the differential equations until the canonical form is reached [14, 103–106]. A recent method [107], based on previous work by [108], allows one to construct a canonical basis starting from a single pure integral. This procedure is completely algorithmic and is implemented in the public MATHEMATICA package INITIAL [107]. Along with these systematic techniques, the literature is scattered with heuristic rules, which often prove useful to find particularly simple pure integrals (e.g. see [14, 109]). As I am writing this section, yet another approach has stemmed from intersection theory [110], proof that this is a very active area of research.

I present here the approach which has had the greatest impact in my work, and to which I have given a small contribution [111]. To understand it, let us start with the simplest pure function,

$$x^\epsilon = 1 + \epsilon \log x + \frac{1}{2}\epsilon^2 \log^2 x + \mathcal{O}(\epsilon^3)\,. \tag{3.278}$$

It is sufficient to introduce any non-constant algebraic factor $n(x)$ to spoil this property. The function $n(x)x^\epsilon$ has transcendental weight 0, but its differential does not have uniform transcendental weight and the function is therefore not pure. So, given a loop integral which evaluates to $n(x)x^\epsilon$—e.g. a bubble integral—we want to normalise it so as to remove the overall algebraic factor $n(x)$. The difficulty lies in the fact that we want to identify the latter *prior* to performing the integration. Moreover, a Feynman integral may have more than one algebraic factor. Following the conjecture on the transcendental weight discussed in Sect. 3.3.4, a generic ℓ-loop integral in $D = 4 - 2\epsilon$ dimensions has the form

$$I^{(\ell)}(x,\epsilon) = \frac{1}{\epsilon^{2\ell}} \sum_{p=0}^{\infty} \epsilon^p \sum_k n_k(x) \sum_{w=0}^{p} h_{p,k}^{(w)}(x)\,, \tag{3.279}$$

where $h_{p,k}^{(w)}(x)$ is a weight-w pure function of the kinematic variables x, and $n_k(x)$ is an algebraic function. Finally, the uniform transcendentality can be spoiled by ϵ-dependent factors as well. All things considered, the situation looks very intricate. Two key ideas allow us to disentangle it: the notion of leading singularities, and the conjecture that the so-called "d log"-integrands having constant leading singularities integrate to pure functions.

3.6.1 Leading Singularities

The loop *integrand* contains all the information about the rational factors n_k in Eq. (3.279). If the integrand has only simple poles in the integration variables, the rational factors can be extracted systematically by taking (multi-variate) residues. The "maximal" residues, namely those which localise all the integrations, are called *leading singularities* [112–115].[8] They give the rational factors arising upon integration. The relationship can be understood qualitatively as follows. The computation of the leading singularities is a generalisation of the unitarity cuts. The latter are related to the discontinuities of the integral, e.g. through the optical theorem. Computing a discontinuity of Eq. (3.279) isolates the rational factors n_k, because only the transcendental functions $h^{(w)}_{p,k}(x)$ are multi valued. This establishes a link between the leading singularities and the rational factors arising upon integration.

Let us consider for instance the bubble integral in $D = 2$ dimensions in the p_1-channel,

$$I^{(D=2)}_{1,1,0} = \int \frac{d^2k}{i\pi} \frac{1}{k^2(k+p_1)^2} =: \frac{1}{i\pi} \int \mathcal{I}^{(D=2)}_{1,1,0} \,. \tag{3.280}$$

The careful readers might notice that I have set $D = 2$, although the integral is divergent. They are right to be worried, but in many cases it turns out that this is actually fine. After all, we are not going to integrate on the entire loop-momentum space, but only take residues. I will comment on the D-dimensional subtleties below. In order to compute the leading singularities, it is convenient to introduce a parameterisation rather than to work with the components of the loop momenta. In two dimensions there are two independent degrees of freedom. We parametrise them as follows. We introduce a basis made of two auxiliary light-like vectors n_1 and n_2, $n_i^2 = 0$, so that

$$p_1 = n_1 + n_2 \,. \tag{3.281}$$

Clearly, $p_1^2 = 2n_1 \cdot n_2$. We expand the loop momentum k in the basis,

$$k = a_1 n_1 + a_2 n_2 \,. \tag{3.282}$$

The two-dimensional integrand then takes the form

$$\mathcal{I}^{(D=2)}_{1,1,0} = \frac{1}{2m_1^2} \frac{da_1 \wedge da_2}{a_1 a_2 (1+a_1)(1+a_2)} \,. \tag{3.283}$$

Hereafter the wedge corresponds to the standard definition of a differential form, giving rise to an oriented volume upon integration (e.g. $da_1 \wedge da_2 = -da_2 \wedge da_1$).

[8] Even in the presence of higher poles in the integration variables, the algebraic factors arising upon integration are often called, by analogy, leading singularities, although the maximal residues of the integrand are in this case not defined.

Note that in this context we only vary the integration variables, and consider the kinematic variables as fixed. The integrand of the two-dimensional bubble has four multi-variate simple poles. The residues are easy to compute. The resulting leading singularities are

$$\mathrm{LS}\left(I_{1,1,0}^{(D=2)}\right) = \pm\frac{1}{2m_1^2}\,. \tag{3.284}$$

The two-dimensional bubble integral normalised by a factor of m_1^2 has thus constant leading singularities. The explicit computation in $D = 2 - 2\epsilon$ shows that this integral is in fact pure,

$$\epsilon m_1^2\, I_{1,1,0}^{(D=2-2\epsilon)} = -2 + 2\epsilon \log\left(-m_1^2\right) - \epsilon^2\left(\log^2\left(-m_1^2\right) - \frac{\pi^2}{6}\right) + \mathcal{O}(\epsilon^3)\,, \tag{3.285}$$

where I have also inserted a factor of ϵ in order to make it weight zero. Using the dimension shifting relations [116, 117], implemented e.g. in LiteRed [24], it is possible to rewrite the two-dimensional bubble in terms of four-dimensional integrals,

$$I_{1,1,0}^{(D=2-2\epsilon)} = I_{2,1,0}^{(D=4-2\epsilon)} + I_{1,2,0}^{(D=4-2\epsilon)} = 2I_{2,1,0}^{(D=4-2\epsilon)}\,, \tag{3.286}$$

where, in the last equality, I have used the graph symmetries. This simple calculation motivates the choice of the three single-scale integrals $g_i, i = 1, 2, 3$, for the one-loop three-mass triangle family given by Eq. (3.28).

At this point it is natural to ask what is wrong about the bubble integrals directly in $D = 4 - 2\epsilon$ dimensions. To see it, we need to parametrise four degrees of freedom. We adopt the spinor-helicity parametrisation[9] for the auxiliary light-like momenta, $n_i = \lambda_i\tilde{\lambda}_i$. The spinors can be used to construct two additional complex vectors, $\lambda_1\tilde{\lambda}_2$ and $\lambda_2\tilde{\lambda}_1$. Together with n_1 and n_2, they form a basis. The loop momentum is decomposed as

$$k = a_1 n_1 + a_2 n_2 + a_3\lambda_1\tilde{\lambda}_2 + a_4\lambda_2\tilde{\lambda}_1\,. \tag{3.287}$$

Note that the two complex momenta are not helicity-free, and thus a_3 and a_4 carry helicity as well. It is possible to normalise the momenta so as to work with scalar parameters only, but it is not necessary. The integrand of the four-dimensional bubble in the p_1-channel is then given by

$$\mathcal{I}_{1,1,0}^{(D=4)} = \frac{1}{4}\frac{da_1 \wedge da_2 \wedge da_3 \wedge da_4}{(a_1a_2 - a_3a_4)(1 + a_1 + a_2 + a_1a_2 - a_3a_4)}\,. \tag{3.288}$$

[9] See e.g. [118–120] for an introduction to the spinor helicity formalism.

Since there are only two poles, one may naïvely think it is impossible to localise all the four integrations. Taking residues, however, introduces jacobian factors which have poles on their own. For instance, taking the following two residues sequentially

$$\oint_{a_3=-\frac{a_2(1+a_2)}{a_4}} \oint_{a_1=\frac{a_3 a_4}{a_2}} \mathcal{I}^{(D=4)}_{1,1,0} = \frac{1}{4}\frac{da_2 \wedge da_4}{a_4}\,, \tag{3.289}$$

introduces a pole at $a_4 = 0$ which was not present in the original integrand. We talk in such a case of *composite leading singularities*. Taking also the residues at $a_4 = 0$ brings to light the problem,

$$\oint_{a_4=0} \oint_{a_3=-\frac{a_2(1+a_2)}{a_4}} \oint_{a_1=\frac{a_3 a_4}{a_2}} \mathcal{I}^{(D=4)}_{1,1,0} = \frac{1}{4} da_2\,. \tag{3.290}$$

This differential form has a double pole at infinity. The latter can be exposed by the change of variables $a_2 = 1/y$,

$$da_2 = -\frac{dy}{y^2}\,, \tag{3.291}$$

which has a double pole at $y = 0$, corresponding to $a_2 \to \infty$. Although higher poles have well-defined residues too—in this case it would be zero—this appears to be an obstruction for the uniform transcendentality of the integrated function. The four-dimensional bubble, in fact, does not have uniform transcendentality. This can be fixed only with an ϵ-dependent prefactor, given by Eqs. (3.25) and (3.29), which translates the four-dimensional bubble into the two-dimensional one. The conjecture presented in the next section sheds some light on the disruptive role of the double poles.

Before we move on to that, let us conclude the computation of the leading singularities of the one-loop three-mass triangle basis integrals. In the four-dimensional parameterisation used for the bubble, the triangle integrand becomes

$$\begin{aligned}\mathcal{I}_{1,1,1} \propto & \frac{da_1 \wedge da_2 \wedge da_3 \wedge da_4}{(a_1 a_2 - a_3 a_4)(1 + a_2 + a_1 + a_1 a_2 - a_3 a_4)} \\ & \times \frac{1}{\left(m_1^2(a_2 + a_1 a_2 - a_3 a_4) - m_2^2(a_2 + a_3) + m_3^2(1 + a_1 + a_4)\right)}\,,\end{aligned} \tag{3.292}$$

where I omit for simplicity the irrelevant overall constant. There are three poles to localise four integration variables. The fourth pole comes from a jacobian, as we have seen in the case of the four-dimensional bubble. This is therefore a composite leading singularity. This computation is significantly more involved than the previous ones. The MATHEMATICA packages MULTIVARIATERESIDUES [121] and DLOGBASIS [122] come to our help. The former uses algebraic geometry methods to compute multivariate residues in general, while the latter is specifically meant for a systematic

analysis of leading singularities. The readers who remember Eq. (3.28) will not be surprised to see that the leading singularity of the triangle integral is given by

$$\mathrm{LS}\left(I_{1,1,1}\right) = \frac{1}{\sqrt{\lambda(m)}}\,, \tag{3.293}$$

where λ is the Källen function (3.16). Once again, we see that an integral whose integrand has only simple poles and which is normalised so as to have constant leading singularities evaluates to a pure function. We have gathered enough evidence to motivate the conjecture presented in the next section.

3.6.2 *d* log *Integrands*

We have seen some evidence that two properties of the loop integrands are correlated with the transcendental purity of the corresponding integrals: the absence of double (or higher) poles in the integration variables, and the constant leading singularities. These properties can be made beautifully manifest in the so called *d* log *forms*. Let us consider an integrand $\mathcal{I}$ with n integration variables, a_i with $i = 1, \ldots, n$. We consider the kinematic variables as fixed, and thus define the differential as

$$d = \sum_{i=1}^{n} da_i \frac{\partial}{\partial a_i}\,. \tag{3.294}$$

An integrand admits a d log form if it can be expressed as

$$\mathcal{I} = \sum_{I=(i_1,\ldots,i_n)} c_I\, d\log r_{i_1} \wedge \cdots \wedge d\log r_{i_n}\,, \tag{3.295}$$

where the r_i are algebraic functions of the kinematic and of the integration variables, while the c_I are algebraic functions of the kinematic variables only. The d log forms clearly behave as dx/x near any singularity $x = 0$, and thus have only simple poles. The coefficients c_I are the leading singularities. They can be computed—at least in principle—by taking residues so as to localise all the n integrations, e.g. by integrating along the contour encircling the poles $r_i = 0$.

It is important to stress the difference between the d log form of the loop integrands (3.295) and the d log forms in Chen's iterated integrals discussed in Sect. 3.3.1: the former are differential forms in the loop integration variables, while the latter are differential forms in the kinematic variables. A study of the intriguing relation between the two has been initiated in [123].

It is instructive to spell out at least one example of d log form. Using the properties of the wedge product it is rather easy to rewrite the integrand of the bubble in $D = 2$ dimensions given by Eq. (3.283) as

$$m_1^2 \mathcal{I}_{1,1,0}^{(D=2)} = \frac{1}{2} d\log\left(\frac{a_1}{1+a_1}\right) \wedge d\log\left(\frac{a_2}{1+a_2}\right). \tag{3.296}$$

With some more algebraic manipulations, it is possible to express this d log form in terms of the loop momentum,

$$m_1^2 \mathcal{I}_{1,1,0}^{(D=2)} = \frac{1}{2} d\log\left(\frac{k^2}{(k-k^*)^2}\right) \wedge d\log\left(\frac{(k+p_1)^2}{(k-k^*)^2}\right), \tag{3.297}$$

where k^* is one of the two solutions of the maximal cut,

$$\begin{cases} (k^*)^2 = 0\,, \\ (k^*+p)^2 = 0\,, \end{cases} \tag{3.298}$$

which in the parameterisation given by Eq. (3.282) are $k^* = -n_1$ and $k^* = -n_2$. An analogous but lengthier d log form can also be worked out for the triangle integrand in four dimensions, but not for the bubble, because of the double pole at infinity.

The conjecture underlying this method states that integrands which admit a d log form with constant leading singularities integrate to pure functions [115, 124]. A lot of evidence has been collected over the years in support of this statement, and important steps towards a deeper understanding have been made in [123].

Apart from the mere theoretical interest, this observation has important implications for the search of pure integrals. The reason is that it is possible to construct algorithmically all the d log forms with constant leading singularities associated with a given integral family. The algorithm, first proposed in [125] and then refined in [122], has also been implemented in the public MATHEMATICA package DLOGBASIS. The systematic nature of this method and the particular simplicity of the resulting pure integrals with respect to other techniques have made this approach extremely successful. As we will see in the next chapter, it played a crucial role in the state-of-the-art computation of all the Feynman integrals required for the massless five-particle scattering amplitudes at two loops. Before moving on to that, however, it is fair to mention also the limitations of this method.

First of all, the presence of double poles in the integrand does not imply that the integral does not have a uniform transcendental weight in general. For example, the two-dimensional bubble, shifted to $D = 4 - 2\epsilon$ dimensions, has a double propagator and thus a clear double pole, as can be seen in Eq. (3.286). Nonetheless, it has uniform transcendental weight. Clearly, the d log integrands do not cover the entire space of integrands which evaluate to uniformly transcendental functions. The algorithm proposed in [107] does not have this limitation, but it requires one pure integral (which couples to all the integrals of the family) to start with, and the resulting canonical bases typically have much more complicated expressions than the d log ones. For this reason I see the two methods as complementary.

Another limitation is the integer-dimensional nature of the analysis of the leading singularities presented in this section. We are typically interested in loop integrals in

$D = D_0 - 2\epsilon$ dimensions, for some integer D_0, whereas we have mostly considered the D_0-dimensional part of the integrands only. While this is sufficient for many highly non-trivial applications, it is in general not enough. It is in fact possible to write down integrands which vanish identically in D_0 dimensions, but yield a finite result upon integration. The contribution of these "evanescent" terms are clearly missed by the D_0-dimensional analysis, and may sometimes be relevant. In [111], my collaborators and I proposed a refined leading singularity analysis based on a D-dimensional parameterisation, which allows us to control such evanescent terms as well. I postpone the discussion of this to Sect. 4.2.1.

This topic concludes a long and hopefully not too tedious chapter, where I have presented all the tools necessary to face an analytic multi-loop computation using the method of the differential equations. Now I owe you, relentless reader who made it to this point, a proof that it is really worthwhile to learn all of this. In the next chapter I discuss the application of these techniques to the computation of several five-particle integrals and scattering amplitudes at two-loop order.

Bibliography

1. Kotikov A (1991) Differential equations method: new technique for massive Feynman diagrams calculation. Phys Lett B 254:158
2. Bern Z, Dixon LJ, Kosower DA (1994) Dimensionally regulated pentagon integrals. Nucl Phys B 412:751. arXiv:hep-ph/9306240
3. Remiddi E (1997) Differential equations for Feynman graph amplitudes. Nuovo Cim A 110:1435. arXiv:hep-th/9711188
4. Gehrmann T, Remiddi E (2000) Differential equations for two loop four point functions. Nucl Phys B 580:485. arXiv:hep-ph/9912329
5. Henn JM (2013) Multiloop integrals in dimensional regularization made simple. Phys Rev Lett 110:251601. arXiv:1304.1806
6. Smirnov A (2016) FIESTA4: optimized Feynman integral calculations with GPU support. Comput Phys Commun 204:189–199
7. Borowka S, Heinrich G, Jahn S, Jones S, Kerner M, Schlenk J (2019) A GPU compatible quasi-Monte Carlo integrator interfaced to pySecDec. Comput Phys Commun 240:120–137
8. Moriello F (2020) Generalised power series expansions for the elliptic planar families of Higgs + jet production at two loops. JHEP 01:150. arXiv:1907.13234
9. Frellesvig H, Hidding M, Maestri L, Moriello F, Salvatori G, The complete set of two-loop master integrals for Higgs + jet production in QCD. arXiv:1911.06308
10. Bonciani R, Del Duca V, Frellesvig H, Henn J, Hidding M, Maestri L et al (2020) Evaluating a family of two-loop non-planar master integrals for Higgs + jet production with full heavy-quark mass dependence. JHEP 01:132. arXiv:1907.13156
11. Abreu S, Ita H, Moriello F, Page B, Tschernow W, Zeng M, Two-loop integrals for planar five-point one-mass processes. arXiv:2005.04195
12. Hidding M, DiffExp, a Mathematica package for computing Feynman integrals in terms of one-dimensional series expansions. arXiv:2006.05510
13. Becchetti M, Bonciani R, Del Duca V, Hirschi V, Moriello F, Schweitzer A, NLO corrections to light-quark mixed QCD-EW contributions to Higgs production. arXiv:2010.09451
14. Henn JM (2015) Lectures on differential equations for Feynman integrals. J Phys A 48:153001. arXiv:1412.2296

15. Chavez F, Duhr C (2012) Three-mass triangle integrals and single-valued polylogarithms. JHEP 11:114. arXiv:1209.2722
16. Chetyrkin K, Tkachov F (1981) Integration by parts: the algorithm to calculate beta functions in 4 loops. Nucl Phys B 192:159
17. Capper DM, Leibbrandt G (1974) On a conjecture by 't Hooft and Veltman. J Math Phys 15
18. Leibbrandt G (1975) Introduction to the technique of dimensional regularization. Rev Mod Phys 47:849
19. Smirnov A, Petukhov A (2011) The number of master integrals is finite. Lett Math Phys 97:37. arXiv:1004.4199
20. Laporta S (2000) High precision calculation of multiloop Feynman integrals by difference equations. Int J Mod Phys A 15:5087. arXiv:hep-ph/0102033
21. Laporta S, Remiddi E (1996) The analytical value of the electron (g-2) at order alpha**3 in QED. Phys Lett B 379:283. arXiv:hep-ph/9602417
22. Anastasiou C, Lazopoulos A (2004) Automatic integral reduction for higher order perturbative calculations. JHEP 07:046. arXiv:hep-ph/0404258
23. von Manteuffel A, Studerus C, Reduze 2 - distributed Feynman integral reduction. arXiv:1201.4330
24. Lee RN (2014) LiteRed 1.4: a powerful tool for reduction of multiloop integrals. J Phys Conf Ser 523:012059. arXiv:1310.1145
25. Maierhöfer P, Usovitsch J, Kira 1.2 release notes. arXiv:1812.01491
26. Smirnov A, Chuharev F, FIRE6: Feynman integral REduction with modular arithmetic. arXiv:1901.07808
27. Goncharov AB (1995) Geometry of configurations, polylogarithms, and motivic cohomology. Adv Math 114:197
28. Remiddi E, Vermaseren J (2000) Harmonic polylogarithms. Int J Mod Phys A 15:725. arXiv:hep-ph/9905237
29. Goncharov AB, Multiple polylogarithms and mixed Tate motives. arXiv:math/0103059
30. Vollinga J, Weinzierl S (2005) Numerical evaluation of multiple polylogarithms. Comput Phys Commun 167:177. arXiv:hep-ph/0410259
31. Goncharov AB (2011) Multiple polylogarithms, cyclotomy and modular complexes
32. Heller M, von Manteuffel A, Schabinger RM, Multiple polylogarithms with algebraic arguments and the two-loop EW-QCD Drell-Yan master integrals. arXiv:1907.00491
33. Brown F, Duhr C, A double integral of dlog forms which is not polylogarithmic. arXiv:2006.09413
34. Brown FCS, Levin A (2011) Multiple elliptic polylogarithms
35. Adams L, Bogner C, Weinzierl S (2014) The two-loop sunrise graph in two space-time dimensions with arbitrary masses in terms of elliptic dilogarithms. J Math Phys 55:102301. arXiv:1405.5640
36. Broedel J, Mafra CR, Matthes N, Schlotterer O (2015) Elliptic multiple zeta values and one-loop superstring amplitudes. JHEP 07:112. arXiv:1412.5535
37. Broedel J, Duhr C, Dulat F, Tancredi L (2018) Elliptic polylogarithms and iterated integrals on elliptic curves. Part I: general formalism. JHEP 05:093. arXiv:1712.07089
38. Broedel J, Duhr C, Dulat F, Tancredi L (2018) Elliptic polylogarithms and iterated integrals on elliptic curves II: an application to the sunrise integral. Phys Rev D 97:116009. arXiv:1712.07095
39. Adams L, Weinzierl S (2018) The ε-form of the differential equations for Feynman integrals in the elliptic case. Phys Lett B 781:270. arXiv:1802.05020
40. Bogner C, Müller-Stach S, Weinzierl S (2020) The unequal mass sunrise integral expressed through iterated integrals on $\overline{\mathcal{M}}_{1,3}$. Nucl Phys B 954:114991. arXiv:1907.01251
41. Huang R, Zhang Y (2013) On genera of curves from high-loop generalized unitarity cuts. JHEP 04:080. arXiv:1302.1023
42. Hauenstein JD, Huang R, Mehta D, Zhang Y (2015) Global structure of curves from generalized unitarity cut of three-loop diagrams. JHEP 02:136. arXiv:1408.3355

43. Vanhove P (2019) Feynman integrals, toric geometry and mirror symmetry. In: KMPB conference: elliptic integrals, elliptic functions and modular forms in quantum field theory, pp 415–458. arXiv:1807.11466
44. Klemm A, Nega C, Safari R (2020) The l-loop banana amplitude from GKZ systems and relative Calabi-Yau periods. JHEP 04:088. arXiv:1912.06201
45. Bourjaily JL, He Y-H, Mcleod AJ, Von Hippel M, Wilhelm M (2018) Traintracks through Calabi-Yau manifolds: scattering amplitudes beyond elliptic polylogarithms. Phys Rev Lett 121:071603. arXiv:1805.09326
46. Bourjaily JL, McLeod AJ, von Hippel M, Wilhelm M (2019) Bounded collection of Feynman integral Calabi-Yau geometries. Phys Rev Lett 122:031601. arXiv:1810.07689
47. Bourjaily JL, McLeod AJ, Vergu C, Volk M, Von Hippel M, Wilhelm M (2020) Embedding Feynman integral (Calabi-Yau) geometries in weighted projective space. JHEP 01:078. arXiv:1910.01534
48. Brown F (2013) Iterated integrals in quantum field theory. In: 6th summer school on geometric and topological methods for quantum field theory, pp 188–240
49. Chen K-T (1977) Iterated path integrals. Bull Am Math Soc 83:831
50. Brown FCS (2006) Multiple zeta values and periods of moduli spaces $\mathfrak{M}_{0,n}$
51. Spence W (1809) An essay on the theory of the various orders of logarithmic transcendents. London and Edinburgh
52. Zagier D (1990) The Bloch-Wigner-Ramakrishnan polylogarithm function. Math Ann 286:613
53. Bloch S (1977) Higher regulators, algebraic K-theory, and zeta functions of elliptic curves. Irvine lecture notes
54. Goncharov A (1996) Volumes of hyperbolic manifolds and mixed Tate motives
55. Duhr C, Dulat F (2019) PolyLogTools — polylogs for the masses. JHEP 08:135. arXiv:1904.07279
56. Ree R (1958) Lie elements and an algebra associated with shuffles. Ann Math 68:210
57. Maitre D (2006) HPL, a mathematica implementation of the harmonic polylogarithms. Comput Phys Commun 174:222. arXiv:hep-ph/0507152
58. Hoffman ME (1997) The algebra of multiple harmonic series. J Algebra 194:477
59. Blumlein J, Broadhurst D, Vermaseren J (2010) The multiple zeta value data mine. Comput Phys Commun 181:582. arXiv:0907.2557
60. Brown F (2012) Mixed Tate motives over $\mathbb{Z}$. Ann Math 175:949
61. Lewin L (1981) Polylogarithms and associated functions. North-Holland, New York
62. Kellerhals R (1995) Volumes in hyperbolic 5-space. Geom Funct Anal GAFA 5:640
63. Frellesvig H, Tommasini D, Wever C (2016) On the reduction of generalized polylogarithms to Li_n and $\mathrm{Li}_{2,2}$ and on the evaluation thereof. JHEP 03:189. arXiv:1601.02649
64. Bauer CW, Frink A, Kreckel R (2002) Introduction to the GiNaC framework for symbolic computation within the C++ programming language. J Symb Comput 33:1. arXiv:cs/0004015
65. Apéry R (1979) Irrationalité de $\zeta(2)$ et $\zeta(3)$. Astérisque 61:11
66. Goncharov AB (2002) Galois symmetries of fundamental groupoids and noncommutative geometry
67. Duhr C (2012) Hopf algebras, coproducts and symbols: an application to Higgs boson amplitudes. JHEP 08:043. arXiv:1203.0454
68. Mitev V, Zhang Y, SymBuild: a package for the computation of integrable symbols in scattering amplitudes. arXiv:1809.05101
69. Peraro T (2019) FiniteFlow: multivariate functional reconstruction using finite fields and dataflow graphs. JHEP 07:031. arXiv:1905.08019
70. Zoia S (2018) Conformal symmetry and Feynman integrals. PoS LL2018:037. arXiv:1807.06020
71. Del Duca V, Duhr C, Smirnov VA (2010) An analytic result for the two-loop hexagon Wilson loop in N = 4 SYM. JHEP 03:099. arXiv:0911.5332
72. Del Duca V, Duhr C, Smirnov VA (2010) The two-loop hexagon Wilson loop in N = 4 SYM. JHEP 05:084. arXiv:1003.1702

73. Goncharov AB, Spradlin M, Vergu C, Volovich A (2010) Classical polylogarithms for amplitudes and Wilson loops. Phys Rev Lett 105:151605. arXiv:1006.5703
74. Goncharov AB (2009) A simple construction of Grassmannian polylogarithms
75. Duhr C, Gangl H, Rhodes JR (2012) From polygons and symbols to polylogarithmic functions. JHEP 10:075. arXiv:1110.0458
76. Bloch SJ (2000) Higher regulators, algebraic K-theory, and zeta functions of elliptic curves. CRM monograph series, vol 11
77. Fomin S, Zelevinsky A (2001) Cluster algebras i: foundations
78. Gaiotto D, Maldacena J, Sever A, Vieira P (2011) Pulling the straps of polygons. JHEP 12:011. arXiv:1102.0062
79. Steinmann O (1960) Über den Zusammenhang zwischen den Wightmanfunktionen und der-retardierten Kommutatoren. Helv Phys Acta 33:257
80. Steinmann O (1960) Wightman-Funktionen und retardierten Kommutatoren. II. Helv Phys Acta 33:347
81. Cahill KE, Stapp HP (1975) Optical theorems and Steinmann relations. Ann Phys 90:438
82. Caron-Huot S, Dixon LJ, McLeod A, von Hippel M (2016) Bootstrapping a five-loop amplitude using Steinmann relations. Phys Rev Lett 117:241601. arXiv:1609.00669
83. Dixon LJ, Drummond J, Harrington T, McLeod AJ, Papathanasiou G, Spradlin M (2017) Heptagons from the Steinmann cluster bootstrap. JHEP 02:137. arXiv:1612.08976
84. Caron-Huot S, Dixon LJ, Dulat F, Von Hippel M, McLeod AJ, Papathanasiou G (2019) The cosmic Galois group and extended Steinmann relations for planar $\mathcal{N} = 4$ SYM amplitudes. JHEP 09:061. arXiv:1906.07116
85. Drummond J, Foster J, Gürdoğan Ö (2018) Cluster adjacency properties of scattering amplitudes in $N = 4$ supersymmetric Yang-Mills theory. Phys Rev Lett 120:161601. arXiv:1710.10953
86. Drummond J, Foster J, Gürdoğan Ö (2019) Cluster adjacency beyond MHV. JHEP 03:086. arXiv:1810.08149
87. Henn JM, Mistlberger B (2019) Four-graviton scattering to three loops in $\mathcal{N} = 8$ supergravity. JHEP 05:023. arXiv:1902.07221
88. Ferguson HRP, Bailey DH (1992) A polynomial time, numerically stable integer relation algorithm. RNR technical report RNR-91-032
89. Chicherin D, Gehrmann T, Henn J, Lo Presti N, Mitev V, Wasser P (2019) Analytic result for the nonplanar hexa-box integrals. JHEP 03:042. arXiv:1809.06240
90. Becchetti M, Bonciani R (2018) Two-loop master integrals for the planar QCD massive corrections to Di-photon and Di-jet hadro-production. JHEP 01:048. arXiv:1712.02537
91. Besier M, Van Straten D, Weinzierl S (2019) Rationalizing roots: an algorithmic approach. Commun Number Theory Phys 13:253. arXiv:1809.10983
92. Besier M, Wasser P, Weinzierl S (2020) RationalizeRoots: software package for the rationalization of square roots. Comput Phys Commun 253:107197. arXiv:1910.13251
93. Besier M, Festi D, Rationalizability of square roots. arXiv:2006.07121
94. Brown F (2009) The massless higher-loop two-point function. Commun Math Phys 287:925. arXiv:0804.1660
95. Panzer E (2015) Algorithms for the symbolic integration of hyperlogarithms with applications to Feynman integrals. Comput Phys Commun 188:148. arXiv:1403.3385
96. Gehrmann T, Henn J, Lo Presti N (2018) Pentagon functions for massless planar scattering amplitudes. JHEP 10:103. arXiv:1807.09812
97. Chicherin D, Sotnikov V, Pentagon functions for scattering of five massless particles. arXiv:2009.07803
98. Ree R (1958) Lie elements and an algebra associated with shuffles. Ann Math 68:210
99. Bourbaki N (1972) Groupes et algèbres de Lie. Hermann, Paris
100. Griffing G (1995) Dual lie elements and a derivation for the cofree coassociative coalgebra. Proc Am Math Soc 123:3269
101. Caron-Huot S, Henn JM (2014) Iterative structure of finite loop integrals. JHEP 06:114. arXiv:1404.2922

102. Wasow W (1965) Asymptotic expansions for ordinary differential equations. Pure and applied mathematics, vol XIV. Interscience Publishers Wiley, New York-London-Sydney
103. Lee RN (2015) Reducing differential equations for multiloop master integrals. JHEP 04:108. arXiv:1411.0911
104. Prausa M (2017) Epsilon: a tool to find a canonical basis of master integrals. Comput Phys Commun 219:361. arXiv:1701.00725
105. Meyer C (2017) Transforming differential equations of multi-loop Feynman integrals into canonical form. JHEP 04:006. arXiv:1611.01087
106. Gituliar O, Magerya V (2017) Fuchsia: a tool for reducing differential equations for Feynman master integrals to epsilon form. Comput Phys Commun 219:329. arXiv:1701.04269
107. Dlapa C, Henn J, Yan K (2020) Deriving canonical differential equations for Feynman integrals from a single uniform weight integral. JHEP 05:025. arXiv:2002.02340
108. Höschele M, Hoff J, Ueda T (2014) Adequate bases of phase space master integrals for gg $\rightarrow$ h at NNLO and beyond. JHEP 09:116. arXiv:1407.4049
109. Henn JM, Smirnov AV, Smirnov VA (2013) Analytic results for planar three-loop four-point integrals from a Knizhnik-Zamolodchikov equation. JHEP 07:128. arXiv:1306.2799
110. Chen J, Xu X, Yang LL, Constructing canonical Feynman integrals with intersection theory. arXiv:2008.03045
111. Chicherin D, Gehrmann T, Henn J, Wasser P, Zhang Y, Zoia S (2019) All master integrals for three-jet production at next-to-next-to-leading order. Phys Rev Lett 123:041603. arXiv:1812.11160
112. Eden RJ, Landshoff PV, Olive DI, Polkinghorne JC (1966) The analytic S-matrix. Cambridge University Press, Cambridge
113. Britto R, Cachazo F, Feng B (2005) Generalized unitarity and one-loop amplitudes in N=4 super-Yang-Mills. Nucl Phys B 725:275. arXiv:hep-th/0412103
114. Cachazo F, Sharpening the leading singularity. arXiv:0803.1988
115. Arkani-Hamed N, Bourjaily JL, Cachazo F, Trnka J (2012) Local integrals for planar scattering amplitudes. JHEP 06:125. arXiv:1012.6032
116. Derkachov S, Honkonen J, Pis'mak Y (1990) Three-loop calculation of the random walk problem: an application of dimensional transformation and the uniqueness method. J Phys A: Math Gen 23:5563
117. Tarasov O (1996) Connection between Feynman integrals having different values of the space-time dimension. Phys Rev D 54:6479. arXiv:hep-th/9606018
118. Dixon LJ (2014) A brief introduction to modern amplitude methods. In: Theoretical advanced study institute in elementary particle physics: particle physics: the Higgs boson and beyond, pp 31–67. arXiv:1310.5353
119. Henn JM, Plefka JC (2014) Scattering amplitudes in gauge theories, vol 883. Springer, Berlin. https://doi.org/10.1007/978-3-642-54022-6
120. Elvang H, Huang Y-T (2015). Scattering amplitudes in gauge theory and gravity. Cambridge University Press, Cambridge
121. Larsen KJ, Rietkerk R (2017) MultivariateResidues - a Mathematica package for computing multivariate residues. PoS RADCOR2017:021. arXiv:1712.07050
122. Henn J, Mistlberger B, Smirnov VA, Wasser P (2020) Constructing d-log integrands and computing master integrals for three-loop four-particle scattering. JHEP 04:167. arXiv:2002.09492
123. Herrmann E, Parra-Martinez J (2020) Logarithmic forms and differential equations for Feynman integrals. JHEP 02:099. arXiv:1909.04777
124. Arkani-Hamed N, Bourjaily JL, Cachazo F, Trnka J (2014) Singularity structure of maximally supersymmetric scattering amplitudes. Phys Rev Lett 113:261603. arXiv:1410.0354
125. Wasser P (2018) Analytic properties of Feynman integrals for scattering amplitudes. PhD thesis, Mainz University

Chapter 4
Two-Loop Five-Particle Scattering Amplitudes

In this chapter I present the first results for complete two-loop five-particle scattering amplitudes. By "complete" I mean that the computation takes into account both the planar and the non-planar Feynman diagrams. In case you are not familiar with this distinction, bear with me until Sect. 4.3.1, where I define it properly. For now it suffices to know that the non-planar contributions are substantially more complicated than their planar counterparts, both in the reduction to basis integrals and in the evaluation of the latter. Indeed, a lot is known about the scattering of five massless particles at two-loop order in the planar limit. The planar integral family and all the five-parton amplitudes in QCD[1] have been computed analytically, in Refs. [1–3] and [1, 4–8], respectively. Even a full-fledged NNLO theoretical prediction is already available in the planar limit, for three-photon production [9–11]. There has even been important progress towards the computation of the planar two-loop five-particle integrals with one massive external leg [2, 12–14]. In this chapter I outline the recent progress towards including the non-planar corrections in massless two-loop five-particle scattering amplitudes.

I begin in Sect. 4.1 by discussing the kinematics of the scattering of five massless particles. Then, I move on to the Feynman integrals in Sect. 4.2. There are two non-planar integral families. One was computed previously in Ref. [15] (see also [16–19]). I took part in the computation of the last non-planar integral family, the so-called "double-pentagon" [20, 21]. I first discuss a D-dimensional extension of the four-dimensional leading-singularity technique introduced in Sect. 3.6.2. I show how we use it to construct a basis of pure integrals for the double-pentagon family, and how we compute the latter in terms of Chen's iterated integrals through the canonical differential equations. Finally, I discuss the resulting function space and highlight certain non-trivial analytic properties.

[1] The available results for the two-loop five-parton amplitudes in the planar limit are valid in the Euclidean region only. Further effort is required to analytically continue them to the physical scattering region, in view of phenomenological applications.

S. Zoia, *Modern Analytic Methods for Computing Scattering Amplitudes*, Springer Theses,
https://doi.org/10.1007/978-3-031-01945-6_4

In Sect. 4.3 I present in parallel the computation of the two-loop five-particle amplitudes in $\mathcal{N} = 4$ super Yang-Mills theory and $\mathcal{N} = 8$ supergravity. Historically, we first computed them at symbol level [20, 22–24], starting from the integrands of Ref. [25]. These were the very first analytic results for complete two-loop five-particle amplitudes. Later, we lifted the results to function level [26]. Here I present directly the final result. First I show that a lot of precious information can be extracted from the integrand prior to integration. This allows us to write down rather restrictive ansätze for the amplitudes, in terms of leading singularities and pure functions. Using the results for the integrals discussed in Sect. 4.2 we can then fix the coefficients of the ansätze, and in this way obtain explicit analytic expressions of the amplitudes which have manifestly uniform transcendental weight. I discuss how their infrared singularities factorise, and extract finite hard functions. To further validate our results, I present several other checks, including the behaviour in collinear and soft limits. Finally, I discuss throughly the asymptotic expansion of the hard functions in the multi-Regge limit.

After warming up with the maximally supersymmetric theories, we raise the stake and tackle Yang-Mills theory. Section 4.5 is devoted to the computation of the two-loop five-gluon all-plus helicity amplitude in pure Yang-Mills theory [27, 28]. Despite the substantial increase in complexity, I show that it is nonetheless possible to make an educated guess for the form of the two-loop hard function. I discuss the renormalisation of ultraviolet divergences and the factorisation of the infrared ones, and define a finite hard function. The fact that the tree-level amplitude vanishes and that the one-loop amplitude is finite and rational (at order ϵ^0) allows us to use four-dimensional unitarity and leading singularities to constrain the form of the two-loop hard function. Then I move on to the actual computation. I show how to rewrite the integrand from Ref. [29] in a form that is suitable for Integration-by-Parts relation (IBP) reduction. After this is achieved, IBP reduction to pure basis integrals, substitution of the latter with their analytic expressions in terms of Chen's iterated integrals, and subtraction of the singularities are performed using the finite field method. Remarkable cancellations take place. The final formula fits in just two lines and involves logarithms and dilogarithms only. The rational prefactors of the latter are conformally invariant, which we proved to be related to the conformal invariance of the one-loop all-plus amplitudes [30].

4.1 Kinematics

We study the scattering of five massless particles. The five light-like momenta p_i are subject to on-shell and momentum conservation conditions,

$$p_i^2 = 0\,, \qquad \sum_{i=1}^{5} p_i = 0\,. \tag{4.1}$$

They give rise to five independent parity-even Lorentz invariants, which can be chosen as the scalar products of adjacent momenta,

$$s = (s_{12}\,, s_{23}\,, s_{34}\,, s_{45}\,, s_{51})\,, \tag{4.2}$$

with $s_{ij} = 2\,p_i \cdot p_j$. We take the external momenta p_i to lie in four-dimensional Minkowski space, while the loop momenta live in $D = 4 - 2\epsilon$ dimensions to regulate the infrared and ultraviolet divergences.

Starting from $n = 5$ particles, the kinematics depends also on parity-odd Lorentz invariants. Since there are four independent momenta, they can be contracted with the Levi-Civita pseudo-tensor. It is therefore possible to construct a parity-odd Lorentz invariant,

$$\mathrm{tr}_5 := \mathrm{tr}(\gamma_5 \not{p}_1 \not{p}_2 \not{p}_3 \not{p}_4) = 4i\,\epsilon_{\mu_1\mu_2\mu_3\mu_4}\, p_1^{\mu_1} p_2^{\mu_2} p_3^{\mu_3} p_4^{\mu_4}\,. \tag{4.3}$$

Space-time parity in fact acts by inverting all the spatial momentum components,

$$\left(p_i^0,\, \vec{p}_i\right) \longrightarrow \left(p_i^0,\, -\vec{p}_i\right)\,, \tag{4.4}$$

which induces a change of sign in tr_5, while leaving the scalar products s_{ij} invariant. Clearly it is not possible to build a parity-odd invariant if fewer than five particles scatter, which makes five-particle scattering particularly interesting. It is convenient to introduce the usual spinor-helicity parameterisation of the external light-like momenta, $p_i = \lambda_i \tilde{\lambda}_i$. In terms of spinor brackets, the parity-odd invariant can be expressed as

$$\mathrm{tr}_5 = [12]\langle 23\rangle[34]\langle 41\rangle - \langle 12\rangle[23]\langle 34\rangle[41]\,. \tag{4.5}$$

The square of tr_5 is a scalar quantity, and can thus be expressed in terms of the scalar invariants s_{ij}. In order to do so, we introduce the so-called *Gram determinants*. Given a set of momenta $\{q_i\}_{i=1}^n$, the Gram matrix $G(q_1, \ldots, q_n)$ is defined by

$$[G(q_1, \ldots, q_n)]_{ij} = 2q_i \cdot q_j\,, \qquad \forall i, j = 1, \ldots, n\,, \tag{4.6}$$

where the factor of 2 is conventional. The Gram determinant of a set of momenta is the determinant of the corresponding Gram matrix. The Gram determinant vanishes if the momenta q_i are linearly dependent and, as a consequence, it is invariant under the shift of any q_i by any of the other momenta. In particular, if the momenta q_i are four-dimensional, the Gram determinant vanishes for any set of n momenta with $n > 4$. This has important implications for the evanescent integrands discussed in Sect. 3.6.2. I will address this in Sect. 4.2.1. Using the properties of the Levi-Civita symbol, it is possible to show that

$$\mathrm{tr}_5^2 = \Delta\,, \tag{4.7}$$

where Δ is the determinant of the Gram matrix constructed with four independent external momenta,

$$\Delta := \det G\,(p_1, p_2, p_3, p_4)\ , \tag{4.8}$$

which is a degree-four polynomial in the s_{ij},

$$\Delta = (s_{12}s_{23} + s_{23}s_{34} - s_{34}s_{45} + s_{45}s_{51} - s_{51}s_{12})^2 - 4s_{12}s_{23}s_{34}(s_{23} - s_{45} - s_{51})\,. \tag{4.9}$$

The parity-odd invariant tr_5 thus introduces an algebraic dependence on the kinematics through Eq. (4.7). We choose the positive branch of the square root,

$$\mathrm{tr}_5 = \sqrt{\Delta}\,. \tag{4.10}$$

The cautious readers might feel quite uneasy looking at this equation: the left-hand side has odd parity, whereas the right-hand side is a function of parity-even invariants. They might fear that this choice washes away the information about parity. In practice, it is sufficient to recall that parity acts on helicity-free functions by flipping the sign of $\sqrt{\Delta}$, which plays the role of parity label.

In Sect. 3.4.1 we have seen that, since the Feynman integrals are multi-valued functions, it is crucial to specify the domain of the variables, namely the kinematic region. The double-pentagon integrals discussed in Sect. 4.2 do not have a Euclidean region. Moreover, we are ultimately interested in phenomenological applications. For these reasons, we work in the $2 \to 3$ physical scattering kinematics. Since any pair of momenta (p_i, p_j) can be incoming, the physical region in Minkowski space consists of ten distinct regions. They are referred to as channels, and are labelled by their initial-state s_{ij} invariant. The different channels are related by permutations of the external momenta. Without any loss of generality, we can take the particles with momenta p_1 and p_2 to be incoming. In other words, we work in the s_{12} channel. The kinematic variables in the s_{12} channel are delimited by requiring that all s-channel invariants are positive,

$$s_{12} > 0\,, \qquad s_{34} > 0\,, \qquad s_{35} > 0\,, \qquad s_{45} > 0\,, \tag{4.11}$$

all t-channel invariants are negative,

$$s_{1j} < 0\,, \qquad s_{2j} < 0\,, \qquad \forall\ j = 3, 4, 5\,, \tag{4.12}$$

and by the negativity of the Gram determinant,

$$\Delta \leq 0\,, \tag{4.13}$$

which follows from the real-valuedness of all momenta. This constraint might sound unusual, and can be understood as follows. The Gram matrix of the external momenta

can be written as

$$G(p_1, p_2, p_3, p_4) = 2M^T(p_1, p_2, p_3, p_4)gM(p_1, p_2, p_3, p_4)\,, \tag{4.14}$$

where $M(p_1, p_2, p_3, p_4)$ is a 4×4 matrix whose columns are the four-dimensional momenta $\{p_i\}_{i=1}^4$, and g is the metric tensor. Since $\det g = -1$,

$$\Delta = -2^4 \det^2 \left[M(p_1, p_2, p_3, p_4)\right]\,. \tag{4.15}$$

It follows that, if all the external momenta p_i are real, Δ must be negative.

4.2 Feynman Integrals

The scattering amplitudes for five massless particles at two loops contain Feynman integrals of the three families shown in Fig. 4.1. The planar "pentagon-box" family in Fig. 4.1a and the nonplanar "hexagon-box" family in Fig. 4.1b were computed in Refs. [1–3] and [15] (see also [16–19]), respectively. The last family, dubbed "double-pentagon" and shown in Fig. 4.1c, was computed at symbol level in Ref. [20], and in terms of Chen's iterated integrals by my collaborators and I [21]. In this section I cover the latter work. I first present a refinement of the technique described in Sect. 3.6, which allowed us to construct a basis of pure master integrals. Then I discuss the ensuing function space.

4.2.1 Pure Integrals from D-Dimensional Leading Singularities

We define the integrals of the double-pentagon family shown in Fig. 4.1c as

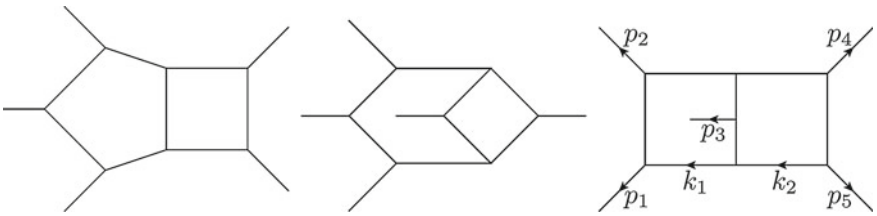

(a) Pentagon-box (b) Hexagon-box (c) Double-pentagon

Fig. 4.1 Integral topologies for massless five-particle scattering at two loops. The arrows in Fig. 4.1c denote the direction of the momenta

$$I_{a_1,a_2,\ldots,a_{11}} = e^{2\epsilon\gamma_{\rm E}} \int \frac{d^D k_1}{i\pi^{\frac{D}{2}}} \frac{d^D k_2}{i\pi^{\frac{D}{2}}} \prod_{j=1}^{11} D_j^{-a_j} \,. \tag{4.16}$$

The inverse propagators D_j are given by

$$\begin{aligned}
D_1 &= k_1^2\,, & D_7 &= (k_1-k_2)^2\,,\\
D_2 &= (k_1-p_1)^2\,, & D_8 &= (k_1-k_2+p_3)^2\,,\\
D_3 &= (k_1-p_1-p_2)^2\,, & D_9 &= (k_1+p_5)^2\,,\\
D_4 &= k_2^2\,, & D_{10} &= (k_2-p_1)^2\,,\\
D_5 &= (k_2+p_4+p_5)^2\,, & D_{11} &= (k_2-p_1-p_2)^2\,,\\
D_6 &= (k_2+p_5)^2\,,
\end{aligned} \tag{4.17}$$

where D_9, D_{10} and D_{11} are Irreducible Scalar Products (ISPs). The IBPs relations indicate that there are 108 independent integrals. Of these, 9 are in the top sector, namely they have all 8 propagators. The integrals with fewer propagators are already known. Some are sub-topologies of the pentagon-box [1, 3] and of the hexagon-box [15] families. Others have less than five, but possibly massive, external momenta [31, 32]. Our goal is therefore to find 9 independent pure integrals in the top sector.

We adopt the approach discussed in Sect. 3.6, and construct all the four-dimensional d log integrands with constant leading singularities using the algorithm of Refs. [33] (further refined in Ref. [34]). In order to perform the loop integration in D dimension, however, one needs to specify how such d log integrands are to be defined away from four dimensions. The easiest way to do so is to simply "upgrade" the loop momenta from four to D dimensions. For obvious reasons, we dubbed this the "naïve upgrade" of a four-dimensional integrand. Despite its name, this method has been successful in many cases. In particular, it is sufficient to construct canonical bases for the other massless two-loop five-particle integral families. Nonetheless, one should expect the freedom involved in the upgrade to strike back, eventually. Indeed, this is what happens for the double-pentagon family.

The naïve upgrade of a four-dimensional d log integrand of the double-pentagon family in general does not integrate to a pure function. Let us make an explicit example. Table 3 of Ref. [35] offers a list of massless two-loop five-particle integrals whose four-dimensional integrands admit a d log form and have constant leading singularities. The sum of the first and the fifth numerators for the double-pentagon diagram (labelled (a) there), which we denote by $B_1 + B_5$, does not produce a pure integral after the naïve upgrade. This can be assessed by computing the differential equation.

The obstruction to the naïve upgrade must be related to missing evanescent terms in the integrands, namely terms which vanish in four dimensions at the integrand level, but which yield finite contributions upon D-dimensional integration. We found a convenient way to construct such terms using the Gram determinants. In Eq. (4.6) I have defined the Gram matrix of a set of vectors. We need to generalise it further to two distinct sets of vectors $\{q_i\}_{i=1}^n$ and $\{r_i\}_{i=1}^n$,

$$\left[G\begin{pmatrix} q_1,\ldots,q_n \\ r_1,\ldots,r_n \end{pmatrix}\right]_{ij} = 2q_i\cdot r_j\,. \tag{4.18}$$

In four dimensions, the determinant of the Gram matrix of any set or any pair of sets of five momenta is zero, because the latter are linearly dependent. If the five momenta involve also loop momenta, the Gram determinant gives a non-trivial integrand term which vanishes in the $D\to 4$ limit. For instance, consider the Gram determinants

$$\mathcal{G}_{ij} = \det G\begin{pmatrix} k_i,\, p_1,\, p_2,\, p_3,\, p_4 \\ k_j,\, p_1,\, p_2,\, p_3,\, p_4 \end{pmatrix}\,, \tag{4.19}$$

with $i,\,j\in\{1,2\}$. An integrand whose numerator is proportional to any combination of $\mathcal{G}_{ij}$ vanishes identically in four dimensions. Whenever such terms are relevant for an integrand to integrate to a pure function, the four-dimensional analysis discussed in Sect. 3.6 may be inaccurate. In particular, the conjectured criterion that four-dimensional d log integrands with constant leading singularities produce pure functions can in such a case fail.

We developed a novel D-dimensional criterion for pure integrals, based on the study of the leading singularities in Baikov representation [36, 37], which captures the D-dimensional features of the integrand as well. For a given four-dimensional d log integrand of the generic form $N/(D_1\ldots D_k)$, the new criterion generates a D-dimensional integrand of the form

$$\frac{\tilde{N}}{\tilde{D}_1\ldots\tilde{D}_k}+\frac{\tilde{S}}{\tilde{D}_1\ldots\tilde{D}_k}\,, \tag{4.20}$$

which is conjectured to integrate to a pure function. The tilde sign here denotes the naïve upgrade, and $\tilde{S}$ is proportional to evanescent Gram determinants. We name Eq. (4.20) the "refined upgrade" of the four-dimensional d log integrand $N/(D_1\ldots D_k)$.

In order to understand how this works it is not necessary to go into the details of the Baikov parameterisation. It is sufficient to recall the key idea: the inverse propagators D_j of a D-dimensional Feynman integrand are taken as the integration variables. I refer e.g. to [38] for a thorough discussion of how to write down the Baikov representation of an integral. The new integration variables, called Baikov variables for obvious reasons, capture also the D-dimensional features of the integrand. One can thus define D-dimensional leading singularities as the maximal residues computed in the Baikov variables. This can be done just as we did for the four-dimensional parameterisations discussed in Sect. 3.6. Then, our new D-dimensional criterion for a pure integral is to require that its integrand in the Baikov parameterisation admits a d log form and that all its leading singularities are constant. In practice, one can feed manually the Baikov parameterisation to the MATHEMATICA package DLOGBASIS [34], and execute its algorithm to construct all the D-dimensional d log forms with constant leading singularities.

There is however a technical complication. For the double-pentagon family, the standard Baikov analysis of the maximal cut [39, 40], based on the two-loop Baikov parameterisation, involves complicated three-fold integrals in the ISPs which are not cut. We by-pass this computational difficulty by adopting the loop-by-loop Baikov cut analysis [38]. Consider a generic double-pentagon integral with numerator N,

$$I_{\text{dp}}[N] := e^{2\epsilon\gamma_{\text{E}}} \int \frac{d^D k_1}{i\pi^{\frac{D}{2}}} \frac{d^D k_2}{i\pi^{\frac{D}{2}}} \frac{N}{D_1 \dots D_8} \,. \tag{4.21}$$

The analysis is analogous if the propagators are raised to some integer power. The integration can be separated loop by loop as

$$I_{\text{dp}}[N] = e^{2\epsilon\gamma_{\text{E}}} \int \frac{d^D k_2}{i\pi^{\frac{D}{2}}} \frac{1}{D_4 D_5 D_6} \int \frac{d^D k_1}{i\pi^{\frac{D}{2}}} \frac{N}{D_1 D_2 D_3 D_7 D_8} \,. \tag{4.22}$$

The two-loop integral $I_{\text{dp}}[N]$ can thus be written as the composition of a pentagon integral with loop momentum k_1 and a triangle integral with loop momentum k_2. The idea is then to apply the Baikov parameterisation loop by loop, namely first for the pentagon integral with numerator N and next for the triangle. Unfortunately, here comes another technical subtlety. The four independent external momenta of the pentagon integral are p_1, p_2, p_3 and $-k_2$. The numerator N may in general contain scalar products between the loop momentum of the pentagon, k_1, and external momenta which do not flow into the pentagon, i.e. $k_1 \cdot p_4$ or $k_1 \cdot p_5$. We refer to the latter as crossed terms. They cannot be Baikov-parameterised straightforwardly in the loop-by-loop approach, because they do not appear as propagators nor as ISPs of the pentagon integral. In other words, the pentagon integral offers no Baikov variables to express them. In such a case, we perform a one-loop integral reduction, i.e. we expand the pentagon integral with numerator k_1^μ in its four independent external momenta,

$$\int \frac{d^D k_1}{i\pi^{\frac{D}{2}}} \frac{k_1^\mu}{D_1 D_2 D_3 D_7 D_8} = I^{(1)} p_1^\mu + I^{(2)} p_2^\mu + I^{(3)} p_3^\mu - I^{(4)} k_2^\mu \,. \tag{4.23}$$

By contracting the two sides of this equations with the external momenta of the pentagon we can construct a linear system, whose solution gives the coefficients $I^{(i)}$ of the expansion. This way we can remove the crossed terms.[2] As a consequence, D_9 drops out from the integrand. We are thus left with 10 Baikov variables, $z_i \equiv D_i$, $i \in \{1, \dots, 11\}\backslash\{9\}$, as opposed to the 11 we would have had in the standard two-loop Baikov representation. Once this parameterisation is complete, we can explore the D-dimensional residues.

[2] Technically, we have solved the problem only for a linear dependence of the numerator on the crossed scalar products. The integral reduction on a quadratic crossed term, e.g. $(k_1 \cdot p_4)^2$, would involve the metric tensor $g^{\mu\nu}$, thus introducing a dependence on ϵ in the integrand. We did not need to address this issue for our purposes, but this remains an interesting open problem.

Let us consider, for example, a double-pentagon integral with an evanescent numerator, e.g. $I_{\text{dp}}[\mathcal{G}_{12}]$. The entire integrand, and thus also its leading singularities, vanishes in four dimensions. The method presented in Sect. 3.6 cannot establish whether this integral is expected to be pure or not. The loop-by-loop Baikov representation described above, on the other hand, does not vanish, and depends on 10 Baikov variables z_i. Using the package DLOGBASIS [34] we can compute systematically all leading singularities. In practice, it is convenient to simplify the calculation by working on the cut integral. So we take the residues in $z_i = 0\ \forall i \in C$ for all the subsets of propagators $C \subseteq \{1, \ldots, 8\}$, we compute the residues of these integrands in the remaining variables, and we make sure that there are no double poles. We find that the leading singularities, computed on different cuts, all evaluate to either $\pm \text{tr}_5/(s_{12} - s_{45})$ or zero. We therefore conclude that the integral

$$\frac{s_{12} - s_{45}}{\text{tr}_5} I_{\text{dp}}[G_{12}] \tag{4.24}$$

fulfills our D-dimensional criterion. Other integrals with purely Gram-determinant numerators satisfy our D-dimensional criterion, for instance

$$\frac{s_{45}}{\text{tr}_5}(G_{11} - G_{12})\,, \qquad \frac{s_{12}}{\text{tr}_5}(G_{22} - G_{12})\,. \tag{4.25}$$

The explicit computation of the differential equations proves that those given by Eqs. (4.24) and (4.25) are indeed pure integrals.

This D-dimensional analysis of the leading singularities also allows us to determine the refined upgrade of the double-pentagon four-dimensional d log integrals in Ref. [35]. For instance, the refined upgrade of $(B_1 + B_5)$ is given by

$$(\tilde{B}_1 + \tilde{B}_5) + \frac{16 s_{45} G_{12}}{\text{tr}_5^2}(s_{12}s_{23} - s_{12}s_{15} + 2s_{12}s_{34} + s_{23}s_{34} + s_{15}s_{45} - s_{34}s_{45})\,. \tag{4.26}$$

We verified that the refined upgrades of the d log integrands of Ref. [35] are indeed pure.

Finally, we can go back to the original goal: finding a canonical basis for the top sector of the double-pentagon integral family. The four-dimensional d logs in Ref. [35], upgraded in the refined sense, together with the Gram-determinant integrals given in Eqs. (4.24) and (4.25), span a 8-dimensional linear space. Only one integral is missing to form a basis.

The last integral was found using computational algebraic geometry. We consider generic ansätze for the numerators,

$$N_{\text{even}} = \sum_{\alpha} c_\alpha m_\alpha \,, \tag{4.27}$$

$$N_{\text{odd}} = \frac{1}{\text{tr}_5} \sum_{\alpha} c_\alpha m_\alpha \,, \tag{4.28}$$

where it is convenient to separate even and odd parity. Each c_α is a polynomial in the Mandelstam invariants s_{ij}, while m_α denotes a monomial in the ISPs. We require the four-dimensional leading singularities of the ansätze to match a given list of rational numbers. The polynomials c_α can then be computed using the module lift techniques [41] in computational algebraic geometry, implemented in the computer algebra system SINGULAR [42]. This produces another linearly independent integral satisfying our D-dimensional criterion.

Putting together all the candidate pure integrals which satisfy our novel D-dimensional criterion for uniform transcendentality gives a basis for the double-pentagon on the top sector. Sub-sector pure integrals are found either via the method described in Sect. 3.6, or taken from the literature [1, 3, 15]. The explicit computation of the differential equations proves that the resulting integral basis is indeed canonical.

4.2.2 Pentagon Functions

The method described in the previous section leads to a basis of 108 pure integrals for the double-pentagon family. We denote it by $\vec{g}$. They satisfy a system of differential equations in the canonical form,

$$d\vec{g} = \epsilon \, d\tilde{A} \, \vec{g} \,, \tag{4.29}$$

with

$$d\tilde{A} = \sum_{i=1}^{31} a_i d \log W_i \,, \tag{4.30}$$

where a_i are constant 108×108 matrices, and $\{W_i\}_{i=1}^{31}$ are the letters of the so-called *pentagon alphabet* [16]. The latter describes not only the double-pentagon family, but all massless five-particle integrals at two loops. This was first conjectured in Ref. [16], based on the results for the planar integrals [1–3], and later proven by exhaustion [15, 19–21]. Let us break it down.

First there is a large group of parity-even letters, $\{W_i\}_{i=1}^{25}$, which are simply given by scalar products of the external momenta,

$$W_i = 2p_i \cdot p_{i+1}\,, \tag{4.31}$$
$$W_{5+i} = 2p_{i+3} \cdot (p_{i+2} + p_{i-1})\,, \tag{4.32}$$
$$W_{10+i} = 2p_{i+2} \cdot (p_{i+3} + p_{i-1})\,, \tag{4.33}$$
$$W_{15+i} = -2p_i \cdot p_{i+2}\,, \tag{4.34}$$
$$W_{20+i} = 2p_{i+2} \cdot (p_i + p_{i+3})\,, \tag{4.35}$$

with $i = 1, \ldots, 5$. Here and in the following, the index that labels the external momenta p_i is understood modulo 5 ($p_{i+5} = p_i$). These letters are clearly related to the collinear and soft singularities of the integrals. Therefore, they could have been anticipated by an analysis of the Landau equations. This block of letters is closed under the 5! permutations of the external momenta. Moreover, it is clearly structured into orbits of the cyclic permutation group, which is apparent from the presentation given by Eqs. (4.31)–(4.35). The letters $\{W_i\}_{i=21}^{25}$ are purely nonplanar, as they do not appear in the planar pentagon-box integrals. This set of letters was conjectured in Ref. [16] by completing in a minimal way the planar alphabet so as to make it closed under all permutations of the external legs. Finally, only the letters $\{W_i\}$ with $i \in \{1, \ldots, 5\} \cup \{16, \ldots, 20\}$ (only for $i \in \{1, \ldots, 5\}$ in the planar case) are allowed as first entries of the symbol. See Sect. 3.3.6 for an explanation. On top of this well understood first-entry condition, a mysterious *second-entry condition* was conjectured in Ref. [16], based on the results available at the time. Iterated integrals of the form $[W_1, W_8, \ldots]$, $[W_5, W_8, \ldots]$ and their permutations appear to be forbidden. Since all the massless two-loop five-particle integrals have now been computed, we can claim that this conjecture is in fact correct, but an understanding of the underlying physical principle is still missing. It is not unreasonable to fantasise about a connection with the Steinmann relations [43–45] discussed in Sect. 3.3.6.

One last even letters is

$$W_{31} = \sqrt{\Delta}\,, \tag{4.36}$$

or, equivalently,

$$W_{31} = \mathrm{tr}\left(\gamma_5 \not{p}_1 \not{p}_2 \not{p}_3 \not{p}_4\right)\,. \tag{4.37}$$

Although $\sqrt{\Delta}$ changes sign under parity, we must remember that the letter really is $d \log W_{31}$, so that the sign of W_{31} is irrelevant. For the same reason, this letter is invariant under any permutations of the external momenta. We recall that Δ is defined by Eq. (4.8) as the determinant of the Gram matrix constructed with four of the external momenta. This means that, if restrict the momenta to $D < 4$ dimensions, the four momenta become linearly dependent and the Gram determinant vanishes. The letter W_{31} is thus related to spurious singularities of the integrals in a lower-dimensional subspace.

The letter W_{31} alone does not imply an algebraic dependence of the alphabet on the Mandelstam invariants, since

$$d\log\sqrt{\Delta} = \frac{1}{2}d\log\Delta\,. \tag{4.38}$$

The algebraic nature is introduced by the five parity-odd letters,

$$W_{25+i} = \frac{a_{i,i+1,i+2,i+3} - \sqrt{\Delta}}{a_{i,i+1,i+2,i+3} + \sqrt{\Delta}}\,, \tag{4.39}$$

with $i = 1, \ldots, 5$, where $a_{i,i+1,i+2,i+3}$ is a degree-two polynomial in the Mandelstam invariants defined by

$$a_{1,2,3,4} = \mathrm{tr}\left(\not{p}_4\not{p}_5\not{p}_1\not{p}_2\right) = s_{12}s_{23} - s_{23}s_{34} + s_{34}s_{45} - s_{12}s_{51} - s_{45}s_{51}\,, \tag{4.40}$$

and similarly for the other indices. Because of the dependence on $\sqrt{\Delta}$, these letters are genuine to five-particle kinematics. They form a set which is closed under permutations of the external momenta. We recall that parity acts by flipping the sign of $\sqrt{\Delta}$. These letters are therefore manifestly odd, i.e. $d\log W_i \to -d\log W_i$ under parity for all $i = 26, \ldots, 30$. In fact, they have exactly the form advocated around Eq. (3.47), and the polynomial $a_{i,i+1,i+2,i+3}$ can be easily anticipated from Δ and from the even letters via the procedure described in Sect. 3.2.1. In the physical scattering region $\Delta < 0$ and these odd letters are therefore complex phases, namely $|W_i| = 1$ for all $i = 26, \ldots, 30$. Their form might look rather complicated, but, as pointed out in Ref. [1], an underlying simplicity emerges when we rewrite them as ratios of traces,

$$W_{26} = \frac{\mathrm{tr}\left[(1-\gamma_5)\not{p}_4\not{p}_5\not{p}_1\not{p}_2\right]}{\mathrm{tr}\left[(1+\gamma_5)\not{p}_4\not{p}_5\not{p}_1\not{p}_2\right]}\,, \tag{4.41}$$

and similarly for the others.

The possibility of the rewriting given by Eqs. (4.37) and (4.41) has important implications. As discussed in Sect. 3.2.1, one could equally well choose the numerators (or denominators) of the odd letters as independent letters. We choose to use the ratios because they have simple transformation properties under parity, but numerators and denominators, separately, have another virtue: they are linear in the momenta. It is therefore possible to express the entire alphabet in a way that is linear in all the external momenta. This suggests immediate parameterisations that are rational in a given variable. Any BCFW-like shift of the momenta [46] would in fact lead to a parameterisation of the alphabet that is linear in the shift parameter. The latter therefore gives a "direction" along which we can very the letters in a rational way. This is in general a very precious property, but in this case we can do even better. We can in fact define changes of variables that completely rationalise the alphabet. One way to see that this is possible, is by noting that all the letters are rational in the spinor-helicity invariants. For example,

$$W_{26} = \frac{\langle 45\rangle[51]\langle 12\rangle[24]}{[45]\langle 51\rangle[12]\langle 24\rangle} \,. \tag{4.42}$$

Any parameterisation in terms of momentum twistors [47] therefore rationalises the alphabet. See e.g. Refs. [48, 49] for explicit parameterisations of this kind. The possibility of rationalising globally the pentagon alphabet implies that it is possible to solve the differential equations systematically in terms of Goncharov Polylogarithms (GPLs) (see Sect. 3.4.3). A basis of functions for the pentagon alphabet up to weight four together with fast numerical routines for their evaluation was provided first in Ref. [3] for the planar subset of letters, and then in Ref. [50] for the complete alphabet. They are dubbed *pentagon functions*.

4.2.3 Boundary Values

Once the function space is well under control, the last missing ingredient to write down the solution of the differential equations are the boundary values. As base point, we choose

$$s_0 = (3, -1, 1, 1, -1) \,, \qquad \text{tr}_5\big|_{s_0} = i\sqrt{3} \,. \tag{4.43}$$

This is the most symmetric point lying in the s_{12} channel. In particular, it is symmetric under the exchange of the incoming momenta, $p_1 \leftrightarrow p_2$, and under any permutation of the outgoing momenta, $\{p_3, p_4, p_5\}$. To determine the values of the integrals at s_0 we exploit the transparent singularity structure of the canonical form (4.29). The method is a refinement of the one discussed in Sect. 3.4.2. I will content myself with describing the procedure. For the technical details I refer to Refs. [3, 15, 51]. The d log basis integrals are by construction ultraviolet-finite. This can be proven e.g. by power counting [34]. We can therefore assign to ϵ a negative value, small enough that we do not spoil the ultraviolet behaviour. For such a value of ϵ, all divergences are regulated, and the integrals are therefore finite. The differential equations however bring into the solution spurious singularities everywhere one of the letters vanishes, even for a small negative value of ϵ. So we solve the differential equations asymptotically close to the hypersurface where one of the letters vanishes, and require the result to be finite for ϵ small and negative. This imposes constraints on the values of the integrals on that hypersurface, which we transport back to the base point using the differential equations. Repeating this procedure for all the letters of the alphabet relates all the boundary values to a few simple integrals. The latter can be computed in closed-form, or found in the literature [31, 32].

There is an important *caveat*. The fact that the integrals are finite everywhere for a small and negative value of ϵ is a conjecture, and should be taken with great caution. In fact, during the computation we realised that the hypersurface $\Delta = 0$, boundary of the physical scattering region, is a very dangerous place. Although it looks like a rather unphysical locus, some of the integrals diverge there. I discuss this interesting

phenomenon in the next section. For now, it suffices to say that we do not require the integrals to be finite at $\Delta = 0$, even for a small negative value of ϵ. We only impose a matching between the full and the asymptotic solution.

Although it might sound slightly intricate, this procedure is very systematic and can be implemented in an automatic way. This allowed us to overcome another technical complication. In previous work, the pentagon-box integrals were computed in all kinematic regions [1–3], whereas the hexagon-box integrals were computed only in the Euclidean region [15]. Similarly, we computed the double-pentagon integrals initially only in the s_{12} channel [21]. We will see in the next sections that the integrals enter the amplitudes in all the orientations of the external momenta. In other words, we need to know them in all the kinematic regions. For instance, imagine that one of the double-pentagon integrals we computed in the s_{12} channel evaluates to

$$I_{\text{dummy}}(s, \text{tr}_5) = 1 + \epsilon \log s_{12} + \mathcal{O}(\epsilon^2) \,. \tag{4.44}$$

The amplitude might contain this integral in another orientation. For instance, we may need to trade $\{p_1, p_2, p_3, p_4, p_5\}$ as in Fig. 4.1c for $\{p_2, p_3, p_4, p_5, p_1\}$. Let me denote this cyclic permutation by σ_1, with $\sigma_1 \circ p_i = p_{i+1}$. If we do this naïvely, we get

$$\left[\sigma_1 \circ I_{\text{dummy}}\right](s, \text{tr}_5) = I_{\text{dummy}}\left(\sigma_1 \circ s, \sigma_1 \circ \text{tr}_5\right) = 1 + \epsilon \log s_{23} + \mathcal{O}(\epsilon^2) \,, \tag{4.45}$$

which is not well defined in the s_{12} scattering region, where $s_{23} < 0$. In principle this can be fixed via analytic continuation (see Sect. 3.4.1). I find this approach to be cumbersome at high transcendental weight, and very error-prone. In Ref. [27] we adopted a different strategy. Consider now the differential equation satisfied by I_{dummy},

$$d\, I_{\text{dummy}} = \epsilon\, d \log s_{12}\; I_{\text{dummy}} \,. \tag{4.46}$$

The permuted integral satisfies the permuted differential equation,

$$d\left(\sigma \circ I_{\text{dummy}}\right) = \epsilon\, d \log s_{23}\; \left(\sigma \circ I_{\text{dummy}}\right) \,. \tag{4.47}$$

Permuting the differential equation is however trivial and completely safe, since only algebraic functions are involved. Given a systematic way of fixing the boundary values for the differential equations in a given base point, the expression of the permuted integral can be obtained by solving the permuted differential equations directly in the kinematic region of interest. No analytic continuation is needed.

Since we do have a systematic procedure to fix the boundary values at a given base point starting from the differential equations, our strategy is the following. We consider each permutation of all the integral families shown in Fig. 4.1 as a distinct integral family. We derive the differential equations and fix the boundary constants for each of them directly at the base point in the s_{12} channel, given by

Eq. (4.43). Moreover, to reduce the number of independent integrals and streamline the calculation, we also derived the relations between integrals of different families and in different orientations. This approach is completely automatic and less error-prone, since we never need to continue analytically.

We verified the boundary values numerically for two orientations of the double-pentagon integrals, and for selected integrals of the hexagon-box family. This was done by computing the integrals numerically using pySecDec [52, 53] at the base point s_0. To simplify this computation, we performed it in $D = 6 - 2\epsilon$ dimensions, and used the dimension shifting relations [54, 55] to relate the results to the integrals in $D = 4 - 2\epsilon$ dimensions. The values of the planar integrals were checked against the program provided with Ref. [3].

In conclusion, we computed analytically the values at the s_{12}-channel base point (4.43) of the basis integrals of the integral families shown in Fig. 4.1 in all the 5! orientations of the external momenta, up to transcendental weight four. This opened up the door to the computation of the first complete—i.e. including the non-planar contributions—five-particle scattering amplitudes at two-loop order. Sections 4.3 and 4.5 are devoted to this topic.

4.2.4 Non-trivial Analytic Behaviour at the Boundary

In this section I present examples of Feynman integrals to illustrate the analytic behaviour near the hypersurface $\mathrm{tr}_5 = 0$, boundary of the physical scattering region. Specifically, we consider the nonplanar two-loop five-particle integrals shown in Fig. 4.2,

$$I_a = e^{2\epsilon\gamma_E} \int \frac{d^D k_1}{i\pi^{D/2}} \frac{d^D k_2}{i\pi^{D/2}} \frac{\mathrm{tr}_5}{k_1^2 (k_1 - p_2)^2 k_2^2 (k_2 - p_1)^2 (k_1 + k_2 + p_3)^2 (k_1 + k_2 + p_3 + p_5)^2}\,, \tag{4.48}$$

and similarly for I_b. The factor of tr_5 in the numerator makes these integrals pure and parity-odd. We study them in the physical s_{12} scattering region. There, $\Delta < 0$ and tr_5 is purely imaginary. We assume that $\mathrm{Im}[\mathrm{tr}_5] > 0$.

Given the factor of tr_5 in the numerator, one might naïvely expect the integrals I_a and I_b to vanish at $\mathrm{tr}_5 = 0$. As a matter of fact, I_b does vanish, but I_a does not. As we will see later, because of the odd parity, the non-zero value at $\mathrm{tr}_5 = 0$ has interesting implications for the analytic behaviour of the integrals. I stress that the two integrals are related by a permutation of the external legs. Nonetheless, they exhibit a completely different behaviour at $\mathrm{tr}_5 = 0$.

Let us start with I_b, shown in Fig. 4.2b. Using the method of the differential equations one can show that, in the s_{12} channel, it takes the form

$$I_b = \frac{1}{\epsilon^2} f_b^{(2)} + \frac{1}{\epsilon} f_b^{(3)} + f_b^{(4)} + \mathcal{O}(\epsilon)\,. \tag{4.49}$$

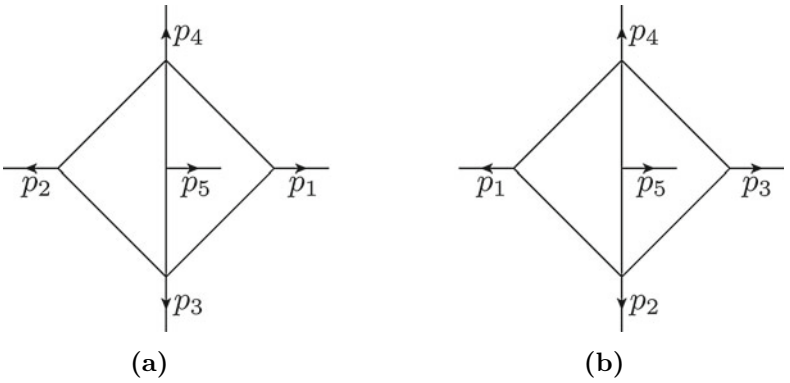

Fig. 4.2 Feynman integrals to illustrate the analytic properties near the hypersurface where $\mathrm{tr}_5 = 0$. The arrows denote the direction of the momenta. The scalar integrals shown here are multiplied by a factor of tr_5. As a result, they are pure and parity-odd. The integral **a** does *not* vanish on the hypersurface $\mathrm{tr}_5 = 0$ (approached from within the s_{12} scattering region), the integral **b** does

For our purposes, it is sufficient to look at the weight-two part. It can be expressed explicitly in terms of dilogarithms,

$$\begin{aligned} f_b^{(2)} = 3\Big[&\mathrm{Li}_2\Big(W_{27}\Big) - \mathrm{Li}_2\Big(\frac{1}{W_{27}}\Big) + \mathrm{Li}_2\Big(W_{28}\Big) - \mathrm{Li}_2\Big(\frac{1}{W_{28}}\Big) \\ &+ \mathrm{Li}_2\Big(\frac{1}{W_{27}W_{28}}\Big) - \mathrm{Li}_2\Big(W_{27}W_{28}\Big)\Big]. \end{aligned} \tag{4.50}$$

This function is single valued in the s_{12} channel. This can be shown by rewriting it in terms of Bloch-Wigner dilogarithms (3.83) with arguments W_{27}, W_{28} and $W_{27}W_{28}$. To this end, I recall that in the s_{12} channel these arguments are pure phases, and their complex conjugation is given by their inverse. Since the odd letters $\{W_i\}_{i=26}^{30}$ become 1 at $\mathrm{tr}_5 = 0$, $f_b^{(2)}$ vanishes on the whole hypersurface $\mathrm{tr}_5 = 0$, in agreement with the naïve expectations.

The integral I_a, shown in Fig. 4.2a, has a more interesting behaviour. Its Laurent expansion reads

$$I_a = \frac{1}{\epsilon^2} f_a^{(2)} + \frac{1}{\epsilon} f_a^{(3)} + f_a^{(4)} + \mathcal{O}(\epsilon)\,. \tag{4.51}$$

The weight-two part $f_a^{(2)}$ has a much more complicated expression than that of I_b. A very careful analysis shows that it is given by

$$f_a^{(2)} = 3\mathcal{P}_a + 6i\pi h_a\,, \tag{4.52}$$

where

$$\mathcal{P}_a = \mathrm{Li}_2\left(\frac{W_{30}}{W_{27}W_{28}}\right) - \mathrm{Li}_2\left(\frac{W_{27}W_{28}}{W_{30}}\right) + \mathrm{Li}_2\left(\frac{W_{28}}{W_{26}W_{30}}\right) - \mathrm{Li}_2\left(\frac{W_{26}W_{30}}{W_{28}}\right) + \mathrm{Li}_2\left(W_{26}W_{27}\right) - \mathrm{Li}_2\left(\frac{1}{W_{26}W_{27}}\right), \tag{4.53}$$

and

$$\begin{aligned} h_a = {} & \log(W_{28})\Theta(a_{28}) + \big(\log(W_{28}) - 2i\pi\big)\Theta(-a_{28}) - i\pi\delta_{a_{28}} \\ & - \log(W_{26})\Theta(a_{26}) - \big(\log(W_{26}) - 2i\pi\big)\Theta(-a_{26}) + i\pi\delta_{a_{26}} \\ & - \log(W_{30})\Theta(-a_{30}) - \big(\log(W_{30}) + 2i\pi\big)\Theta(a_{30}) - i\pi\delta_{a_{30}}\,. \end{aligned} \tag{4.54}$$

Here, I introduced the short-hand notation $a_i := a_{i,i+1,i+2,i+3}$ for the polynomial appearing in the odd letters (see Eq. (4.39)), Θ is the Heaviside function (with $\Theta(0) \equiv 0$), and

$$\delta_x = \begin{cases} 1\,, & \text{if } x = 0\,, \\ 0\,, & \text{otherwise}\,. \end{cases} \tag{4.55}$$

Both $\mathcal{P}_a$ and h_a are single-valued in the s_{12} channel. While $\mathcal{P}_a$ vanishes identically like $f_b^{(2)}$ if $\mathrm{tr}_5 = 0$, h_a does not vanish in a generic point where $\mathrm{tr}_5 = 0$. Therefore, in contrast to I_b, I_a does not vanish on the whole hypersurface $\mathrm{tr}_5 = 0$.

The analytic expressions given by Eqs. (4.53) and (4.54) were checked against numerical evaluations performed with pySecDec [52]. In particular, we integrated numerically the convenient integral representation given in Ref. [16],

$$I_a = -\epsilon_5 e^{2\epsilon\gamma_E}\left(-\frac{\Gamma^3(-\epsilon)\Gamma(2+2\epsilon)}{\Gamma(-3\epsilon)}\right)\int_0^1 d\alpha_1 \int_0^1 d\alpha_2 \int_0^1 d\alpha_3\, F^{-2-2\epsilon}\,, \tag{4.56}$$

where

$$F = (-s_{23})\alpha_2 + (-s_{13})\alpha_3 + (-s_{35})\alpha_1 + (-s_{25})\alpha_1\alpha_2 + (-s_{15})\alpha_1\alpha_3 + (-s_{12})\alpha_2\alpha_3\,, \tag{4.57}$$

and similarly for I_b. The analytic expressions are in agreement with the numerical evaluations within the error estimates.

Finally, we can appreciate the interesting analytic consequences of the seemingly innocuous fact that I_a does not vanish on the entire hypersurface $\mathrm{tr}_5 = 0$. The key point is that I_a is a parity-odd integral. As such, it changes sign under parity, which acts by flipping the sign of tr_5. Approaching a point on the hypersurface $\mathrm{tr}_5 = 0$ from within the scattering region but with different sigs of $\mathrm{Im}[\mathrm{tr}_5]$ therefore gives values with opposite signs,

$$f_a^{(2)}\Big|_{\mathrm{Im}[\mathrm{tr}_5]=0^\pm} = \pm 12\pi^2\Big(\Theta(-a_{28}) - \Theta(-a_{26}) + \Theta(a_{30})\Big)\,. \tag{4.58}$$

Here, the superscript $\pm$ indicates whether the offending hypersurface is reached along a path with $\mathrm{Im}[\mathrm{tr}_5] > 0$ or $\mathrm{Im}[\mathrm{tr}_5] < 0$, respectively. In other words, any parity-odd integral which does not vanish on the entire hypersurface $\mathrm{tr}_5 = 0$ has a discontinuity across the latter, even though the scattering region is never left. We can therefore think of the scattering region as composed of two copies, one with $\mathrm{Im}[\mathrm{tr}_5] > 0$ and one with $\mathrm{Im}[\mathrm{tr}_5] < 0$. I stress however that this is a feature of the individual Feynman integrals. The scattering amplitudes are expected to be analytic throughout the physical scattering region. While this is obvious for the two-loop five-gluon all-plus helicity amplitude presented in Sect. 4.5, we checked numerically that also the supersymmetric amplitudes discussed in Sect. 4.3 are continuous at the point

$$s = \left(3, -1 + \frac{\sqrt{3}}{2}, 1, 1, -1\right), \qquad \mathrm{tr}_5 = 0\,, \tag{4.59}$$

where some of the contributing Feynman integrals are discontinuous and even divergent.

4.3 Maximally Supersymmetric Amplitudes

In this section I discuss the two-loop five-particle (super) amplitudes in $\mathcal{N} = 4$ super Yang-Mills theory and $\mathcal{N} = 8$ supergravity.[3] Since they share many properties, I treat them in parallel. My collaborators and I, alongside another group of researchers, computed them first at symbol level [20, 22–24]. Later, we supplied the information about the boundary constants of the Feynman integrals, and lifted the results to function level [26]. In the same work we also investigated the multi-Regge limit of the amplitudes. The discussion is structured as follows. First, in Sect. 4.3.1, I introduce the two amplitudes and define the notation. A lot of information on the form of the amplitudes can be inferred from the integrands even prior to integration. In particular, both amplitudes are expected to have uniform transcendental weight. This allows us to make ansätze for the amplitudes in terms of a finite set of rational factors and pure pentagon integrals, which I discuss in Sect. 4.3.2. Then I move on to the actual computation. In Sect. 4.3.3 I use the known analytic expressions of the pentagon integrals to integrate the integrands computed in Ref. [25], this way fixing the coefficients in the ansätze and confirming the expected structure. In Sect. 4.3.4 I show how the infrared singularities of the amplitudes factorise, and define finite hard functions (or remainder functions), for which I provide the numerical values at a reference point. Our results are further validated in Sect. 4.3.5, where I present several checks, such as the behaviour in collinear and soft limits. Section 4.4 is devoted to discussing the multi-Regge limit of the hard functions. After defining the multi-Regge kinematics in Sect. 4.4.1, I show how we computed the asymptotic expansions in the limit using the procedure presented in Sect. 3.5. A basis of the transcendental

[3] I refer the readers who are not familiar with these theories e.g. to the textbooks [56, 57].

functions appearing in the Regge limit up to two loops is presented in Sect. 4.4.3. In Sections 4.4.4 and 4.4.5 I present and discuss the asymptotic expansion of the hard functions in $\mathcal{N}=4$ super Yang-Mills and $\mathcal{N}=8$ supergravity, respectively. I comment on the results in Sect. 4.4.6.

4.3.1 Notation

It is convenient to expand the amplitude in $\mathcal{N}=4$ super Yang-Mills theory in a modified coupling constant,

$$a = \frac{e^{-\epsilon\gamma_{\rm E}}}{(4\pi)^{\frac{D}{2}}} g^2 \,, \tag{4.60}$$

where g is the coupling of the Lagrangian. This way we absorb in the new coupling a the factor of $e^{\epsilon\gamma_{\rm E}}$ introduced in the normalisation of the integrals to remove Euler's constant from the expressions, and the different loop integration measure of the Feynman diagrams, $d^D k/(2\pi)^D$, with respect to the Feynman integrals, $d^D k/\pi^{D/2}$. We expand the five-gluon super-amplitude as

$$\mathcal{A}_5 = \delta^{(4)}\left(p_1+p_2+p_3+p_4+p_5\right)\delta^{(8)}(Q)\, g^3 \sum_{\ell\geq 0} a^\ell A_5^{(\ell)} \,, \tag{4.61}$$

extracting the overall momentum and super-momentum Q conservation delta functions. The latter implements all the supersymmetric Ward identities and packages the information on how to extract from the super-amplitude the various amplitudes for the states in the super-multiplet (see e.g. Refs. [56, 57] for an introduction to the super-field formalism).

We make the $SU(N_c)$ colour dependence explicit by further decomposing the amplitudes $A_5^{(\ell)}$ up to $\ell=2$ as

$$A_5^{(0)} = \sum_{\lambda=1}^{12} A_\lambda^{(0)} \mathcal{T}_\lambda \,, \tag{4.62}$$

$$A_5^{(1)} = \sum_{\lambda=1}^{12} N_c A_\lambda^{(1,0)} \mathcal{T}_\lambda + \sum_{\lambda=13}^{22} A_\lambda^{(1,1)} \mathcal{T}_\lambda \,, \tag{4.63}$$

$$A_5^{(2)} = \sum_{\lambda=1}^{12} \left(N_c^2 A_\lambda^{(2,0)} + A_\lambda^{(2,2)} \right) \mathcal{T}_\lambda + \sum_{\lambda=13}^{22} \left(N_c A_\lambda^{(2,1)} \right) \mathcal{T}_\lambda \,, \tag{4.64}$$

where $\{\mathcal{T}_\lambda\}_{\lambda=1}^{22}$ is a colour basis introduced in Ref. [58]. It is composed of 12 single traces,

$$\begin{aligned}
\mathcal{T}_1 &= \mathrm{Tr}(12345) - \mathrm{Tr}(15432)\,, & \mathcal{T}_2 &= \mathrm{Tr}(14325) - \mathrm{Tr}(15234)\,,\\
\mathcal{T}_3 &= \mathrm{Tr}(13425) - \mathrm{Tr}(15243)\,, & \mathcal{T}_4 &= \mathrm{Tr}(12435) - \mathrm{Tr}(15342)\,,\\
\mathcal{T}_5 &= \mathrm{Tr}(14235) - \mathrm{Tr}(15324)\,, & \mathcal{T}_6 &= \mathrm{Tr}(13245) - \mathrm{Tr}(15423)\,,\\
\mathcal{T}_7 &= \mathrm{Tr}(12543) - \mathrm{Tr}(13452)\,, & \mathcal{T}_8 &= \mathrm{Tr}(14523) - \mathrm{Tr}(13254)\,,\\
\mathcal{T}_9 &= \mathrm{Tr}(13524) - \mathrm{Tr}(14253)\,, & \mathcal{T}_{10} &= \mathrm{Tr}(12534) - \mathrm{Tr}(14352)\,,\\
\mathcal{T}_{11} &= \mathrm{Tr}(14532) - \mathrm{Tr}(12354)\,, & \mathcal{T}_{12} &= \mathrm{Tr}(13542) - \mathrm{Tr}(12453)\,,
\end{aligned} \tag{4.65}$$

and 10 double traces,

$$\begin{aligned}
\mathcal{T}_{13} &= \mathrm{Tr}(12)[\mathrm{Tr}(345) - \mathrm{Tr}(543)]\,, & \mathcal{T}_{14} &= \mathrm{Tr}(23)[\mathrm{Tr}(451) - \mathrm{Tr}(154)]\,,\\
\mathcal{T}_{15} &= \mathrm{Tr}(34)[\mathrm{Tr}(512) - \mathrm{Tr}(215)]\,, & \mathcal{T}_{16} &= \mathrm{Tr}(45)[\mathrm{Tr}(123) - \mathrm{Tr}(321)]\,,\\
\mathcal{T}_{17} &= \mathrm{Tr}(51)[\mathrm{Tr}(234) - \mathrm{Tr}(432)]\,, & \mathcal{T}_{18} &= \mathrm{Tr}(13)[\mathrm{Tr}(245) - \mathrm{Tr}(542)]\,,\\
\mathcal{T}_{19} &= \mathrm{Tr}(24)[\mathrm{Tr}(351) - \mathrm{Tr}(153)]\,, & \mathcal{T}_{20} &= \mathrm{Tr}(35)[\mathrm{Tr}(412) - \mathrm{Tr}(214)]\,,\\
\mathcal{T}_{21} &= \mathrm{Tr}(41)[\mathrm{Tr}(523) - \mathrm{Tr}(325)]\,, & \mathcal{T}_{21} &= \mathrm{Tr}(52)[\mathrm{Tr}(134) - \mathrm{Tr}(431)]\,.
\end{aligned} \tag{4.66}$$

Here I introduced the short-hand notation

$$\mathrm{Tr}(ij\ldots) := \mathrm{Tr}(\tilde{T}^{a_i}\tilde{T}^{a_j}\ldots)\,, \tag{4.67}$$

where $\tilde{T}^a = \sqrt{2}T^a$ and T^a are generators of the symmetry group $SU(N_c)$ in the fundamental representation, normalised so that $\mathrm{Tr}(T^aT^b) = 1/2\delta^{ab}$.

The components $A_n^{(\ell,0)}$ in this decomposition dominate in the large N_c limit, and they are therefore referred to as leading-colour components. From the diagrammatic point of view, they receive contributions only from planar Feynman diagrams with the external legs ordered as the generators in the corresponding trace. In this sense they constitute the *planar* part of the amplitude. Conversely, the subleading-colour components are dubbed *nonplanar*.

The partial amplitudes $A_\lambda^{(\ell,k)}$ are related by group-theoretic identities [58, 59]. As a result, the one-loop double-trace components $A_\lambda^{(1,1)}$ are entirely determined by the planar ones $A_\lambda^{(1,0)}$. At two loops, the colour-subleading single-trace components $A_\lambda^{(2,2)}$ are given by linear combinations of the planar $A_\lambda^{(2,0)}$ and of the double-trace $A_\lambda^{(2,1)}$ components. Moreover, the complete amplitude is symmetric under any permutation of the external legs. This symmetry interplays with the transformation properties of the colour structures $\mathcal{T}_\lambda$, inducing relations among the different partial amplitudes $A_\lambda^{(\ell,k)}$. Two components $A_\lambda^{(\ell,k)}$ and $A_{\lambda'}^{(\ell,k)}$ are related by the permutation of the external legs which maps $\mathcal{T}_\lambda$ into $\mathcal{T}_{\lambda'}$. Therefore, there is only one independent component at tree level and at one loop, say $A_1^{(0)}$ and $A_1^{(1,0)}$, and only two at two loops, e.g. $A_1^{(2,0)}$ and $A_1^{(2,1)}$. However, because of the complicated interplay between permutations and analytic continuation (see the discussion in Sect. 4.2.3), we prefer to compute all the components, and to use these relations as checks.

At tree level, the amplitude is given by the famous Parke-Taylor formula [60, 61],

$$A_1^{(0)} = \frac{1}{\langle 12\rangle\langle 23\rangle\langle 34\rangle\langle 45\rangle\langle 51\rangle}\,. \tag{4.68}$$

The Parke-Taylor factors play an important role in the following, and it is thus convenient to define the short-hand notation

$$\mathrm{PT}(i_1 i_2 i_3 i_4 i_5) = \frac{1}{\langle i_1 i_2\rangle\langle i_2 i_3\rangle\langle i_3 i_4\rangle\langle i_4 i_5\rangle\langle i_5 i_1\rangle}\,. \tag{4.69}$$

The integrands of the amplitude at one and two loops can be found e.g. in Refs. [25, 62].

For the five-graviton amplitude in $\mathcal{N}=8$ supergravity we adopt a similar expansion in the gravitational coupling constant κ, with $\kappa^2 = 32\pi G$,

$$\mathcal{M}_5 = \delta^{(4)}\left(p_1+p_2+p_3+p_4+p_5\right)\delta^{(16)}(Q)\left(\frac{\kappa}{2}\right)^3 \sum_{\ell\geq 0}\left[\left(\frac{\kappa}{2}\right)^2 \frac{e^{-\epsilon\gamma_{\mathrm{E}}}}{(4\pi)^{\frac{D}{2}}}\right]^\ell M_5^{(\ell)}\,. \tag{4.70}$$

As in the super Yang-Mills case, we have absorbed in the coupling the conventional normalisation of the Feynman integrals, and we have extracted the momentum and super-momentum Q conservation delta functions. There are important differences with respect to the $\mathcal{N}=4$ super Yang-Mills amplitude. The gravitational coupling κ has the dimension of an inverse energy, $1/E$. Moreover, there is no concept of colour in supergravity. All the partial amplitudes $M_5^{(\ell)}$ are thus intrinsically nonplanar. Similarly to the super Yang-Mills amplitude, on the other hand, also the supergravity amplitude is invariant under any permutation of the external legs. The explicit representation of the amplitude may however obscure this symmetry. An example of this is the following expression for the amplitude at tree level [63],

$$M_5^{(0)} = s_{12}s_{34}\mathrm{PT}(12345)\mathrm{PT}(21435) + s_{13}s_{24}\mathrm{PT}(13245)\mathrm{PT}(31425)\,. \tag{4.71}$$

It is instructive for the following to investigate how this formula actually manages to be permutation invariant. The rational factors appearing in Eq. (4.71) have the generic form

$$s_{ij}s_{kl}\mathrm{PT}(\sigma)\mathrm{PT}(\rho)\,, \tag{4.72}$$

where the Greek letters σ and ρ denote arbitrary permutations of the external momenta. There are many relations among these factors, and only 146 of them are linearly independent. These relations are responsible for the permutation symmetry of the expression given by Eq. (4.71). Through them, we can rewrite the tree-level amplitude in a manifestly symmetric form,

$$M_5^{(0)} = \frac{1}{60}\sum_{\sigma\in S_5}\sigma\circ\left[-s_{12}s_{34}\mathrm{PT}(12345)\mathrm{PT}(21435)\right], \tag{4.73}$$

where the sum runs over all the permutations of the external momenta. These relations among the rational functions play an even more important role at loop level. Unintegrated expressions of the one and two-loop five-graviton amplitudes are given for instance in Refs. [25, 64].

4.3.2 *Expected Structure of the Two-Loop Amplitudes*

The computation of a scattering amplitude can be simplified dramatically by having an insight into its final structure. For the two amplitudes under consideration, it turns out that we can actually write down rather constrained ansätze before even starting to integrate the known integrands [25].

We know from the explicit computation discussed in Sect. 4.2 that all the Feynman integrals which contribute to the massless two-loop five-particle amplitudes can be expressed as linear combinations of pure integrals. It follows that a generic (partial) amplitude $\mathcal{F}_5^{(2)}$ has the form

$$\mathcal{F}_5^{(2)} = \sum_i R_i(\lambda, \tilde{\lambda}, \epsilon)\, \mathcal{I}_i^{(2)\text{pure}}\,, \tag{4.74}$$

where $\mathcal{I}_i^{(2)\text{pure}}$ are pure two-loop integrals, and the factors R_i depend rationally on both the external spinors and the dimensional regulator ϵ. In the special case in which the rational factors R_i do not depend on ϵ, the (partial) amplitude $\mathcal{F}_5^{(2)}$ has uniform transcendental weight. We have seen in Sect. 3.6.2 that this property of the amplitude is conjecturally related to its integrand admitting a d log form. We recall that a d log form by definition has only simple poles in the integration variables. The study of the poles of the integrands can therefore lead to reasonable expectations about whether an amplitude has uniform transcendental weight or not [33, 34, 65, 66].

The absence of double poles in $\mathcal{N} = 4$ super Yang-Mills has been shown for several amplitude integrands [67, 68]. In particular, a lot is known about the Maximally-Helicity-Violating amplitudes, such as the one we are now considering. Not only they are all conjectured to have uniform transcendental weight [67, 69–71], but their leading singularities are in fact known [72]: they are given by permutations of the Parke-Taylor tree-level amplitudes (4.69) only.[4] In the five-particle case, only six of them are linearly independent. We choose

$$\begin{aligned} \text{PT}_1 &= \text{PT}(12345)\,, & \text{PT}_2 &= \text{PT}(12354)\,, \\ \text{PT}_3 &= \text{PT}(12453)\,, & \text{PT}_4 &= \text{PT}(12534)\,, \\ \text{PT}_5 &= \text{PT}(13425)\,, & \text{PT}_6 &= \text{PT}(15423)\,. \end{aligned} \tag{4.75}$$

[4] For the two-loop five-gluon amplitude, these properties are made manifest in the representation of the four-dimensional integrand given by Ref. [35].

Therefore, the partial amplitudes in Eq. (4.64) are expected to have the form

$$A_{\lambda}^{(2,k)} = \sum_{i=1}^{6} \sum_{j} a_{\lambda,ij}^{(2,k)} \, \mathrm{PT}_i \, \mathcal{I}_j^{(2)\mathrm{pure}} \,, \tag{4.76}$$

where $a_{\lambda,ij}^{(k)}$ are constant rational numbers and $\mathcal{I}_j^{(2)\mathrm{pure}}$ are pure two-loop integrals.

The amplitude integrands in $\mathcal{N} = 8$ supergravity in general exhibit double or higher poles. However, the two-loop five-graviton amplitude is free of double poles at least at infinity [73, 74]. This is a convincing hint that the integrated amplitude has uniform transcendentality, which was in fact confirmed by the explicit computations. For the leading singularities, we can make a guess based on the known expressions for the tree-level and one-loop five-graviton amplitudes. Since the gravitational coupling κ is dimensionful, the leading singularities must have a different dimension at each order in κ^2. At tree level we have already seen that the rational factors building blocks of the amplitude (4.71) have the form (4.72). The naïve one-loop generalisation of the latter is

$$s_{ij} s_{kl} s_{mn} \mathrm{PT}(\sigma) \mathrm{PT}(\rho) \,. \tag{4.77}$$

The extra factor of s_{ij} with respect to the tree-level case compensates the dimensionality of the gravitational coupling κ. These objects form a 290-dimensional space over $\mathbb{Q}$. In order to assess the validity of this guess, we look at the one-loop amplitude. It can be expressed as [64]

$$M_5^{(1)} = -\sum_{S_5} \Big[s_{45} s_{12}^2 s_{23}^2 \mathrm{PT}(12345) \mathrm{PT}(12354) \mathcal{I}_4^{(45)} + 2\epsilon \frac{[12][23][34][45][51]}{\langle 12\rangle\langle 23\rangle\langle 34\rangle\langle 45\rangle\langle 51\rangle} \mathcal{I}_5^{6-2\epsilon} \Big] , \tag{4.78}$$

where $\mathcal{I}_4^{(45)}$ is the one-mass box integral with external momenta p_1, p_2, p_3 and $p_4 + p_5$ in $D = 4 - 2\epsilon$ dimensions, while $\mathcal{I}_5^{6-2\epsilon}$ denotes the massless pentagon integral in $D = 6 - 2\epsilon$ dimensions. It suffices to know that these two integrals evaluate to pure functions, with overall leading singularity $1/(s_{12}s_{23})$ and $1/\mathrm{tr}_5$, respectively. The one-loop amplitude therefore contains two classes of rational factors. As we expected, there is the generalisation of the tree-level factors, given by Eq. (4.77). In particular, the leading singularities of this form are spanned by 15 $\mathbb{Q}$-linearly independent permutations of

$$r_1^{(1)} = s_{12} s_{23} s_{34} \mathrm{PT}(34125) \mathrm{PT}(43215) \,. \tag{4.79}$$

In addition, the six-dimensional pentagon integral introduces

$$r_{16}^{(1)} = \frac{1}{\mathrm{tr}_5} \frac{[12][23][34][45][51]}{\langle 12\rangle\langle 23\rangle\langle 34\rangle\langle 45\rangle\langle 51\rangle} \,, \tag{4.80}$$

which is independent of the factors in Eq. (4.77) and, quite remarkably, is invariant under permutations of the external momenta.

A few observations are in order. First, the new one-loop factor in Eq. (4.80) enters the amplitude only at order ϵ, as it is manifest in Eq. (4.78). This "$D > 4$"-dimensional nature—spoiler alert—is confirmed at two loops: the two-loop generalisation of Eq. (4.80) in fact drops out of the infrared-finite hard function. Secondly, it is a good moment to highlight the wealth of non-trivial relations existing among these rational functions. For instance, the prefactor of the one-mass box in the one-loop amplitude given by Eq. (4.78) vanishes upon summing over all its S_5 permutations

$$\sum_{\sigma\in S_5} \sigma \circ [s_{12}s_{23}s_{45}\,\mathrm{PT}(12345)\mathrm{PT}(12354)] = 0\,. \tag{4.81}$$

Interestingly, the same remains true even if we multiply it by *any* function of $x \in \{s_{34}, s_{35}, s_{14}, s_{15}\}$,

$$\sum_{\sigma\in S_5} \sigma \circ [s_{12}s_{23}s_{45}\,\mathrm{PT}(12345)\mathrm{PT}(12354)\; f(x)] = 0\,. \tag{4.82}$$

This identity follows from the interplay between the permutation symmetries of the rational factor and of the argument of f. It does not imply any non-trivial functional identity for the latter. These examples indicate that the study of the relations among the leading singularities is crucial in order to find a "good"—according to more or less subjective criteria of elegance and compactness—expression for the amplitude. In this view, I highlight that both the tree-level and the one-loop amplitude, can be expressed in a fairly elegant way by summing over the permutations of a compact "seed" function (see Eqs. (4.73) and (4.78)).

We can draw inspiration from the information collected at tree level and one loop to make an ansatz for the leading singularities of the two-loop amplitude. The minimal expectation is that the following two classes of rational factors are required,

$$s_{ij}s_{kl}s_{mn}s_{op}\mathrm{PT}(\sigma)\mathrm{PT}(\rho)\,, \tag{4.83}$$

and

$$\frac{s_{ij}}{\mathrm{tr}_5}\frac{[12][23][34][45][51]}{\langle 12\rangle\langle 23\rangle\langle 34\rangle\langle 45\rangle\langle 51\rangle}\,. \tag{4.84}$$

Of the two sets, 510 and 5 are linearly independent, respectively. While this guess is correct, it is convenient—in order to simplify the notation—to anticipate that only 45 of them actually appears in the amplitude. They are spanned by 40 independent permutations of

$$r_1^{(2)} = s_{12}s_{23}s_{34}s_{45}\mathrm{PT}(12345)\mathrm{PT}(21435)\,, \tag{4.85}$$

and by

$$r^{(2)}_{40+k} = \frac{s_{k\,k+1}}{\mathrm{tr}_5}\frac{[12][23][34][45][51]}{\langle 12\rangle\langle 23\rangle\langle 34\rangle\langle 45\rangle\langle 51\rangle}\,, \qquad \text{for } k = 1,\ldots,5\,, \tag{4.86}$$

where the indices of the Mandelstam invariants are understood modulo 5. The rational factors $\{r^{(2)}_i\}_{i=1}^{45}$, like the tree-level and one-loop ones, have the property of having at most simple poles at all locations where $\langle ij\rangle = 0$. This set of rational factors can be further motivated by studying the leading singularities of the integrand using the method discussed in Sect. 3.6.1 [24]. Also in this approach the factors given by Eq. (4.84) remain slightly elusive, and can be caught only by employing a D-dimensional parameterisation, as proposed in Sect. 4.2.1. In conclusion, we arrive at the following ansatz for the two-loop five-graviton amplitude in $\mathcal{N} = 8$ supergravity,

$$M^{(2)}_5 = \sum_{i=1}^{45}\sum_j m^{(2)}_{ij} r^{(2)}_i \mathcal{I}^{(2)\text{pure}}_j\,, \tag{4.87}$$

where $m^{(2)}_{ij}$ are constant rational numbers and $\mathcal{I}^{(2)\text{pure}}_j$ are pure two-loop integrals.

4.3.3 *Integrating the Integrands*

In this section I describe how explicit results for the amplitudes in the form given by Eqs. (4.76) and (4.87) are obtained starting from known un-integrated expressions. The latter were computed in Ref. [25] using D-dimensional unitarity and colour-kinematics duality [75].

The integrand of the $\mathcal{N} = 4$ super-Yang-Mills amplitude can be expressed as

$$A^{(2)}_5 = \sum_{\sigma\in S_5}\sigma\circ\left(\frac{1}{2}\mathcal{I}^{(a)}_{\mathcal{N}=4} + \frac{1}{4}\mathcal{I}^{(b)}_{\mathcal{N}=4} + \frac{1}{4}\mathcal{I}^{(c)}_{\mathcal{N}=4} + \frac{1}{2}\mathcal{I}^{(d)}_{\mathcal{N}=4} + \frac{1}{4}\mathcal{I}^{(e)}_{\mathcal{N}=4} + \frac{1}{4}\mathcal{I}^{(f)}_{\mathcal{N}=4}\right), \tag{4.88}$$

where $\mathcal{I}^{(x)}_{\mathcal{N}=4}$ with $x = a, b, \ldots, f$, denotes a Feynman integral whose propagator structure is given by the graph (x) in Fig. 4.3. Each of the integrals in Eq. (4.88) has the form

$$\mathcal{I}^{(x)}_{\mathcal{N}=4} = e^{2\epsilon\gamma_{\mathrm{E}}}\int\frac{d^Dk_1}{i\pi^{D/2}}\frac{d^Dk_2}{i\pi^{D/2}}\frac{c^{(x)}N^{(x)}}{D^{(x)}_1\ldots D^{(x)}_8}, \quad \text{for } x = a, b, \ldots, f\,. \tag{4.89}$$

The inverse propagators $D^{(x)}_i$ can be read off from the graph (x) in Fig. 4.3 (for $x = d, e, f$ one of the inverse propagators is given by s_{12}). The colour factor $c^{(x)}$ is given by a product of Lie-algebra structure constants. We find it convenient to write it as a vector in the colour basis $\{\mathcal{T}_\lambda\}_{\lambda=1}^{22}$ given by Eqs. (4.65) and (4.66). Finally,

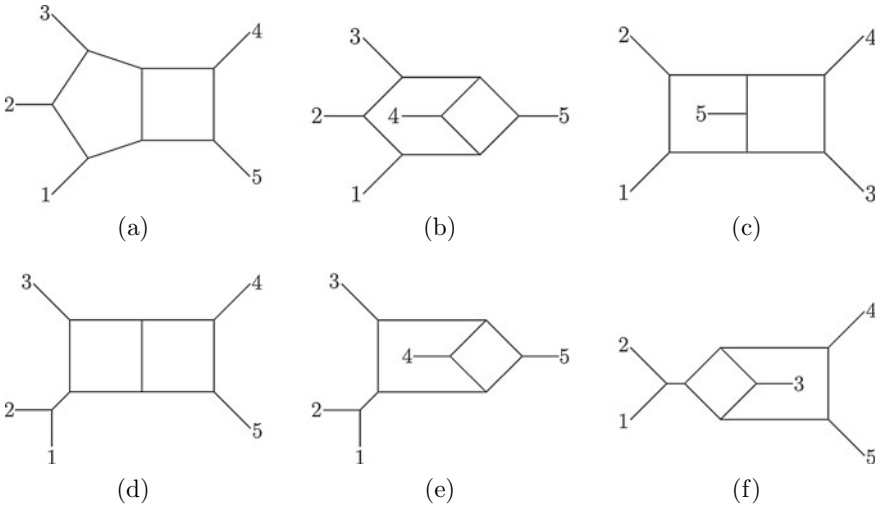

Fig. 4.3 Graphs representing the integrals appearing in the two-loop five-particle integrands given by Eqs. (4.88) and (4.90)

$N^{(x)}$ is a kinematic factor. For the explicit expressions I refer to Eqs. (4.15) and Table I of the original work [25]. Note that the numerator factors there contain the super-momentum conservation delta function, which we have extracted from the definition of the two-loop amplitude $A_5^{(2)}$ (see Eq. (4.61)).

The $\mathcal{N} = 4$ super Yang-Mills integrand given by Eq. (4.88) is in the so-called Bern-Carrasco-Johansson form [75, 76]: the kinematic factors $N^{(x)}$ in the numerator appear on equal footing with the colour factors $c^{(x)}$, i.e. they satisfy same algebraic relations as the colour factors. This is a manifestation of the colour-kinematics duality [75]. Therefore, the integrand of the $\mathcal{N} = 8$ supergravity amplitude can be obtained by "squaring" the $\mathcal{N} = 4$ super Yang-Mills one as dictated by the double-copy mechanism [75, 76]. In practice, one trades the colour factors $c^{(x)}$ for copies of the kinematic factors $N^{(x)}$. Such copies, which we denote by $\tilde{N}^{(x)}$, are identical to the original factors $N^{(x)}$ from the kinematic point of view, but have shifted R-symmetry indices for a correct bookkeeping of the individual states. We delegate this bookkeeping to the overall super-momentum conservation delta function, which we have extracted from the two-loop amplitude $M_5^{(2)}$ (see Eq. (4.70)). We thus keep only the purely kinematic part of the numerator factors, which is identical between the two copies $N^{(x)}$ and $\tilde{N}^{(x)}$. The resulting expression for the $\mathcal{N} = 8$ supergravity amplitude is

$$M_5^{(2)} = \sum_{\sigma \in S_5} \sigma \circ \left(\frac{1}{2} \mathcal{I}^{(a)}_{\mathcal{N}=8} + \frac{1}{4} \mathcal{I}^{(b)}_{\mathcal{N}=8} + \frac{1}{4} \mathcal{I}^{(c)}_{\mathcal{N}=8} + \frac{1}{2} \mathcal{I}^{(d)}_{\mathcal{N}=8} + \frac{1}{4} \mathcal{I}^{(e)}_{\mathcal{N}=8} + \frac{1}{4} \mathcal{I}^{(f)}_{\mathcal{N}=8} \right), \tag{4.90}$$

where the integrals are double-copies of the $\mathcal{N} = 4$ ones given by Eq. (4.89),

$$\mathcal{I}^{(x)}_{\mathcal{N}=8} = e^{2\epsilon\gamma_{\rm E}} \int \frac{d^D k_1}{i\pi^{D/2}} \frac{d^D k_2}{i\pi^{D/2}} \frac{\left[N^{(x)}\right]^2}{D_1^{(x)} \dots D_8^{(x)}}, \quad \text{for } x = a, b, \dots, f\,. \tag{4.91}$$

As discussed in Sect. 4.2, all massless two-loop five-particle integrals have been computed. Integrating the integrands given by Eqs. (4.88) and (4.90) therefore amounts to rewriting them in terms of the known pure basis integrals. Our workflow is the following. First, we rewrite the numerator factors $N^{(x)}$ in terms of inverse propagators $D_i^{(x)}$ and ISPs, and map the integrals $\mathcal{I}^{(x)}_{\mathcal{N}=4}$ and $\mathcal{I}^{(x)}_{\mathcal{N}=8}$ to (permutations of) the three integral families discussed in Sect. 4.2 (see Fig. 4.1). Then, we use IBP relations to express the summands of Eqs. (4.88) and (4.90) for the first orientation of the external momenta in terms of basis integrals. I stress that at this stage we are focusing on one specific orientation of the external legs, and postpone the sum over the 5! permutations. Thanks to the recent advances in the IBP-reduction techniques, this step no longer represents a bottleneck. The numerators are in fact rather simple: they depend at most linearly (quadratically) on the loop momenta in the $\mathcal{N} = 4$ ($\mathcal{N} = 8$) case. Therefore, the IBP reduction can be performed using either the public IBP packages like FIRE6 [77], Kira [78] and Reduze2 [79], or private IBP solvers with novel approaches [6, 80–82]. The resulting form of the $\mathcal{N} = 4$ super Yang-Mills amplitude is

$$A_5^{(2)} = \sum_{\sigma\in S_5} \sigma \circ \left[\sum_{\lambda=1}^{22} \left(\sum_{j=1}^{61} c^{(a)}_{\lambda,j}\, I^{(a)}_j + \sum_{j=1}^{73} c^{(b)}_{\lambda,j}\, I^{(b)}_j + \sum_{j=1}^{108} c^{(c)}_{\lambda,j}\, I^{(c)}_j \right) \mathcal{T}_\lambda \right], \tag{4.92}$$

where $\{I^{(a)}_i\}_{i=1}^{61}$, $\{I^{(b)}_i\}_{i=1}^{73}$ and $\{I^{(c)}_i\}_{i=1}^{108}$ denote the integral bases for the pentagon-box, for the hexagon-box, and for the double-pentagon integral family, respectively, in the orientation of the external legs given by Fig. 4.3. The choice of these integral bases depends on the specific IBP solver used. In general, they are not pure integrals. The factors $c^{(x)}_{\lambda,j}$ in Eq. (4.92) depend on N_c, on the spinor products of the external momenta, and on ϵ. An analogous expression holds for the supergravity amplitude.

Next, we change the integral bases to the known canonical bases, which we denote by $\{\tilde{I}^{(a)}_i\}_{i=1}^{61}$, $\{\tilde{I}^{(b)}_i\}_{i=1}^{73}$ and $\{\tilde{I}^{(c)}_i\}_{i=1}^{108}$. See Sect. 4.2 for the relevant references. In order to perform this change of basis, we first reduce the canonical bases to those chosen by the IBP solver. This gives the transformation matrices $T^{(x)}$ such that

$$\tilde{I}^{(x)} = T^{(x)} \cdot I^{(x)}\,. \tag{4.93}$$

The inverse transformation matrices $\left(T^{(x)}\right)^{-1}$ are computed using the sparse linear algebra method of Ref. [81]. They allow us to rewrite the summands of the amplitudes in terms of pure integrals,

$$A_5^{(2)} = \sum_{\sigma\in S_5} \sigma \circ \left[\sum_{\lambda=1}^{22} \left(\sum_{j=1}^{61} \tilde{c}^{(a)}_{\lambda,j}\, \tilde{I}^{(a)}_j + \sum_{j=1}^{73} \tilde{c}^{(b)}_{\lambda,j}\, \tilde{I}^{(b)}_j + \sum_{j=1}^{108} \tilde{c}^{(c)}_{\lambda,j}\, \tilde{I}^{(c)}_j \right) \mathcal{T}_\lambda \right], \tag{4.94}$$

and similarly for the $\mathcal{N} = 8$ supergravity amplitude. It is interesting that also at this stage the prefactors of the integrals $\tilde{c}^{(x)}_{\lambda,j}$ are functions not only of the kinematics and of N_c, but also of ϵ. In other words, these expressions for the amplitudes do not exhibit uniform transcendentality. The sum over the permutations of the external legs therefore appears to play a crucial role in making this property manifest.

To permute the integrals, we follow the strategy introduced in Ref. [27] and outlined in Sect. 4.2.3. We do not compute the integrals for one orientation of the external legs and then permute the result, which would require a careful analytic continuation. Instead, we treat every permutation of each integral family as a different family, for which we write down the differential equations and compute the boundary values at the base point in the s_{12} channel given by Eq. (4.43). This way, we can express all permutations of any basis integral in terms of iterated integrals or of the basis of functions of Ref. [50] straightforwardly and directly in the s_{12} channel. In addition, we construct the relations between integrals of different families and in different orientations, so that the remaining pure integrals are linearly independent.

The rational factors, on the other hand, come with a different issue. Although they are trivial from the analytic point of view, their proliferation in the sum over the permutations causes an uncontrolled growth in size of the expression. We can tame this easily because we have a very precise idea of which leading singularities should appear in the amplitudes. The latter, in fact, should ultimately take the forms given by Eqs. (4.76) and (4.87). Our strategy then is to evaluate the prefactors of the pure integrals in random kinematic points, leaving the integrals as symbolic expressions. In particular, we use rational rather than floating-point numbers to avoid any loss in accuracy. This way, the intermediate expressions are as compact as they could possibly be. Using just 6 (45) independent random evaluations we can easily fit the expected form of the $\mathcal{N} = 4$ super Yang-Mills ($\mathcal{N} = 8$ supergravity) amplitude. A few more evaluations are used to validate the result. At this stage it is important that only a set of independent pure integrals are left. Unresolved identities among the pure integrals could in fact lead to spurious terms which do not have the expected form.

Finally, after summing up all the permutations, the dependence on ϵ in the rational factors drops out, and the amplitudes exhibit uniform transcendentality in full glory. We obtain expressions for the two amplitudes with the expected form, given by Eqs. (4.76) and (4.87). The leading singularities are those discussed in Sect. 4.3.2, and the pure integrals are the independent canonical basis integrals which span all the permutations of the three relevant integral families. These expressions give us full analytical and numerical control over the amplitudes. Using the differential equations we can in fact rewrite them in terms of iterated integrals, Goncharov polylogarithms or the basis of functions of Ref. [50], and evaluate them anywhere in the physical scattering regions. The expressions are however too bulky for me to write them out here. They can be found in ancillary files of the original papers [22, 23, 26]. The remarkable cancellations that ultimately lead to uniformly transcendent amplitudes with precisely the expected leading singularities are on their own a compelling sign that the computation is correct. Nonetheless, we carried out a number of tests to validate our results, which I present in the next two sections.

4.3.4 Divergence Structure and Hard Functions

In Sect. 2.3 I have shown how the divergences in loop scattering amplitudes stem from either the infrared or the ultraviolet region of the loop integration. Ultraviolet divergences can be removed through renormalisation, but we do not need to worry about them in the present case. $\mathcal{N} = 4$ super Yang-Mills theory is in fact known to be ultraviolet finite [83–85]. The potential ultraviolet (UV) finiteness of $\mathcal{N} = 8$ supergravity is still an extremely intriguing open problem. Various arguments rule out UV divergences in supergravity amplitudes up to at least seven loops [86–92]. Therefore, the two-loop five-particle amplitudes in $\mathcal{N} = 4$ super Yang-Mills and $\mathcal{N} = 8$ supergravity have infrared divergences only.

The infrared divergences of scattering amplitudes in gauge and gravity theories factorise in well understood ways. Through the infrared factorisation theorems, the infrared-divergent part of a loop amplitude is determined entirely by information of lower loop order. This provides a precious check on amplitude computations. Moreover, it means that the infrared divergences can be subtracted, this way defining an infrared-safe hard (or remainder) function where the regulator ϵ can be removed. The hard functions are interesting objects for several reasons. Because the infrared divergences are determined by lower-loop information, the hard functions contain the truly new piece of information. Moreover, the Kinoshita-Lee-Nauenberg theorem [93, 94] implies that infrared divergences of virtual amplitudes cancel out against corresponding divergences from real emissions in any physical observable. The hard functions thus capture the physically most relevant part of the amplitudes. Finally, there is also a practical reason. Experience shows that the hard functions are substantially simpler than the corresponding amplitudes, and they typically allow for much more compact expressions.

In the next section I review the infrared factorisation of massless amplitudes in gauge and gravity theories, and then present our results for the $\mathcal{N} = 4$ super Yang-Mills and $\mathcal{N} = 8$ supergravity hard functions.

Infrared factorisation in $\mathcal{N} = 4$ super Yang-Mills theory

The infrared (IR) divergences of (renormalised) massless amplitudes in gauge theories factorise to all perturbative orders as [95–99]

$$\mathcal{A}_5\left(\frac{s_{ij}}{\mu^2}, a(\mu^2), \epsilon\right) = \mathbf{Z}_5\left(\frac{s_{ij}}{\mu_F^2}, a(\mu_F^2), \epsilon\right) \mathcal{A}_5^f\left(\frac{s_{ij}}{\mu^2}, \frac{\mu^2}{\mu_F^2}, a(\mu^2), \epsilon\right), \tag{4.95}$$

where $\mathbf{Z}_5$ is an operator which captures all the poles in ϵ, and the amplitude $\mathcal{A}_5^f$ is thus finite in the $\epsilon \to 0$ limit. Treating the amplitudes as vectors in colour space, $\mathbf{Z}_5$ is a matrix. I denote matrices in colour space in bold face. In Eq. (4.95) μ and μ_F are the renormalisation and factorisation scale. For simplicity we choose them to be equal, $\mu = \mu_F$, and eventually set $\mu = 1$. The explicit dependence can be recovered a posteriori.

The hard (or remainder) function is then defined by letting letting $\epsilon \to 0$ in the finite amplitude,

$$\mathcal{H}_5 = \lim_{\epsilon \to 0} \mathcal{A}_5^f \,. \tag{4.96}$$

This definition is of course ambiguous, as different choices for the finite part of the pole operator $\mathbf{Z}_5$ can be made. We adopt the $\overline{\text{MS}}$ scheme, i.e. we keep only the pure pole part in $\mathbf{Z}_5$. The latter may then be expressed as the path-ordered exponential of an anomalous dimension, which up to two loops is given by the elegant "dipole" form,

$$\Gamma_5 \equiv -\gamma_{\text{cusp}} \sum_{i<j}^{5} \left(\mathbf{T}_i \cdot \mathbf{T}_j\right) \log\left(\frac{-s_{ij}}{\mu^2}\right) + \sum_{i=1}^{5} \gamma_{\text{c}} \,, \tag{4.97}$$

where the operator $\mathbf{T}_i^a$ inserts a $SU(N_c)$ generator in the adjoint representation on the i^{th} leg. For convenience of the reader I spell out the action of the colour-insertion operator on the $SU(N_c)$ generators T^{a_i},

$$\mathbf{T}_i^b \circ T^{a_j} = \begin{cases} 0 \,, & j \neq i \,, \\ -i f^{b a_i c_i} T^{c_i} \,, & j = i \,. \end{cases} \tag{4.98}$$

Keeping into account the vanishing of the (four-dimensional part of the) β-function in $\mathcal{N} = 4$ super Yang-Mills, the pole operator $\mathbf{Z}_5$ takes the form [98]

$$\log \mathbf{Z}_5 = a \left(\frac{\Gamma_5'^{(1)}}{4\epsilon^2} + \frac{\Gamma_5^{(1)}}{2\epsilon}\right) + a^2 \left(\frac{\Gamma_5'^{(2)}}{16\epsilon^2} + \frac{\Gamma_5^{(2)}}{4\epsilon}\right) + O(a^3) \,, \tag{4.99}$$

where $\Gamma_5^{(\ell)}$ is the coefficient of a^ℓ in Γ_5 and

$$\Gamma_5' = \mu \frac{\partial}{\partial \mu} \Gamma_5 = 2\gamma_{\text{cusp}} \sum_{i<j}^{5} \left(\mathbf{T}_i \cdot \mathbf{T}_j\right) = -5 C_A \gamma_{\text{cusp}} \,, \tag{4.100}$$

with $C_A = N_c$. Finally, in Eq. (4.97) γ_{cusp} is the cusp anomalous dimension normalised by the quadratic Casimir in the adjoint representation C_A [100–106],

$$\gamma_{\text{cusp}} = 4a - \frac{4\pi^2}{3} C_A a^2 + O(a^3) \,, \tag{4.101}$$

and γ_{c} is the collinear anomalous dimension,

$$\gamma_{\text{c}} = 2\zeta_3 C_A^2 a^2 + O(a^3) \,. \tag{4.102}$$

The logarithms in Γ_5 (4.97) need to be analytically continued to the kinematic region of interest. This can be achieved by adding a small positive imaginary part to each Mandelstam invariant s_{ij}, and results in

$$\log\left(-s_{ij}-i0^+\right)=\begin{cases}\log s_{ij}-i\pi\,, & \text{if } s_{ij}>0\,,\\ \log\left(-s_{ij}\right)\,, & \text{if } s_{ij}<0\,.\end{cases} \tag{4.103}$$

Denoting by $A^{(\ell)}_{5;k}$ the order-ϵ^k term of ℓ-loop amplitude $A^{(\ell)}_5$, the one and two-loop hard functions in the $\overline{\text{MS}}$ scheme are explicitly given by

$$\mathcal{H}^{(1)}_5=A^{(1)}_{5;0}\,, \tag{4.104}$$

$$\mathcal{H}^{(2)}_5=A^{(2)}_{5;0}+5C_A\,A^{(1)}_{5;2}+2\sum_{i<j}^{5}\left(\mathbf{T}_i\cdot\mathbf{T}_j\right)\log\left(\frac{-s_{ij}}{\mu^2}\right)A^{(1)}_{5;1}\,. \tag{4.105}$$

We see in Eq. (4.105) that the two-loop hard function depends on the coefficients of the one-loop amplitude up to order ϵ^2. We computed the latter starting from the integrand given in Ref. [25] and following the same strategy presented in Sect. 4.3.3 for the two-loop amplitude. The result has uniform transcendental weight, with the same leading singularities of the two-loop amplitude,

$$A^{(1,k)}_{\lambda}=\sum_{i=1}^{6}\sum_{j}a^{(1,k)}_{\lambda,ij}\,\text{PT}_i\,\mathcal{I}^{(1)\text{pure}}_j\,, \tag{4.106}$$

where $a^{(1,k)}_{\lambda,ij}\in\mathbb{Q}$ and $\mathcal{I}^{(1)\text{pure}}_j$ are pure one-loop integrals.

Infrared factorisation in $\mathcal{N}=8$ supergravity

The IR structure of perturbative gravity is much simpler as compared to gauge theories. Graviton amplitudes are in fact free of collinear divergences [107]. As a result, they have only a single pole in ϵ per loop order, associated with soft graviton exchanges, rather than a double pole as in gauge theories. The soft divergences exponentiate in a strikingly simple way [107–113],

$$\mathcal{M}_5=\mathcal{S}_5\,\mathcal{M}^f_5\,. \tag{4.107}$$

The gravitational soft function $\mathcal{S}_5$ is the analogue of the pole operator $\mathbf{Z}_5$ in Eq. (4.95) for the Yang-Mills case: it captures all the singularities, leaving a finite amplitude $\mathcal{M}^f_5$. Thanks to the absence of colour, $\mathcal{S}_5$ is not an operator, and it is given by a simple exponential, as opposed to the path-ordered exponential in the Yang-Mills IR-pole operator $\mathbf{Z}_5$. In particular, the gravitational soft function $\mathcal{S}_5$ is given to all orders in the coupling by

$$\mathcal{S}_5 = \exp\left[\frac{\sigma_5}{\epsilon}\right], \tag{4.108}$$

where σ_5/ϵ is the infrared-divergent part of the one-loop amplitude,

$$\sigma_5 = \left(\frac{\kappa}{2}\right)^2 \sum_{j=1}^{5} \sum_{i<j} s_{ij} \log\left(\frac{-s_{ij}}{\mu^2}\right). \tag{4.109}$$

Here μ is a factorisation scale, which we set to 1 for simplicity. In this sense the divergences of graviton amplitudes are said to be *one-loop exact*. The logarithms in Eq. (4.109) are analytically continued to the desired scattering region according to Eq. (4.103).

In complete analogy with the Yang-Mills case, we let $\epsilon \to 0$ in the finite amplitude $\mathcal{M}_5^f$, and define an infrared-safe hard function,

$$\mathcal{F}_5 \equiv \lim_{\epsilon\to 0} \mathcal{M}_5^f \,. \tag{4.110}$$

The one and two-loop contributions are given explicitly by

$$\mathcal{F}_5^{(1)} = M_{5;0}^{(1)}\,, \tag{4.111}$$

$$\mathcal{F}_5^{(2)} = M_{5;0}^{(2)} - \sigma_5\, M_{5;1}^{(1)}\,, \tag{4.112}$$

where $M_{5;k}^{(\ell)}$ denotes the order-ϵ^k term of the ℓ-loop amplitude $M_5^{(\ell)}$.

Computing the two-loop hard function requires the knowledge of the one-loop amplitude up to order ϵ. We obtained the latter by applying the workflow discussed in Sect. 4.3.3 to the integrand given in Ref. [25]. The result exhibits uniform transcendental weight,

$$M^{(1)} = \sum_{i=1}^{16} m_{ij}^{(1)} r_i^{(1)} \mathcal{I}_j^{(1)\text{pure}}, \tag{4.113}$$

where $m_{ij}^{(1)} \in \mathbb{Q}$, $r_i^{(1)}$ are the one-loop leading singularities discussed in Sect. 4.3.2, and $\mathcal{I}_j^{(1)\text{pure}}$ are pure one-loop integrals.

The two-loop hard functions

In this section I present our results for the hard functions. We begin with $\mathcal{N} = 4$ super Yang-Mills theory. We adopt for the hard functions the same colour decomposition used for the amplitudes, given for the latter by Eqs. (4.63) and (4.64). The results for the one and two-loop amplitudes have the form given by Eqs. (4.106) and (4.76), respectively. Substituting them into Eqs. (4.104) and (4.105) gives expressions for the hard functions of the form

$$\mathcal{H}_{\lambda}^{(1,k)} = \sum_{i=1}^{6} \sum_{j} b_{\lambda,ij}^{(1,k)} \, \mathrm{PT}_i \, P_j^{(2)} \,, \tag{4.114}$$

$$\mathcal{H}_{\lambda}^{(2,k)} = \sum_{i=1}^{6} \sum_{j} b_{\lambda,ij}^{(2,k)} \, \mathrm{PT}_i \, P_j^{(4)} \,, \tag{4.115}$$

where $b_{\lambda,ij}^{(\ell,k)} \in \mathbb{Q}$ and $P_j^{(w)}$ are weight-w pentagon functions. We observe that the letter W_{31}, defined in Eq. (4.36) and present in the amplitudes, drops out of the hard function, as it was already noted at symbol level [20, 22]. We have full analytical and numerical control over the hard functions in the form given by Eqs. (4.114) and (4.115). For instance, this allows us to compute their asymptotic behaviour in any kinematic limit. I give an explicit example of this in Sect. 4.4, where I discuss the multi-Regge limit. Moreover, we can evaluate the hard functions anywhere in the physical scattering region. To prove this and to facilitate future cross-checks, we provide in Table 4.1 the numerical values of the two-loop hard function at the randomly-chosen kinematic point

$$s_R = \left(\frac{13}{4} \,, -\frac{9}{11} \,, \frac{3}{2} \,, \frac{3}{4} \,, -\frac{2}{3} \right) \,, \quad \text{with } \mathrm{tr}_5 = i \frac{\sqrt{222767}}{264} \,. \tag{4.116}$$

We find it interesting to note that the planar and the non-planar colour components of the two-loop hard function are numerically of the same order of magnitude, as can be seen in Table 4.1. We stress however that the impact of the non-planar corrections on the theory predictions can be assessed systematically only at the level of the physical observable. We provide the explicit expressions of the one- and two-loop hard function in terms of the pentagon functions defined in Ref. [50] at

pentagonfunctions.hepforge.org/downloads/2l_5pt_hardfunctions_N=4_N=8.tar.gz.

The one and two-loop hard functions in $\mathcal{N} = 8$ supergravity are given by Eqs. (4.111) and (4.112) in terms of the finite part of the two-loop amplitude $M_5^{(2)}$ and of the one-loop amplitude $M_5^{(1)}$ up to order ϵ. Substituting our results for the amplitudes, which have the form given by Eqs. (4.113) and (4.87), gives

$$\mathcal{F}_5^{(1)} = \sum_{i=1}^{15} \sum_{j} c_{ij}^{(1)} r_i^{(1)} P_j^{(2)} \,, \tag{4.117}$$

$$\mathcal{F}_5^{(2)} = \sum_{i=1}^{40} \sum_{j} c_{ij}^{(2)} r_i^{(2)} P_j^{(4)} \,, \tag{4.118}$$

where $c_{ij}^{(\ell)} \in \mathbb{Q}$ and $P_j^{(w)}$ are weight-w pentagon functions. It is very interesting that the rational factors $r_{16}^{(1)}$ at one loop and $r_{40+k}^{(2)}$, with $k = 1, \ldots, 5$, at two loops drop out of the hard function. At one loop this is already obvious from the integrand

Table 4.1 Numerical values of the two-loop five-particle hard function in $\mathcal{N}=4$ super Yang-Mills theory normalised by the Parke-Taylor factor PT_1 (4.75), $\mathcal{H}_5^{(2)}/\mathrm{PT}_1$, at the kinematic point s_R (4.116). The rows correspond to the colour decomposition in the basis defined by Eqs. (4.65) and (4.66), and the columns to the power of N_c

	N_c^2	N_c	N_c^0
$\mathcal{T}_1$	$74.92986 - 61.83635i$	0	$-617.3565 + 294.7986i$
$\mathcal{T}_2$	$92.3051 + 108.9834i$	0	$-1024.0932 + 532.1760i$
$\mathcal{T}_3$	$-49.51614 + 73.37582i$	0	$258.3246 + 558.5523i$
$\mathcal{T}_4$	$7.50918 + 52.48750i$	0	$427.1264 + 340.3532i$
$\mathcal{T}_5$	$-95.8105 - 124.8597i$	0	$-73.4024 - 741.5020i$
$\mathcal{T}_6$	$-134.93821 + 4.43862i$	0	$853.1018 - 590.6476i$
$\mathcal{T}_7$	$-12.39259 + 33.13533i$	0	$494.0699 + 262.7033i$
$\mathcal{T}_8$	$37.35506 + 120.68054i$	0	$87.3332 + 500.0807i$
$\mathcal{T}_9$	$80.04433 + 33.19817i$	0	$-839.1711 + 349.2263i$
$\mathcal{T}_{10}$	$50.71731 - 21.09889i$	0	$-670.3692 + 131.0271i$
$\mathcal{T}_{11}$	$-39.34196 - 85.68420i$	0	$-263.6325 - 106.3503i$
$\mathcal{T}_{12}$	$-27.72786 + 22.45736i$	0	$662.8718 + 44.5041i$
$\mathcal{T}_{13}$	0	$-125.2669 + 216.9434i$	0
$\mathcal{T}_{14}$	0	$-696.3813 - 209.4301i$	0
$\mathcal{T}_{15}$	0	$-344.4732 + 447.8376i$	0
$\mathcal{T}_{16}$	0	$-127.9880 + 116.6798i$	0
$\mathcal{T}_{17}$	0	$-444.5692 - 325.7655i$	0
$\mathcal{T}_{18}$	0	$-510.7351 - 321.1812i$	0
$\mathcal{T}_{19}$	0	$459.3389 + 210.4025i$	0
$\mathcal{T}_{20}$	0	$-120.7437 + 267.2953i$	0
$\mathcal{T}_{21}$	0	$711.4669 + 60.1616i$	0
$\mathcal{T}_{22}$	0	$-460.7431 - 329.6070i$	0

given by Eq. (4.78). There, in fact, it is clear that the factor $r_{16}^{(1)}$ appears only at order ϵ, which does not enter the one-loop hard function. Its absence at two loops is instead non-trivial. In this regards it is interesting to note that, while the other factors can be computed using the four-dimensional analysis of the leading singularities, $r_{16}^{(1)}$ and its two-loop versions can be caught only with a D-dimensional analysis (e.g. using Baikov representation, as suggested in Sect. 4.2.1) [24]. In this sense the hard function, which is a four-dimensional object, appears to contain only the four-dimensional leading singularities. Another interesting observation is that the letter W_{31} in the supergravity case is absent not only in the hard function, but also in the amplitude. I complete this section by providing the value of the two-loop hard function at the kinematic point s_R defined in Eq. (4.116),

$$\left.\frac{\mathcal{F}_5^{(2)}}{\mathrm{PT}_1^2}\right|_{s_R} = -1211.9365 - 215.6087i\,, \tag{4.119}$$

where the normalisation was chosen so as to cancel the helicity weight. The explicit expressions of the one- and two-loop hard functions in terms of the pentagon functions defined in Ref. [50] can be downloaded at

pentagonfunctions.hepforge.org/downloads/2l_5pt_hardfunctions_N=4_N=8.tar.gz.

4.3.5 *Further Validation of the Results*

We verified that our results for the two-loop five-particle amplitudes in $\mathcal{N} = 4$ super Yang-Mills theory and $\mathcal{N} = 8$ supergravity satisfy several highly non-trivial constraints, in addition to having the correct infrared structure. All the checks discussed in this section have been carried out at symbol level, where we also successfully cross-check with the results of Refs. [20, 24].

Soft limit of the supergravity amplitude

The leading term in the asymptotic expansion of a n-graviton amplitude as one of the gravitons becomes soft factorises into a $(n-1)$-graviton amplitude times a universal soft factor [64]. The latter does not receive quantum corrections [107, 114], which explains the much simpler soft structure of supergravity amplitudes discussed in Sect. 4.3.4 as compared to their super Yang-Mills counterparts. Since the four-graviton amplitude in $\mathcal{N} = 8$ supergravity is known up to two loops [109, 115, 116], we can check that our result for the two-loop five-graviton amplitude has the correct leading behaviour in the soft limit. I stress that here we consider the leading soft behaviour only. The subleading soft operators are substantially more complicated: they are realised as differential operators in the spinor variables and they do receive quantum corrections [117].

Recall that we are actually working with a *super*-amplitude, which comprises different component amplitudes related by supersymmetry. It is convenient to focus on a specific component, without any loss of generality. In particular, we choose the component amplitude describing the scattering of five gravitons with helicity configuration $(1^-, 2^-, 3^+, 4^+, 5^+)$. As one of the external momenta becomes soft, say $p_5 \to 0$, the five-point amplitude factorises as [64]

$$\lim_{p_5 \to 0} \mathcal{M}_5^{(\ell)}(1^-, 2^-, 3^+, 4^+, 5^+) \sim \mathcal{S}(5^+) \times \mathcal{M}_4^{(\ell)}(1^-, 2^-, 3^+, 4^+)\,, \tag{4.120}$$

where all subleading terms are omitted. The leading soft factor for a positive-helicity graviton is given at all orders by [107, 114]

$$\mathcal{S}(5^+) = -\frac{1}{\langle 15\rangle\langle 54\rangle}\left[\frac{\langle 12\rangle\langle 24\rangle[25]}{\langle 25\rangle} + \frac{\langle 13\rangle\langle 34\rangle[35]}{\langle 35\rangle}\right]. \tag{4.121}$$

We use momentum twistor variables Z_i to parameterise the kinematics in the limit. In particular, we find it convenient to use the Poincaré dual of the standard momentum twistors [47],

$$Z_i = \begin{pmatrix} \tilde{\lambda}_i^{\dot{\alpha}} \\ x_{i\,\alpha\dot{\alpha}}\,\tilde{\lambda}_i^{\dot{\alpha}} \end{pmatrix}, \tag{4.122}$$

where

$$x_i - x_{i+1} = \lambda_i\tilde{\lambda}_i = p_i\,, \tag{4.123}$$

and the subscript of x_i is defined modulo 5. Swapping the helicity spinors $\lambda \leftrightarrow \tilde{\lambda}$ in Eq. (4.122) gives the standard momentum twistors. In momentum twistor space, the soft limit $p_5 \to 0$ can be parameterised as [118]

$$Z_5 \to Z_4 + a_1 Z_1 + \delta\,(a_2 Z_2 + a_3 Z_3)\,, \tag{4.124}$$

where $\delta \to 0$ controls the limit, and the parameters a_1, a_2, a_3 are fixed. It follows from the parameterisation given by Eq. (4.124) that $\lambda_5 \sim \mathcal{O}(\delta)$ and $\tilde{\lambda}_5 \sim \mathcal{O}(1)$ as $\delta \to 0$. The soft factor (4.121) thus diverges as $\mathcal{S}(5^+) \sim 1/\delta^3$. The Mandelstam invariants are given by

$$\begin{aligned}
s_{12} &= \frac{s}{1+\delta\left[\frac{y_1}{x} + \left(1+\frac{1}{x}\right)\frac{y_1}{y_3}\right]}\,,\\
s_{23} &= t \equiv s\,x\,,\\
s_{34} &= \frac{s}{1+\delta\left(1+\frac{1}{x}\right)y_2(1+y_3)}\,,\\
s_{45} &= \frac{y_1 s\,\delta}{1+\delta\left[\frac{y_1}{x} + \left(1+\frac{1}{x}\right)\frac{y_1}{y_3}\right]}\,,\\
s_{15} &= \frac{y_2\,(s+t)\,\delta}{1+\delta\,y_2\left(1+\frac{1}{x}\right)(1+y_3)}\,,
\end{aligned} \tag{4.125}$$

where the fixed parameters y_1, y_2 and y_3 specify how the soft limit is approached. The ratio $x = t/s$ is also introduced to simplify the expressions. Letting $p_5 = 0$ or equivalently $\delta = 0$, the five-particle invariants reduce to the usual Mandelstam variables s and t describing four-point scattering,

$$s_{12} \to s\,, \qquad s_{23} \to t\,, \qquad s_{34} \to s\,, \qquad s_{45} \to 0\,, \qquad s_{15} \to 0\,. \tag{4.126}$$

Substituting the parameterisation given by Eq. (4.125) into the pentagon alphabet $\{W_i\}_{i=1}^{31}$ (see Sect. 4.2.2 for the definitions), and expanding the letters up to the leading order in δ, produces a much simpler 15-letter alphabet. As expected, it contains the sub-alphabet $\{x, 1+x, s\}$, which describes the scattering of four massless particles. Only they can appear in the right-hand side of Eq. (4.120). The remaining 12 letters—δ and other functions of the non-universal parameters y_1, y_2, y_3—must drop out in the limit. This alone is already a highly non-trivial check of our result. Working out the soft asymptotics of the symbol of the two-loop amplitudes we can also match the leading terms—of order $1/\delta^3$—on both sides of Eq. (4.120), finding agreement.

Collinear limit of the supergravity amplitude

The leading behaviour of gravity amplitudes in the asymptotic limit as two gravitons become collinear is also very well understood. The leading term in the limit of a n-graviton amplitude factorises into a $(n-1)$-graviton amplitude times a universal collinear splitting amplitude [64]. Just like the soft factor regulating the leading soft behaviour, also the leading collinear splitting amplitude does not receive quantum corrections [107, 114]. Without any loss of generality, we consider the collinear limit of particles 4 and 5, i.e.

$$\lim_{4\|5} p_4 = zP\,, \qquad \lim_{4\|5} p_5 = (1-z)P\,, \tag{4.127}$$

with $P = p_4 + p_5$ to preserve momentum conservation. Moreover, we focus on the amplitude component corresponding to the helicity configuration $(1^-, 2^-, 3^+, 4^+, 5^+)$. The leading term in the asymptotic expansion of the five-particle amplitude then factorises as

$$\lim_{4\|5} \mathcal{M}_5^{(\ell)}(1^-, 2^-, 3^+, 4^+, 5^+) \sim \text{Split}_-^{(0)}(z; 4^+, 5^+) \times \mathcal{M}_4^{(\ell)}(1^-, 2^-, 3^+, P^+)\,, \tag{4.128}$$

where $\text{Split}_-^{(0)}$ is the universal tree-level splitting amplitude,

$$\text{Split}_-^{(0)}(z; 4^+, 5^+) = -\frac{1}{z(1-z)}\frac{[45]}{\langle 45\rangle}\,, \tag{4.129}$$

$\mathcal{M}_4^{(\ell)}(1^-, 2^-, 3^+, P^+)$ is the four-graviton amplitude with external momenta p_1, p_2, p_3 and P [64, 119], and the subleading terms are omitted. Once again we find it convenient to use momentum-twistor variables to parameterise the kinematics in this limit [120, 121],

$$Z_5 \to Z_4 + \delta\,(a_1 Z_1 + a_3 Z_3) + \delta^2 a_2 Z_2\,, \tag{4.130}$$

where δ approaches 0 in the limit, while the parameters a_1, a_2, a_3 are fixed. The Mandelstam invariants take the form

$$\begin{aligned} s_{12} &= \frac{s}{1+\delta\left(1+\frac{1}{x}\right)\frac{1}{y}+\delta^2\left(1+\frac{1}{x}\right)}\,, \\ s_{23} &= t \equiv s\,x\,, \\ s_{34} &= \frac{sz}{1+\delta\,y(1+x)(1-z)}\,, \\ s_{45} &= \frac{(s+t)\delta^2}{1+\delta\left(1+\frac{1}{x}\right)\frac{1}{y}+\delta^2\left(1+\frac{1}{x}\right)}\,, \\ s_{15} &= \frac{t(1-z)}{1+\delta\,y(1+x)(1-z)}\,, \end{aligned} \tag{4.131}$$

where the fixed parameter y specifies how the limit is approached. In the limit, they reduce to the Mandelstam invariants s and t of the four-point amplitude,

$$s_{12} \to s\,, \qquad s_{23} \to t\,, \qquad s_{34} \to z\,s\,, \qquad s_{45} \to 0\,, \qquad s_{15} \to (1-z)\,t\,. \tag{4.132}$$

Substituting the parameterisation given by Eq. (4.131) into the letters of the pentagon alphabet, and keeping up to the leading order in δ, produces a 14-letter alphabet. The right-hand side of Eq. (4.128) can contain the letters $\{s, x, 1+x\}$ only, which describe the scattering of four massless particles. The remaining 11 letters have to cancel out in the limit, making this test very stringent. The symbol of our expression for the two-loop five-point supergravity amplitude passes this test as well, and exhibits the expected leading collinear behaviour given by Eq. (4.128).

Collinear limit of the super Yang-Mills amplitude

Scattering amplitudes in (super) Yang-Mills theory factorise in the collinear limit, but their behaviour is more complicated as compared to supergravity. Colour in fact gives additional structure, and the leading collinear splitting amplitudes receive quantum corrections. Nonetheless, the leading behaviour in the collinear limit is well known. Without loss of generality, we consider the collinear limit of particles 4 and 5, which we choose to be positive-helicity gluons. The two-loop five-particle amplitude then factorises as

$$\begin{aligned} \lim_{4\|5}\left(A_5^{(2)}\right)^{a_1,a_2,a_3,a_4,a_5} \sim f^{a_4a_5b}\Big[&\mathrm{Split}_-^{(0)}(z;4^+,5^+)\,A_4^{(2)} + N_c\,\mathrm{Split}_-^{(1)}(z;4^+,5^+)\,A_4^{(1)} \\ &+ N_c^2\,\mathrm{Split}_-^{(2)}(z;4^+,5^+)\,A_4^{(0)}\Big]^{a_1,a_2,a_3,b}\,, \end{aligned} \tag{4.133}$$

where $\mathrm{Split}_-^{(\ell)}(z;4^+,5^+)$ and $\mathcal{A}_4^{(\ell)}$ are the ℓ-loop splitting amplitude, and the four-particle amplitude with external momenta p_1, p_2, p_3, and p_4+p_5. For the sake

of clarity I have spelled out the colour indices in Eq. (4.133). We adopt the same momentum-twistor inspired parameterisation introduced in Sect. 4.3.5. The alphabet is also the same as in the supergravity case, and simplifies in the limit to the same 14 letters. Because of the quantum corrections to the splitting amplitudes, the right-hand side of Eq. (4.133) contains also the letters $\{z, 1-z\}$, on top of the massless four-particle alphabet $\{s, x, 1+x\}$. Still, most of the letters have to drop out in the limit, making this check very constraining. Using the two-loop splitting amplitudes given in Ref. [122] and the four-point amplitude up to $\mathcal{O}(\epsilon^2)$ from Ref. [123] we find that our result for the two-loop five-particle amplitude exhibits the expected collinear factorisation, given by Eq. (4.133).

Other checks of the super Yang-Mills amplitude

Thanks to the $SU(N_c)$ symmetry, the super Yang-Mills amplitude has more structure than its supergravity counterpart, and thus offers more checks. The partial amplitudes $A_\lambda^{(\ell,k)}$ are related by group-theoretic identities [58, 59]. We checked that our result satisfies these relations, which are spelled out explicitly for the five-particle case up to two loops in Ref. [58]. More than an actual check on the calculation of the amplitude, these identities should be viewed as checks on the implementation of the colour algebra. In fact, they follow automatically from rearranging the colour structure of the amplitude in the basis defined by Eqs. (4.65) and (4.66).

The notion of colour also allows us to separate a planar amplitude, corresponding to the leading-colour partial amplitudes $A_\lambda^{(2,0)}$. In Refs. [69, 124], the authors proposed a formula expressing the planar amplitude in $\mathcal{N}=4$ super Yang-Mills theory to all orders in the coupling in terms of the one-loop amplitude and other known ingredients. This prediction, known as the ABDK/BDS ansatz from the names of the authors, was confirmed numerically for the two-loop five-particle amplitude in Refs. [125, 126], and was later shown to follow from a dual conformal Ward identity [127]. The planar component of our result is in perfect agreement with the ABDK/BDS ansatz.

A stringent check on the non-planar part of the amplitude comes from the multi-Regge limit. In Ref. [26] we computed the asymptotic behaviour of the $\mathcal{N}=4$ super Yang-Mills amplitude (and of the supergravity amplitude as well). Section 4.4 is devoted to this topic. What matters here is that, in the same work, a completely independent computation of the multi-Regge limit for certain non-planar colour structures is performed using the BFKL effective theory. Needless to say, the results agree. I stress that this check is performed at function level, including the terms beyond the symbol.

4.4 Multi-Regge Limit of the Maximally Supersymmetric Amplitudes

The expressions for the amplitudes in $\mathcal{N} = 4$ super Yang-Mills theory and $\mathcal{N} = 8$ supergravity in terms of rational factors and pure integrals allow us to study their asymptotic behaviour in any kinematic limit. The rational factors are in fact trivial in this context, and the asymptotics of the pure integrals can be studied in a very systematic and straightforward way through the canonical differential equations they satisfy. To some extent we have already done this in the previous section, where the soft and the collinear limits of the amplitudes were computed to validate our results. The analysis there was however simplified: we worked at symbol level and focused on the leading terms in the limit. Two classes of contributions were thus omitted: the terms beyond the symbol and the power-suppressed terms in the asymptotic expansion of the integrals. In this section I present the computation of another kinematic limit, the so-called *multi-Regge limit* [128, 129]. We perform it at function level, and do not restrict ourselves to the leading behaviour only, but rather we omit only the terms which vanish in the limit. The technique presented in Sect. 3.5 to compute the asymptotic expansion of pure integrals is therefore employed in full glory.

Loosely speaking, in the Regge limit the interacting objects are highly boosted and have a fixed transverse profile. There is therefore a hierarchy between transverse and longitudinal momenta, which allows one to expand the scattering amplitudes in powers and logarithms of a small parameter. The leading-logarithmic terms in this expansion are universal. They are controlled by the gluon Regge trajectory and are related to light-like cusp anomalous dimension. Much less is known about the subleading-logarithmic and power-suppressed terms. They are substantially more complicated, but they can be numerically relevant and thus important for phenomenology. Understanding these subleading contributions in the Regge limit, as well as in other kinematic limits, is an active area of research.

The interest in the Regge kinematics initially arose from the goal of interpreting data from high-energy experiments. One of the aims is therefore to describe better certain phase space regions of collider experiments. The Regge limit is however also a very useful probe into the structure of scattering amplitudes in quantum field theory. One of the most interesting questions in this field is to what extent scattering amplitudes are determined by general principles and properties. The Regge limit sheds some light into the answer. For example, studies of this limit gave the first hints that planar $\mathcal{N} = 4$ super Yang-Mills theory is integrable [130, 131]. More recently, it played an important role in studying multi-particle amplitudes in the context of the Wilson loop/scattering amplitude duality. While it is difficult to formulate crossing symmetry for multi-particle amplitudes in general, it is relatively well understood in the Regge kinematics. Moreover, the absence of certain "overlapping" discontinuities in the Regge limit gave early hints that the ABDK/BDS ansatz mentioned in Sect. 4.3.5 was incomplete [132], and helps to constrain the form of the required corrections [133]. Such constraints are an example of how the Regge limit can be useful in a bootstrap approach to amplitudes, where an ansatz based on certain assumptions

is made, and the free coefficients are fixed using various conditions [70, 134]. The Regge limit can be used as an input in such a procedure, but whenever the ansatz can be constrained by other means, it gives a prediction. See also Ref. [135] for recent work on multi-particle amplitudes in the Regge limit. Although most studies in Regge theory are restricted to the scattering of massless particles, an intriguing pattern of exponentiation was observed also for certain massive amplitudes [136]. There, also the subleading-power terms were found to be governed by the anomalous dimension of a certain Wilson line operator. Relatedly, the power corrections to energy-energy correlators have also revealed a surprisingly simple pattern [137].

Another restrictions of most studies of the Regge limit in $\mathcal{N} = 4$ super Yang-Mills is that of planarity. In the limit of large 't Hooft coupling, scattering amplitudes in $\mathcal{N} = 4$ super Yang-Mills enjoy a dual conformal symmetry [138], which restricts substantially their variable dependence and the transcendental functions appearing. This is very interesting and helpful, but it is natural to wonder how universal the structures found in this limit are. An answer to this question can be found only by considering non-planar amplitudes as well. The latter are important for several reasons. For phenomenology, it is unclear whether the non-planar terms are numerically negligible with respect to the planar ones, especially in QCD, where $N_c = 3$. Non-planar results are necessary also in order to understand if it is possible, and eventually how, to make use of integrability in $\mathcal{N} = 4$ super Yang-Mills [18, 139–141] beyond the planar limit. Moreover, it is in itself interesting to investigate how the Regge limit interplays with the much richer non-planar colour structures. Finally, (super)gravity theories have no notion of colour. Any attempt to understand scattering amplitudes in these theories necessarily includes also the terms which in a Yang-Mills theory would count as non planar.

Conceptual advances in understanding the Regge limit in quantum field theory [142–144] have led to predictions that were successfully compared against the explicit computation of the full-colour four-gluon amplitudes in $\mathcal{N} = 4$ super Yang-Mills theory [123] at three loops. Furthermore, there are recent efforts in understanding certain terms in the Regge limit in supergravity theories [145–149], and perturbative results for the four-graviton amplitudes are available up to three-loop order [51, 109, 115, 116].

Non-planar studies at two-loop order have been limited to the scattering of four massless particles until recently, because of the technical difficulty of computing full-colour higher-point Feynman integrals and amplitudes. As I discussed in the previous sections, for massless five-particle scattering this bottleneck has been overcome. All the required integral families have been computed [15, 16, 19–21], a number of full-colour amplitudes are now available [20, 22–24, 26, 27], and my collaborators and I computed the Regge limit of the two-loop five-particle amplitudes in $\mathcal{N} = 4$ super Yang-Mills theory and $\mathcal{N} = 8$ supergravity [26]. In the same work we have also extended to the five-particle case the ideas of Ref. [144]. This allowed us to predict the Regge limit of certain non-planar colour structures of the super Yang-Mills amplitude, which we found to be in perfect agreement with the perturbative computation. Here I content myself with discussing the latter.

I start in Sect. 4.4.1 by introducing the multi-Regge kinematics and showing how we parameterise it. Next, in Sect. 4.4.2 I discuss how we compute the asymptotic behaviour of the pure five-particle integrals, which we describe using the basis of transcendental functions given in Sect. 4.4.3. I present our results for the multi-Regge limit of the five-particle hard functions up to two loops in Sections 4.4.4 and 4.4.5, respectively. I give a summary of our conclusions in Sect. 4.4.6.

4.4.1 Multi-Regge Kinematics

The multi-Regge kinematics [128, 129] is defined as a scattering process in which the outgoing particles have strongly ordered rapidities and comparable transverse momenta. Without any loss of generality we take the particles with momenta p_1 and p_2 to be incoming, and assume that they travel along the z-axis. In order to define quantitatively the multi-Regge kinematics, we introduce the light-cone coordinates for the external momenta,

$$p_j = \left(p_j^+, p_j^-, \mathbf{p}_j\right) , \tag{4.134}$$

with

$$p_j^\pm = p_j^0 \pm p_j^3 , \qquad \mathbf{p}_j = p_j^1 + i p_j^2 . \tag{4.135}$$

The multi-Regge kinematics is then defined by

$$|p_3^+| \gg |p_4^+| \gg |p_5^+| , \qquad |p_3^-| \ll |p_4^-| \ll |p_5^-| , \qquad |\mathbf{p}_3| \simeq |\mathbf{p}_4| \simeq |\mathbf{p}_5| . \tag{4.136}$$

We can implement the constraints given by Eq. (4.136) by introducing a parameter x to regulate the size of the light-cone components as

$$\begin{aligned} &|p_1^-| \sim |p_2^+| \sim |p_3^+| \sim |p_5^-| \sim \mathcal{O}\left(\frac{1}{x}\right) , \\ &|p_4^+| \sim |p_4^-| \sim |\mathbf{p}_3| \sim |\mathbf{p}_4| \sim |\mathbf{p}_5| \sim \mathcal{O}(1) , \\ &|p_5^+| \sim |p_3^-| \sim \mathcal{O}(x) . \end{aligned} \tag{4.137}$$

The limit $x \to 0^+$ gives the multi-Regge kinematics.

Scattering amplitudes and Feynman integrals are functions of Lorentz invariants. It is therefore convenient to implement the scalings in Eq. (4.137) at the level of the Mandelstam invariants. This can be done by parameterising the latter as

$$s_{12} = \frac{s}{x^2} , \quad s_{23} = t_1 , \quad s_{34} = \frac{s_1}{x} , \quad s_{45} = \frac{s_2}{x} , \quad s_{15} = t_2 , \tag{4.138}$$

where $t_1, t_2 < 0$ and $s, s_1, s_2 > 0$ are fixed in the limit. One way to see the equivalence between Eqs. (4.138) and (4.137) is by rewriting the Mandelstam invariants in terms of light-cone components,

$$\begin{aligned} s_{12} &= p_1^- p_2^+ = p_3^+ p_5^- \equiv \frac{s}{x^2}\,, \\ s_{23} &= -|\mathbf{p}_3|^2 \equiv t_1\,, \\ s_{15} &= -|\mathbf{p}_5|^2 \equiv t_2\,, \\ s_{34} &= p_3^+ p_4^- \equiv \frac{s_1}{x}\,, \\ s_{45} &= p_4^+ p_5^- \equiv \frac{s_2}{x}\,. \end{aligned} \tag{4.139}$$

In order to express the transverse momenta, we introduce the complex variables z and $\bar{z}$, defined by

$$z\bar{z} = -\frac{t_1 s}{s_1 s_2}\,, \qquad (1-z)(1-\bar{z}) = -\frac{t_2 s}{s_1 s_2}\,. \tag{4.140}$$

The transverse momenta then are given by

$$|\mathbf{p}_3| = z\sqrt{\frac{s_1 s_2}{s}}\,, \quad |\bar{\mathbf{p}}_3| = \bar{z}\sqrt{\frac{s_1 s_2}{s}}\,, \quad |\mathbf{p}_5| = (1-z)\sqrt{\frac{s_1 s_2}{s}}\,, \quad |\bar{\mathbf{p}}_5| = (1-\bar{z})\sqrt{\frac{s_1 s_2}{s}}\,, \tag{4.141}$$

and $\mathbf{p}_1 = \mathbf{p}_2 = 0$. In the s_{12} physical scattering region, z and $\bar{z}$ are complex-conjugate to each other. I give a pictorial representation of the multi-Regge kinematics in Fig. 4.4.

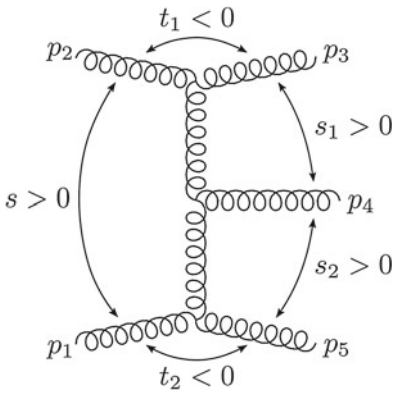

Fig. 4.4 Pictorial representation of the multi-Regge kinematics in the s_{12} channel

4.4.2 Multi-Regge Limit of the Pentagon Functions

The starting point of the computation of the multi-Regge limit are the expressions of the amplitudes in terms of rational factors and pure integrals. They have the form given by Eqs. (4.76) and (4.87) for the super Yang-Mills and for the supergravity amplitude, respectively. The asymptotic expansion in the multi-Regge limit of the rational factors is trivial. The pure integrals are a subset of the ensemble of the canonical bases of all the permutations of the three integral families shown in Fig. 4.1. In order to work out their asymptotic expansion, we apply the procedure discussed in Sect. 3.5 to each canonical basis.

We parameterise the kinematics according to Eq. (4.138). We denote cumulatively by

$$y = (s, s_1, s_2, z, \bar{z}) \tag{4.142}$$

the set of kinematic variables which stay fixed in the limit. Let $\vec{g}$ be the canonical basis of one of the two-loop five-particle integral families with a given orientation of the external legs. It satisfies a system of differential equations in the canonical form,

$$d\vec{g}(x, y, \epsilon) = \epsilon d\tilde{A}(x, y)\vec{g}(x, y, \epsilon)\,. \tag{4.143}$$

The matrix of 1-forms $d\tilde{A}$ has the form given by Eq. (4.30). The alphabet is presented in Sect. 4.2.2.

From the differential equations (4.143), following Sect. 3.5, we can systematically derive an asymptotic expansion in the multi-Regge limit $x \to 0$ of the form

$$\vec{g}(x, y, \epsilon) = T(x, y, \epsilon)\, x^{\epsilon A_0}\, \mathbb{P}\exp\left[\epsilon \int_\gamma d\tilde{B}\right] \vec{h}_0(\epsilon)\,. \tag{4.144}$$

Let us us break this down piece by piece. The matrix T is a transformation matrix defined by

$$T^{-1}\left(\epsilon \frac{\partial \tilde{A}}{\partial x} T - \frac{\partial T}{\partial x}\right) = \epsilon \frac{A_0}{x}\,, \tag{4.145}$$

where A_0 is a matrix of constant rational numbers, defined as the residue of $\partial\tilde{A}/\partial x$ at $x = 0$,

$$\frac{\partial}{\partial x}\tilde{A}(x, y) = \frac{A_0}{x} + \sum_{k\geq 0} x^k A_{k+1}(y)\,. \tag{4.146}$$

The matrix $\tilde{A}$ is guaranteed to have such a form because Feynman integrals can only have regular singularities (see Sect. 3.2). The transformation matrix T admits the expansion

$$T(x, y, \epsilon) = \mathbb{1} + \sum_{k\geq 1} \sum_{m\geq 1} x^k \epsilon^m T_{k,m}(y)\,, \tag{4.147}$$

from which it is clear that it is responsible for the power corrections in x. If one is interested only in the leading behaviour of the integrals, she can simply let $T = \mathbb{1}$. The asymptotic expression given by Eq. (4.144) then contains divergent logarithms of x, produced by the matrix exponential $x^{\epsilon A_0}$ and governed by the matrix A_0. The path-ordered exponential produces the polylogarithmic functions. The contour γ goes from a base point y_0 in the multi-Regge kinematics to a generic point y. We choose

$$y_0 = \left(s = 1\,, s_1 = 1\,, s_2 = 1\,, z = e^{\frac{i\pi}{3}}\,, \bar{z} = e^{-\frac{i\pi}{3}}\right), \tag{4.148}$$

which corresponds to $t_1 = t_2 = -1$. The matrix $\tilde{B}$ is obtained from the original $\tilde{A}$ through

$$\left.\frac{\partial \tilde{A}}{\partial y_i}\right|_{x=0} = \frac{\partial \tilde{B}}{\partial y_i}\,, \qquad \forall y_i \in y\,. \tag{4.149}$$

Finally, $\vec{h}_0(\epsilon)$ denotes the boundary values at y_0 for the auxiliary system of differential equations

$$d\vec{h}(y, \epsilon) = \epsilon \tilde{B}(y)\vec{h}(y, \epsilon)\,. \tag{4.150}$$

The letters appearing in the matrix $\tilde{B}$ are obtained from the original pentagon alphabet by expanding it in x and keeping only the leading terms in the limit.

The alphabet in the limit is substantially simpler. First of all, it is rational, because the Gram determinant is given by a perfect square at the leading order,

$$\Delta \underset{x\to 0}{\sim} \frac{s_1^2 s_2^2 (z-\bar{z})^2}{x^4} + \mathcal{O}\left(\frac{1}{x^3}\right). \tag{4.151}$$

We choose the branch of the square root as

$$\mathrm{tr}_5 \underset{x\to 0}{\sim} \frac{s_1 s_2 (z-\bar{z})}{x^2} + \mathcal{O}\left(\frac{1}{x}\right). \tag{4.152}$$

Since z and $\bar{z}$ are complex conjugate to each other in the physical scattering region, tr_5 is purely imaginary. This guarantees that $\Delta < 0$, i.e. that the momenta are real. On top of becoming rational, the pentagon alphabet in the multi-Regge limit reduces to just 12 letters, factorised into four independent sub-alphabets:

$$\begin{aligned}
&\{x\}\,,\\
&\left\{\frac{s_1 s_2}{s}\right\}\,,\\
&\{s_1, s_2, s_1 - s_2, s_1 + s_2\}\,,\\
&\{z, \bar{z}, 1-z, 1-\bar{z}, z-\bar{z}, 1-z-\bar{z}\}\,.
\end{aligned} \tag{4.153}$$

The function space of massless two-loop five-particle amplitudes therefore becomes remarkably simple in the multi-Regge limit. The alphabets in the first two lines simply correspond to logarithms, while the third and the fourth lines encode the harmonic polylogarithms [150] and the two-dimensional harmonic polylogarithms [151], respectively. I stress that the logarithms of x are produced exclusively by the matrix exponential in Eq. (4.144), whereas the remaining 11 letters appear through the path-ordered exponential. A functional basis to express the latter is presented in Sect. 4.4.3.

We compute the boundary values $\vec{h}_0(\epsilon)$ in Eq. (4.144) by integrating the canonical differential equation along a path going from the base point s_0 (4.43) in the bulk of the s_{12} channel, where the values of the integrals are already known, to a tangential end-point in the multi-Regge limit, $(x = 0, y = y_0)$. The power corrections in x are not relevant for this purpose, and the transformation matrix T can thus be ignored. At the end-point the integrals develop logarithmic divergences. Since the end-point is defined in a tangential sense (see Sect. 3.3.1), it is important to make sure that the divergent logarithms which are formally set to zero match those produced by the matrix exponential $x^{\epsilon A_0}$ in Eq. (4.144). After the divergent logarithms are moved, what is left are the boundary values $\vec{h}_0(\epsilon)$ at y_0. This procedure has to be repeated for all the permutations of the relevant integral families. Thanks to the simple functional dependence in the multi-Regge limit, implied by the alphabet shown in Eq. (4.153), the transcendental constants appearing in the values of the integrals at y_0 can be anticipated to be harmonic polylogarithms of argument 1, and two-dimensional harmonic polylogarithms of arguments z and $\bar{z}$ as given by Eq. (4.148). It is therefore relatively simple to fit to analytic transcendental numbers the numerical values obtained by integrating the differential equation in terms of GPLs and evaluating the latter at very high precision with GiNaC [152]. For this purpose we use MATHEMATICA's built-in function FINDINTEGERNULLVECTOR. I present in Table 4.2 a basis of independent transcendental constants which spans the values of all the integrals at y_0 up to weight 4. We could achieve an even greater simplification in the constants by going to $z = \bar{z} = 0$ (or equivalently $t_1 = t_2 = 0$), but we find y_0 more convenient as it is less singular.

Before moving on to presenting the basis of polylogarithmic functions required for the asymptotic expansion of the integrals, I should warn the readers about a treacherous subtlety, related to the non-trivial analytic behaviour at the hypersurface $\mathrm{tr}_5 = 0$ discussed in Sect. 4.2.4. The multi-Regge base point y_0 (4.148) is in the upper half of the complex z plane, namely $\mathrm{Im}[z] > 0$. The physical scattering region in the multi-Regge kinematics is defined by

Table 4.2 Basis of transcendental constants appearing in the values of the pentagon integrals at the base point in the multi-Regge kinematics y_0 (4.148)

Weight	Real	Imaginary
1	0	$i\pi$
2	π^2	$i\,\mathrm{Im}\,\mathrm{Li}_2(e^{\frac{i\pi}{3}})$
3	$\zeta_3,\ \pi\,\mathrm{Im}\,\mathrm{Li}_2(e^{\frac{i\pi}{3}}),\ \pi^2\log(3)$	$i\pi^3,\ i\pi\log^2(3) - 48i\,\mathrm{Im}\,\mathrm{Li}_3\left(\frac{i}{\sqrt{3}}\right)$
4	$\pi^4,\ \left(\mathrm{Im}\,\mathrm{Li}_2(e^{\frac{i\pi}{3}})\right)^2,$ $\pi^2\log^2(3),\ \pi\,\mathrm{Im}\,\mathrm{Li}_3\left(\frac{i}{\sqrt{3}}\right)$	$i\pi\zeta_3,\ i\pi^2\,\mathrm{Im}\,\mathrm{Li}_2(e^{\frac{i\pi}{3}}),\ i\,\mathrm{Im}\,\mathrm{Li}_4(e^{\frac{i\pi}{3}}),\ i\pi^3\log(3),$ $i\pi\log^3(3) + 288i\,\mathrm{Im}\,\mathrm{Li}_4\left(\frac{i}{\sqrt{3}}\right)$

$$s > 0\,, \qquad s_1 > 0\,, \qquad s_2 > 0\,. \tag{4.154}$$

The transverse variables z and $\bar{z}$ are complex conjugate to each other, and span the whole complex plane. However, it is highly non-trivial to analytically continue from the upper half of the complex plane, where the base point y_0 lies, to the lower half. In Sect. 4.2.4, in fact, we have seen that certain non-planar integrals contributing to the amplitudes have discontinuities across the hypersurface $\mathrm{tr}_5 = 0$. The latter corresponds to $z = \bar{z}$, or equivalently $\mathrm{Im}[z] = 0$, in the multi-Regge kinematics.

We prefer to avoid this perilous analytic continuation, and follow a less error-prone strategy. We work in the two halves of the complex z plane separately. In both we choose the branch of the square root for tr_5 as in Eq. (4.152). We integrate the canonical differential equations for the pure integrals from y_0 and obtain expressions valid for $\mathrm{Im}[z] > 0$. We then take the conjugate of y_0 as base point in the lower half of the complex plane,

$$\bar{y}_0 = \left(s = 1\,, s_1 = 1\,, s_2 = 1\,, z = e^{-\frac{i\pi}{3}}\,, \bar{z} = e^{\frac{i\pi}{3}}\right). \tag{4.155}$$

Since we have chosen the pure basis integrals in such a way that they have definite parity, the boundary values at $\bar{y}_0$ can be obtained by those at y_0 by flipping the sign of the odd integrals. Integrating the differential equations starting from $\bar{y}_0$ then gives expressions of the amplitudes valid for $\mathrm{Im}[z] < 0$.

An equivalent approach to construct representations of the amplitudes valid in the lower half of the complex plane consists in keeping $\mathrm{Im}[z] > 0$ and choosing the opposite branch of tr_5 with respect to Eq. (4.152). This affects the boundary values at y_0 by flipping both the sign of the odd integrals and of the odd letters. We followed both approaches and found agreement between the two.

4.4.3 Basis of Transcendental Functions in the Multi-Regge Limit

In this section I present a basis of the transcendental functions appearing in the multi-Regge limit of the five-particle hard functions in $\mathcal{N} = 4$ super Yang-Mills theory and $\mathcal{N} = 8$ supergravity up to two loops. I recall that we neglect all terms which vanish in the limit. The functions have transcendental weight up to four. The basis functions at weight three and, in particular, at weight four are rather bulky, and do not add anything conceptually to the presentation. For this reason, I prefer to discuss here the basis only up to weight two. The remaining functions can be found explicitly in our paper [26].

The transcendental functions in the multi-Regge limit have two sources, manifest in Eq. (4.144). The matrix exponential $x^{\epsilon A_0}$ produces logarithms of x up to power four, which correspond to the alphabet in the first line of Eq. (4.153). The path-ordered exponential, on the other hand, produces non-trivial transcendental functions of s, s_1, s_2, z and $\bar{z}$. They belong to the sub-alphabets given by the other three lines of Eq. (4.153). From the latter we can anticipate the loci of all singularities. Some are physical,

$$z = 0\,, \qquad z = 1\,, \qquad s_1 = 0\,, \qquad s_2 = 0\,, \qquad s = 0\,. \tag{4.156}$$

Others are spurious,

$$z + \bar{z} = 1\,, \qquad z = \bar{z}\,, \qquad s_1 = s_2\,. \tag{4.157}$$

The latter manifest themselves in the representation of the basis functions, but drop out in the hard functions. We construct a basis of functions that are well defined and real analytic in both the upper and the lower half of the complex z plane. Some of the functions are however discontinuous across the real z axis, corresponding to the dangerous hypersurface where $\mathrm{tr}_5 = 0$.

The presentation is organised by transcendental weight. Starting from transcendental weight two, the supergravity hard function appears to be richer in the multi-Regge limit than its super Yang-Mills counterpart. It involves more independent functions, including several genuine weight-four functions. The weight-four part of the super Yang-Mills hard function in the Regge limit, instead, is reducible. In other words, it can be expressed in terms of products of lower weight functions.

Weight 1. The hard functions in both $\mathcal{N} = 4$ super Yang-Mills theory and $\mathcal{N} = 8$ supergravity contain five manifestly single-valued logarithms,

$$
\begin{aligned}
g_1^{(1)} &= \log(s_1)\,, \\
g_2^{(1)} &= \log(s_2)\,, \\
g_3^{(1)} &= \log\left(\frac{s}{s_1 s_2}\right)\,, \\
g_4^{(1)} &= \log(z\bar{z})\,, \\
g_5^{(1)} &= \log((1-z)(1-\bar{z}))\,,
\end{aligned}
\tag{4.158}
$$

and two more logarithms whose analytic structure requires some attention,

$$
\begin{aligned}
g_6^{(1)} &= \log(z) - \log(\bar{z})\,, \\
g_7^{(1)} &= \log(1-z) - \log(1-\bar{z})\,.
\end{aligned}
\tag{4.159}
$$

We can express $g_6^{(1)}$ and $g_7^{(1)}$ in a way that is manifestly well defined in both halves of the complex plane. For $g_6^{(1)}$, we parametrise z using polar coordinates as $z = re^{i\varphi}$, with $\varphi \in [0, \pi]$ for $\mathrm{Im}[z] > 0$, and as $z = re^{-i\varphi}$ with $\varphi \in [0, \pi]$ for $\mathrm{Im}[z] < 0$. Then $g_6^{(1)}$ is given by

$$
g_6^{(1)} = \begin{cases} 2i\varphi\,, & \text{for } \mathrm{Im}[z] > 0\,, \\ -2i\varphi\,, & \text{for } \mathrm{Im}[z] < 0\,. \end{cases}
\tag{4.160}
$$

Similarly, for $g_7^{(1)}$ we parametrise z as $z = 1 + re^{i\varphi}$ for $\mathrm{Im}[z] > 0$, and as $z = 1 + re^{-i\varphi}$ for $\mathrm{Im}[z] < 0$. In both cases, $\varphi \in [0, \pi]$. Then $g_7^{(1)}$ becomes

$$
g_7^{(1)} = \begin{cases} -2i\pi + 2i\varphi\,, & \text{for } \mathrm{Im}[z] > 0\,, \\ 2i\pi + 2i\varphi\,, & \text{for } \mathrm{Im}[z] < 0\,. \end{cases}
\tag{4.161}
$$

It is thus clear that $g_6^{(1)}$ and $g_7^{(1)}$ are well defined in the entire complex z plane except for the real axis, across which they have a discontinuity for $\mathrm{Re}[z] < 0$ and for $\mathrm{Re}[z] > 1$, respectively.

Weight 2. The $\mathcal{N} = 4$ super Yang-Mills amplitude depends on just two weight-two irreducible functions:

$$
g_1^{(2)} = \mathrm{Li}_2(z) - \mathrm{Li}_2(\bar{z}) + \frac{1}{2}\left(\log(1-z) - \log(1-\bar{z})\right)\log(z\bar{z})\,,
\tag{4.162}
$$

$$
g_2^{(2)} = \mathrm{Li}_2(z) + \mathrm{Li}_2(\bar{z})\,.
\tag{4.163}
$$

We have already encountered the first one several times. It is the Bloch-Wigner dilogarithm defined by Eq. (3.83). Therefore, $g_1^{(2)}$ is manifestly single-valued in the entire punctured complex plane $z \in \mathcal{C}\backslash\{0, 1\}$. As for $g_2^{(2)}$, it is continuous, but not real analytic along the real axis $\mathrm{Im}[z] = 0$ for $\mathrm{Re}[z] > 1$.

Two more weight-two functions need to be introduced in order the describe the multi-Regge asymptotics of the $\mathcal{N} = 8$ supergravity hard function:

$$\begin{aligned} g_3^{(2)} &= \mathrm{Li}_2\left(\frac{z}{1-\bar{z}}\right) + \mathrm{Li}_2\left(\frac{\bar{z}}{1-z}\right) + g_3'^{(2)}\,, \\ g_4^{(2)} &= D_2\left(\frac{z}{1-\bar{z}}\right) + g_4'^{(2)}\,, \end{aligned} \tag{4.164}$$

where D_2 denotes the Bloch-Wigner dilogarithm defined by Eq. (3.83), and $g_3'^{(3)}$ and $g_4'^{(2)}$ are corrections to make the functions real-analytic away from the real axis. The correction terms involve only logarithms and step functions. In order to express them, it is convenient to introduce the short-hand notations

$$\ell = \Theta(1-z-\bar{z})\,\log(1-z-\bar{z}) + \Theta(z+\bar{z}-1)\,\log(z+\bar{z}-1) \equiv \log(|1-z-\bar{z}|)\,, \tag{4.165}$$

and

$$\theta = \mathrm{sign}\,(\mathrm{Im}[z])\,\Theta\left(\mathrm{Re}[z] - \frac{1}{2}\right)\,. \tag{4.166}$$

Then,

$$\begin{aligned} g_3'^{(2)} &= \left(g_4^{(1)} - g_5^{(1)}\right)\ell + i\pi\left(g_6^{(1)} + g_7^{(1)}\right)\theta\,, \\ g_4'^{(2)} &= \left(g_6^{(1)} + g_7^{(1)}\right)\ell\,. \end{aligned} \tag{4.167}$$

The function $g_3^{(2)}$ is real valued. The arguments of the dilogarithms cross the real axis as z varies in either the lower or the upper half of the complex plane. Away from the real axis, i.e. for $\mathrm{Im}[z] \neq 0$, the arguments become real only on the line $\mathrm{Re}[z] = 1/2$, where the letter $1 + z + \bar{z}$ of the alphabet vanishes. There, however, the arguments of the dilogarithms in $g_3^{(2)}$ evaluate to 1. As a result, the branch cut of the dilogarithm is never crossed as z ranges in the upper or the lower half of the complex plane. Equation (4.164) thus defines an unambiguous function away from the real axis. The function $g_4^{(2)}$ is manifestly single valued everywhere in the complex plane. The Bloch-Wigner dilogarithm contains logarithms which are singular at $1 + z + \bar{z} = 0$, but the correction term $g_4'^{(2)}$ is constructed so as to cancel them. It is interesting to note that the two additional weight-two functions required in $\mathcal{N} = 8$ supergravity are actually derivatives of certain weight-three functions present in the $\mathcal{N} = 4$ super Yang-Mills hard function.

4.4.4 *Multi-Regge Limit of the $\mathcal{N} = 4$ Super Yang-Mills Amplitude*

In this section I present the asymptotic expansion in the multi-Regge limit of the five-particle hard function in $\mathcal{N} = 4$ super Yang-Mills theory up to two-loop order. We compute explicit analytic expressions for all the divergent and finite contributions of the full-colour hard function, neglecting terms which vanish as $x \log^k(x)$ in the limit $x \to 0$.

The planar part has already been investigated in Ref. [132], where the ABDK/BDS formula [69, 124, 127] was shown to be Regge-exact at five points. My collaborators and I extended the analysis to the full-colour amplitude first at symbol level [22]. There, the double-trace colour structures given by Eq. (4.66) were found to vanish in the limit $x \to 0$, and the leading-logarithmic part of the subleading-power terms was provided analytically. Later we lifted the computation to function level [26].

The starting point of our computation are the expressions of the amplitudes in terms of rational factors of the spinor-helicity variables, and of pure pentagon integrals. They have the form given by Eq. (4.76) for the two-loop amplitude, and similarly for the one-loop one. I have discussed how to work out the asymptotic expansion of the pure integrals in the previous two sections. It is now time to talk about the rational factors. They have an extremely simple behaviour in the limit. In order to see it, we have to normalise the rational factors, because we defined the multi-Regge limit for helicity-free quantities only. We choose to normalise them by the Parke-Taylor factor PT_1, defined in Eq. (4.75), which also gives the tree-level amplitude. Then, all but two of the six rational factors vanish, with the remaining ones becoming 1 (up to power corrections):

$$\frac{\mathrm{PT}_i}{\mathrm{PT}_1} = r_i + \mathcal{O}(x)\,, \tag{4.168}$$

with

$$\{r_i\}_{i=1}^{6} = \{1, 0, 0, 0, 0, 1\}. \tag{4.169}$$

It is particularly important that the rational factors do not exhibit any pole in x. As a result, we can neglect the power corrections to the pure integrals, produced by the transformation matrix T in Eq. (4.144). This also implies that the expressions for the Regge asymptotics of the hard function do not contain any rational function, and that the uniform transcendental weight is preserved. This constitutes a major simplification in both the computation and the presentation of the results. In contrast, they are relevant in the $\mathcal{N} = 8$ supergravity case. Putting together Eq. (4.168) for the rational factors and computing the asymptotics of the pure pentagon integrals according to Eq. (4.144) gives the asymptotic expansion of the amplitudes. Finally, we assemble them in the hard function according to Eqs. (4.104) and (4.105).

In order to present our results in a more meaningful way, it is convenient to first introduce a colour decomposition based on the colour flowing in the t channels. This emphasises certain properties of the Regge regime, and yields more compact expressions. Then I discuss the asymptotic expansion of the one and two-loop hard function. All the explicit expressions can be found in ancillary files of our paper [26].

Colour flow in the multi-Regge limit

We treat the super Yang-Mills amplitude as a vector in colour space. In Sect. 4.3.1 I have defined a basis of this vector space made of certain traces of generators of $SU(N_c)$ in the fundamental representation. This choice of basis is convenient because it highlights the distinction between planar and non-planar components, as well as the permutation symmetries. A different colour basis is more meaningful when discussing the Regge limit. We decompose the ℓ-loop five-particle amplitude $A_5^{(\ell)}$ into a colour basis $\{\mathcal{S}_J\}$ where each element corresponds to a definite exchange in the t-channels,

$$A_5^{(\ell)} = \sum_J A_J^{(\ell)} \mathcal{S}_J \,. \tag{4.170}$$

Here, the sum runs over all possible pairs $J = (r_1, r_2)$, where r_1 (r_2) denotes an irreducible representation of the state propagating in the t_1 (t_2) channel. These representations are obtained by reducing the tensor products of the representations corresponding to the particles 2 and 3, and 1 and 5,

$$R_2 \otimes R_3 = \bigoplus_{r_1} r_1 \,, \qquad\qquad R_1 \otimes R_5 = \bigoplus_{r_2} r_2 \,, \tag{4.171}$$

where R_i labels the irreducible representation of the ith particle. Multiple occurrences of equivalent representations are counted as distinct. In the case of two adjoint representations, the decomposition is given by

$$\mathbf{8}_a \otimes \mathbf{8}_a = \mathbf{1} \oplus \mathbf{8}_s \oplus \mathbf{8}_a \oplus \mathbf{10} \oplus \overline{\mathbf{10}} \oplus \mathbf{27} \oplus \mathbf{0} \,, \tag{4.172}$$

where the subscripts a and s are used to distinguish the anti-symmetric adjoint representation $\mathbf{8}_a$ from the 8-dimensional symmetric representation $\mathbf{8}_s$. We label the representations of $SU(N_c)$ with their $SU(3)$ dimensions, but all the expressions are valid for generic N_c. We thus keep also the "null" representation $\mathbf{0}$, which does not contribute for $N_c = 3$ since its dimension vanishes,

$$\dim[\mathbf{0}] = \frac{N_c^2 (N_c - 3)(N_c + 1)}{4} \,. \tag{4.173}$$

In order to understand better the decomposition into t-channel colour structures given by Eq. (4.170), we introduce colour operators associated with the colour flowing in the t-channels [153, 154],

$$\mathbf{T}_{t_1} = \mathbf{T}_2 + \mathbf{T}_3\,, \tag{4.174}$$
$$\mathbf{T}_{t_2} = \mathbf{T}_2 + \mathbf{T}_3 + \mathbf{T}_4 = -\mathbf{T}_1 - \mathbf{T}_5\,, \tag{4.175}$$

where we used colour conservation, i.e. $\sum_{i=1}^{5} \mathbf{T}_i = 0$, and $\mathbf{T}_i$ denotes the colour insertion operator introduced in Sect. 4.3.4 and defined by Eq. (4.98) for the adjoint representation. Clearly, the Casimir operators $\mathbf{T}^2_{t_1}$ and $\mathbf{T}^2_{t_2}$ commute,

$$\left[\mathbf{T}^2_{t_1}, \mathbf{T}^2_{t_2}\right] = 0, \tag{4.176}$$

and can thus be diagonalised simultaneously. The colour structures $\mathcal{S}_J$ are by definition their simultaneous eigenvectors:

$$\mathbf{T}^2_{t_k} \circ \mathcal{S}_J = C_{r_k} \mathcal{S}_J\,, \tag{4.177}$$

for $k = 1, 2$. I recall that $J = (r_1, r_2)$, where r_k is the representation of the state propagating in the t_k channel.

We then expand the hard function as

$$\mathcal{H}_5^{(\ell)} = \mathrm{PT}_1 \sum_{a=1}^{22} H_a^{(\ell)} \mathcal{S}_a\,, \tag{4.178}$$

where the factor of PT_1 is extracted so that the coefficient functions $H_a^{(\ell)}$ are helicity-free. Table 4.3 shows our explicit choice for the eigenvectors of the t-channel operators, $\{\mathcal{S}_a\}_{a=1}^{22}$.

This choice of basis greatly simplifies the analysis of the Regge limit, since it is controlled by the quantum numbers propagating in the t_i channels. For example, $(\mathbf{8}_a, \mathbf{8}_a)$ is the only non-vanishing colour structure at tree level,

$$\begin{aligned} h_3^{(0)} &= 1\,, \\ h_a^{(0)} &= 0\,, \quad \forall a \neq 3\,, \end{aligned} \tag{4.179}$$

and the only structure at leading-logarithmic order (LL) to all loop orders.

For convenience of the readers, I write here in terms of the trace-based basis defined by Eqs. (4.65) and (4.66) the eigenvectors of the t-channel operators which are of particular interest for this presentation:

Table 4.3 Characterisation of the colour basis $\{\mathcal{S}_a\}_{a=1}^{22}$. The first column refers to the element in the basis. The second shows the pairs (r_1, r_2), where r_i is the irreducible representation corresponding to the state flowing in the t_i-channel, labelled by its $SU(3)$ dimensions (with **1** being the singlet). The last two columns contain the associated Casimirs. The **10** stand for certain combinations of **10** and $\overline{\mathbf{10}}$. The last two structures denote two invariant tensors between **10**, $\overline{\mathbf{10}}$ and the central gluon's **8** (for $N_c \geq 4$)

$\mathcal{S}_a$	(r_1, r_2)	C_{r_1}	C_{r_2}
1	$(\mathbf{1}, \mathbf{8}_a)$	0	$2N_c$
2	$(\mathbf{8}_a, \mathbf{1})$	N_c	0
3	$(\mathbf{8}_a, \mathbf{8}_a)$	N_c	N_c
4	$(\mathbf{8}_a, \mathbf{8}_s)$	N_c	N_c
5	$(\mathbf{8}_a, \mathbf{0})$	N_c	$2(N_c-1)$
6	$(\mathbf{8}_a, \mathbf{27})$	N_c	$2(N_c+1)$
7	$(\mathbf{8}_a, \mathbf{10})$	N_c	$2N_c$
8	$(\mathbf{8}_s, \mathbf{8}_a)$	N_c	N_c
9	$(\mathbf{8}_s, \mathbf{8}_s)$	N_c	N_c
10	$(\mathbf{8}_s, \mathbf{10})$	N_c	$2N_c$
11	$(\mathbf{0}, \mathbf{8}_a)$	$2(N_c-1)$	N_c

$\mathcal{S}_a$	(r_1, r_2)	C_{r_1}	C_{r_2}
12	$(\mathbf{0}, \mathbf{0})$	$2(N_c-1)$	$2(N_c-1)$
13	$(\mathbf{0}, \mathbf{10})$	$2(N_c-1)$	$2N_c$
14	$(\mathbf{27}, \mathbf{8}_a)$	$2(N_c+1)$	N_c
15	$(\mathbf{27}, \mathbf{27})$	$2(N_c+1)$	$2(N_c+1)$
16	$(\mathbf{27}, \mathbf{10})$	$2(N_c+1)$	$2N_c$
17	$(\mathbf{10}, \mathbf{8}_a)$	$2N_c$	N_c
18	$(\mathbf{10}, \mathbf{8}_s)$	$2N_c$	N_c
19	$(\mathbf{10}, \mathbf{0})$	$2N_c$	$2(N_c-1)$
20	$(\mathbf{10}, \mathbf{27})$	$2N_c$	$2(N_c+1)$
21	$(\mathbf{10}, \mathbf{10})_1$	$2N_c$	$2N_c$
22	$(\mathbf{10}, \mathbf{10})_2$	$2N_c$	$2N_c$

$$\mathcal{S}_3 = \mathcal{T}_1 + \mathcal{T}_2 - \mathcal{T}_5 - \mathcal{T}_6\,, \tag{4.180}$$

$$\mathcal{S}_9 = \mathcal{T}_1 - \mathcal{T}_2 - \mathcal{T}_5 + \mathcal{T}_6\,, \tag{4.181}$$

$$\mathcal{S}_{12} = \mathcal{T}_1 - \mathcal{T}_2 - \mathcal{T}_5 + \mathcal{T}_6 - (N_c-2)\,(\mathcal{T}_7 - \mathcal{T}_9 - \mathcal{T}_{10} + \mathcal{T}_{12} + \mathcal{T}_{13} + \mathcal{T}_{18} + \mathcal{T}_{20} + \mathcal{T}_{22})\,, \tag{4.182}$$

$$\mathcal{S}_{15} = \mathcal{T}_1 - \mathcal{T}_2 - \mathcal{T}_5 + \mathcal{T}_6 + (N_c+2)\,(\mathcal{T}_7 - \mathcal{T}_9 - \mathcal{T}_{10} + \mathcal{T}_{12} - \mathcal{T}_{13} - \mathcal{T}_{18} - \mathcal{T}_{20} - \mathcal{T}_{22})\,, \tag{4.183}$$

$$\mathcal{S}_{21} = \frac{N_c}{2}\,(\mathcal{T}_9 - \mathcal{T}_7 + \mathcal{T}_{12} - \mathcal{T}_{10}) - \mathcal{T}_{13} + \mathcal{T}_{15} + \mathcal{T}_{16} + \mathcal{T}_{18} - \mathcal{T}_{19} - \mathcal{T}_{20} - \mathcal{T}_{21} + \mathcal{T}_{22}\,, \tag{4.184}$$

$$\mathcal{S}_{22} = \mathcal{T}_1 + \mathcal{T}_2 - \mathcal{T}_5 - \mathcal{T}_6 + N_c\,(\mathcal{T}_{18} - \mathcal{T}_{13} + \mathcal{T}_{22} - \mathcal{T}_{20})\,. \tag{4.185}$$

The transformation matrix E relating the two colour bases as

$$\mathcal{S}_a = \sum_{b=1}^{22} E_{ab}\mathcal{T}_b \tag{4.186}$$

is provided in an ancillary file of Ref. [26].

One-loop hard function

Thanks to the simple behaviour of the rational factors, the uniform transcendental weight property of the hard function is preserved in the multi-Regge limit. The one-loop hard function is therefore simply given by a weight-two function. We organise

it in powers of $\log(x)$,

$$H_a^{(1)} = \sum_{k=0}^{1} h_{a,k}^{(1)}\left(N_c, s, s_1, s_2, z, \bar{z}\right) \log^k(x) + o(1)\,, \tag{4.187}$$

where the coefficient $h_{a,k}^{(1)}$ has transcendental weight $(2-k)$. Although the hard function has weight 2, it exhibits only a single power of $\log x$. In fact, this observation generalises: there is at most one power of $\log x$ per loop order. This is a well-known result of the BFKL formalism [128, 155] (see e.g. Ref. [144] for a recent discussion in the scattering amplitudes context), related to the fact that boosting a projectile does not introduce new collinear singularities.

There is only one non-vanishing component at order $\log x$,

$$\begin{aligned} h_{3,1}^{(1)} &= -2N_c\left[2\log\left(\frac{s}{s_1 s_2}\right) - \log\left((1-z)(1-\bar{z})\right) - \log\left(z\bar{z}\right)\right], \\ h_{a,1}^{(1)} &= 0\,, \quad \forall a \neq 3\,. \end{aligned} \tag{4.188}$$

The non-trivial colour structure corresponds to the pair of t-channel representations $(\mathbf{8}_a, \mathbf{8}_a)$. This is also well known. The leading logarithmic (LL) terms, of order $(g^2)^\ell \log^\ell x$ at ℓ loops, have the same colour structure as the tree-level amplitude. The underlying reason is that only a single elementary excitation (the reggeised gluon) propagates in each channel at LL order. The other colour structures are suppressed kinematically: either they have a lower power of $\log x$, or they are suppressed by powers of x [128, 155]. There are similar selection rules also at Next-to-LL (NLL) order, where a (symmetrical) pair of adjoint excitations can be exchanged as well. Since such a pair cannot carry the colour representation **10**, many components vanish at order $\log^0 x$ too. We find

$$h_{a,0}^{(1)} = 0\,, \quad \forall a \in \{7, 10, 13, 16, 17, 18, 19, 20, 21, 22\}\,. \tag{4.189}$$

The non-vanishing components are expressed in terms of the function basis presented in Sect. 4.4.3. In particular, only functions which are single-valued in the whole s_{12} scattering region appear at one loop. The explicit expressions are provided in ancillary files of Ref. [26].

Two-loop hard function

At two loops the hard function is given by a weight-4 function. We expand it in powers of $\log x$ as

$$H_a^{(2)} = \sum_{k=0}^{2} h_{a,k}^{(2)}\left(N_c, s, s_1, s_2, z, \bar{z}\right) \log^k(x) + o(1)\,, \tag{4.190}$$

where the coefficient $h_{a,k}^{(2)}$ has transcendental weight $4-k$. Two colour components are particularly simple, and we can spell them out. They are the eigenvectors corresponding to the representation (**10**, **10**). One vanishes,

$$H_{21}^{(2)} = \mathcal{O}(x)\,. \tag{4.191}$$

Interestingly, this follows from the behaviour of the rational factors alone, given by Eq. (4.168). The transcendental functions are irrelevant here. The second eigenvector of (**10**, **10**) is finite in the limit $x \to 0$,

$$\begin{aligned} H_{22}^{(2)} = 2\pi^2\Bigg[&\log^2\left(\frac{s}{s_1 s_2}\right) - 2\log\left(\frac{s}{s_1 s_2}\right)\log\left(z\bar{z}(1-z)(1-\bar{z})\right) + \log^2(z\bar{z}) \\ &+ \log^2\left((1-z)(1-\bar{z})\right) + \log\left((1-z)(1-\bar{z})\right)\log(z\bar{z}) \\ &- 2\left(\mathrm{Li}_2(z) - \mathrm{Li}_2(\bar{z}) - \frac{1}{2}\left(\log(1-z) - \log(1-\bar{z})\right)\log(z\bar{z})\right)\Bigg] + \mathcal{O}(x)\,. \end{aligned} \tag{4.192}$$

This function is manifestly single valued in the entire s_{12} physical scattering region. In particular, we recognise the Bloch-Wigner dilogarithm in the third line.

Let us now discuss the separate orders in $\log x$. As anticipated at weight one, only the colour structure associated with ($\mathbf{8}_a$, $\mathbf{8}_a$) contains the leading logarithm $\log^2 x$,

$$\begin{aligned} h_{3,2}^{(2)} &= 2N_c^2\left(2\log\left(\frac{s}{s_1 s_2}\right) - \log\left(z\bar{z}\right) - \log\left((1-z)(1-\bar{z})\right)\right)^2\,, \\ h_{a,2}^{(2)} &= 0\,, \quad \forall a \neq 3\,. \end{aligned} \tag{4.193}$$

Many components vanish at order $\log x$ too,

$$h_{a,1}^{(2)} = 0 \qquad \forall a \in \{7, 10, 13, 16, 17, 18, 19, 20, 21, 22\}\,. \tag{4.194}$$

Comparing this with Eq. (4.189), it is clear that these are the same components which vanish at order $\log^0 x$ at one loop (4.189). This is a general feature: only the colour representations with non-vanishing coefficients at the previous loop order can exhibit a logarithm of x. The non-vanishing two-loop components at order $\log x$ are very simple. They contain manifestly single-valued logarithms and dilogarithms only. Moreover, they are all proportional to $i\pi$ and thus vanish at symbol level, except for $h_{3,1}^{(2)}$. The latter is non-zero at symbol level, but does not contain any genuine weight-3 function.

The finite terms, i.e. $h_{a,0}^{(2)}$, have transcendental weight 4, but only $h_{3,0}^{(2)}$ is non-zero at symbol level. Nonetheless, the latter is rather simple: it involves only logarithms and the Bloch-Wigner dilogarithm. The other colour components are proportional

to either $i\pi$ or π^2. Three vanish, $h^{(2)}_{a,0} = 0$ for $a = 10, 18, 21$. Some contain genuine weight-3 functions.

The $\mathcal{N} = 4$ super Yang-Mills hard function in the multi-Regge limit contains several functions which are not real-analytic in the entire complex z plane. They appear only in the order-$\log^0 x$ components $h^{(2)}_{a,0}$ with $a \in \{1, 2, 5, 6, 11, 12, 14, 15\}$. Among these, $h^{(2)}_{12,0}$ and $h^{(2)}_{15,0}$ are particularly simple, as they involve—of the functions which are not real-analytic—only the logarithms given by Eq. (4.159). For instance,

$$h^{(2)}_{12,0} = \frac{i\pi}{6}\left[\left(g^{(1)}_7\right)^3 - \left(g^{(1)}_6\right)^3\right] + \frac{2i\pi^3}{3}\left(g^{(1)}_7 - g^{(1)}_6\right) + (\text{analytic})\,. \tag{4.195}$$

The other components, $h^{(2)}_{a,0}$ with $a \in \{1, 2, 5, 6, 11, 14\}$, involve also weight-2 and 3 functions which are not real analytic. Interestingly, we observe that the latter appear in a specific combination. Nonetheless, we introduced them separately, as they enter the hard function in $\mathcal{N} = 8$ supergravity.

Although the hard function is continuous in the entire complex z plane, certain colour components are not analytic across the real z axis. In particular, the second derivatives of certain components have discontinuities: at $\mathrm{Re}[z] > 0$ for components 1, 11 and 14; at $\mathrm{Re}[z] < 1$ for components 2, 5 and 6; and at $\mathrm{Re}[z] < 0$ and $\mathrm{Re}[z] > 1$ for components 12 and 15. Such a non-analyticity of the non-planar amplitudes in the multi-Regge limit, while absent in the planar limit, is not a new phenomenon. It was already observed, for instance, in the computation of the non-planar impact factor at one loop [156]. In our work [26] we also use the latter to compute in the BFKL framework the non-analytic terms. We find agreement with the results of the computation discussed here.

We provide the explicit expressions of the coefficients $h^{(2)}_{a,k}$ of the asymptotic expansion given by Eq. (4.190) in both the upper and lower half of the complex z plane in ancillary files of Ref. [26].

4.4.5 *Multi-Regge Limit of the $\mathcal{N} = 8$ Supergravity Amplitude*

In this section I discuss the multi-Regge asymptotics of the five-graviton amplitude in $\mathcal{N} = 8$ supergravity up to two-loop order. My collaborators and I initiated this analysis at symbol level in Ref. [23], and then lifted it to function level in Ref. [26]. There are several novel features with respect to the corresponding $\mathcal{N} = 4$ super Yang-Mills case. First of all, the behaviour of the rational factors of supergravity amplitude is substantially more complicated. In order to see this, we need to normalise the amplitudes and the hard functions so as to cancel the helicity. We choose to extract a factor of PT_1^2,

$$\widetilde{\mathcal{M}}_5^{(\ell)} = \frac{\mathcal{M}_5^{(\ell)}}{\mathrm{PT}_1^2}\,, \qquad \widetilde{\mathcal{F}}_5^{(\ell)} = \frac{\mathcal{F}_5^{(\ell)}}{\mathrm{PT}_1^2}\,. \tag{4.196}$$

With this normalisation, the tree-level amplitude given by Eq. (4.71) is finite in the multi-Regge limit,

$$\widetilde{\mathcal{M}}_5^{(0)} = -\frac{s_1^2 s_2^2}{s^2} z(1-\bar{z})(z-\bar{z}) + \mathcal{O}(x)\,. \tag{4.197}$$

The rational factors of the supergravity amplitude however diverge in general as $1/x^2$ at one loop and as $1/x^4$ at two loops. As a result, the asymptotic expansion of the hard function is a double series of terms of the form $x^{-m}\log^k(x)$. Moreover, in order to compute the leading contributions in the limit $x \to 0$, the power corrections to the asymptotic expansion of the pentagon integrals have to be taken into account. They are given by the transformation matrix T in Eq. (4.144). This implies a drop in transcendentality: the asymptotics of the hard function does not have uniform and maximal weight, but contains lower-weight functions and rational factors.

At first it is natural to suspect that these complications are consequences of the chosen normalisation, but they are in fact inevitable. We want a common normalisation factor at all loop orders. The dimensionality of the gravitational coupling κ however implies that the dimension of the rational factors depends on the loop order. We know that the latter diverge in the limit $x \to 0$ as $1/x^2$ at one loop and as $1/x^4$ at two loops with the normalisation given by Eq. (4.196). Therefore, any correction to the latter which makes the two-loop rational factors finite also makes the one-loop ones vanish, and does not cure the three-loop ones. Moreover, the normalisation given by Eq. (4.196) is motivated. The minimal choice of normalisation factor to cancel the helicity is given by a product of two Parke-Taylor factors. Among all possible combinations, the one chosen in Eq. (4.196) is particularly good. In fact, most other pairs of Parke-Taylor factors develop even higher poles in the limit. No product of two Parke-Taylor factors leads to a less divergent behaviour of the rational factors with respect to Eq. (4.196).

The rational factors are also related to another new feature. Some of them become singular at $z = \bar{z}$ in the multi-Regge limit, namely on the hypersurface where tr_5 vanishes. This property is a consequence of the power corrections in the pentagon integrals. We have seen in Sect. 4.2.4 that certain non-planar integrals are discontinuous across the hypersurface $\mathrm{tr}_5 = 0$. Moreover, the Regge asymptotics of the five-gluon hard function in $\mathcal{N} = 4$ super Yang-Mills theory is not real analytic there, as its second derivatives are discontinuous. If we were to look at the subleading power corrections, we would encounter rational factors singular at $z = \bar{z}$ in the super Yang-Mills hard function as well. Again, we cannot remove this uncomfortable feature by changing the normalisation. The only way to cancel to poles at $z = \bar{z}$ in the Regge asymptotics of the supergravity hard function is the trivial one, i.e. to multiply it by an appropriate power of $(z - \bar{z})$. Higher poles at $z = \bar{z}$ would however show up in the higher power corrections, so that there is no overall fixed power of $(z - \bar{z})$ that would remove this singularity altogether.

In the next two sections I present our results for the multi-Regge asymptotics of the hard function at one and two-loop order. All the explicit expressions, written in terms of the transcendental functions presented in Sect. 4.4.3, are provided in ancillary files of Ref. [26].

One-loop hard function

The one-loop rational factors $r_i^{(1)}$, normalised by PT_1^2, are in general divergent in the multi-Regge limit as

$$\frac{r_i^{(1)}}{\mathrm{PT}_1^2} \underset{x\to 0}{\sim} \mathcal{O}\left(\frac{1}{x^2}\right). \tag{4.198}$$

Therefore, in order to compute the asymptotics of the one-loop hard function up to infinitesimal terms, we have to take into account power corrections up to x^2 in the asymptotic expansion of the pentagon integrals (4.144). We organise the asymptotic expansion in the multi-Regge limit of the (normalised) one-loop hard function as

$$\widetilde{\mathcal{F}}_5^{(1)} = \sum_{m=0}^{2}\sum_{k=0}^{2} \frac{1}{x^m} \log^k(x)\, F_{m,k}^{(1)}(s_1, s_2, s, z, \bar{z}) + o(1)\,. \tag{4.199}$$

The infinitesimal terms, i.e. those of the form $x^m \log^k(x)$ with $m > 0$ and $k \geq 0$, are neglected, but may be computed following the same procedure. The coefficients $F_{m,k}^{(1)}$ contain a mixture of rational and transcendental functions with up to weight two. The latter can be expressed entirely in terms of the single-valued logarithms given by Eq. (4.158). The expression of the one-loop hard function in the multi-Regge limit is thus straightforwardly valid in the whole s_{12} physical scattering region. As an example, I spell out the leading power term,

$$F_{2,0}^{(1)} = 2i\pi \frac{s_1^2 s_2^2 z(1-\bar{z})}{s}\left[g_5^{(1)} + z\left(g_3^{(1)} - g_5^{(1)}\right) + \bar{z}\left(g_4^{(1)} - g_3^{(1)}\right)\right]. \tag{4.200}$$

I comment on the other terms proceeding by powers of $\log x$.

Unlike the Yang-Mills theory case, the hard function in supergravity does exhibit the maximal logarithms compatible with its transcendental weight. At one loop this means $\log^2 x$. It is present only at power-suppressed order ($\mathcal{O}(x^0)$), so $F_{2,2}^{(1)} = 0$ and $F_{1,2}^{(1)} = 0$, and is multiplied by the rational function

$$F_{0,2}^{(1)} = \frac{2s_1^3 s_2^3 z(1-\bar{z})(3z - 3z^2 - \bar{z} + 4z^2\bar{z} + \bar{z}^2 - 4z\bar{z}^2)}{s^3}. \tag{4.201}$$

Also $\log^1 x$ appears only at order $\mathcal{O}(x^0)$, i.e. $F^{(1)}_{2,1} = 0$ and $F^{(1)}_{1,1} = 0$. Its coefficient, $F^{(1)}_{0,1}$, contains a rational and a weight-1 part.

The order-$\log^0 x$ part is the most complicated. Equation (4.200) shows the leading-power term, $F^{(1)}_{2,0}$. We find that $F^{(1)}_{0,0}$ and $F^{(1)}_{1,0}$ contain a mixture of terms of transcendentalities ranging from 0 to 2. The expressions are too bulky to be given explicitly here. Nonetheless, I can present them in a schematic way which highlights their transcendentality structure:

$$\begin{aligned}
&F^{(1)}_{2,2} = 0\,, && F^{(1)}_{1,2} = 0\,, && F^{(1)}_{0,2} = \mathcal{Q}^{(0)}_{0,2}\,,\\
&F^{(1)}_{2,1} = 0\,, && F^{(1)}_{1,1} = 0\,, && F^{(1)}_{0,1} = \mathcal{Q}^{(1)}_{0,1} + i\pi\mathcal{Q}^{(0)}_{0,1} + \mathcal{Q}^{(0)'}_{0,1}\,,\\
&F^{(1)}_{2,0} = i\pi\mathcal{Q}^{(1)}_{2,0}\,, && F^{(1)}_{1,0} = i\pi\mathcal{Q}^{(1)}_{1,0} + i\pi\mathcal{Q}^{(0)}_{1,0}\,, && F^{(1)}_{0,0} = \mathcal{Q}^{(2)}_{0,0} + i\pi\mathcal{Q}^{(1)}_{0,0} + \mathcal{Q}^{(1)'}_{0,0} + i\pi\mathcal{Q}^{(0)}_{0,0} + \mathcal{Q}^{(0)'}_{0,0}\,.
\end{aligned} \tag{4.202}$$

where $\mathcal{Q}^{(w)}_{a,b}$ denotes a uniform weight-w function, possibly containing rational factors. These formulae show which components vanish and what transcendental weights the others have. The explicit expressions are given in ancillary files of Ref. [26].

As I anticipated in the introduction of this section, the hard function becomes singular for $z = \bar{z}$ in the multi-Regge limit, because of its rational factors. In particular, at one loop, $F^{(1)}_{1,0}$ and $F^{(1)}_{0,0}$ are divergent. $\mathcal{Q}^{(1)}_{1,0}$ and $\mathcal{Q}^{(1)}_{0,0}$ exhibit a simple pole at $z = \bar{z}$, and $\mathcal{Q}^{(1)}_{0,0}$ has a third-order pole. I stress that these poles do not cancel out upon series expansion of the transcendental functions around $z = \bar{z}$.

Two-loop hard function

The two-loop rational factors $r^{(2)}_i$ in general diverge as $1/x^4$ in the multi-Regge limit,

$$\frac{r^{(2)}_i}{\mathrm{PT}^2_1} \underset{x\to 0}{\sim} \mathcal{O}\left(\frac{1}{x^4}\right). \tag{4.203}$$

The soft factor σ_5 is singular as well,

$$\sigma_5 = -\frac{2i\pi s}{x^2} - \frac{2s_1 s_2}{s}(1 - z - \bar{z} + 2z\bar{z})\log(x) + \mathcal{O}(1)\,. \tag{4.204}$$

Therefore, computing the multi-Regge asymptotics of the two-loop hard function up to infinitesimal terms requires the knowledge of the two-loop rational factors $r^{(2)}_i$ up to order x^0, while the one-loop rational factors $r^{(1)}_i$ and the soft factor σ_5 are needed up to order x^2. As for the pentagon integrals, the power corrections in the asymptotic expansion given by Eq. (4.144) have to computed up to order x^4 at both one and two loops.

We arrange the multi-Regge asymptotics of the (normalised) hard function at two-loop order as

$$\widetilde{\mathcal{F}}_5^{(2)} = \sum_{m=0}^{4} \sum_{k=0}^{4} \frac{1}{x^m} \log^k(x)\, F_{m,k}^{(2)}(s_1, s_2, s, z, \bar{z}) + o(1)\,. \tag{4.205}$$

The coefficients $\mathcal{F}_5^{(2)}$ have mixed transcendentality up to weight $(4-k)$. The leading-power contribution is compact enough that I can present it here explicitly,

$$\begin{aligned} F_{4,0}^{(2)} = & -2\pi^2 s_1^2 s_2^2 z(-1+\bar{z}) \Big(-\bar{z} \left(g_3^{(1)} - g_4^{(1)} \right)^2 + z \left(g_3^{(1)} - g_5^{(1)} \right)^2 + 2 g_3^{(1)} g_5^{(1)} \\ & - g_4^{(1)} g_5^{(1)} - \left(g_5^{(1)} \right)^2 + 2 g_1^{(2)} \Big)\,. \end{aligned} \tag{4.206}$$

I discuss the remaining terms order by order in $\log x$, adopting the same schematic notation of Eq. (4.202) to emphasise the transcendentality structure.

The leading logarithm, $\log^4(x)$, is associated with the simplest part of the hard function. As at one loop, in fact, it appears only at order x^0,

$$F_{4,4}^{(2)} = 0\,, \qquad F_{3,4}^{(2)} = 0\,, \qquad F_{2,4}^{(2)} = 0\,, \qquad F_{1,4}^{(2)} = 0\,, \qquad F_{0,4}^{(2)} = \mathcal{Q}_{0,4}^{(0)}\,. \tag{4.207}$$

where $\mathcal{Q}_{0,4}^{(0)}$ is a weight-0, i.e. rational, function. It is interesting to point out that the power corrections of the pentagon integrals and of the soft factor σ_5 do not contribute at LL order.

At order $\log^3(x)$ we find

$$F_{4,3}^{(2)} = 0\,, \quad F_{3,3}^{(2)} = 0\,, \quad F_{2,3}^{(2)} = i\pi \mathcal{Q}_{2,3}^{(0)}\,, \quad F_{1,3}^{(2)} = i\pi \mathcal{Q}_{1,3}^{(0)}\,, \quad F_{0,3}^{(2)} = \mathcal{Q}_{0,3}^{(1)} + i\pi \mathcal{Q}_{0,3}^{(0)} + \mathcal{Q}_{0,3}^{(0)'}\,, \tag{4.208}$$

where the apostrophe is simply meant to distinguish different functions. $\mathcal{Q}_{0,3}^{(1)}$ involves only the manifestly single-valued logarithms given by Eq. (4.158), together with rational factors. The appearance of a rational term $\mathcal{Q}_{0,3}^{(0)'}$ in $F_{0,3}^{(2)}$ is a clear manifestation of the transcendentality drop. Some rational functions, $\mathcal{Q}_{1,3}^{(0)}$ and $\mathcal{Q}_{0,3}^{(0)}$, have poles at $z = \bar{z}$, of order 1 and 3, respectively.

At order $\log^2(x)$ we find

$$\begin{aligned} F_{4,2}^{(2)} &= 0\,, \\ F_{3,2}^{(2)} &= 0\,, \\ F_{2,2}^{(2)} &= i\pi \mathcal{Q}_{2,2}^{(1)} + \pi^2 \mathcal{Q}_{2,2}^{(0)} + i\pi \mathcal{Q}_{2,2}^{(0)'}\,, \\ F_{1,2}^{(2)} &= i\pi \mathcal{Q}_{1,2}^{(1)} + \pi^2 \mathcal{Q}_{1,2}^{(0)} + i\pi \mathcal{Q}_{1,2}^{(0)'}\,, \\ F_{0,2}^{(2)} &= \mathcal{Q}_{0,2}^{(2)} + i\pi \mathcal{Q}_{0,2}^{(1)} + \pi^2 \mathcal{Q}_{0,2}^{(0)} + \mathcal{Q}_{0,2}^{(1)'} + i\pi \mathcal{Q}_{0,2}^{(0)'} + \mathcal{Q}_{0,2}^{(0)''}\,. \end{aligned} \tag{4.209}$$

The transcendental part of the previous expressions can be entirely expressed in terms of (products of) the single-valued logarithms in Eq. (4.158). Some rational functions have poles at $z = \bar{z}$ with order up to three.

At order $\log(x)$ we find

$$
\begin{aligned}
F^{(2)}_{4,1} &= 0\,,\\
F^{(2)}_{3,1} &= 0\,,\\
F^{(2)}_{2,1} &= i\pi\mathcal{Q}^{(2)}_{2,1} + \pi^2\mathcal{Q}^{(1)}_{2,1} + i\pi^3\mathcal{Q}^{(0)}_{2,1} + i\pi\mathcal{Q}^{(1)'}_{2,1} + \pi^2\mathcal{Q}^{(0)'}_{2,1} + i\pi\mathcal{Q}^{(0)''}_{2,1}\,,\\
F^{(2)}_{1,1} &= i\pi\mathcal{Q}^{(2)}_{1,1} + \pi^2\mathcal{Q}^{(1)}_{1,1} + i\pi^3\mathcal{Q}^{(0)}_{1,1} + i\pi\mathcal{Q}^{(1)'}_{1,1} + \pi^2\mathcal{Q}^{(0)'}_{1,1} + i\pi\mathcal{Q}^{(0)''}_{1,1}\,,\\
F^{(2)}_{0,1} &= \mathcal{Q}^{(3)}_{0,1} + i\pi\mathcal{Q}^{(2)}_{0,1} + \pi^2\mathcal{Q}^{(1)}_{0,1} + i\pi^3\mathcal{Q}^{(0)}_{0,1} + \zeta_3\mathcal{Q}^{(0)'}_{0,1} + \mathcal{Q}^{(2)'}_{0,1} + i\pi\mathcal{Q}^{(1)'}_{0,1}\\
&\quad + \pi^2\mathcal{Q}^{(0)''}_{0,1} + \mathcal{Q}^{(1)''}_{0,1} + i\pi\mathcal{Q}^{(0)'''}_{0,1} + \mathcal{Q}^{(0)''''}_{0,1}\,.
\end{aligned}
\tag{4.210}
$$

Almost all the weight-1 and 2 functions in these expressions involve only the single-valued logarithms (4.158) and dilogarithm (4.162). The coefficient $F^{(2)}_{0,1}$ alone has a more complicated functional structure, especially at weight two and three.

Finally, at order $\log^0(x)$ we find

$$
\begin{aligned}
F^{(2)}_{4,0} &= \pi^2\mathcal{Q}^{(2)}_{4,0}\\
F^{(2)}_{3,0} &= \pi^2\mathcal{Q}^{(2)}_{3,0} + \pi^2\mathcal{Q}^{(1)}_{3,0}\,,\\
F^{(2)}_{2,0} &= i\pi\mathcal{Q}^{(3)}_{2,0} + \pi^2\mathcal{Q}^{(2)}_{2,0} + i\pi^3\mathcal{Q}^{(1)}_{2,0} + i\pi\zeta_3\mathcal{Q}^{(0)}_{2,0} + \pi^4\mathcal{Q}^{(0)'}_{2,0} + \pi^2\mathcal{Q}^{(1)'}_{2,0}\\
&\quad + i\pi^3\mathcal{Q}^{(0)''}_{2,0} + i\pi\mathcal{Q}^{(1)''}_{2,0} + \pi^2\mathcal{Q}^{(0)'''}_{2,0} + i\pi\mathcal{Q}^{(0)''''}_{2,0}\,,\\
F^{(2)}_{1,0} &= i\pi\mathcal{Q}^{(3)}_{1,0} + \pi^2\mathcal{Q}^{(2)}_{1,0} + i\pi^3\mathcal{Q}^{(1)}_{1,0} + i\pi\zeta_3\mathcal{Q}^{(0)}_{1,0} + \pi^4\mathcal{Q}^{(0)'}_{1,0} + i\pi\mathcal{Q}^{(2)'}_{1,0}\\
&\quad + \pi^2\mathcal{Q}^{(1)'}_{1,0} + i\pi^3\mathcal{Q}^{(0)''}_{1,0} + i\pi\mathcal{Q}^{(1)''}_{1,0} + \pi^2\mathcal{Q}^{(0)'''}_{1,0} + i\pi\mathcal{Q}^{(0)''''}_{1,0}\,,\\
F^{(2)}_{0,0} &= \mathcal{Q}^{(4)}_{0,0} + i\pi\mathcal{Q}^{(3)}_{0,0} + \pi^2\mathcal{Q}^{(2)}_{0,0} + i\pi^3\mathcal{Q}^{(1)}_{0,0} + \zeta_3\mathcal{Q}^{(1)'}_{0,0} + \pi^4\mathcal{Q}^{(0)}_{0,0} + i\pi\zeta_3\mathcal{Q}^{(0)'}_{0,0}\\
&\quad + \mathcal{Q}^{(3)'}_{0,0} + i\pi\mathcal{Q}^{(2)'}_{0,0} + \pi^2\mathcal{Q}^{(1)''}_{0,0} + i\pi^3\mathcal{Q}^{(0)''}_{0,0} + \zeta_3\mathcal{Q}^{(0)'''}_{0,0} + \mathcal{Q}^{(2)''}_{0,0}\\
&\quad + i\pi\mathcal{Q}^{(1)'''}_{0,0} + \pi^2\mathcal{Q}^{(0)''''}_{0,0} + \mathcal{Q}^{(1)''''}_{0,0} + i\pi\mathcal{Q}^{(0)'''''}_{0,0} + \mathcal{Q}^{(0)''''''}_{0,0}\,.
\end{aligned}
\tag{4.211}
$$

The leading-power coefficient $F^{(2)}_{4,0}$ is given explicitly in Eq. (4.206). Both $F^{(2)}_{4,0}$ and $F^{(2)}_{3,0}$ are non-zero only at this order in $\log x$, where they are rather simple. They involve only the single-valued logarithms (4.158) and the dilogarithm (4.162). The structure of the coefficients $F^{(2)}_{2,0}$, $F^{(2)}_{1,0}$ and $F^{(2)}_{0,0}$ is more complicated. In particular, $F^{(2)}_{2,0}$ and $F^{(2)}_{1,0}$ contain functions with genuine weight three, while genuine weight-4 functions appear in $F^{(2)}_{0,0}$.

We can now make a few general observations. All the transcendental functions appearing in the multi-Regge asymptotics of the hard function up to two loops are real-analytic in both the upper and lower half of the complex z plane. In particular, I stress that the hard function is real analytic across the line $1 - z - \bar{z} = 0$. The rational factors bring in singularities on the real axis, i.e. for $z - \bar{z} = 0$. It is thus impossible to check the continuity of the full hard function across the real axis. The coefficients which are not singular there—$F^{(2)}_{0,4}$, $F^{(2)}_{2,3}$, $F^{(2)}_{2,2}$, $F^{(2)}_{2,1}$ and $F^{(2)}_{4,0}$—do match at $\mathrm{Im}[z] = 0$,

although their derivatives are discontinuous. The coefficients $F^{(2)}_{1,3}$, $F^{(2)}_{0,3}$, $F^{(2)}_{1,2}$, $F^{(2)}_{0,2}$, $F^{(2)}_{1,1}$, $F^{(2)}_{3,0}$ are instead singular at $z = \bar{z}$, but contain only functions which are single-valued in the entire complex plane. In particular, $F^{(2)}_{1,3}$ is purely rational. $F^{(2)}_{0,1}$ diverges at $z = \bar{z}$, and involves also functions which are defined separately in the two halves of the complex plane. The singular rational factors however multiply single-valued functions only, while the part which is finite at $z = \bar{z}$ is continuous across the real axis. This separation is impossible for $F^{(2)}_{0,0}$ and $F^{(2)}_{1,0}$, in which singular rational factors appear alongside with non-single-valued functions. The coefficient $F^{(2)}_{0,0}$ is the most complicated, and contains the highest pole at $z = \bar{z}$, of order 7.

4.4.6 Discussion

The two-loop five-particle hard function in $\mathcal{N} = 4$ super Yang-Mills theory has a substantially simpler multi-Regge asymptotics as compared to its supergravity counterpart. The extremely simpler behaviour of the rational factors allows the hard function to maintain the uniform transcendental weight in the limit. The transcendental functions appearing in the limit are also very simple: they can be expressed in terms of classical polylogarithms of at most weight three. Nonetheless, the result exhibits a very non-trivial analytic property, related to the pseudo-scalar invariant tr_5. The kinematics of the physical scattering constrains tr_5 to be pure imaginary. Its sign distinguishes two copies of the scattering region, separated by the hypersurface $\mathrm{tr}_5 = 0$. The Regge asymptotics of the super Yang-Mills hard function is continuous across this hypersurface, but not real-analytic, as the second derivatives of certain colour structures have discontinuities. This non-trivial analytic property stems from the discontinuity of certain individual non-planar integrals, which I discussed in Sect. 4.2.4. The sum over all Feynman integrals smoothens this discontinuity, but leaves a trace in the second derivatives of the hard function. In Ref. [26] we independently reproduced this non-analyticity using the BFKL effective theory. Using the latter we also computed the multi-Regge limit of certain colour structures of the super Yang-Mills hard function, finding agreement with the direct computation discussed here.

The $\mathcal{N} = 8$ supergravity hard function has a much richer structure. The main reason is that the rational factors develop poles in the Regge limit. This forces one to include also power corrections in the asymptotic expansion of the integrals. As a result, the Regge asymptotics of the hard function contains a mixture of terms of different transcendental weight (up to four) and rational functions. Unlike the $\mathcal{N} = 4$ super Yang-Mills case, some of the rational factors become singular on the hypersurface where $\mathrm{tr}_5 = 0$. The transcendental functions are more complicated as well: they involve genuine weight-four functions and multiple polylogarithms.

4.5 The All-Plus Amplitude in Pure Yang-Mills Theory

In this Section I present the computation of the amplitude describing the scattering of five positive-helicity gluons at two-loop order in pure Yang-Mills theory [27]. This constituted the very first fully-analytic result for a two-loop five-particle amplitude including the non-planar contributions. We achieved it by employing the knowledge of the massless two-loop five-particle integral families discussed in Sect. 4.2, starting from the integrand constructed in Ref. [29]. The same result was independently reached also in Ref. [28]. In the latter, the authors make a very smart use of the particularly simple structure of the all-plus gluonic amplitudes, and adopt a completely different approach based on four-dimensional unitarity and recursion methods. Our goal, on the other hand, was not to compute this specific amplitude, but to prepare for the computation of *all* two-loop five-parton amplitudes in QCD. For this reason we did not take advantage of the simplicity of the all-plus helicity configuration, and tackled head-on a fully-fledged two-loop five-particle computation. The success of our computation shows that the doors are now open for the analytic computation of all the two-loop amplitudes entering the virtual corrections to processes with three particles in the final state at NNLO in QCD. Ultimately, this will enable the computation of NNLO theoretical predictions for several processes of great phenomenological interest, such as the production of three hadronic jets, of two photons and a jet, and of one photon and two jets.

Moreover, the result presented in this section gives one more example of why collecting analytic "data" is not only important for phenomenology, but is also crucial to the advance of our theoretical understanding. It allows one to uncover structures and patterns which may lead to deeper insights in the underlying theory, and to test new ideas. Discovering patterns and structures is of course simpler if the expressions are compact. This is why we put a lot of effort in simplifying our result for the all-plus hard function, until it eventually fit in just two lines. This effort was rewarded. It allowed us to notice that certain pieces of the hard function are conformally invariant, i.e. they are annihilated by the generator of (special) conformal transformations [157],

$$k_{\alpha\dot{\alpha}} = \sum_{i=1}^{5} \frac{\partial^2}{\partial\lambda_i^{\alpha}\partial\tilde{\lambda}_i^{\dot{\alpha}}} \,. \tag{4.212}$$

The pure Yang-Mills Lagrangian is conformally invariant at the classical level. This symmetry is however obscured by quantum corrections, due to the introduction of scales to regularise the divergences. Finding signs of it at loop level is intriguing. Indeed, another work stemmed from this observation. My collaborators and I proved that the one-loop all-plus amplitude is conformally invariant for any number of external gluons, which also explains the signs of conformal symmetry observed at two loops [30].

I begin in Sect. 4.5.1 by defining the notation and discussing the tree-level and one-loop amplitudes. Section 4.5.2 is devoted to the divergence structure of the two-loop amplitude: I show how the UV divergences are removed via renormalisation,

and how the IR divergences factorise and can be subtracted to define a finite hard function. Anticipating the form of the latter is much more complicated than in the supersymmetric cases discussed in Sect. 4.3. Nonetheless, in Sect. 4.5.3 I show how, using four-dimensional unitarity and making a guess for the rational factors based on the known planar part of the amplitude, we can write down a rather constrained ansatz for the two-loop hard function. Having set our expectations, we can proceed with the actual computation. The workflow is similar to the one adopted for the supersymmetric amplitudes in Sect. 4.3, but requires some additional work at the beginning. The expression for the integrand in the literature [29] is written in a form which cannot be directly fed into the IBP reductions. I show in Sect. 4.5.4 how we can rewrite it in a suitable form, i.e. in terms of inverse propagators. This procedure introduces numerators which depend on the loop momenta with a much higher degree with respect to the supersymmetric cases. The IBP reduction to canonical basis integrals is therefore substantially more involved. In Sect. 4.5.5 I show how this bottleneck is overcome thanks to the finite field approach. I present and validate the result for the two-loop hard function in Sect. 4.5.6. The expression is remarkably compact, agrees with the expectations formulated in Sect. 4.5.3 and shows intriguing signs of conformal symmetry. Finally, I comment on the result in Sect. 4.5.7.

4.5.1 Notation

We study the scattering of five gluons with positive helicity. The kinematics is discussed in Sect. 4.1. I recall that the loop momenta are D-dimensional, whereas we take the external momenta p_i to lie in four-dimensional Minkowski space. The algebra in the numerators of the integrand introduces the spin dimension of the gluon, $D_s = g^\mu_\mu$. We keep the dependence on the latter explicit. Results in the Four-Dimensional-Helicity [158] and t'Hooft-Veltman [159] schemes are obtained by setting $D_s = 4$ and $D_s = 4 - 2\epsilon$, respectively. In order the make the expressions more compact, we introduce the short-hand notation

$$\kappa = \frac{D_s - 2}{6} \,. \tag{4.213}$$

We absorb the difference between the loop-integration measure of Feynman diagrams and of Feynman integrals in the coupling,

$$a = g^2 \, \frac{e^{-\epsilon \gamma_{\rm E}}}{(4\pi)^{2-\epsilon}} \,. \tag{4.214}$$

We expand the five-gluon all-plus amplitude in a as

$$\mathcal{A}_5 = i g^3 \, \delta^{(4)}(p_1 + \ldots + p_5) \sum_{\ell \geq 0} a^\ell \, \mathcal{A}_5^{(\ell)} \,. \tag{4.215}$$

Thanks to the particular helicity configuration, the amplitude enjoys a symmetry under any permutation of the external gluons. Moreover, the amplitude vanishes at tree-level [160, 161], and is thus finite at one loop.

We treat the amplitude as a vector in colour space. We use the trace-based basis $\{\mathcal{T}_\lambda\}_{\lambda=1}^{22}$ defined by Eqs. (4.65) and (4.66), and decompose the one and two-loop amplitudes as

$$\mathcal{A}_5^{(1)} = \sum_{\lambda=1}^{12} N_c\, A_\lambda^{(1,0)} \mathcal{T}_\lambda + \sum_{\lambda=13}^{22} A_\lambda^{(1,1)} \mathcal{T}_\lambda\,, \tag{4.216}$$

$$\mathcal{A}_5^{(2)} = \sum_{\lambda=1}^{12} \left(N_c^2 A_\lambda^{(2,0)} + A_\lambda^{(2,2)}\right) \mathcal{T}_\lambda + \sum_{\lambda=13}^{22} N_c A_\lambda^{(2,1)} \mathcal{T}_\lambda\,. \tag{4.217}$$

The partial amplitudes $A_\lambda^{(\ell,k)}$ satisfy the same group-theoretic identities [58, 59] which I discuss in Sect. 4.3.1 for the $\mathcal{N} = 4$ super Yang-Mills amplitude.

The one-loop partial amplitudes $A_\lambda^{(1,k)}$ can be expressed in terms of permutations of one leading-colour component, say $A_1^{(1,0)}$. An expression for the latter can be found in Ref. [48],

$$A_1^{(1,0)} = \frac{\kappa}{2} \frac{s_{12}s_{23} + s_{23}s_{34} + s_{34}s_{45} + s_{45}s_{51} + s_{51}s_{12} + \mathrm{tr}_5}{\langle 12\rangle\langle 23\rangle\langle 34\rangle\langle 45\rangle\langle 51\rangle} + \mathcal{O}(\epsilon)\,. \tag{4.218}$$

The rationality of the one-loop all-plus amplitude at order ϵ^0 follows from the vanishing of the all-plus and single-minus tree-level amplitudes through cutting rules. For similar reasons the only allowed singularities are those where two colour-adjacent momenta become collinear. The expression given by Eq. (4.218) makes manifest both the permutation symmetry and the absence of spurious poles. We can sacrifice the apparent expression of these two properties to highlight another: conformal symmetry. The four-dimensional part of the one-loop all-plus amplitude is in fact annihilated by the generator of special conformal transformations given by Eq. (4.212),[5]

$$k_{\alpha\dot\alpha} A_\lambda^{(1,k)} = \mathcal{O}(\epsilon)\,. \tag{4.219}$$

This property is not at all obvious from Eq. (4.218), but becomes apparent if we rewrite it as [27, 30]

$$A_1^{(1,0)} = \kappa \left(\frac{[45]^2}{\langle 12\rangle\langle 23\rangle\langle 31\rangle} + \frac{[23]^2}{\langle 45\rangle\langle 51\rangle\langle 14\rangle} + \frac{[52]^2}{\langle 41\rangle\langle 13\rangle\langle 34\rangle} \right) + \mathcal{O}(\epsilon)\,. \tag{4.220}$$

[5] We are interested in generic configurations of the external momenta, and we therefore neglect contact terms arising from differentiation [157, 162–165]. Moreover, the complete amplitude also contains an overall momentum conservation δ function. Thanks to Lorentz and dilatation invariance, the generator $k_{\alpha\dot\alpha}$ commutes with the δ function [157, 166].

Conformal symmetry is now manifest term by term. Each addend is trivially annihilated by the generator $k_{\alpha\dot{\alpha}}$, due to the form of the latter. See Ref. [30] for a thorough discussion of the conformal properties of the n-gluon all-plus amplitudes. Note that the higher orders in ϵ of the one-loop all-plus amplitude are substantially more complicated, and involve functions with transcendental weight up to 4 at order ϵ^2. In fact, they play a crucial role in simplifying the expression of the two-loop hard function by cancelling out the most complicated part of the two-loop amplitude.

Thanks to the complete permutation symmetry, the two-loop amplitude can be expressed in terms permutations of just three partial amplitudes, e.g. as

$$\mathcal{A}_5^{(2)} = \sum_{\sigma\in S_5/S_{\mathcal{T}_1}} \sigma\circ\left[\left(N_c^2 A_1^{(2,0)} + A_1^{(2,2)}\right)\mathcal{T}_1\right] + \sum_{\sigma\in S_5/S_{\mathcal{T}_{13}}} \sigma\circ\left[N_c A_{13}^{(2,1)}\mathcal{T}_{13}\right], \tag{4.221}$$

where the sums run over the permutations of the external legs, S_5, modulo the subsets $S_{\mathcal{T}_\lambda}$ of permutations that leave $\mathcal{T}_\lambda$ invariant. The two-loop planar partial amplitude $A_1^{(2,0)}$ was computed in Refs. [1, 4]. The most sub-leading colour component, $A_1^{(2,2)}$, can be expressed in terms of planar and double-trace components through colour relations [58]. The truly new piece of information that my collaborators and I computed in Ref. [27] is thus the double-trace component $A_{13}^{(2,1)}$.

4.5.2 Divergence Structure and Hard Function

The divergence structure of the five-gluon all-plus amplitude in pure Yang-Mills theory is very similar to that of the MHV amplitude in $\mathcal{N}=4$ super Yang-Mills theory discussed in Sect. 4.3.4. The main difference is that the former has ultraviolet divergences as well. Before we subtract the infrared divergences, therefore, we need to renormalise the amplitude. The ultraviolet divergences in pure Yang-Mills amplitudes can be universally absorbed into a renormalisation of the coupling. In other words, we need to replace the bare coupling a with the running coupling $a_R(\mu)$,

$$a = Z(\mu)a_R(\mu)\mu^{2\epsilon}, \tag{4.222}$$

where μ and Z are the renormalisation scale and the coupling renormalisation factor, respectively. The running of the coupling is governed by the β function,

$$\beta(a_R) = -2a_R^2\beta_0 + \mathcal{O}(a_R^3), \tag{4.223}$$

through

$$\frac{da_R}{d\log\mu} = -2\epsilon a_R + \beta(a_R). \tag{4.224}$$

Differentiating both sides of Eq. (4.222) gives an evolution equation for the renormalisation factor Z,

$$\frac{d\log Z}{d\log\mu} = -\frac{\beta(a_R)}{a_R}\,, \tag{4.225}$$

whose solution is given up to order a_R by

$$Z = 1 - \frac{\beta_0}{\epsilon}a_R + \mathcal{O}(a_R^2)\,. \tag{4.226}$$

Substituting the bare with the running coupling in the expansion of the amplitude (4.215) and series expanding in the running coupling a_R gives the renormalised amplitudes,

$$\mathcal{A}^{(1)}_{5,\text{ren.}} = \mathcal{A}^{(1)}_5\,, \tag{4.227}$$

$$\mathcal{A}^{(2)}_{5,\text{ren.}} = \mathcal{A}^{(2)}_5 - \frac{5\beta_0}{2\epsilon}\mathcal{A}^{(1)}_5\,. \tag{4.228}$$

Hereafter I will often set the renormalisation scale to 1. The explicit dependence can be recovered by dimensional analysis. The renormalised amplitudes inherit the colour decomposition from the bare amplitudes.

The infrared singularities of the renormalised amplitude then factorise according to the same dipole formula (4.95) discussed in Sect. 4.3.4 for the $\mathcal{N}=4$ super Yang-Mills case. The cusp and collinear anomalous dimensions are in this case given by [167]

$$\gamma_{\text{cusp}} = \sum_{k=0}^{\infty}\gamma^{(k)}_{\text{cusp}}a_R^{k+1} = 4a_R + O(a_R^2)\,, \tag{4.229}$$

$$\gamma_{\text{c}} = \sum_{k=0}^{\infty}\gamma^{(k)}_{\text{c}}a_R^{k+1} = -\beta_0 a_R + O(a_R^2)\,. \tag{4.230}$$

The specific value of β_0 is irrelevant here, as we are about to see. Since the tree-level amplitude vanishes, we need the infrared pole operator $\mathbf{Z}_5$ only up to order a,

$$\mathbf{Z}_5 = \mathbb{1} + a\,\mathbf{Z}_5^{(1)} + \mathcal{O}(a^2). \tag{4.231}$$

Putting together Eqs. (4.97), (4.99), and (4.100) gives

$$\mathbf{Z}_5^{(1)} = \frac{1}{2\epsilon^2}\gamma^{(0)}_{\text{cusp}}\left[\sum_{i<j}^{5}\mathbf{T}_i\cdot\mathbf{T}_j - \epsilon\sum_{i<j}^{5}\left(\mathbf{T}_i\cdot\mathbf{T}_j\right)\log\left(\frac{-s_{ij}}{\mu^2}\right)\right] + \frac{5}{2\epsilon}\gamma^{(0)}_{\text{c}}\,, \tag{4.232}$$

where I recall that $\mathbf{T}_i$ is the colour-insertion operator defined by Eq. (4.98), and that the logarithms have to be analytically continued to the s_{12} channel according to Eq. (4.103). The finite two-loop amplitude is then given by

$$\begin{aligned}\mathcal{A}_{5,\text{finite}}^{(2)} &= \mathcal{A}_{5,\text{ren.}}^{(2)} - \mathbf{Z}_5^{(1)}\mathcal{A}_{5,\text{ren.}}^{(1)} = \\ &= \mathcal{A}_5^{(2)} - \frac{5\beta_0}{2\epsilon}\mathcal{A}_5^{(1)} - \mathbf{Z}_5^{(1)}\mathcal{A}_5^{(1)}\,.\end{aligned} \tag{4.233}$$

Thanks to the specific value of the collinear anomalous dimension, given by Eq. (4.230), a nice simplification occurs. The contribution coming from the ultraviolet renormalisation cancels out with the contribution proportional to the collinear anomalous dimension in the infrared pole operator, given by Eq. (4.232). As a result, the finite two-loop amplitude is simply given by

$$\mathcal{A}_{5,\text{finite}}^{(2)} = \mathcal{A}_5^{(2)} - \frac{1}{2\epsilon^2}\gamma_{\text{cusp}}^{(0)}\left[\sum_{i<j}^{5}\mathbf{T}_i\cdot\mathbf{T}_j - \epsilon\sum_{i<j}^{5}\left(\mathbf{T}_i\cdot\mathbf{T}_j\right)\log\left(\frac{-s_{ij}}{\mu^2}\right)\right]\mathcal{A}_5^{(1)}\,. \tag{4.234}$$

I recall that we are currently working in the $\overline{\text{MS}}$ subtraction scheme of infrared singularities, namely that the infrared pole operator contains only the pure pole part. We are however free to modify the finite part of $\mathbf{Z}_5^{(1)}$, this way defining a different scheme. In the square brackets on the right-hand side of Eq. (4.234) we recognise the first two terms of a series expansion. We find it convenient to lift the latter to the complete series,

$$\mathbf{Z}_5^{(1)'} := \frac{1}{2\epsilon^2}\gamma_{\text{cusp}}^{(0)}\sum_{i<j}^{5}\mathbf{T}_i\cdot\mathbf{T}_j\left(\frac{\mu^2}{-s_{ij}}\right)^{\epsilon}\,. \tag{4.235}$$

We observe that a further simplification in the hard function can be achieved by multiplying the infrared pole operator by a constant,

$$\frac{e^{\epsilon\gamma_{\text{E}}}}{\Gamma(1-\epsilon)} = 1 - \frac{\pi^2\epsilon^2}{12} + \mathcal{O}(\epsilon^3)\,, \tag{4.236}$$

which affects only the finite part. In fact, this constant factor is present in Catani's original subtraction operators [95]. Finally, we define the two-loop five-gluon all-plus hard function as

$$\mathcal{H}^{(2)} = \lim_{\epsilon\to 0}\left[\mathcal{A}_5^{(2)} - \tilde{\mathbf{Z}}_5^{(1)}\mathcal{A}_5^{(1)}\right]\,, \tag{4.237}$$

with

$$\tilde{\mathbf{Z}}_5^{(1)} = \frac{\gamma_{\text{cusp}}^{(0)}}{2} \frac{e^{\epsilon\gamma_{\text{E}}}}{\epsilon^2\Gamma(1-\epsilon)} \sum_{i<j}^{5} \mathbf{T}_i \cdot \mathbf{T}_j \left(\frac{\mu^2}{-s_{ij}}\right)^{\epsilon} . \tag{4.238}$$

We decompose the hard function in colour space similarly to the amplitudes. Renormalisation and infrared factorisation scales are set to 1.

4.5.3 Expected Structure of the Hard Function

We have seen in Sect. 4.3 that having a prior insight into the structure of the integrated amplitude can simplify dramatically its computation. Things are however much more complicated in Yang-Mills theory than in the maximally supersymmetric theories. The two-loop five-particle amplitudes in $\mathcal{N} = 4$ super Yang-Mills theory and $\mathcal{N} = 8$ supergravity could in fact be constrained significantly before actually computing them. They were both expected to have uniform transcendental weight and, thanks to the absence of double poles in the integrands, the rational factors can be computed using the leading singularity technique discussed in Sects. 3.6.1 and 4.2.1. The Yang-Mills amplitude is instead a mixture of functions with different weight, bounded from the conjecture expressed by Eq. (3.110). Moreover, the integrand has double poles and the analysis of the leading singularities allows us to determine only a small subset of the potential rational factors. The all-plus helicity configuration is however special, and we can actually say quite a lot about the hard function.

We start by separating the two-loop hard function into a transcendental $\mathcal{P}^{(2)}$ and a rational part $\mathcal{R}^{(2)}$,

$$\mathcal{H}^{(2)} = \mathcal{P}^{(2)} + \mathcal{R}^{(2)} . \tag{4.239}$$

The hard function is a four dimensional object, and we can thus compute its transcendental part $\mathcal{P}^{(2)}$ using four-dimensional unitarity methods [168, 169]. The one-loop all-plus amplitude is rational in four dimensions, and can effectively be used as an additional on-shell vertex. The four-dimensional cuts of the two-loop amplitude this way become one-loop cuts with an insertion of this effective vertex [28]. In this spirit, the one and two-loop all-plus amplitudes are treated as tree-level and one-loop, respectively. This implies that the functions appearing in the two-loop all-plus amplitude have at most transcendental weight two. We can go even further. The analysis carried out in Ref. [28] shows that only the quadruple cuts contribute to the hard function. In other words, the polylogarithmic part of the two-loop hard function can be expressed in terms of box integrals. In particular, box integrals with one massive leg, since they have to accommodate five external particles. The finite part of the one-mass box integral with external momenta $\{p_1, p_2, p_3, p_4 + p_5\}$ is given by

$$I_{123;45} = \text{Li}_2\left(1 - \frac{s_{12}}{s_{45}}\right) + \text{Li}_2\left(1 - \frac{s_{23}}{s_{45}}\right) + \log^2\left(\frac{s_{12}}{s_{23}}\right) + \frac{\pi^2}{6} . \tag{4.240}$$

Permuting in all possible ways the external legs produces 30 linearly-independent one-mass box functions. We introduce an arbitrary basis, $\{I_k^{\text{box}}\}_{k=1}^{30}$. Thanks to their simplicity, they can be analytically continued to the s_{12} channel by simply adding a small positive imaginary part to each two-particle Mandelstam invariant, $s_{ij} \to s_{ij} + i0^+$. The leading singularities associated with the quadruple cuts can be computed e.g. using the method of the on-shell diagrams [170] (see Ref. [57] for a pedagogical introduction). They are given by permutations of the finite part of the one-loop all-plus amplitude. Thanks to our new formula for the latter, Eq. (4.220), we can express these leading singularities as permutations of the basic conformally invariant object,

$$R = \frac{[45]^2}{\langle 12\rangle\langle 23\rangle\langle 31\rangle}\,. \tag{4.241}$$

The permutations of the latter span a six-dimensional space. We introduce an arbitrary basis, $\{R_i\}_{k=i}^{6}$. As a result, the transcendental part of the two-loop hard function has a very constrained form,

$$\mathcal{P}_\lambda^{(2)} = \sum_{i=1}^{6}\sum_{k=1}^{30} c_{i,k}^{(\lambda)} R_i\, I_k^{\text{box}}\,, \tag{4.242}$$

where $c_{i,k}^{(\lambda)}$ are rational numbers. Indeed, the planar hard function, previously computed in Refs. [1, 4], perfectly matches the form given by Eq. (4.242). In order to emphasise this, we rewrite it as

$$\begin{aligned}\mathcal{H}_1^{(2,0)} = \sum_{\sigma\in S_{\mathcal{T}_1}} \sigma\circ\Bigg\{-\kappa\,\frac{[45]^2}{\langle 12\rangle\langle 23\rangle\langle 31\rangle}\,I_{123;45} + \\ + \kappa^2\frac{1}{\langle 12\rangle\langle 23\rangle\langle 34\rangle\langle 45\rangle\langle 51\rangle}\left[5\,s_{12}s_{23} + s_{12}s_{34} + \frac{\text{tr}_+^2(1245)}{s_{12}s_{45}}\right]\Bigg\}\,,\end{aligned} \tag{4.243}$$

where

$$\text{tr}_+(ijkl) = \frac{1}{2}\text{tr}\left((1+\gamma_5)\not{p}_i\not{p}_j\not{p}_k\not{p}_l\right) = [ij]\langle jk\rangle[kl]\langle li\rangle\,, \tag{4.244}$$

and $S_{\mathcal{T}_1}$ is the set of all permutations of the external legs which leave the trace $\mathcal{T}_1$—defined in Eq. (4.65)—invariant. In other words, $S_{\mathcal{T}_1}$ contains the cyclic permutations of the external legs.

The rational part of the two-loop hard function, $\mathcal{R}^{(2)}$, is more elusive. The authors of Ref. [28] computed it using recursive methods. For our purpose, we just want to constrain it so as to simplify the assembly of amplitude. We adopt a heuristic but very easy and quick approach. We assume that the rational functions appearing in the non-planar amplitude are just non-cyclic permutations of the ones appearing in the planar one. The rational factors in the planar hard function given by Eq. (4.243),

permuted in all possible ways, generate a 76-dimensional vector space over $\mathbb{Q}$. We extract an arbitrary basis, $\{r_i\}_{i=1}^{76}$, preferring the most compact functions. If our guess is correct, then the rational part of the two-loop hard function is simply given by

$$\mathcal{R}_\lambda^{(2)} = \sum_{i=1}^{76} c_i^{(\lambda)} r_i \,, \tag{4.245}$$

for some rational numbers $c_i^{(\lambda)}$. As we will see, this is correct.

One might argue that such a guess is a bit far-fetched. The choice of which rational functions we consider as separate in the planar hard function, for instance, is completely arbitrary, and highly depends on the specific expression of the result. Different people may have different tastes in this regard, and might thus come up with different guesses for the basis of rational functions. Even so, it would still be convenient to attempt this approach. Constructing such a simple ansatz costs no effort and is very quick. If it is incorrect, there is no solution for the constant coefficients. There is no risk of ending up with a wrong result, and no reason to despair (typically). In fact, even without having any idea about the form of the result, we can still reconstruct it analytically from the evaluation in a finite number of random points. This idea reaches its peak of performance in the combination of finite field arithmetics (also known as modular arithmetics) and multivariate functional reconstruction algorithms [171, 172], implemented in the extremely flexible framework FiniteFlow [173]. Moreover, even when a full-fledged finite field reconstruction is needed, having a basis that covers a good portion of the functions appearing in the result can reduce the complexity of the problem.[6] If the ansatz is correct, on the other hand, the result is reconstructed from just as many evaluations as the number of unfixed constants, which is typically much smaller than the number of evaluations required by even the most efficient reconstruction algorithm.

4.5.4 *How to Express the Integrand in Terms of Inverse Propagators*

Our starting point is the integrand computed in Ref. [29] using modern generalised unitarity techniques. I show it in a pictorial way in Fig. 4.5. It is given as a sum over all the permutations of the external legs of a summand, written in terms of colour factors and integrals of the families shown in Fig. 4.1. In the figure, I indicates

[6] The idea is to first reconstruct only the linear relations among the functions that need to be reconstructed—e.g. the rational prefactors of the iterated integrals or of a transcendental function basis—together with the ones we guessed. This typically requires fewer evaluations than the full reconstruction. We can then use the linear relations to express the most complicated functions in terms of simpler ones and of functions we guessed, which do not need to be reconstructed at all. Note that this pays off only if the functions which remain to be reconstructed require fewer evaluations than the original ones. For this reason having a good guess can be crucial.

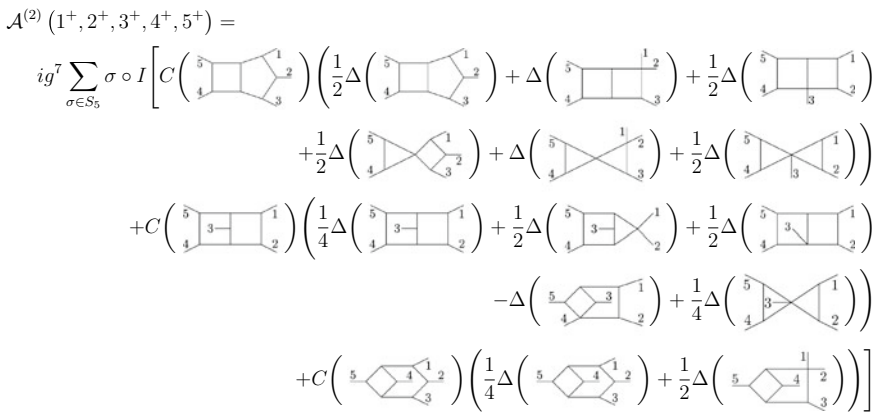

Fig. 4.5 Pictorial representation of the two-loop five-gluon all-plus amplitude in pure Yang-Mills theory as presented in Ref. [29]

loop integration and $C(X)$ stands for the colour factor of the diagram X, which we express as a vector in the colour basis $\{\mathcal{T}_\lambda\}_{\lambda=1}^{22}$ defined in Eqs. (4.65) and (4.66). Finally, $\Delta(X)$ indicates that the Feynman integral X is decorated with a numerator dependent on the loop momenta. For the explicit expressions of the latter I refer to the original paper [29]. What matters here is that the numerators are written in terms of the $D > 4$-dimensional part of the loop momenta, the so-called "μ *terms*."

A loop momentum k_i in $D = 4 - 2\epsilon$ dimensions can be decomposed as

$$k_i = k_i^{[4]} + k_i^{[-2\epsilon]}\,, \tag{4.246}$$

where $k_i^{[4]}$ lives in the same four-dimensional subspace as the external momenta p_i, and all the extra dimensionality is contained in $k_i^{[-2\epsilon]}$. The latter is perpendicular to the four-dimensional subspace,

$$k_i^{[-2\epsilon]} \cdot k_j^{[4]} = 0 = k_i^{[-2\epsilon]} \cdot p_j \quad \forall i = 1, 2\,, \forall j = 1, \ldots, 5\,. \tag{4.247}$$

In the regularisation scheme we adopted, therefore, only the scalar products involving two loop momenta receive contribution from the extra dimensions,

$$\mu_{ij} = k_i^{[-2\epsilon]} \cdot k_j^{[-2\epsilon]}\,. \tag{4.248}$$

In other words, the extra dimensionality of a loop integrand can be entirely described by of these μ terms. At two loops there are three of them: μ_{11}, μ_{12}, and μ_{22}. In order to employ the IBP machinery, we need to rewrite them in terms of inverse propagators and kinematic variables.

In Sect. 4.2.1 we have seen another way of capturing the extra dimensionality of the loop integrands, namely through Gram determinants involving the loop momenta. Clearly the Gram determinants must be related to the μ terms, and indeed offer one way to rewrite the latter in terms of inverse propagators,

$$\mu_{ij} = \frac{1}{2\Delta} \text{det}G \begin{pmatrix} k_i, p_1, p_2, p_3, p_4 \\ k_j, p_1, p_2, p_3, p_4 \end{pmatrix} , \tag{4.249}$$

where I recall that the Gram matrix of two sets of momenta is defined by Eq. (4.18). The Gram determinant in this relation evaluates to a polynomial in the scalar products of loop and external momenta, which can then expressed in terms of inverse propagators using simple linear algebra. Proving Eq. (4.249) is rather easy. First, note that only the extra-dimensional part of the loop momenta give a non-vanishing contribution to the Gram determinant on the right-hand side of Eq. (4.249),

$$\text{det}G \begin{pmatrix} k_i, p_1, p_2, p_3, p_4 \\ k_j, p_1, p_2, p_3, p_4 \end{pmatrix} = \text{det}G \begin{pmatrix} k_i^{[-2\epsilon]}, p_1, p_2, p_3, p_4 \\ k_j^{[-2\epsilon]}, p_1, p_2, p_3, p_4 \end{pmatrix} , \tag{4.250}$$

because the four-dimensional parts of the loop momenta are linearly dependent on the external momenta $\{p_i\}_{i=1}^4$. Since $k_i^{[-2\epsilon]}$ is perpendicular to the external momenta, the only term which survives in the determinant is the one proportional to $k_i^{[-2\epsilon]} \cdot k_j^{[-2\epsilon]}$,

$$\text{det}G \begin{pmatrix} k_i^{[-2\epsilon]}, p_1, p_2, p_3, p_4 \\ k_j^{[-2\epsilon]}, p_1, p_2, p_3, p_4 \end{pmatrix} = 2(k_i^{[-2\epsilon]} \cdot k_j^{[-2\epsilon]}) \text{det}G \begin{pmatrix} p_1, p_2, p_3, p_4 \\ p_1, p_2, p_3, p_4 \end{pmatrix} . \tag{4.251}$$

Putting together Eqs. (4.250) and (4.251) and recalling the definitions of the Gram determinant of the external legs Δ and of the μ terms then gives Eq. (4.249).

Having dealt with the μ terms, there is one last ingredient of the integrand of Ref. [29] which requires some work to be expressed in terms of inverse propagators: the spinor chains involving a loop momentum k_j, such as

$$\langle i|k_j|k]\langle kl\rangle[li] , \tag{4.252}$$

where k_i is understood as the double spinor $k_{i\,\alpha\dot{\alpha}} = k_{i\,\mu}(\sigma^\mu)_{\alpha\dot{\alpha}}$, with $\sigma^\mu = (\mathbb{1}, \vec{\sigma})$ being the four-vector of the Pauli matrices σ_i (see e.g. any of Refs. [56, 57, 174] for a pedagogical discussion of the spinor-helicity formalism). In order to deal with spinor chains such as the one given by Eq. (4.252), let us take one step back and trade k_j for an external momentum p_j. Then, the trace in the $SU(2)$ indices can be turned into a trace in the Dirac indices through the well-known relation

$$\langle ij\rangle[jk]\langle kl\rangle[li] = \text{tr}\left[\frac{1-\gamma_5}{2} \not{p}_i \not{p}_j \not{p}_k \not{p}_l\right] . \tag{4.253}$$

This identity actually holds also if one of the light-like momenta, say p_j, is substituted by an off-shell momentum k_j,

$$\langle i|k_j|k]\langle kl\rangle[li] = \mathrm{tr}\left[\frac{1-\gamma_5}{2}\not{p}_i\not{k}_j\not{p}_k\not{p}_l\right] . \tag{4.254}$$

Since the external momenta p_i lie in the four-dimensional subspace, also any complex vector $\lambda_i\tilde{\lambda}_j$ does, so that—because of Eq. (4.247)—the left-hand side of Eq. (4.254) only sees the four-dimensional component of the off-shell momentum, $k_j^{[4]}$. The latter can always be decomposed into two auxiliary four-dimensional light-like momenta $n^{(a)}$,

$$k_j^{[4]} = \sum_{a=1}^{2} n^{(a)} . \tag{4.255}$$

For each of the light-like momenta $n^{(a)}$ Eq. (4.253) holds, and the linearity of the trace then implies Eq. (4.254). The use of Eq. (4.254) produces ϵ-contractions involving loop momenta,

$$\mathrm{tr}\left(\gamma_5\not{p}_i\not{k}_j\not{p}_k\not{p}_l\right) = -4i\epsilon\left(p_i, k_j, p_k, p_l\right) , \tag{4.256}$$

which also need to be rewritten in terms of scalar products and tr_5. In order to do this, consider the identity relating the product of two Levi-Civita symbols to the metric tensor $g^{\mu\nu}$,

$$\epsilon^{\mu_1\mu_2\mu_3\mu_4}\epsilon^{\nu_1\nu_2\nu_3\nu_4} = -\det\left(g^{\mu_i\nu_j}\right) , \tag{4.257}$$

where the factor of -1 comes from the Minkowskian signature, and on the right-hand side there is the determinant of the matrix whose entries are $g^{\mu_i\nu_j}$, with $i, j = 1, \ldots, 4$. It follows that an ϵ-contraction involving one loop momentum k_i can be rewritten as

$$\epsilon(k_i, p_j, p_k, p_l) = \frac{i}{4\,\mathrm{tr}_5}\mathrm{det}G\begin{pmatrix} k_i, p_j, p_k, p_l \\ p_1, p_2, p_3, p_4 \end{pmatrix} , \tag{4.258}$$

where we used that $\mathrm{tr}_5 = -4i\epsilon(p_1, p_2, p_3, p_4)$, and the Gram determinant is defined by Eq. (4.18). On the right-hand side of Eq. (4.258) the loop momentum k_i appears only in scalar products, and thus in inverse propagators. There is however a subtlety. The identity (4.257) is four-dimensional, whereas the Gram determinant is defined for D-dimensional vectors. One has thus to be careful when using Eq. (4.258). On the left-hand side, the loop momentum k_i is projected onto the four-dimensional subspace by the Levi-Civita symbol. On the right-hand side, the loop momentum k_i always appears in scalar products with the external momenta p_i, and is thus projected on the four-dimensional subspace as well. Only the four-dimensional component of

k_i thus contributes on both sides. This happens because we have chosen the auxiliary set of momenta in the Gram determinant—i.e. the lower one—to be made by four-dimensional momenta only. For this reason, Eq. (4.258) holds also if there is more than one loop momentum in the ϵ-contraction on the left-hand side, but fails if a loop momentum is present in the auxiliary set of vectors, too. Let us consider, for instance, a product of two ϵ-contractions both containing a loop momentum, e.g.

$$\epsilon(k_i, p_1, p_2, p_3)\epsilon(k_j, p_1, p_2, p_3)\,. \tag{4.259}$$

One might naïvely use Eq. (4.257) to rewrite this product as

$$\epsilon(k_i, p_1, p_2, p_3)\epsilon(k_j, p_1, p_2, p_3) = -\frac{1}{16}\text{det}G\begin{pmatrix} k_i, p_1, p_2, p_3 \\ k_j, p_1, p_2, p_3 \end{pmatrix}\,. \tag{4.260}$$

This is wrong, because Eq. (4.257) holds only in $D = 4$ dimensions. On the right-hand side there are contributions from the extra-dimensional components $k_i^{[-2\epsilon]}$ and $k_j^{[-2\epsilon]}$, which are instead absent on the left-hand side. Equation (4.260) therefore needs to be corrected by some μ-terms (4.248),

$$\epsilon(k_i, p_1, p_2, p_3)\epsilon(k_j, p_1, p_2, p_3) = -\frac{1}{16}\text{det}G\begin{pmatrix} k_i, p_1, p_2, p_3 \\ k_j, p_1, p_2, p_3 \end{pmatrix} + (\mu \text{ terms})\,. \tag{4.261}$$

On the other hand, it is straightforward to rewrite correctly a product of two ϵ-contractions containing loop momenta such as Eq. (4.259) by applying Eq. (4.258) to each of the ϵ-contractions separately, so that the loop momenta are everywhere projected onto the four-dimensional subspace, as they should. By comparing the outcome of the two different procedures, we can also fix the μ-terms needed to correct Eq. (4.260),

$$(\mu \text{ terms}) = \frac{s_{12}s_{23}(s_{12} + s_{23} - s_{45})}{2}\mu_{12}\,. \tag{4.262}$$

Using Eqs. (4.249) and (4.254) we can express the integrand of Ref. [29] in terms of inverse propagators, and feed it into the IBP machinery. I discuss all the steps which take us from the integrand to the fully-analytic result for the hard function in the next section.

4.5.5 Computation of the Hard Function

The procedure discussed in the previous section returns a form of the integrand which can be immediately fed into the usual IBP workflow. Conceptually there is no difference in the next steps with respect to what we have already done for the

maximally supersymmetric amplitudes in Sect. 4.3. There is however an important practical difference. The integrand of the two-loop five-particle all-plus amplitude in pure Yang-Mills theory features numerators with up to degree five for the eight-propagator integrals shown in Fig. 4.1, and six for some of the one-loop squared sectors. This is substantially higher as compared to the $\mathcal{N} = 4$ super Yang-Mills and $\mathcal{N} = 8$ supergravity amplitudes, whose integrands have numerators with up to degree one and two in the loop momenta, respectively. This means that the IBPs identities required to reduce the all-plus amplitude to basis integrals are dramatically more complicated. Recent conceptual and technical advances have finally brought the solution of IBP systems of such a complexity within reach. In particular, what was crucial in our computation was the finite-field method [171–173].

In the maximally supersymmetric theories discussed in Sect. 4.3 we have simplified the sums over the permutations of the external legs in the amplitudes by performing them "numerically," i.e. we evaluated the rational functions in random rational kinematic points. The analytic results were recovered from a small number of evaluations by fitting well-motivated ansätze. The basic idea of finite fields is similar: the rational functions are evaluated in random rational kinematic points modulo some (big) prime number. This ensures that there is no loss of accuracy, which would occur using floating point numbers, and no overflow, which could instead occur if arbitrarily large integers were allowed to appear. Note that also ϵ can be evaluated numerically. The fully analytic result can then be recovered from a finite number of evaluations using very efficient multi-variate functional reconstruction algorithms. The different evaluations are independent and can therefore be carried out in parallel on a computing cluster. We used the framework FINITEFLOW [173], which combines the "speed" of C++ with the flexibility and user-friendliness of a MATHEMATICA interface.

One important advantage of using finite fields is that we can really target what we are interested in, namely the amplitude or hard function, and treat *all* the intermediate steps numerically. In particular, one is in general not interested in the solution of the IBP system on its own. It is typically more complicated than the amplitude itself, and its purpose is usually only to express the un-integrated amplitude in terms of basis integrals. Determining the solution of the IBP system analytically may often be a waste of time. All the steps from the integrand[7] to the integrated hard function can be performed numerically over finite fields, including the solution of the IBP system. Only the final expression for the hard function is then reconstructed analytically. This strategy has by now become the state of the art, and several cutting-edge computations have benefited from it. Just to mention one example, see the computation of all the two-loop five-parton amplitudes in planar QCD in the Euclidean scattering region [6, 8]. More recently there have been even further advances in simplifying the system of IBP relations [175] and the coefficients of the IBP reductions [176].

In Sect. 4.5.3 we made a reasonable ansatz for the two-loop five-gluon all-plus amplitude. In such a case it is not necessary to perform a full-fledged functional reconstruction. We just need to "fit" the constants in the ansatz. However, one of

[7] Even the integrand can be constructed using finite fields.

our main goals is to assess the feasibility of the computation of non-planar five-parton amplitudes at two loops in general. For this reason, we also carried out the computation ignoring the ansatz. We set up a system of IBPs identities with the help of LiteRed [177]. We solve it over finite fields to express the one and two-loop integrands in terms of pure basis integrals (see Sect. 4.2). We use the differential equations in the canonical form and the boundary constants discussed in Sect. 4.2 to rewrite all the pure integrals in terms of Chen's iterated integrals. We assemble the two amplitudes in the hard function as shown in Eq. (4.237). In order to have a common notation, we express also the infrared pole operator $\tilde{\mathbf{Z}}_5$ in terms of iterated integrals. At every step the rational functions are evaluated in a random (rational) kinematic point (including ϵ) modulo some prime number. Finally, we reconstruct analytically the rational factors of the iterated integrals and of the transcendental constants. The workflow is implemented in the framework FiniteFlow [173].

4.5.6 Result

Expressing all the ingredients of the hard function in terms of Chen's iterated integrals offers a useful practical advantage: all the simplifications due to functional relations among the transcendental functions are automatically implemented. Before carrying out the functional reconstruction we can already see marvellous simplifications: all the weight one, three and four iterated integrals cancel out altogether. Only the weight-two iterated integrals survive, which can be easily expressed in terms of (products of) logarithms and dilogarithms, e.g.

$$[W_1]_{s_0}(s) = \log\left(\frac{s_{12}}{3}\right), \tag{4.263}$$

$$\left[\frac{W_5}{W_2}, \frac{W_{12}}{W_2}\right]_{s_0}(s) = -\mathrm{Li}_2\left(1 - \frac{s_{51}}{s_{23}}\right). \tag{4.264}$$

All the relevant functions are manifestly real valued in the s_{12}-channel. The imaginary parts appear explicitly through the boundary values. Moreover, all logarithms and dilogarithms, including their imaginary parts, can be absorbed into permutations of the one-mass box functions defined in Eq. (4.240). Finally, the functional reconstruction shows that the two-loop hard function has precisely the form we guessed in Sect. 4.5.3. After some effort to simplify the expression, the result fits in just two lines,

$$\begin{aligned}\mathcal{H}_{13}^{(2,1)} = \sum_{\sigma\in S_{\mathcal{T}_{13}}} \sigma\circ\Bigg\{6\kappa^2\left[\frac{3}{2}\frac{[12]^2}{\langle 34\rangle\langle 45\rangle\langle 53\rangle} - \frac{s_{23}\,\mathrm{tr}_-(1345)}{s_{34}\,\langle 12\rangle\langle 23\rangle\langle 34\rangle\langle 45\rangle\langle 51\rangle}\right] + \\ + \kappa\,\frac{[15]^2}{\langle 23\rangle\langle 34\rangle\langle 42\rangle}\left[I_{234;15} + I_{243;15} - I_{324;15} - 4\,I_{345;12} - 4\,I_{354;12} - 4\,I_{435;12}\right]\Bigg\},\end{aligned} \tag{4.265}$$

where

$$\mathrm{tr}_-(ijkl) = \frac{1}{2}\mathrm{tr}\left((1-\gamma_5)\not{p}_i\not{p}_j\not{p}_k\not{p}_l\right) = \langle ij\rangle[jk]\langle kl\rangle[li]\,. \tag{4.266}$$

All the other partial amplitudes can be obtained from Eqs. (4.243) and (4.265) through permutations of the external legs and colour relations (see Eq. (4.221) and below). Thanks to the simplicity of the special functions involved, the resulting expressions for the independent partial amplitudes can be analytically continued to any other region by simply adding a small positive imaginary part to each two-particle Mandelstam invariant.

A number of non-trivial checks proves the validity of our result. The planar part agrees with the previous computations [1, 4]. The ultraviolet poles of the amplitudes cancel out upon renormalisation, and the infrared poles factorise as they should (see Sect. 4.5.2). The agreement of the hard function with the expected form argued in Sect. 4.5.3 based on four-dimensional unitarity and leading singularities, with the enormous cancellations involved in the intermediate steps, is also a strong indication that the result is correct. Furthermore, we also verified that our expression for the two-loop amplitude exhibits the correct leading behaviour in the collinear limit. In particular, we checked the limits $p_1 \parallel p_2$, $p_2 \parallel p_3$ and $p_3 \parallel p_4$ of the double trace term $\mathcal{T}_{13}$. In the first one, for instance, the two-loop all-plus amplitude is expected to factorise as

$$\begin{aligned}\lim_{p_1\parallel p_2}\mathcal{A}^{(2)}(1^+,2^+,3^+,4^+,5^+) \sim\ & \mathrm{Split}^{(0)}(-P^-;1^+,2^+)\,\mathcal{A}^{(2)}(P^+,3^+,4^+,5^+)+\\ &+\mathrm{Split}^{(1)}(-P^-;1^+,2^+)\,\mathcal{A}^{(1)}(P^+,3^+,4^+,5^+)+\\ &+\mathrm{Split}^{(1)}(-P^+;1^+,2^+)\,\mathcal{A}^{(1)}(P^-,3^+,4^+,5^+)\,,\end{aligned} \tag{4.267}$$

where we must sum over the colour index of the intermediate gluon labelled by "P." After inserting the expressions of the splitting amplitudes $\mathrm{Split}^{(\ell)}$ [168, 178–180] and of the four-gluon amplitudes [181, 182], we decompose the collinear limit in the basis $\{\mathcal{T}_\lambda\}_{\lambda=1}^{22}$ defined by Eqs. (4.65) and (4.66). The component of the two-loop hard function corresponding to the double trace $\mathcal{T}_{13}$ vanishes in the limits $p_1 \parallel p_2$ and $p_2 \parallel p_3$, but has a non-trivial structure in the limit $p_3 \parallel p_4$. Finally, there is agreement with the independent computation of Ref. [28].

4.5.7 Discussion

In this section I have presented the analytic computation of the five-gluon all-plus helicity amplitude at two loops in pure Yang-Mills theory. This was the very first fully-analytic result for a full-colour two-loop five-particle amplitude. The hard function has a remarkably simple form, which we could anticipate based on four-dimensional unitarity and leading singularities. The polylogarithmic part can be entirely expressed

in terms of the finite part of the one-mass box integral. Intriguingly, the rational prefactors of the latter are conformally invariant. In another work, which I do not discuss in this thesis, my collaborators and I showed this to be related to the conformal invariance of the one-loop all-plus amplitude [30].

The work presented in this chapter has opened the door for the analytic computation of all two-loop five-parton amplitudes in QCD. The complete information on all the relevant Feynman integrals integrals is now available in the physical scattering region. Furthermore, the IBP reductions carried out in this computation are of comparable complexity as to what is expected to be required for other helicity amplitudes, or amplitudes including fermions.

Bibliography

1. Gehrmann T, Henn J, Lo Presti N (2016) Analytic form of the two-loop planar five-gluon all-plus-helicity amplitude in QCD. Phys Rev Lett 116:062001. https://doi.org/10.1103/PhysRevLett.116.062001. arXiv:1511.05409
2. Papadopoulos CG, Tommasini D, Wever C (2016) The pentabox master integrals with the simplified differential equations approach. JHEP 04:078. https://doi.org/10.1007/JHEP04(2016)078. arXiv:1511.09404
3. Gehrmann T, Henn J, Lo Presti N (2018) Pentagon functions for massless planar scattering amplitudes. JHEP 10:103. https://doi.org/10.1007/JHEP10(2018)103. arXiv:1807.09812
4. Dunbar DC, Perkins WB (2016) Two-loop five-point all plus helicity Yang-Mills amplitude. Phys Rev D93:085029. https://doi.org/10.1103/PhysRevD.93.085029. arXiv:1603.07514
5. Badger S, Brönnum-Hansen C, Hartanto HB, Peraro T (2019) Analytic helicity amplitudes for two-loop five-gluon scattering: the single-minus case. JHEP 01:186. https://doi.org/10.1007/JHEP01(2019)186. arXiv:1811.11699
6. Abreu S, Febres Cordero F, Ita H, Page B, Sotnikov V (2018) Planar two-loop five-parton amplitudes from numerical unitarity. JHEP 11:116. https://doi.org/10.1007/JHEP11(2018)116. arXiv:1809.09067
7. Abreu S, Dormans J, Febres Cordero F, Ita H, Page B (2019) Analytic form of planar two-loop five-gluon scattering amplitudes in QCD. Phys Rev Lett 122:082002. https://doi.org/10.1103/PhysRevLett.122.082002. arXiv:1812.04586
8. Abreu S, Dormans J, Febres Cordero F, Ita H, Page B, Sotnikov V (2019) Analytic form of the planar two-loop five-parton scattering amplitudes in QCD. JHEP 05:084. https://doi.org/10.1007/JHEP05(2019)084. arXiv:1904.00945
9. Chawdhry HA, Czakon ML, Mitov A, Poncelet R (2020) NNLO QCD corrections to three-photon production at the LHC. JHEP 02:057. https://doi.org/10.1007/JHEP02(2020)057. arXiv:1911.00479
10. Kallweit S, Sotnikov V, Wiesemann M. Triphoton production at hadron colliders in NNLO QCD. arXiv:2010.04681
11. Abreu S, Page B, Pascual E, Sotnikov V. Leading-color two-loop QCD corrections for three-photon production at hadron colliders. arXiv:2010.15834
12. Papadopoulos CG, Wever C (2020) Internal reduction method for computing Feynman integrals. JHEP 02:112. https://doi.org/10.1007/JHEP02(2020)112. arXiv:1910.06275
13. Abreu S, Ita H, Moriello F, Page B, Tschernow W, Zeng M. Two-loop integrals for planar five-point one-mass processes. arXiv:2005.04195
14. Canko DD, Papadopoulos CG, Syrrakos N. Analytic representation of all planar two-loop five-point master integrals with one off-shell leg. arXiv:2009.13917

15. Chicherin D, Gehrmann T, Henn J, Lo Presti N, Mitev V, Wasser P (2019) Analytic result for the nonplanar hexa-box integrals. JHEP 03:042. https://doi.org/10.1007/JHEP03(2019)042. arXiv:1809.06240
16. Chicherin D, Henn J, Mitev V (2018) Bootstrapping pentagon functions. JHEP 05:164. https://doi.org/10.1007/JHEP05(2018)164. arXiv:1712.09610
17. Chicherin D, Henn JM, Sokatchev E (2018) Scattering amplitudes from superconformal ward identities. Phys Rev Lett 121:021602. https://doi.org/10.1103/PhysRevLett.121.021602. arXiv:1804.03571
18. Chicherin D, Henn J, Sokatchev E (2018) Implications of nonplanar dual conformal symmetry. JHEP 09:012. https://doi.org/10.1007/JHEP09(2018)012. arXiv:1807.06321
19. Abreu S, Page B, Zeng M (2019) Differential equations from unitarity cuts: nonplanar hexa-box integrals. JHEP 01:006. https://doi.org/10.1007/JHEP01(2019)006. arXiv:1807.11522
20. Abreu S, Dixon LJ, Herrmann E, Page B, Zeng M (2019) The two-loop five-point amplitude in $\mathcal{N} = 4$ super-Yang-Mills theory. Phys Rev Lett 122:121603. https://doi.org/10.1103/PhysRevLett.122.121603. arXiv:1812.08941
21. Chicherin D, Gehrmann T, Henn J, Wasser P, Zhang Y, Zoia S (2019) All master integrals for three-jet production at next-to-next-to-leading order. Phys Rev Lett 123:041603. https://doi.org/10.1103/PhysRevLett.123.041603. arXiv:1812.11160
22. Chicherin D, Gehrmann T, Henn J, Wasser P, Zhang Y, Zoia S (2019) Analytic result for a two-loop five-particle amplitude. Phys Rev Lett 122:121602. https://doi.org/10.1103/PhysRevLett.122.121602. arXiv:1812.11057
23. Chicherin D, Gehrmann T, Henn JM, Wasser P, Zhang Y, Zoia S (2019) The two-loop five-particle amplitude in $\mathcal{N} = 8$ supergravity. JHEP 03:115. https://doi.org/10.1007/JHEP03(2019)115. arXiv:1901.05932
24. Abreu S, Dixon LJ, Herrmann E, Page B, Zeng M (2019) The two-loop five-point amplitude in $\mathcal{N} = 8$ supergravity. JHEP 03:123. https://doi.org/10.1007/JHEP03(2019)123. arXiv:1901.08563
25. Carrasco JJ, Johansson H (2012) Five-point amplitudes in $N = 4$ super-Yang-Mills theory and $N = 8$ supergravity. Phys Rev D85:025006. https://doi.org/10.1103/PhysRevD.85.025006. arXiv:1106.4711
26. Caron-Huot S, Chicherin D, Henn J, Zhang Y, Zoia S (2020) Multi-Regge limit of the two-loop five-point amplitudes in $\mathcal{N} = 4$ super Yang-Mills and $\mathcal{N} = 8$ supergravity. JHEP 10:188. https://doi.org/10.1007/JHEP10(2020)188. arXiv:2003.03120
27. Badger S, Chicherin D, Gehrmann T, Heinrich G, Henn J, Peraro T, et al (2019) Analytic form of the full two-loop five-gluon all-plus helicity amplitude. Phys Rev Lett 123:071601. https://doi.org/10.1103/PhysRevLett.123.071601. arXiv:1905.03733
28. Dunbar DC, Godwin JH, Perkins WB, Strong JM (2020) Color dressed unitarity and recursion for Yang-Mills two-loop all-plus amplitudes. Phys Rev D 101:016009. https://doi.org/10.1103/PhysRevD.101.016009. arXiv:1911.06547
29. Badger S, Mogull G, Ochirov A, O'Connell D (2015) A complete two-loop, five-gluon helicity amplitude in Yang-Mills theory. JHEP 10:064. https://doi.org/10.1007/JHEP10(2015)064. arXiv:1507.08797
30. Henn J, Power B, Zoia S (2020) Conformal invariance of the one-loop all-plus helicity scattering amplitudes. JHEP 02:019. https://doi.org/10.1007/JHEP02(2020)019. arXiv:1911.12142
31. Gehrmann T, Remiddi E (2001) Two loop master integrals for gamma* —> 3 jets: the planar topologies. Nucl Phys B 601:248. https://doi.org/10.1016/S0550-3213(01)00057-8. arXiv:hep-ph/0008287
32. Gehrmann T, Remiddi E (2001) Two loop master integrals for gamma* –> 3 jets: the non-planar topologies. Nucl Phys B 601:287. https://doi.org/10.1016/S0550-3213(01)00074-8. arXiv:hep-ph/0101124
33. Wasser P (2018) Analytic properties of Feynman integrals for scattering amplitudes. PhD thesis, Mainz U
34. Henn J, Mistlberger B, Smirnov VA, Wasser P (2020) Constructing d-log integrands and computing master integrals for three-loop four-particle scattering. JHEP 04:167. https://doi.org/10.1007/JHEP04(2020)167. arXiv:2002.09492

35. Bern Z, Herrmann E, Litsey S, Stankowicz J, Trnka J (2016) Evidence for a nonplanar amplituhedron. JHEP 06:098. https://doi.org/10.1007/JHEP06(2016)098. arXiv:1512.08591
36. Baikov P (1997) Explicit solutions of the multiloop integral recurrence relations and its application. Nucl Instrum Meth A 389:347. https://doi.org/10.1016/S0168-9002(97)00126-5. arXiv:hep-ph/9611449
37. Baikov P (1996) Explicit solutions of the three loop vacuum integral recurrence relations. Phys Lett B 385:404. https://doi.org/10.1016/0370-2693(96)00835-0. arXiv:hep-ph/9603267
38. Frellesvig H, Papadopoulos CG (2017) Cuts of Feynman integrals in Baikov representation. JHEP 04:083. https://doi.org/10.1007/JHEP04(2017)083. arXiv:1701.07356
39. Bosma J, Sogaard M, Zhang Y (2017) Maximal cuts in arbitrary dimension. JHEP 08:051. https://doi.org/10.1007/JHEP08(2017)051. arXiv:1704.04255
40. Harley M, Moriello F, Schabinger RM (2017) Baikov-Lee representations of cut Feynman integrals. JHEP 06:049. https://doi.org/10.1007/JHEP06(2017)049. arXiv:1705.03478
41. Greuel G-M, Pfister G (2007) A singular introduction to commutative algebra, 2nd edn. Springer, Incorporated
42. Decker W, Greuel GM, Pfister G, Schönemann H (2018) SINGULAR 4-1-1 — a computer algebra system for polynomial computations. http://www.singular.uni-kl.de
43. Steinmann O (1960) Über den Zusammenhang zwischen den Wightmanfunktionen und der-retardierten Kommutatoren. Helv. Physica Acta 33:257
44. Steinmann O (1960) Wightman-Funktionen und retardierten Kommutatoren. II. Helv. Physica Acta 33:347
45. Cahill KE, Stapp HP (1975) Optical theorems and Steinmann relations. Ann Phys 90:438. https://doi.org/10.1016/0003-4916(75)90006-8
46. Britto R, Cachazo F, Feng B, Witten E (2005) Direct proof of tree-level recursion relation in Yang-Mills theory. Phys Rev Lett 94:181602. https://doi.org/10.1103/PhysRevLett.94.181602. arXiv:hep-th/0501052
47. Hodges A (2013) Eliminating spurious poles from gauge-theoretic amplitudes. JHEP 05:135. https://doi.org/10.1007/JHEP05(2013)135. arXiv:0905.1473
48. Bern Z, Dixon LJ, Kosower DA (1993) One loop corrections to five gluon amplitudes. Phys Rev Lett 70:2677. https://doi.org/10.1103/PhysRevLett.70.2677. arXiv:hep-ph/9302280
49. Badger S (2016) Automating QCD amplitudes with on-shell methods. J Phys Conf Ser 762:012057. https://doi.org/10.1088/1742-6596/762/1/012057. arXiv:1605.02172
50. Chicherin D, Sotnikov V. Pentagon functions for scattering of five massless particles. arXiv:2009.07803
51. Henn JM, Mistlberger B (2019) Four-graviton scattering to three loops in $\mathcal{N} = 8$ supergravity. JHEP 05:023. https://doi.org/10.1007/JHEP05(2019)023. arXiv:1902.07221
52. Borowka S, Heinrich G, Jahn S, Jones S, Kerner M, Schlenk J, et al (2018) pySecDec: a toolbox for the numerical evaluation of multi-scale integrals. Comput Phys Commun 222:313. https://doi.org/10.1016/j.cpc.2017.09.015. arXiv:1703.09692
53. Borowka S, Heinrich G, Jahn S, Jones S, Kerner M, Schlenk J (2019) A GPU compatible quasi-Monte Carlo integrator interfaced to pySecDec. Comput Phys Commun 240:120. https://doi.org/10.1016/j.cpc.2019.02.015. arXiv:1811.11720
54. Derkachov S, Honkonen J, Pis'mak Y (1990) Three-loop calculation of the random walk problem: an application of dimensional transformation and the uniqueness method. J Phys A Math Gen 23:5563. https://doi.org/10.1088/0305-4470/23/23/028
55. Tarasov O (1996) Connection between Feynman integrals having different values of the space-time dimension. Phys Rev D 54:6479. https://doi.org/10.1103/PhysRevD.54.6479. arXiv:hep-th/9606018
56. Henn JM, Plefka JC (2014) Scattering amplitudes in gauge theories, vol 883. Springer, Berlin. https://doi.org/10.1007/978-3-642-54022-6
57. Elvang H, Huang Y-t (2015) Scattering amplitudes in gauge theory and gravity, vol 4. Cambridge University Press
58. Edison AC, Naculich SG (2012) SU(N) group-theory constraints on color-ordered five-point amplitudes at all loop orders. Nucl Phys B 858:488. https://doi.org/10.1016/j.nuclphysb.2012.01.019. arXiv:1111.3821

59. Bern Z, Kosower DA (1991) Color decomposition of one loop amplitudes in gauge theories. Nucl Phys B 362:389. https://doi.org/10.1016/0550-3213(91)90567-H
60. Parke SJ, Taylor TR (1986) Amplitude for n-gluon scattering. Phys Rev Lett 56:2459. https://doi.org/10.1103/PhysRevLett.56.2459
61. Nair V (1988) A current algebra for some gauge theory amplitudes. Phys Lett B 214:215. https://doi.org/10.1016/0370-2693(88)91471-2
62. Bern Z, Dixon L, Dunbar DC, Kosower DA (1997) One-loop self-dual and $N = 4$ super Yang-Mills. Phys Lett B 394:105. https://doi.org/10.1016/S0370-2693(96)01676-0. arXiv:hep-th/9611127
63. Berends F, Giele W, Kuijf H (1988) On relations between multi-gluon and multi-graviton scattering. Phys Lett B 211:91. https://doi.org/10.1016/0370-2693(88)90813-1
64. Bern Z, Dixon LJ, Perelstein M, Rozowsky JS (1999) Multileg one loop gravity amplitudes from gauge theory. Nucl Phys B546:423. https://doi.org/10.1016/S0550-3213(99)00029-2. arXiv:hep-th/9811140
65. Arkani-Hamed N, Bourjaily JL, Cachazo F, Trnka J (2012) Local integrals for planar scattering amplitudes. JHEP 06:125. https://doi.org/10.1007/JHEP06(2012)125. arXiv:1012.6032
66. Henn JM (2013) Multiloop integrals in dimensional regularization made simple. Phys Rev Lett 110:251601. https://doi.org/10.1103/PhysRevLett.110.251601. arXiv:1304.1806
67. Arkani-Hamed N, Bourjaily JL, Cachazo F, Goncharov AB, Postnikov A, Trnka J (2016) Grassmannian geometry of scattering amplitudes. Cambridge University Press. arXiv:1212.5605
68. Arkani-Hamed N, Bourjaily JL, Cachazo F, Trnka J (2014) Singularity structure of maximally supersymmetric scattering amplitudes. Phys Rev Lett 113:261603. https://doi.org/10.1103/PhysRevLett.113.261603. arXiv:1410.0354
69. Bern Z, Dixon LJ, Smirnov VA (2005) Iteration of planar amplitudes in maximally supersymmetric Yang-Mills theory at three loops and beyond. Phys Rev D72:085001. https://doi.org/10.1103/PhysRevD.72.085001. arXiv:hep-th/0505205
70. Dixon LJ, Drummond JM, Henn JM (2011) Bootstrapping the three-loop hexagon. JHEP 11:023. https://doi.org/10.1007/JHEP11(2011)023. arXiv:1108.4461
71. Kotikov A, Lipatov L (2007) On the highest transcendentality in $n = 4$ susy. Nucl Phys B 769:217. https://doi.org/10.1016/j.nuclphysb.2007.01.020
72. Arkani-Hamed N, Bourjaily JL, Cachazo F, Postnikov A, Trnka J (2015) On-shell structures of MHV amplitudes beyond the planar limit. JHEP 06:179. https://doi.org/10.1007/JHEP06(2015)179. arXiv:1412.8475
73. Herrmann E, Trnka J (2019) UV cancellations in gravity loop integrands. JHEP 02:084. https://doi.org/10.1007/JHEP02(2019)084. arXiv:1808.10446
74. Bourjaily JL, Herrmann E, Trnka J (2019) Maximally supersymmetric amplitudes at infinite loop momentum. Phys Rev D 99:066006. https://doi.org/10.1103/PhysRevD.99.066006. arXiv:1812.11185
75. Bern Z, Carrasco J, Johansson H (2008) New relations for Gauge-Theory amplitudes. Phys Rev D 78:085011. https://doi.org/10.1103/PhysRevD.78.085011. arXiv:0805.3993
76. Bern Z, Carrasco JJM, Johansson H (2010) Perturbative quantum gravity as a double copy of gauge theory. Phys Rev Lett 105:061602. https://doi.org/10.1103/PhysRevLett.105.061602. arXiv:1004.0476
77. Smirnov A, Chuharev F. FIRE6: Feynman Integral REduction with modular arithmetic. arXiv:1901.07808
78. Klappert J, Lange F, Maierhöfer P, Usovitsch J. Integral reduction with Kira 2.0 and finite field methods. arXiv:2008.06494
79. von Manteuffel A, Studerus C. Reduze 2 - distributed Feynman integral reduction. arXiv:1201.4330
80. Ita H (2016) Two-loop integrand decomposition into master integrals and surface terms. Phys Rev D94:116015. https://doi.org/10.1103/PhysRevD.94.116015. arXiv:1510.05626
81. Boehm J, Georgoudis A, Larsen KJ, Schönemann H, Zhang Y (2018) Complete integration-by-parts reductions of the non-planar hexagon-box via module intersections. JHEP 09:024. https://doi.org/10.1007/JHEP09(2018)024. arXiv:1805.01873

82. Bendle D, Boehm J, Decker W, Georgoudis A, Pfreundt F-J, Rahn M, et al. Integration-by-parts reductions of Feynman integrals using Singular and GPI-Space. arXiv:1908.04301
83. Mandelstam S (1984) Light-cone superspace and the finiteness of the $N = 4$ model. AIP Conf Proc 116:99. https://doi.org/10.1063/1.34597
84. Brink L, Lindgren O, Nilsson BE (1983) The ultraviolet finiteness of the $N = 4$ Yang-Mills theory. Phys Lett B 123:323. https://doi.org/10.1016/0370-2693(83)91210-8
85. Howe PS, Stelle K, Townsend P (1984) Miraculous ultraviolet cancellations in supersymmetry made manifest. Nucl Phys B 236:125. https://doi.org/10.1016/0550-3213(84)90528-5
86. Bern Z, Carrasco J, Dixon LJ, Johansson H, Roiban R (2009) The ultraviolet behavior of $N = 8$ supergravity at four loops. Phys Rev Lett 103:081301. https://doi.org/10.1103/PhysRevLett.103.081301. arXiv:0905.2326
87. Bossard G, Howe P, Stelle K (2011) On duality symmetries of supergravity invariants. JHEP 01:020. https://doi.org/10.1007/JHEP01(2011)020. arXiv:1009.0743
88. Beisert N, Elvang H, Freedman DZ, Kiermaier M, Morales A, Stieberger S (2011) E7(7) constraints on counterterms in $N = 8$ supergravity. Phys Lett B 694:265. https://doi.org/10.1016/j.physletb.2010.09.069. arXiv:1009.1643
89. Vanhove P. The critical ultraviolet behaviour of $N = 8$ supergravity amplitudes. arXiv:1004.1392
90. Bjornsson J, Green MB (2010) 5 loops in 24/5 dimensions. JHEP 08:132. https://doi.org/10.1007/JHEP08(2010)132. arXiv:1004.2692
91. Bjornsson J (2011) Multi-loop amplitudes in maximally supersymmetric pure spinor field theory. JHEP 01:002. https://doi.org/10.1007/JHEP01(2011)002. arXiv:1009.5906
92. Bossard G, Howe P, Stelle K, Vanhove P (2011) The vanishing volume of $D = 4$ superspace. Class Quant Grav 28:215005. https://doi.org/10.1088/0264-9381/28/21/215005. arXiv:1105.6087
93. Kinoshita T (1962) Mass singularities of Feynman amplitudes. J Math Phys 3:650. https://doi.org/10.1063/1.1724268
94. Lee T, Nauenberg M (1964) Degenerate systems and mass singularities. Phys Rev 133:B1549. https://doi.org/10.1103/PhysRev.133.B1549
95. Catani S (1998) The singular behavior of QCD amplitudes at two loop order. Phys Lett B427:161. https://doi.org/10.1016/S0370-2693(98)00332-3. arXiv:hep-ph/9802439
96. Sterman GF, Tejeda-Yeomans ME (2003) Multiloop amplitudes and resummation. Phys Lett B552:48. https://doi.org/10.1016/S0370-2693(02)03100-3. arXiv:hep-ph/0210130
97. Dixon LJ, Magnea L, Sterman GF (2008) Universal structure of subleading infrared poles in gauge theory amplitudes. JHEP 08:022. https://doi.org/10.1088/1126-6708/2008/08/022. arXiv:0805.3515
98. Becher T, Neubert M (2009) Infrared singularities of scattering amplitudes in perturbative QCD. Phys Rev Lett 102:162001. https://doi.org/10.1103/PhysRevLett.102.162001, https://doi.org/10.1103/PhysRevLett.111.199905, arXiv:0901.0722
99. Almelid O, Duhr C, Gardi E (2016) Three-loop corrections to the soft anomalous dimension in multileg scattering. Phys Rev Lett 117:172002. https://doi.org/10.1103/PhysRevLett.117.172002. arXiv:1507.00047
100. Korchemsky GP, Radyushkin AV (1986) Loop space formalism and renormalization group for the infrared asymptotics of QCD. Phys Lett B171:459. https://doi.org/10.1016/0370-2693(86)91439-5
101. Korchemskaya IA, Korchemsky GP (1992) On lightlike Wilson loops. Phys Lett B287:169. https://doi.org/10.1016/0370-2693(92)91895-G
102. Moch S, Vermaseren JAM, Vogt A (2004) The three loop splitting functions in QCD: the nonsinglet case. Nucl Phys B688:101. https://doi.org/10.1016/j.nuclphysb.2004.03.030. arXiv:hep-ph/0403192
103. Beisert N, Eden B, Staudacher M (2007) Transcendentality and crossing. J Stat Mech 0701:P01021. https://doi.org/10.1088/1742-5468/2007/01/P01021. arXiv:hep-th/0610251
104. Bern Z, Czakon M, Dixon LJ, Kosower DA, Smirnov VA (2007) The four-loop planar amplitude and cusp anomalous dimension in maximally supersymmetric Yang-Mills theory. Phys Rev D75:085010. https://doi.org/10.1103/PhysRevD.75.085010. arXiv:hep-th/0610248

105. Henn JM, Korchemsky GP, Mistlberger B. The full four-loop cusp anomalous dimension in $\mathcal{N} = 4$ super Yang-Mills and QCD. arXiv:1911.10174
106. von Manteuffel A, Panzer E, Schabinger RM. Analytic four-loop anomalous dimensions in massless QCD from form factors. arXiv:2002.04617
107. Weinberg S (1965) Infrared photons and gravitons. Phys Rev 140:B516. https://doi.org/10.1103/PhysRev.140.B516
108. Dunbar DC, Norridge PS (1997) Infinities within graviton scattering amplitudes. Class Quant Grav 14:351. https://doi.org/10.1088/0264-9381/14/2/009. arXiv:hep-th/9512084
109. Naculich SG, Nastase H, Schnitzer HJ (2008) Two-loop graviton scattering relation and IR behavior in $N = 8$ supergravity. Nucl Phys B805:40. https://doi.org/10.1016/j.nuclphysb.2008.07.001. arXiv:0805.2347
110. Naculich SG, Schnitzer HJ (2011) Eikonal methods applied to gravitational scattering amplitudes. JHEP 05:087. https://doi.org/10.1007/JHEP05(2011)087. arXiv:1101.1524
111. White CD (2011) Factorization properties of soft graviton amplitudes. JHEP 05:060. https://doi.org/10.1007/JHEP05(2011)060. arXiv:1103.2981
112. Akhoury R, Saotome R, Sterman G (2011) Collinear and soft divergences in perturbative quantum gravity. Phys Rev D84:104040. https://doi.org/10.1103/PhysRevD.84.104040. arXiv:1109.0270
113. Beneke M, Kirilin G (2012) Soft-collinear gravity. JHEP 09:066. https://doi.org/10.1007/JHEP09(2012)066. arXiv:1207.4926
114. Berends FA, Giele WT, Kuijf H (1988) On relations between multi-gluon and multigraviton scattering. Phys Lett B211:91. https://doi.org/10.1016/0370-2693(88)90813-1
115. Brandhuber A, Heslop P, Nasti A, Spence B, Travaglini G (2009) Four-point amplitudes in $N = 8$ supergravity and Wilson loops. Nucl Phys B807:290. https://doi.org/10.1016/j.nuclphysb.2008.09.010. arXiv:0805.2763
116. Boucher-Veronneau C, Dixon LJ (2011) $N \geq 4$ supergravity amplitudes from gauge theory at two loops. JHEP 12:046. https://doi.org/10.1007/JHEP12(2011)046. arXiv:1110.1132
117. Bern Z, Davies S, Nohle J (2014) On loop corrections to subleading soft behavior of gluons and gravitons. Phys Rev D90:085015. https://doi.org/10.1103/PhysRevD.90.085015. arXiv:1405.1015
118. Bianchi M, He S, Huang Y-t, Wen C (2015) More on soft theorems: trees, loops and strings. Phys Rev D92:065022. https://doi.org/10.1103/PhysRevD.92.065022. arXiv:1406.5155
119. Bern Z, Dixon LJ, Perelstein M, Rozowsky JS (1998) One loop n point helicity amplitudes in (selfdual) gravity. Phys Lett B444:273. https://doi.org/10.1016/S0370-2693(98)01397-5. arXiv:hep-th/9809160
120. Caron-Huot S (2011) Superconformal symmetry and two-loop amplitudes in planar $N = 4$ super Yang-Mills. JHEP 12:066. https://doi.org/10.1007/JHEP12(2011)066. arXiv:1105.5606
121. Bullimore M, Skinner D. Descent equations for superamplitudes. arXiv:1112.1056
122. Bern Z, Dixon LJ, Kosower DA (2004) Two-loop g —> gg splitting amplitudes in QCD. JHEP 08:012. https://doi.org/10.1088/1126-6708/2004/08/012. arXiv:hep-ph/0404293
123. Henn JM, Mistlberger B (2016) Four-Gluon scattering at three loops, infrared structure, and the Regge limit. Phys Rev Lett 117:171601. https://doi.org/10.1103/PhysRevLett.117.171601. arXiv:1608.00850
124. Anastasiou C, Bern Z, Dixon LJ, Kosower DA (2003) Planar amplitudes in maximally supersymmetric Yang-Mills theory. Phys Rev Lett 91:251602. https://doi.org/10.1103/PhysRevLett.91.251602. arXiv:hep-th/0309040
125. Bern Z, Czakon M, Kosower DA, Roiban R, Smirnov VA (2006) Two-loop iteration of five-point $N = 4$ super-Yang-Mills amplitudes. Phys Rev Lett 97:181601. https://doi.org/10.1103/PhysRevLett.97.181601. arXiv:hep-th/0604074
126. Cachazo F, Spradlin M, Volovich A (2006) Iterative structure within the five-particle two-loop amplitude. Phys Rev D74:045020. https://doi.org/10.1103/PhysRevD.74.045020. arXiv:hep-th/0602228

127. Drummond J, Henn J, Korchemsky G, Sokatchev E (2010) Conformal Ward identities for Wilson loops and a test of the duality with gluon amplitudes. Nucl Phys B 826:337. https://doi.org/10.1016/j.nuclphysb.2009.10.013. arXiv:0712.1223
128. Kuraev EA, Lipatov LN, Fadin VS (1976) Multi-Reggeon processes in the Yang-Mills theory. Sov Phys JETP 44:443
129. Del Duca V. An introduction to the perturbative QCD pomeron and to jet physics at large rapidities. arXiv:hep-ph/9503226
130. Lipatov LN (1994) Asymptotic behavior of multicolor QCD at high energies in connection with exactly solvable spin models. JETP Lett 59:596. arXiv:hep-th/9311037
131. Faddeev LD, Korchemsky GP (1995) High-energy QCD as a completely integrable model. Phys Lett B342:311. https://doi.org/10.1016/0370-2693(94)01363-H. arXiv:hep-th/9404173
132. Bartels J, Lipatov LN, Sabio Vera A (2009) BFKL Pomeron, Reggeized gluons and Bern-Dixon-Smirnov amplitudes. Phys Rev D80:045002. https://doi.org/10.1103/PhysRevD.80.045002. arXiv:0802.2065
133. Caron-Huot S, Dixon LJ, McLeod A, von Hippel M (2016) Bootstrapping a five-loop amplitude using Steinmann relations. Phys Rev Lett 117:241601. https://doi.org/10.1103/PhysRevLett.117.241601. arXiv:1609.00669
134. Caron-Huot S, Dixon LJ, Dulat F, von Hippel M, McLeod AJ, Papathanasiou G (2019) Six-Gluon amplitudes in planar $\mathcal{N} = 4$ super-Yang-Mills theory at six and seven loops. JHEP 08:016. https://doi.org/10.1007/JHEP08(2019)016. arXiv:1903.10890
135. Del Duca V, Druc S, Drummond JM, Duhr C, Dulat F, Marzucca R, et al. All-order amplitudes at any multiplicity in the multi-Regge limit. arXiv:1912.00188
136. Brüser R, Caron-Huot S, Henn JM (2018) Subleading Regge limit from a soft anomalous dimension. JHEP 04:047. https://doi.org/10.1007/JHEP04(2018)047. arXiv:1802.02524
137. Moult I, Vita G, Yan K. Subleading power resummation of rapidity logarithms: the energy-energy correlator in $\mathcal{N} = 4$ SYM. arXiv:1912.02188
138. Drummond JM, Henn J, Smirnov VA, Sokatchev E (2007) Magic identities for conformal four-point integrals. JHEP 01:064. https://doi.org/10.1088/1126-6708/2007/01/064. arXiv:hep-th/0607160
139. Bern Z, Enciso M, Ita H, Zeng M (2017) Dual conformal symmetry, integration-by-parts reduction, differential equations and the nonplanar sector. Phys Rev D96:096017. https://doi.org/10.1103/PhysRevD.96.096017. arXiv:1709.06055
140. Bern Z, Enciso M, Shen C-H, Zeng M. Dual conformal structure beyond the planar limit. arXiv:1806.06509
141. Ben-Israel R, Tumanov AG, Sever A. Scattering amplitudes – Wilson loops duality for the first non-planar correction. arXiv:1802.09395
142. Caron-Huot S (2015) When does the gluon reggeize? JHEP 05:093. https://doi.org/10.1007/JHEP05(2015)093. arXiv:1309.6521
143. Del Duca V, Falcioni G, Magnea L, Vernazza L (2015) Analyzing high-energy factorization beyond next-to-leading logarithmic accuracy. JHEP 02:029. https://doi.org/10.1007/JHEP02(2015)029. arXiv:1409.8330
144. Caron-Huot S, Gardi E, Vernazza L (2017) Two-parton scattering in the high-energy limit. JHEP 06:016. https://doi.org/10.1007/JHEP06(2017)016. arXiv:1701.05241
145. Bartels J, Lipatov LN, Sabio Vera A (2014) Double-logarithms in Einstein-Hilbert gravity and supergravity. JHEP 07:056. https://doi.org/10.1007/JHEP07(2014)056. arXiv:1208.3423
146. Sabio Vera A (2019) Double-logarithms in $\mathcal{N} = 8$ supergravity: impact parameter description & mapping to 1-rooted ribbon graphs. JHEP 07:080. https://doi.org/10.1007/JHEP07(2019)080. arXiv:1904.13372
147. Sabio Vera A (2020) Double logarithms in $\mathcal{N} \geq 4$ supergravity: weak gravity and Shapiro's time delay. JHEP 01:163. https://doi.org/10.1007/JHEP01(2020)163. arXiv:1912.00744
148. Di Vecchia P, Luna A, Naculich SG, Russo R, Veneziano G, White CD (2019) A tale of two exponentiations in $\mathcal{N} = 8$ supergravity. Phys Lett B798:134927. https://doi.org/10.1016/j.physletb.2019.134927. arXiv:1908.05603

149. Di Vecchia P, Naculich SG, Russo R, Veneziano G, White CD. A tale of two exponentiations in $\mathcal{N} = 8$ supergravity at subleading level. arXiv:1911.11716
150. Remiddi E, Vermaseren J (2000) Harmonic polylogarithms. Int J Mod Phys A 15:725. https://doi.org/10.1142/S0217751X00000367. arXiv:hep-ph/9905237
151. Gehrmann T, Remiddi E (2002) Numerical evaluation of two-dimensional harmonic polylogarithms. Comput Phys Commun 144:200. https://doi.org/10.1016/S0010-4655(02)00139-X. arXiv:hep-ph/0111255
152. Bauer CW, Frink A, Kreckel R (2002) Introduction to the GiNaC framework for symbolic computation within the C++ programming language. J Symb Comput 33:1. https://doi.org/10.1006/jsco.2001.0494. arXiv:cs/0004015
153. Dokshitzer YuL, Marchesini G (2006) Soft gluons at large angles in hadron collisions. JHEP 01:007. https://doi.org/10.1088/1126-6708/2006/01/007. arXiv:hep-ph/0509078
154. Del Duca V, Duhr C, Gardi E, Magnea L, White CD (2011) The infrared structure of gauge theory amplitudes in the high-energy limit. JHEP 12:021. https://doi.org/10.1007/JHEP12(2011)021. arXiv:1109.3581
155. Lipatov LN (1976) Reggeization of the vector meson and the vacuum singularity in nonabelian gauge theories. Sov J Nucl Phys 23:338
156. Fadin VS, Fiore R, Kotsky MI, Papa A (2000) The Gluon impact factors. Phys Rev D61: 094005. https://doi.org/10.1103/PhysRevD.61.094005. arXiv:hep-ph/9908264
157. Witten E (2004) Perturbative gauge theory as a string theory in twistor space. Commun Math Phys 252:189. https://doi.org/10.1007/s00220-004-1187-3. arXiv:hep-th/0312171
158. Bern Z, De Freitas A, Dixon LJ, Wong HL (2002) Supersymmetric regularization, two loop QCD amplitudes and coupling shifts. Phys Rev D66:085002. https://doi.org/10.1103/PhysRevD.66.085002. arXiv:hep-ph/0202271
159. 't Hooft G, Veltman MJG (1972) Regularization and renormalization of gauge fields. Nucl Phys B44:189. https://doi.org/10.1016/0550-3213(72)90279-9
160. Parke SJ, Taylor TR (1985) Perturbative QCD utilizing extended supersymmetry. Phys Lett 157B:81. https://doi.org/10.1016/0370-2693(85)91216-X
161. Mangano ML, Parke SJ (1991) Multiparton amplitudes in gauge theories. Phys Rept 200:301. https://doi.org/10.1016/0370-1573(91)90091-Y. arXiv:hep-th/0509223
162. Cachazo F, Svrcek P, Witten E (2004) Gauge theory amplitudes in twistor space and holomorphic anomaly. JHEP 10:077. https://doi.org/10.1088/1126-6708/2004/10/077. arXiv:hep-th/0409245
163. Bargheer T, Beisert N, Galleas W, Loebbert F, McLoughlin T (2009) Exacting $N = 4$ superconformal symmetry. JHEP 11:056. https://doi.org/10.1088/1126-6708/2009/11/056. arXiv:0905.3738
164. Korchemsky GP, Sokatchev E (2010) Symmetries and analytic properties of scattering amplitudes in $N = 4$ SYM theory. Nucl Phys B832:1. https://doi.org/10.1016/j.nuclphysb.2010.01.022. arXiv:0906.1737
165. Beisert N, Henn J, McLoughlin T, Plefka J (2010) One-loop superconformal and Yangian symmetries of scattering amplitudes in $N = 4$ super Yang-Mills. JHEP 04:085. https://doi.org/10.1007/JHEP04(2010)085. arXiv:1002.1733
166. Chicherin D, Sokatchev E (2018) Conformal anomaly of generalized form factors and finite loop integrals. JHEP 04:082. https://doi.org/10.1007/JHEP04(2018)082. arXiv:1709.03511
167. Becher T, Neubert M (2009) On the structure of infrared singularities of gauge-theory amplitudes. JHEP 06:081. https://doi.org/10.1088/1126-6708/2009/06/081. arXiv:0903.1126
168. Bern Z, Dixon LJ, Dunbar DC, Kosower DA (1994) One loop n point gauge theory amplitudes, unitarity and collinear limits. Nucl Phys B 425:217. https://doi.org/10.1016/0550-3213(94)90179-1. arXiv:hep-ph/9403226
169. Bern Z, Dixon LJ, Dunbar DC, Kosower DA (1995) Fusing gauge theory tree amplitudes into loop amplitudes. Nucl Phys B 435:59. https://doi.org/10.1016/0550-3213(94)00488-Z. arXiv:hep-ph/9409265
170. Arkani-Hamed N, Bourjaily JL, Cachazo F, Goncharov AB, Postnikov A, Trnka J (2016) Grassmannian geometry of scattering amplitudes, vol 4. Cambridge University Press. https://doi.org/10.1017/CBO9781316091548. arXiv:1212.5605

171. von Manteuffel A, Schabinger RM (2015) A novel approach to integration by parts reduction. Phys Lett B 744:101. https://doi.org/10.1016/j.physletb.2015.03.029. arXiv:1406.4513
172. Peraro T (2016) Scattering amplitudes over finite fields and multivariate functional reconstruction. JHEP 12:030. https://doi.org/10.1007/JHEP12(2016)030. arXiv:1608.01902
173. Peraro T (2019) FiniteFlow: multivariate functional reconstruction using finite fields and dataflow graphs. JHEP 07:031. https://doi.org/10.1007/JHEP07(2019)031. arXiv:1905.08019
174. Dixon LJ (2014) A brief introduction to modern amplitude methods. In: Theoretical advanced study institute in elementary particle physics: particle physics: the Higgs Boson and Beyond, pp 31–67. https://doi.org/10.5170/CERN-2014-008.31. arXiv:1310.5353
175. Guan X, Liu X, Ma Y-Q (2020) Complete reduction of two-loop five-light-parton scattering amplitudes. Chin Phys C 44:093106. https://doi.org/10.1088/1674-1137/44/9/093106. arXiv:1912.09294
176. Boehm J, Wittmann M, Wu Z, Xu Y, Zhang Y. IBP reduction coefficients made simple. arXiv:2008.13194
177. Lee RN (2014) LiteRed 1.4: a powerful tool for reduction of multiloop integrals. J Phys Conf Ser 523:012059. https://doi.org/10.1088/1742-6596/523/1/012059. arXiv:1310.1145
178. Parke SJ, Taylor TR (1986) An amplitude for n gluon scattering. Phys Rev Lett 56:2459. https://doi.org/10.1103/PhysRevLett.56.2459
179. Berends FA, Giele WT (1988) Recursive calculations for processes with n gluons. Nucl Phys B306:759. https://doi.org/10.1016/0550-3213(88)90442-7
180. Mangano ML, Parke SJ, Xu Z (1988) Duality and multi-gluon scattering. Nucl Phys B298:653. https://doi.org/10.1016/0550-3213(88)90001-6
181. Bern Z, Kosower DA (1992) The computation of loop amplitudes in gauge theories. Nucl Phys B379:451. https://doi.org/10.1016/0550-3213(92)90134-W
182. Bern Z, Dixon LJ, Kosower DA (2000) A two loop four gluon helicity amplitude in QCD. JHEP 01:027. https://doi.org/10.1088/1126-6708/2000/01/027. arXiv:hep-ph/0001001

Chapter 5
Conclusions and Outlook

Scattering amplitudes play a crucial role in the way we study the fundamental laws of the universe. Their importance is at least two-fold. On the one hand, they connect theory and experiment, allowing us to submit our theoretical understanding to the judgement of the experimental data. On the other hand, they often unveil unexpected properties of the underlying theory, which are nowhere to be seen in the usual Lagrangian formulation of QFT. To both ends, truncating the perturbative expansion of scattering amplitudes to the tree level is unacceptable, and we must endeavour to compute higher corrections to the perturbative series. This is made difficult by the necessity of integrating over the degrees of freedom associated with the virtual particles.

Among the current challenges in this field, I have taken up that of computing the scattering amplitudes for processes involving five massless particles at two-loop order. There is growing demand to obtain these amplitudes due to their phenomenological relevance. They are the main bottleneck towards a theoretical description of processes of great interest, such as three-jet and di-photon + jet production, at the next-to-next-to-leading order in QCD. Reaching such a level of accuracy is imperative in order to match the corresponding experimental precision and exploit fully the LHC's enormous physics potential. In the last few years there has been tremendous progress in this direction, thanks to the work of several groups. I have joined this endeavour, and in this thesis I have presented my contributions to it.

Firstly, my collaborators and I computed all the required two-loop five-particle Feynman integrals [1, 2]. We used the method of the differential equations in the canonical form. Our results are fully analytic and valid in the physical scattering region. In order to reach this end, we refined the technique of the leading singularities used to put the differential equations in the canonical form. This approach typically relies on the computation of the leading singularities in four dimensions. In this way, all terms which vanish in four dimensions at the integrand level but give non-vanishing contributions upon D-dimensional integration are missed. Such "evanescent" terms may be fundamental in constructing integrands which integrate

S. Zoia, *Modern Analytic Methods for Computing Scattering Amplitudes*, Springer Theses,
https://doi.org/10.1007/978-3-031-01945-6_5

to pure functions and satisfy a system of differential equations in the canonical form. We showed how to parametrise the evanescent terms using Gram determinants and proposed a notion of D-dimensional leading singularities based on the Baikov parameterisation of the integrals. We expect this approach to be useful also in future computations. The functions needed to write down the analytic expressions of all massless two-loop five-particle integrals have later been systematically classified and implemented [3], and are therefore ready for phenomenology applications.

Making use of our results for the Feynman integrals, we provided the first analytic results for two-loop five-particle scattering amplitudes including the contributions from the non-planar diagrams. We started by computing the (super) amplitudes in $\mathcal{N} = 4$ super Yang-Mills theory [4] and $\mathcal{N} = 8$ supergravity [5] at symbol level. In Ref. [6] we lifted these results to functions, and computed their asymptotic expansion in the multi-Regge limit. The computations in the maximally supersymmetric theories served two purposes. They provided precious analytic data to study the properties of these theories in a particle configuration never-before investigated beyond the planar limit. This is particularly important for supergravity, where no notion of colour exists and the amplitudes are therefore intrinsically non-planar. We highlighted a non-trivial analytic property of certain non-planar Feynman integrals that it is not possible to have if fewer than five particles scatter: they exhibit a discontinuity within the physical scattering region. This feature disappears from the complete amplitudes, but manifests itself in their multi-Regge asymptotics. Our results may help shedding light on very interesting open problems, such as—just to name a couple—whether it is possible to make use of integrability in $\mathcal{N} = 4$ super Yang-Mills theory beyond the planar limit, and whether it is possible to formulate an effective theory to explain the Regge limit of supergravity as the BFKL theory explains that of Yang-Mills theory. On a more practical note, the computations in the supersymmetric theories served us to test and improve our workflow in view of the computation of the amplitudes in QCD required for the phenomenological predictions.

We took one further step in this direction by computing the two-loop amplitude for the scattering of five positive-helicity gluons in pure Yang-Mills theory [2]. This amplitude is not required in any NNLO QCD prediction because it interferes with a vanishing tree-level amplitude, but its computation is substantially more complicated than those in the supersymmetric theories. Therefore, it allows us to better assess the feasibility of the computation of the MHV helicity amplitudes which are needed for phenomenology. Our formula for the two-loop all-plus five-gluon amplitude is remarkably compact. It contains only logarithms and dilogarithms, and can therefore be analytically continued to any kinematic region with little or no effort. Interestingly, the rational factors of the transcendental functions are conformally invariant, and we managed to write them in a form that makes this symmetry beautifully manifest. In a spin-off devoted to conformal symmetry, my collaborators and I showed that this follows from the conformal invariance of the one-loop all-plus amplitude for any number of external gluons [7].

The ultimate goal of this program is to compute analytically all the massless five-particle amplitudes required to produce predictions for the processes of phenomenological interest—three-jet and di-photon + jet production in primis—at NNLO

accuracy in QCD. With the state-of-the-art workflow based on finite fields, the typical bottlenecks of such amplitude computations are: achieving suitable expressions for the Feynman integrals, IBP-reducing the amplitudes, and reconstructing the rational functions in the amplitudes. Thanks to the recent progress, which I have partly presented in this thesis, the bottleneck of the Feynman integrals is completely removed. The IBP reductions we performed for the all-plus amplitude are of comparable complexity to what is required for other helicity amplitudes or for amplitudes including fermions. Our computation has therefore shown that such IBP reductions are now accessible. The remaining obstacle is time. The plain reconstruction of the rational factors may require the evaluation of the IBP-reduced amplitude millions of times. If we want to achieve our goals within a reasonable timeframe, further work is necessary to optimise all the steps in the workflow and reduce the evaluation time. Moreover, a refined reconstruction strategy is desirable. Several approaches are being pursued in this sense: choosing carefully the kinematic variables, making use of the linear relations among the rational functions, guessing frequent factors, constructing good ansätze... Some of these or other ideas may reduce dramatically the complexity of the computation. I have no doubt that the amplitude community—hopefully with some contribution from me—will soon be able to overcome these challenges.

Bibliography

1. Chicherin D, Gehrmann T, Henn J, Wasser P, Zhang Y, Zoia S (2019) All Master integrals for three-jet production at next-to-next-to-leading order. https://doi.org/10.1103/PhysRevLett.123.041603. arXiv:1812.11160
2. Badger S, Chicherin D, Gehrmann T, Heinrich G, Henn J, Peraro T et al (2019) Analytic form of the full two-loop five-gluon all-plus helicity amplitude. https://doi.org/10.1103/PhysRevLett.123.071601. arXiv:1905.03733
3. Chicherin D, Sotnikov V, Pentagon functions for scattering of five massless particles. arXiv:2009.07803
4. Chicherin D, Gehrmann T, Henn J, Wasser P, Zhang Y, Zoia S (2019) Analytic result for a two-loop five-particle amplitude. https://doi.org/10.1103/PhysRevLett.122.121602. arXiv:1812.11057
5. Chicherin D, Gehrmann T, Henn JM, Wasser P, Zhang Y, Zoia S, The two-loop five-particle amplitude in $\mathcal{N} = 8$ supergravity. https://doi.org/10.1007/JHEP03(2019)115. arXiv:1901.05932
6. Caron-Huot S, Chicherin D, Henn J, Zhang Y, Zoia S, Multi-Regge limit of the two-loop five-point amplitudes in $\mathcal{N} = 4$ super Yang-Mills and $\mathcal{N} = 8$ supergravity. https://doi.org/10.1007/JHEP10(2020)188. arXiv:2003.03120
7. Henn J, Power B, Zoia S, Conformal invariance of the one-loop all-plus helicity scattering amplitudes. https://doi.org/10.1007/JHEP02(2020)019. arXiv:1911.12142